Ecosystem oxygen metabolism in an impacted temperate river network: Application of the δ^{18}O-DO approach

by

Gao Chen

A thesis
presented to the University of Waterloo
in fulfillment of the
thesis requirement for the degree of
Doctor of Philosophy
in
Biology

Waterloo, Ontario, Canada, 2013

AUTHOR'S DECLARATION

I hereby declare that I am the sole author of this thesis. This is a true copy of the thesis, including any required final revisions, as accepted by my examiners.

I understand that my thesis may be made electronically available to the public.

Abstract

Ecosystem metabolism is an important indicator of aquatic ecosystem function. This thesis concerns ecosystem metabolism as recorded by daily variation in dissolved oxygen (DO) and δ^{18}O-DO in an impacted temperate river network, the Grand River, Ontario, Canada, and specifically addresses the effects of stream size and human disturbance including agriculture, deforestation, and wastewater treatment plants (WWTPs). A suite of 14 sites in the Grand River network was selected with stream sizes varying from 2nd to 7th order.

A transient model of river ecosystem oxygen metabolism, ROM-TM, was developed in order to calculate river ecosystem metabolic rates and reaeration rates from field observation of changes in DO and δ^{18}O-DO. ROM-TM is an inverse modeling approach programmed using MATLAB. Key parameters describing the main metabolic processes, gas exchange, and isotopic fractionation, such as maximum photosynthetic rate ($\boldsymbol{P_m}$), photosynthetic efficiency ($\boldsymbol{a}$), respiration rate at 20℃ ($\boldsymbol{R_{20}}$), gas exchange coefficient ($\boldsymbol{k}$), respiration isotopic fractionation factor ($\boldsymbol{\alpha_R}$), and photorespiration coefficient ($\boldsymbol{\beta_R}$), can be obtained by matching of model predictions with field data. Besides being capable of teasing apart metabolic processes and gas exchange to provide daily average estimates of metabolic parameters at the ecosystem level, ROM-TM can be used to address issues related to light including light saturation phenomena at the ecosystem level, the effect of cloud cover on metabolic balance and photorespiration.

Primary production responses to light along a longitudinal gradient in the Grand River network were described by means of *P-I* curves. Both light-limited and light-saturated conditions were observed. Production parameters $\boldsymbol{P_m}$ and $\boldsymbol{I_k}$ in the Grand River network exhibited an increase with stream order, while $\boldsymbol{a}$ was independent of stream size. However, $\boldsymbol{a}$ did vary among and within sites.

Higher light availability in small and middle-sized streams without riparian trees was associated with high $\boldsymbol{P_m}$, $\boldsymbol{I_k}$ and $\boldsymbol{E_c}$, but low $\boldsymbol{a}$. Ecosystem-level $\boldsymbol{P_m}$ in both small periphyton-dominated streams and large macrophyte-dominated rivers in the Grand River basin were generally less than community-level $\boldsymbol{P_m}$ values from the literature. However, two Grand River sites had comparable $\boldsymbol{P_m}$ to literature-derived $\boldsymbol{P_m}$ due to the prolific growth of macrophytes supported by high nutrient effluents from upstream WWTPs. Ecosystem-level $\boldsymbol{a}$ in my study streams were also less than

those at the community level, indicating there was a declining trend of this parameter with scale, from individual, community to ecosystem. Derived parameters (e.g., $\boldsymbol{I_k}$, $\boldsymbol{E_c}$, and saturation point) increased from the individual level to the community level, and then to the ecosystem level.

From May to early October, metabolic rates in the Grand River network (gross primary production, GPP = 0.4 to 20 and ecosystem respiration, ER = 2 to 33 g O_2 m^{-2} day^{-1}) were within the broad range of metabolic rates occurring in the temperate region, regardless of stream size. The Grand River network is a net heterotrophic system. The total GPP and ER for whole basin was 3.3e+08 and 4.2e+08 g O_2 day^{-1}, respectively.

Reach geomorphology controls the spatial patterns of stream metabolism in the Grand River network, although the spatial patterns may be modified by effects of human disturbance on riparian vegetation, nutrients and other factors. Stream order and channel width, as measures of stream size, are good predictors of metabolic rates and ratios of GPP: ER from small streams to the central Grand River. Ecosystem metabolic rates and ratios generally increase with stream size, but with site-specific variation.

The Grand River network is experiencing effects of human disturbance, mostly downstream of the urban areas and least in small streams with remaining riparian forest. The small and middle-sized streams (2^{nd} to 4^{th} order) without riparian trees in agriculture regions in the Grand River basin did not exhibit significantly different GPP and ER than their counterparts with riparian trees. The stimulative effect of increased light availability due to open canopy on GPP in non-shaded streams may be offset by shading from stream banks and riparian grasses, and unstable sediments resulting from agricultural activities. Large river sites impacted by WWTPs had significantly increased metabolic rates, both GPP and ER, compared to two upstream sites impacted by agriculture only. This result suggests that urban areas cause impacts on the Grand River that are superimposed on the impacts of agriculture.

Three aspects of metabolism of the Grand River differ from the general pattern for the temperate regions: (1) a increase trend of GPP: ER ratios with stream size from 2^{nd} to 7^{th} order; (2) overall, human activities in the Grand River watershed have stronger positive effects on the GPP than on the ER; (3) the middle-sized to large river sites (5^{th}-7^{th} order) had greater influence than small to middle-sized streams (2^{nd}-5^{th} order) in the Grand River on overall GPP and ER.

The general trend of GPP: ER ratio in tropical, subtropical, temperate, and global data approximately conforms to the predictions of the River Continuum Concept (RCC). However, the maximum ratio of GPP: ER in mid-reaches of river networks is not usually >1 as proposed in the RCC. There is a latitude and stream size shift phenomenon regarding where the peak ratio of GPP: ER occurs in each climate zone. The maximum GPP: ER ratio is higher at higher latitudes and occurs at higher order streams.

The study of stream ecosystem metabolism can benefit from the addition of the second oxygen budget, δ^{18}O-DO, in four ways: (1) it is better to use both DO and δ^{18}O-DO budgets, rather than DO only, in sampling protocols with low temporal frequency but high spatial frequency; (2) the δ^{18}O-DO time series data can provide relatively independent constraints on parameter estimation; (3) the addition of δ^{18}O-DO in using two oxygen budgets to quantify metabolic rates provides a way, the cross-plot of δ^{18}O-DO against fraction of DO saturation, to indicate trophic status of an aquatic ecosystem; and (4) the addition of δ^{18}O-DO can provide an estimate of $\boldsymbol{a_R}$ at the ecosystem level that can be used to understand factors affecting respiration.

Acknowledgements

I sincerely thank my supervisors, Profs. William D Taylor and Sherry L Schiff, for their consistently academic and financial support. They provided me a diversity of expertise and support with their different supervisory approaches and areas of specialization. This study would not have been completed without their guidance and valuable and thoughtful suggestions. I am especially appreciative of their patient corrections of my thesis. I will always be grateful for their guidance and their friendship.

I gladly thank the remaining members of my doctoral committees for their time and helpful advice: Prof. Ralph Smith, Prof. Mark Servos and Prof. Barry Warner.

I am forever grateful for the laboratory and field assistance offered by the remarkable Earth Sciences technician, Richard Elgood. All the time, he made things possible for me.

For his assistance with various aspects of my research, I would like to thank Dr. Jason Venkiteswaran. Thanks especially for his great suggestions on the calculation of SSE and model development, and many aspects in my writings.

I appreciate my friend, Li Wang, for her great help with the design and initial programming of the model, ROM-TM.

For field assistance and lab analysis in planning, collecting and analyzing water samples, chemical and isotope data from 2006 to 2012, I would like to thank Justin Harbin, Madeline Rosamond, Jennifer Hood, Simon Thuss, Amy Wong, Haruka Shoji, Ryan Hutchins, Bonnie DeBaets, Adrian Rajkumar, Heather Geertsma, Shannon Walsh, Yuxuan (Ariel) Guo, Jason Gomes, Clive Fernandes, Zhi (Jenessa) Zheng, Amy Morrison, and Eduardo Cejudo.

I would like to sincerely acknowledge Mark Anderson and the Grand River Conservation Authority for support in providing data. I also would like to thank Natural Sciences and Engineering Research Council (NSERC) for providing funding to support my research.

I would also like to thank the people who are not mentioned here, but provided assistance.

Dedication

I would like to dedicate this work to Aquatic Ecology, and

My lovely family, especially to my mother, who provides me unbounded love and support throughout my life, and my lovely wife with her steadfast love, friendship and emotional support since we met thirteen years ago. Also, the two little young men, Eddy and Daniel, who give me lots of fun, I love you all!

Table of Contents

List of Symbols and Abbreviations

2F,2NF	A 2nd order stream with riparian trees, a 2nd order stream without riparian trees
3F,3NF	A 3rd order stream with riparian trees, a 3rd order stream without riparian trees
4F,4NF	A 4th order stream with riparian trees, a 4th order stream without riparian trees
5F,5NF	A 5th order stream with riparian trees, a 5th order stream without riparian trees
α	Production efficiency
APHA	American Public Health Association
BaMM	Bayesian metabolism model
BL	Blair sampling site
BP	Bridgeport sampling site
CCME	Canadian Council of Ministers of the Environment
CR	Community respiration
D	Mean depth of the river channel
DIC	Dissolved inorganic carbon
DO	Dissolved oxygen concentration
DOC	Dissolved organic carbon
DOM	Dissolved organic matter
$\mathbf{DO_{sat}}$	Dissolved oxygen concentration at atmospheric equilibrium
ER	Ecosystem respiration
G or GE	Gas exchange
GDPP	Gross daily primary production
GM	Glen Morris sampling site
$\mathbf{G_n}$, $\mathbf{G_t}$	Net flux of gas exchange, Total flux of gas exchange
GPP	Gross primary production
GRCA	Grand River Conservation Authority
GRB	Grand River Basin
GRN	Grand River network
GRW	Grand River watershed
I	Irradiance intensity
IPCC	Intergovernmental Panel on Climate Change
I_k	Onset of light saturation (the ratio of P_m to α)
k	Gas transfer coefficient
NDM	Net daily metabolisms
NDPP	Net daily primary production
NPP	Net production (GPP-ER)
NPRI	Environment Canada National Pollutant Release Inventory
$\mathbf{O_{2sat}}$	Dissolved oxygen concentration at atmospheric equilibrium
OAT	One-at-a-time technique
P	Photosynthesis
PAR	Photosynthetically active radiation
P-I	Photosynthesis-irradiance curve or production-irradiance curve

P_m	Maximum photosynthetic rate or maximum production rate
P_{max}	Maximum gross primary production rate
PoRGy	PoRGy model
pR	Photorespiration
Q	River discharge
R	Respiration
R^2	Coefficient of determination
R_{20}	Normalized respiration rate at temperature 20℃
R_{air}	Isotopic ratio (^{18}O:^{16}O) of air, a constant 23.5‰
RCC	River Continuum Concept
R_{H2O}	Isotopic ratio (^{18}O:^{16}O) of water
RMS	Root mean squared error
ROM-TM	Transient model of river oxygen metabolism
SPa	A sampling site named SPa, in Speed river
SPb	B sampling site named SPb, in Speed river
SRP	Soluble reaction phosphorus
SSE	Sum of square errors
TIN	Total inorganic nitrogen
TN	Total nitrogen
TON	Total organic nitrogen
TP	Total phosphorus
V	Mean river velocity
VSMOW	Vienna Standard Mean Ocean Water
WM	West Montrose sampling site
WWTP	Wastewater treatment plant

$\alpha_{G\text{-}eq}$	Isotopic fractionation factor for gas-exchange equilibrium
$\alpha_{G\text{-}k}$	Isotopic fractionation factor for gas-exchange kinetic
α_p	Isotopic fractionation factor for photosynthesis
α_R	Isotopic fractionation factor for respiration
β_R	Photorespiration factor
δ	Isotopic signature of dissolved oxygen in delta notation
δ^{18}O-DO	Isotopic signature of dissolved oxygen, in delta notation
δ^{18}O-H_2O	Isotopic signature of molecular oxygen in water, in delta notation

List of Figures

List of Tables

– Chapter 1 –

Introduction

1.1 Background

Healthy river ecosystems can provide humans the most basic necessity of life, water, as well as a variety of other ecosystem services (e.g., fisheries, transportation, recreation, education and esthetic values). However, development of human societies and associated land use changes have greatly altered and damaged natural freshwater environments. The growth of both human and animal populations will impose further demands and stresses on river ecosystems. To reach sustainability, action must be taken to preserve the stressed ecosystems and restore damaged ones. Scientific knowledge can provide the foundation for managing ecosystems. However, good cooperation is needed among scientists, stakeholders, local communities and governments.

Water, both quality and quantity, is one of the most important issues for a populated region, and greatly depend on the preservation of local freshwater ecosystems. Providing sufficient water of good quality for local people by means of effective management of local freshwater ecosystems is a long-term management objective of the Grand River Conservation Authority (GRCA) in the Grand River Watershed, Ontario, Canada.

Dissolved oxygen (DO) is often used as the primary indicator of water quality in rivers. It not only supports respiration for most of organisms on earth, but also mediates biogeochemical cycles. The DO in a river is largely controlled by biological processes (i.e., photosynthesis and respiration) and as well as by physical and hydrological processes. The metabolic balance of a river ecosystem reflects ecological structure and

function and therefore it is often considered an important indicator of river ecosystem health (Mulholland et al. 2005, Fellows et al. 2006a, Young et al. 2008). Better understanding of river ecosystem metabolism will improve our management of water sources, as well as contribute to ecosystem science.

New techniques and scientific approaches can often enlarge our capability to explore science questions and advance our understanding and knowledge. This is true of the study of aquatic ecosystem metabolism using oxygen isotope ($\delta^{18}O$) techniques in recent years. The $\delta^{18}O$ approach has come into widespread use in metabolic balance research in various aquatic ecosystems due to the advent of continuous-flow isotope-ratio mass spectrometry (CF-IRMS), which has reduced the onerous sample requirements of conventional dual-inlet analysis by orders of magnitude with only a slight loss in precision over dual-inlet analysis (Wassenaar and Koehler 1999). Hence, O_2 isotopic analysis is not as time-consuming as it once was.

1.2 Motivations and Objectives

The Grand River network is an agriculture and urban mixed impacted river system with long history of inhabitation in the watershed. My objective is to address the effects of human activity on the ecosystem metabolism of the Grand River, and examine the utility of using $\delta^{18}O$ analysis in the study of river ecosystem metabolism, following a few pioneer studies in oceans (Luz and Barkan 2000, Quay et al. 2010, Viviani et al. 2011), lakes (Quay et al. 1995, Russ et al. 2004), and productive rivers (Parker et al. 2005, Tobias et al. 2007, Venkiteswaran et al. 2007). This work may provide answers to practical and scientific questions that initially motivated this study. The specific research objectives of this work can be summarized as follows:

1) Develop a new, dynamic, transient model of river ecosystem oxygen metabolism (ROM-TM) which is capable of using both DO ($^{16}O^{16}O$) and $^{18}O^{16}O$ time series, to quantify photosynthesis, respiration and gas exchange rates (Chapter 4);

2) Address the responses of primary production to light in streams of different stream size and stress, at the ecosystem level (Chapter 5);

3) Assess the effects of anthropogenic perturbations on Grand River ecosystem metabolism from multiple aspects and scales. The main disturbances include agricultural activities and deforestation in the headwaters and wastewater plant effluents in the main channel of the Grand River (Chapter 6); and

4) Examine current concepts and theories of stream ecology, e.g., heterotrophy of streams and the applicability of the River Continuum Concept (RCC) in the Grand River and other rivers that have been the subject of metabolic studies (Chapter 7).

1.3 Organization of the Thesis

Eight chapters are presented in this thesis. It can be logically divided into four parts. The first part sets out the context from which this work emerged: the reasons to conduct this study and the objectives (Chapter 1), relevant literature background (Chapter 2), and the study sites and methods (Chapter 3). The second part develops the method (a new model) with which metabolic rates can be quantified (Chapter 4). The third part addresses a few key scientific questions at the ecosystem/watershed level (Chapters 5 and 6) and the global level (Chapter 7). The last part is the summary of the thesis (Chapter 8). Chapters are as follows:

Chapter 1: Introduction

This chapter introduces the context of this research and outlines the objectives of this research.

Chapter 2: River Ecosystem Oxygen Metabolism: Background and Current Knowledge

This chapter provides a context for the thesis by means of a literature review on the study of ecosystem oxygen metabolism in streams and rivers.

Chapter 3: Study Area and Methods

Chapter 1-

This chapter describes the natural environmental characteristics (e.g., location, climate, soils and ecology) of the Grand River Watershed, sites chosen for this study and methods.

Chapter 4: Inverse Modeling of Dissolved O_2 and $\delta^{18}O$-DO to Estimate Aquatic Metabolism, Reaeration and Respiration Isotopic Fractionation: Effects of Variable Light Regimes and Input Uncertainties

A new river ecosystem metabolism model, ROM-TM, is presented in this chapter. Its ecological applications and new functions are examined.

Chapter 5: The Responses of primary production to Light at the Ecosystem Level in an Impacted Temperate River Network

This chapter systematically addresses ecosystem-level responses of production to light through a series of stream and river sites with different size and stress.

Chapter 6: Stream Ecosystem Metabolism in an Impacted Temperate River Network: Magnitude, Variability and Temporal-Spatial Patterns

Magnitude, variability and temporal-spatial patterns of ecosystem metabolism of the Grand River are reported. The effects of human activities on ecosystem metabolism are systematically addressed from various aspects.

Chapter 7: A Global Perspective on Ecosystem Metabolism in Streams and Rivers

A global review dataset of stream ecosystem metabolism is developed. River Continuum Concept is examined using the data of the Grand River, and literature data of different climate zones and the globe.

Chapter 8: Summary, Conclusions and Recommendations

In the last summary chapter, conclusions and the significance of this study are addressed as well as the prospect of future challenges and frontiers.

– Chapter 2 –

River ecosystem oxygen metabolism: background and current knowledge

2.1 Introduction

Oxygen (O_2) is one of the most important chemical elements on the earth. It makes up 49.2% of the earth's crust and 88.8% of the oceans by mass. Molecular oxygen is the second largest gaseous component of modern earth's atmosphere, 21% on a volume basis. Acting as the primary oxidizing agent, oxygen regulates biogeochemical cycles and provides aerobic conditions for metabolic activities of organisms in our biosphere. It is essential for the respiration of almost all life. In aquatic ecosystems, dissolved O_2 (DO) is vital for higher aquatic life (Davis 1975, Kramer 1987, Seibel 2011) and aquatic ecosystem health (Bunn et al. 1999, Brisbois et al. 2008, Young et al. 2008). Usually, DO levels no less than 7.0 mg L^{-1} are desired to maintain aquatic ecosystem health. DO level below 5.0 mg L^{-1} may impair the function and survival of aquatic biota, and below 2 mg L^{-1} can directly lead to death of most fishes (Davis 1975, Seibel 2011).

The local DO levels in an aquatic ecosystem are generally determined by oxygen solubility, biological metabolic processes (including photosynthesis and respiration) and air-water gas exchange. The study of aquatic ecosystem metabolism concerns the partitioning and quantification of these processes in aquatic ecosystems. Efforts to measure metabolism in aquatic ecosystems have contributed to theoretical and conceptual foundations of aquatic ecology (Odum 1957b, Vannote et al. 1980, Ward et al. 2002) and guided management and manipulation of stressed aquatic ecosystems (Kaenel et al. 2000, Caraco and Cole 2002, Cronin et al. 2007, Suren 2009). However, despite a

long history of study (Odum 1956, Edwards and Owens 1962), our understanding of aquatic metabolism is still limited, particularly in lotic ecosystems (Bayley 1995, Naegeli and Uehlinger 1997, Gomi et al. 2002, Del Giorgio and Williams 2005, Berman-Frank et al. 2009). The challenges mainly lie in four aspects: (1) the complexity of river ecosystems; (2) correct mathematical description (expression) of metabolic processes at the ecosystem level; (3) the confounding effects of some hydraulic and physical processes on the variation of DO (e.g., ground water input with lower concentration of DO, gas exchange with atmosphere), and, more importantly; (4) the lack of direct and efficient methods (Bott et al. 1978, Marzolf et al. 1994, Mulholland et al. 1997, Dodds and Brock 1998, Uzarski et al. 2004, Warkentin et al. 2007).

2.2 Dissolved O_2: supplying and consuming pathways

DO often has daily fluctuations in rivers, reflecting the balance between O_2 supplying and consuming pathways. The baseline is determined by the solubility of O_2. Major DO sources include O_2 production during photosynthesis by aquatic plants and algae, and reaeration from the atmosphere. O_2 sinks include various metabolic respiration pathways, chemical O_2 consumption, and O_2 flux to the atmosphere. Photosynthesis and respiration largely determine the daily variation in DO in aquatic ecosystems. Most aquatic phototrophs produce O_2 through photosynthesis during the day, however, respiration consumes O_2 throughout the night. Air-water gas exchange drives the O_2 flux into or out of the system depending on the difference between saturation O_2 and the actual DO level, dampening the daily fluctuation of DO level. The addition of water with different DO may also cause changes in the local level of DO.

2.2.1 Oxygen solubility

The solubility of O_2 provides the basic level of DO in water. About 9.1 mg L^{-1} O_2 can be dissolved into distilled water at 20℃ and standard pressure. Three factors co-determine the level of O_2 solubility. Water temperature is the primary controlling factor. Colder

water can hold more O_2. The next most important factor is atmospheric pressure. According to Henry's law, the barometric pressure has a positive relationship with the solubility of O_2. For example, decreasing atmosphere pressure with increasing altitude lowers the solubility of O_2. Similar situations can occur in deep lakes and oceans because of the higher hydrostatic pressure with depth. The third factor to be considered is salinity. Salinity decreases the solubility of O_2 in water.

Widely accepted equations predicting the amount of DO in equilibrium with the atmosphere at a certain temperature, pressure and salinity are the Weiss (1970) equations, later revised equations by Benson and Krause (1980 & 1984). They all can provide accurate predictions, with discrepancies less than 0.1 mg L^{-1} in general and have been recommended as standard methods. These equations are provided in Chapter 4.

2.2.2 Photosynthesis and respiration

Photosynthesis (P) is the biological conversion of light energy to chemical bond energy that is stored in the form of organic carbon compounds, and can be written as an oxidation-reduction reaction of the general form:

$$2H_2A + CO_2 + \text{Light} \xrightarrow{\text{Pigments}} (CH_2O) + H_2O + 2A \quad (2.1)$$

Where, A is usually oxygen in plants, algae and cyanobacteria. They are often called primary producers or phototrophs. In stream and river ecosystems, major aquatic primary producers include a diverse group of macrophytes, periphyton and phytoplankton.

Respiration (R) is the process by which all organisms obtain vital energy from a variety of reduced carbon compounds (del Giorgio 2005). Respiration represents the largest sink of organic matter in the biosphere. It covers a variety of very different processes that can be broadly categorized as: (1) Reactions that occur in the light and involve O_2 cycling and energy dissipation, and (2) Reactions that occur both in the light and dark and effect the acquisition of energy.

Carbon fixation in rivers is accompanied by oxygen evolution during photosynthesis and the reverse process, respiration, occurs concurrently. Both oxygen and carbon are widely used in the definition and quantification of metabolism. The conversion factor is close to 1.0 but needs to be modified by the photosynthetic quotient (PQ) and respiration quotient (RQ) according to the specifies of metabolism. The RQ values can broadly range from 0.5 to 1.33 according to the organic material oxidized, e.g., methane (RQ = 0.5), saturated fatty acid (RQ = 0.67), nucleic acid (RQ = 1.24) and glycolic acid (RQ = 1.33). The oxidation of organic materials can be generally described by equation 2.2 (Del Giorgio and Williams 2005). The RQ is the ratio of α/γ.

$$C_\alpha H_\beta O_\chi N_\delta P_\varepsilon S_\phi + \gamma O_2 = \alpha CO_2 + \delta NH_3 + \varepsilon H_3PO_4 + 0.5[\beta - 3(\delta+\varepsilon) + 2\phi]\ H_2O + \phi H_2SO_4$$

$$\gamma = \alpha + 0.25\beta - 0.5\chi - 0.75\delta + 1.25\varepsilon + 1.5\phi \qquad (2.2)$$

Oxygen is commonly used as a currency for the measurement of respiration and carbon is used as a currency in ecosystem models. Hereafter, I adopt oxygen as the currency for metabolism. This use has a potential advantage when I talk about gross photosynthesis (P_g) or gross primary production (GPP). However, high photorespiratory rates lead to critical differences between measures based on oxygen evolution and carbon fixation (Hough 1974, Lloyd et al. 1977, Bauwe et al. 2010).

At the ecosystem level, photosynthesis and respiration can be regarded as a summation of anabolism and catabolism of all organisms or all ecological components within an ecosystem (Falkowski and Raven 1997, Del Giorgio and Williams 2005). Essential measures of stream and river ecosystem metabolism include gross primary production (GPP), ecosystem respiration (ER), net ecosystem production (NPP = GPP - ER), and the ratio of GPP/ER. GPP, identical to gross photosynthesis often used by physiologists, represents the total conversion of inorganic carbon to organic forms by autotrophs within an ecosystem. It accounts for all O_2 produced during photosynthesis, whether or not part of evolved O_2 has been reused via rubisco activity inside autotrophs as photorespiration. Ecosystem respiration accounts for the consumption of O_2 and organic matter. In a narrow sense, it represents total oxidation of organic carbon to inorganic carbon within an ecosystem. However, in a generalized sense, ecosystem

respiration often includes a variety of biotic O_2 consumption pathways and abiotic oxidative processes as well. It should be noted that ecosystem respiration is often called community respiration (CR) in aquatic ecosystems. Strictly speaking, CR denotes only a subset of the ecosystem components.

Net primary production is the difference between gross primary production and ecosystem respiration within a specified time periods. The GPP/ER ratios are dimensionless, but still time-specific (e.g., daily, annual, etc).

2.2.3 Gas exchange

In open water, air-water O_2 exchange occurs continuously to reach a dynamic equilibrium of DO with the atmosphere, with net entry of O_2 into the water from air while DO is under saturated, or net loss of DO from the water while DO is supersaturated. According to the surface-renewal theory, it is assumed that the net O_2 transfer velocity is dependent on the turbulence and the diffusion rate of O_2 in water. The air-water O_2 exchange in streams is generally described using a standard flux equation under the assumption that the water column is well-mixed with a homogeneous DO concentration (Equation 2.3). The difference between saturation DO and actual O_2 drive the O_2 flux into or out of the system:

$$G_t = k \bullet (DO_{sat} - DO) \tag{2.3}$$

Where, G_t is gas exchange, the mass flux of O_2 in DO concentration time^{-1}. The key parameter of this process is $\boldsymbol{k}$, the gas exchange coefficient (in *distance* t^{-1} or t^{-1}). DO_{sat} is the amount of O_2 dissolved in the water at saturation.

The gas exchange coefficient is a key parameter in analyzing metabolic rates, but is a difficult measurement to make precisely. There are three main approaches used to estimate $\boldsymbol{k}$ in the study of stream and river ecosystem metabolism. One common approach that can produce accurate measurements of $\boldsymbol{k}$ is using tracer techniques. A diverse array of tracers has been used, including inert gases, e.g., propane, SF6, methyl chloride and ethylene (Tsivoglou and Neal 1976, Wanninkhof et al. 1990, Genereux and

Hemond 1992, Tobias et al. 2009), radioactive gases (^{85}Kr) , and the reaeration of deoxygenated water (Churchill et al. 1962). However, the use of tracers often requires sophisticated instrumentation, and is time consuming and costly. In addition, the accuracy and reproducibility of ***k*** estimates is always an issue while using gas tracers. Potential hazardous effects of radioactive tracers limit their use, although they have yielded accurate ***k*** estimates.

Another common approach is to estimate ***k*** using empirical and theoretical equations based on the relationship between gas exchange and channel geometric parameters (e.g., mean depth and bed slope) and hydrological parameters (e.g., water flow). A formula is often chosen arbitrarily, basing on similarity between the river under study and the river used to calibrate the empirical relationship. A large database of empirical parameters (river conditions) is required, otherwise, poor estimates, may be obtained using this approach (Melching and Flores 1999). Furthermore, this approach needs to be used with care in analyzing the effects of changes in hydrology on metabolism because of undesired circularity (Marcarelli et al. 2010).

A third general approach has been developed and widely used in modeling DO balance. When Odum first presented the whole-ecosystem approach to tease apart the photosynthesis, respiration and gas exchange rates through DO diel curves, he also proposed that ***k*** represented the slope of the regression between DO deficit and the rate of change in DO during the night (Odum 1956). This method is called the nighttime regression technique (Hornberger and Kelly 1975). It is a robust method in relative deep rivers. However, if no significant reaeration rates are determined on that date, valid daily metabolism estimates cannot be obtained and should be excluded (Aristegi et al. 2009). An alternative analytical solution for yielding ***k*** from DO diel curves has also been developed, the Delta method (Chapra and Ditoro 1991, McBride 2002, McBride and Chapra 2005). The ***k*** is calculated as a function of the time lag between solar noon and DO maximum. However, this method is not appropriate for small headwater streams with $k > 10/d$. This method is also less useful on cloudy days because of irregular DO diel curves with multiple DO peaks after solar noon, or sites with short time lags due to high

reaeration rates. Fully sunny days are not always common in summer in temperate regions, limiting the application of the Delta method in estimating ***k***. In recent years, with the rapid development of computational techniques and the application of inverse modeling techniques in DO mass balance modeling, the ***k*** value can be directly treated as an unknown parameter and estimated through least squares methods (Tobias et al. 2007, Venkiteswaran et al. 2007) or maximum probability (Holtgrieve et al. 2010). The ***k*** estimate obtained in this way is an average value over a specified time period of ecological relevance, e.g., hourly or daily (Venkiteswaran et al. 2007, Holtgrieve et al. 2010). Oxygen dual or triple isotopes have been used to help in constraining the uncertainty of ***k*** estimates (Tobias et al. 2007, Venkiteswaran et al. 2007, Holtgrieve et al. 2010, Sarma et al. 2010).

In addition, some particular methods have been recently developed to provide an estimation of the ***k*** in streams, such as sound pressure (Morse et al. 2007). The sound pressure method is similar to the gas-evasion approach using gas tracers, but in this case the relationship is built up between sound level (noise) and turbulence driven by channel features to obtain ***k*** estimates. Compared to gas-evasion methods, the sound pressure method has a few advantages. It is modest in cost and effort because a simple and inexpensive sound level meter is enough to measure sound levels, and is easily calibrated and deployed. Continuous reaeration estimation can be achieved by combining the k-sound pressure relationship with the sound pressure-stage rating curve; and most importantly, measurements are made on a similar time scale to DO, temperature, and light values to calculate whole-stream metabolism. Hence, the sound pressure method is particularly useful for long-term whole-stream experiments and monitoring plans.

2.3 Evolution of methodologies and techniques

The primary task on the study of aquatic ecosystem metabolism is to quantify metabolic rates at the ecosystem scale. Based on these rates, relevant ecological issues can be addressed, for example, cross-system comparison, metabolic responses to disturbance,

etc. A variety of methods to estimate ecosystem metabolic rates in streams and rivers have been developed, basically belonging to two different approaches. One is the microcosm approach and the other is the *in situ*, whole-ecosystem approach (Table 2.1).

2.3.1 Comparison of microcosm vs. in situ approaches

The microcosm approach follows the idea of reductionism, i.e., the assumption that the quantification of whole ecosystem metabolism can be obtained through simply summing up directly quantified metabolic rates of individual ecological components. For example, a series of light and dark chambers can be used to incubate ecological components such as seston, macrophytes, etc., so their relevant rates of P and R can be calculated. Dark chambers can provide the respiration rates of incubated parts, and gross photosynthesis rates can be obtained as the sum of R and NPP from light and dark chambers.

The whole-ecosystem approach exploits DO time series as a representation of whole-ecosystem metabolism, and metabolic rates can be abstracted through model-fitting. Photosynthesis, respiration and gas exchange rates can be teased apart from DO diel curves through night-time regression, and other modeling methods. The whole-ecosystem approach includes the one-station method and the two-station method. The choice of method is mainly dependent on the homogeneity of upstream reaches, labor and time cost, resource availability, and data quality requirements. The one-station method uses measures at one location and assumes the upstream reaches to be homogeneous on the scale of the measurement, i.e., no drains and significant tributary inputs, without changes in biology, chemistry, and morphology. The length of the distance upstream that influences the sampling station downstream is empirically approximated by $3v/k$ (v is flow velocity, k is gas exchange coefficient) according to Chapra and Ditoro (1991), which typically spans from 100 m to 10 km (Reichert et al. 2009).

Table 2.1 Approaches, methods and techniques used in estimating stream/river ecosystem metabolism

Approach	Method	Temporal-Spatial scale	Strengths	Weaknesses
Incubation	Closed chamber or light/dark bottle (^{14}C,O_2)	Hourly-daily; patch scale (within habitats)	○ Isolation of certain components ○ Highly controllable ○ Direct and precise measurement	○ Difficult to scale up because of high heterogeneity ○ Transferring of biological material and causing: changes in water velocity; nutrient depletion; light attenuation; O_2 or CO_2 bubble formation ○ Neglect of other components (e.g., deep sediments) ○ Labor intensive
Open channel (whole-stream)	Diel O_2 time-series (DIC, pH time-series in few cases)	Daily-annual; reach scale	○ Integrated measurement of all components, reliable for scaling up ○ Labor saving (multi-variable sensors & remote data collection: YSI, Hydrolab,etc.) ○ Precise measurements ○ High resolution data	○ Requiring accurate determination of reaeration ○ Mixing physical, chemical and biological processes (e.g., ecosystem respiration) ○ No component rates ○ Spatial heterogeneity of longitudinal, horizontal and vertical, e.g., ○ Length of upper reach considered as homogeneity must be > $3v/k$ while using one-station method; ○ Tributary water input; ○ Groundwater input;
	Diel $\delta^{18}O$-DO time-series	Daily mainly; reach scale	○ Integrated measurement of all components ○ precise and insightful ○ sensitive method	○ Dependant on and being enhancements to diel O_2 time-series ○ model dependency ○ Requires determination of both reaeration and fractionation factors ○ time and labor costly, both in field sampling and lab analysis
others	Ecosystem budget	Seasonal-annual; Ecosystem scale	Integrated measurement of all components	○ NPP only ○ Large aggregation error

Both microcosm approaches and whole-ecosystem approaches have strengths and weaknesses (Table 2.1). Both are widely accepted methods of measuring aquatic ecosystem metabolism and have even been used in combination in some cases. However, care must be taken to choose an appropriate method for answering the questions at hand.

Whole-ecosystem approaches are gradually accepted as the best choice for estimates of metabolic balance at the ecosystem level due to the complexity of aquatic ecosystems. Although the whole-ecosystem approach does not provide direct measurements of metabolism of ecosystem components, it does avoid the issue of scaling-up to the ecosystem level and is useful for obtaining system wide measurements (across habitats, reach scale), whereas the microcosm approach is limited to the patch scale (within habitats) or even less. The use of chambers to estimate reach-scale metabolism requires extrapolation and assumption of minimal within-reach heterogeneity (Mulholland et al. 1997). Marzolf et al. (1994) clearly demonstrates the limitations in extrapolating patch-scale measurements to the reach scale, as they found that chamber and whole ecosystem approaches can result in very different estimates of metabolism. Scaling up to the ecosystem produces errors that are unknown, but likely underestimates GPP and ER (Uzarski et al. 2004) . This distinction between the two techniques reinforces the importance of considering scale when choosing an appropriate method (Uzarski et al. 2001, Uzarski et al. 2004).

Limitations of the microcosm approach may arise, in part, from transferring biological communities or components into metabolic chambers. On the other hand, the microcosm approach improves control over conditions for experimental manipulation, and so offers the only experimental means of addressing controlling factors. However, experimental manipulation does not accurately reproduce hydrodynamic environment and irradiance from those occurring in situ. Other problems include nutrient depletion, and bubble formation under supersaturated conditions (McIntire and Phinney 1965, Sumner and Fisher 1979, Bott et al. 1985). Also, enclosed communities may not adequately represent the entire stream ecosystem. Neglect of metabolism of deep sediments can lead to serious underestimates of river ecosystem metabolism (Grimm and

Fisher 1984). Estimates of photosynthetic rates may be altered by light attenuation by chambers, which also can reduce the harmful effects of UV irradiance on biofilm (Dodds and Brock 1998).

In contrast, methods from whole-system approach do not at all alter the environmental conditions for primary producers and other organisms. NPP and ER results can be extracted at different time scales, from minutes to hours. Measurements based on open-system changes in dissolved O_2 can occur continuously without extraordinarily high costs. However, they usually require accurate determination of reaeration across the air-water interface which can be difficult to quantify, especially if the studied reach is highly spatial heterogeneous (e.g., non-uniform hydraulic characteristics). Although techniques to measure reaeration using tracer compounds are available, this approach involves sophisticated equipment, e.g., pumps, regulators, gas chromatograph and integrator, etc (Kilpatrick F.A. 1989). Currently, O_2 exchange with the atmosphere is often only estimated by models. There are dozens of re-aeration models available. The results differ, sometimes by a lot (Jamieson 2010). Commonly, open-stream techniques produce relatively low estimates of net community productivity (Bott 1978). Updated ecosystem metabolism models based on the one-station method treat the gas exchange coefficient $\boldsymbol{k}$ as an estimated parameter.

Spatial heterogeneity is an important concern using whole-system, open-channel methods (Reichert et al. 2009), particularly using the one-station method, but has been often ignored (Chapra and Ditoro 1991). Open-channel methods are more suitable for less turbulent streams with moderately high metabolic rates (McCutchan et al. 1998). The length of the reach considered to be homogeneous must be $> 3\boldsymbol{v}/\boldsymbol{k}$ ($\boldsymbol{v}$ is flow velocity and $\boldsymbol{k}$ is gas exchange coefficient) while using one-station method (Chapra and Ditoro 1991). Inflow of water from tributaries and groundwater with different O_2 concentration might lead to errors in estimates of metabolic rates (McCutchan et al. 2002). In headwater streams with small channels, shallow water depths and turbulence, it might be difficult to obtain reliable k estimates (Young and Huryn 1999, McBride and Chapra 2005, Clapcott and Barmuta 2010a). In this case, benthic chambers are more suitable, and they might

provide metabolic responses of specific in-stream habitats to perturbation (Hill et al. 1997, Whitledge and Rabeni 2000, Fellows et al. 2001, Clapcott and Barmuta 2010b). Benthic chambers are also favored where lateral or groundwater inflow and/or O_2 exchange across the air-water interface is expected to be high, compartmentalization of metabolism is desired, and an estimate of variance is required. Whole stream metabolism method is preferred where a range of habitat types are going to be incorporated in the measurement and/or where nutrient limitation is expected to occur if closed chambers are used. Recent findings of significant hyporheic respiration in many streams (Grimm and Fisher 1984, Jones 1995, Mulholland et al. 1997, Baker et al. 1999) may explain why the two methods often give conflicting results when used in the same system (Bott et al. 1978, Grimm and Fisher 1984, McCutchan et al. 1998, McCutchan et al. 2002). Mulholland et al. (1997) concluded that non-disruptive, whole-stream methods are needed to accurately measure stream ecosystem metabolism and respiration in particular.

2.3.2 Application of O_2 stable isotopes

Oxygen has three naturally occurring stable isotopes: ^{16}O, ^{17}O and ^{18}O. Their nuclei all contain 8 protons, but with 8, 9 and 10 neutrons, respectively. The most abundant is ^{16}O (99.76%), next is ^{18}O (0.201%) and an even smaller percentage for ^{17}O (0.039%). Because of the difference in atomic mass of these isotopologues, they exhibit slightly different behaviors in chemical reactions or state transformation in physical processes. Usually, ‘heavy’ isotopes (with more neutrons, sometimes called ‘enriched’) react or transform more slowly, whereas ‘light’ isotopes (sometimes called ‘depleted’) react or transform more quickly. Hence, this difference in reactivity can be detected and used in relevant research, such as aquatic ecosystem oxygen metabolism.

Traditional oxygen metabolism studies use DO concentration only, and ignore DO isotopic composition, $^{18}O^{16}O$. In recent years, the $\delta^{18}O$ approach has come into widespread use in metabolic balance research in various aquatic ecosystems because of the advent of continuous-flow isotope-ratio mass spectrometry (CF-IRMS), which has reduced the large sample requirements of conventional dual-inlet analysis by orders of

magnitude with only a slight loss in precision (Wassenaar and Koehler 1999). O_2 isotopic analysis is no longer as time-consuming. However, large volumes may be required for low DO samples. Currently, oxygen isotope analysis considers only the ratio of ^{18}O to ^{16}O present in a sample in most of cases. A considerable amount of work using duel oxygen isotope analysis (^{18}O and ^{16}O) has occurred in diverse aquatic ecosystems, e.g., lakes, oceans and rivers (Quay et al. 1995, Tobias et al. 2007, Venkiteswaran et al. 2007, Holtgrieve et al. 2010, Quay et al. 2010, Karim et al. 2011, Luz and Barkan 2011). Triple oxygen isotopes (^{18}O, ^{17}O and ^{16}O) have been used in estimating primary production in estuaries and oceans (Luz 1999, Luz and Barkan 2000, Sarma and Abe 2006, Sarma et al. 2008, Luz and Barkan 2009, Juranek and Quay 2010, Sarma et al. 2010, Kaiser 2011, Prokopenko et al. 2011), however, not in rivers and lakes yet.

2.3.2.1 Notation of O_2 stable isotopes

For the sake of results being straightforward and comparable from various sources and analyses, the isotopic ratio of a sample is measured and reported in delta per mill notation (‰) as the part per thousand deviation from a standard reference (Equation 2.5). For the ^{18}O: ^{16}O ratio of O_2, the reference used is Vienna Standard Mean Ocean Water (VSMOW), which is a constant 0.0020052. $\delta^{18}O$ is then

$$\delta^{18}O = \left(\frac{R_{sample}}{R_{std}} - 1\right) \bullet 1000 \qquad (2.5)$$

Where, R is the ^{18}O:^{16}O ratio. R_{sample} is the ratio of the heavy isotope ^{18}O to the light isotope ^{16}O of dissolved O_2 or H_2O in the sample. R_{std} is the ^{18}O:^{16}O of VSMOW.

Isotope fractionation factors for different processes are denoted as α values ($\alpha = R_b/R_a$), where R is the ^{18}O:^{16}O ratio of the reactant (a) and product (b).

2.3.2.2 Application of ^{18}O stable isotope in river ecosystem metabolism

DO budgets describing O_2 dynamics in rivers usually consider three processes: photosynthesis (P), producing oxygen from water; respiration, consuming oxygen and converting it into carbon dioxide, nitrate, and other species; and air-water O_2 exchanges between DO with atmospheric O_2. When adding $\delta^{18}O$-DO time-series data as the second O_2 budget, we need to know two additional things:

1) $\delta^{18}O$ value in the oxygen sources, i.e., $\delta^{18}O$ in H_2O and $\delta^{18}O$ in air O_2. $\delta^{18}O$ value in river water usually range from -7 to -12 per mill, but are usually stable at the daily scale. The $\delta^{18}O$ value of atmospheric oxygen is a constant 23.5 per mill.
2) We must know isotopic fractionation factors for each process. The fractionation factor for photosynthesis ($\boldsymbol{a_p}$) is often considered as a constant 1 (Helman et al. 2005). The fractionation factor for respiration ($\boldsymbol{a_R}$) ranges from 0.970 to 1. Gas exchange process includes two fractionation factors, kinetic ($\boldsymbol{a_{G\text{-}k}}$) and equilibrium ($\boldsymbol{a_{G\text{-}eq}}$). They are 0.9972 and 1.0007, respectively.

By integrating delta ^{18}O values and isotopic fractionation factors into the convention oxygen budget equation, we will have another differential equation to describe dynamic of $^{18}O^{16}O$ in DO (Venkiteswaran et al. 2007, Tobias et al. 2009). Some of the uncertainties of P and R determinations may be resolved by measuring the isotopic composition of dissolved O_2 ($\delta^{18}O$-DO). Relevant assumptions and models appeared for various aquatic ecosystems (Quay et al. 1995, Russ et al. 2004, Parker et al. 2005, Tobias et al. 2007). Meanwhile, Venkiteswaran (2007) developed a dynamic O_2 stable isotope model, PoRGy (photosynthesis - respiration - gas exchange) for non-steady state assumptions in river ecosystems. Based on this model, the $\delta^{18}O$ approach can be easily applied to estimate oxygen dynamics and metabolic balance in river ecosystems, even avoiding the measurement of gas exchange by modeling rather than complex field experimentation (Venkiteswaran et al. 2007).

Holtgrieve et al. (2010) presented a Bayesian statistical model, BaMM, describing diel oxygen dynamics in aquatic ecosystems. This model can use both oxygen

budgets (DO and δ^{18}O-DO) and is suited to low-gas exchange, high-productivity systems. One advantage of this model is that it is capable of uncertainty analysis while generating estimates of metabolic rates and oxygen exchange with the atmosphere through Bayesian statistical methods (Holtgrieve et al. 2010).

The traditional whole-ecosystem metabolism methods, based on DO only, serve a variety of research purposes (Marzolf et al. 1994). In general, high-resolution DO diel data can provide enough information to estimate metabolic parameters (Marzolf et al. 1994, Loperfido et al. 2009, Holtgrieve et al. 2010). However, Holtgrieve et al. (2010) indicated that it was better to use both DO and δ^{18}O-DO budgets, rather than DO only, in sampling protocols with low temporal frequency but high spatial frequency. The δ^{18}O-DO time series data can provide relatively independent constraints on parameter estimation. As for how low a frequency is acceptable, this needs further study. Although the δ^{18}O-DO trend is substantially determined by the DO trend, one property of δ^{18}O-DO diel data suggests that it is irreplaceable. This property is that the dynamic equilibria of DO and its isotopic composition are not necessarily synchronous. Two isotope fractionation processes for gas exchange, kinetic and equilibrium, co-determine the establishment of oxygen isotopic equilibrium between atmospheric O_2 and water DO. When DO is at 100% saturation, ^{18}O isotope exchange still occurs, so δ^{18}O-DO provides unique information. Jamieson (2010) stressed the application of δ^{18}O-DO data in the estimation of night-time $\boldsymbol{k}$ and ER and suggested that the inclusion of isotope data was not necessary in the daytime; the DO diel curve alone was enough to provide reasonable estimates of the gas exchange coefficient. As well, addition of δ^{18}O-DO provides us an estimate of $\boldsymbol{a_R}$ at the ecosystem level.

2.4 Current knowledge of river ecosystem metabolism

Essential measures of stream ecosystem metabolism include gross primary production (GPP), ecosystem respiration (ER), and net ecosystem production (P_n). The primary goal of measuring metabolism usually is to obtain the magnitude and variability of these rates

and their ratios. Our knowledge of stream ecosystem metabolism can be categorized as follows (Figure 2.1):

1) Approaches, methods and techniques in estimating river metabolism;
2) Drivers and controlling factors;
3) Partitioning of contributors to GPP and ER;
4) Cross-system comparisons of magnitude and variability of metabolic rates;
5) Ecosystem metabolism responses to both natural and human perturbation;
6) Contribution of P and R to organic matter budgets and nutrient cycling;
7) Concepts and hypotheses related to stream ecosystem metabolism.

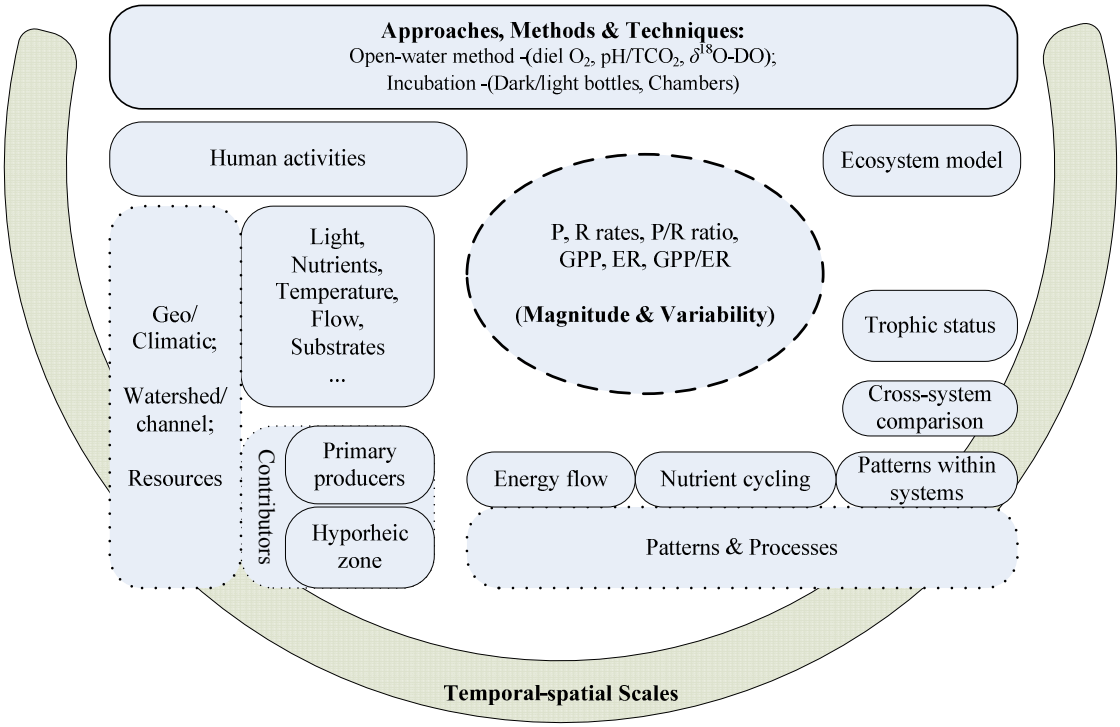

Figure 2.1 Objective-based scheme of understanding of river ecosystem metabolism

2.4.1 Drivers and controlling factors

Metabolic rates and their ratios for stream and river ecosystems are directly determined by a variety of abiotic factors, such as light (Kelly et al. 1983, Bott et al. 1985, Fleituch 1998, Mulholland et al. 2001), temperature (Bott et al. 1985, Fleituch 1998, Acuna et al. 2008, Demars et al. 2011), nutrients (Mulholland et al. 2001, Uehlinger and Brock 2005), river hydraulics (Fisher et al. 1982, Biggs et al. 1999, Uehlinger 2000, Uehlinger et al. 2003, Acuna et al. 2004, Colangelo 2007), sediment stability (Biggs et al. 1999, Parkhill and Gulliver 2002, Uehlinger et al. 2002, Atkinson et al. 2008), organic matter supply (Meyer and Edwards 1990, Whitledge and Rabeni 2000, Crenshaw et al. 2002), and water chemistry (Schafer et al. 2012).

Light

As the ultimate energy source for primary producers and the first driving variable for primary production, light is the single most important factor for photosynthetic production (Kirk 1994). Light intensity not only directly governs gross photosynthesis, it also controls primary production indirectly through influencing the distribution and abundance of aquatic primary producers (Sandjensen and Madsen 1991, Arscott et al. 2000, Julian et al. 2011). It affects the photo-adaptive state of phytoplankton, which controls the depth over which photosynthesis takes place. GPP of streams and rivers has been observed to be most strongly correlated with light intensity, i.e., PAR or photosynthetically active radiation (Mulholland et al. 2001). Most of the variation in NPP in some streams and rivers can be explained by PAR (Duncan and Brusven 1985, Mulholland et al. 2001). The log of PAR and soluble reactive phosphorus (SRP) concentration explained 90% of the variation in log GPP in diverse streams from a large geographic range (Mulholland et al. 2001). The relationship between photosynthesis and light is empirically described by the photosynthesis-irradiance (*P-I*) curve. It involves three typical responses of photosynthesis to irradiance: light-limited, light-saturated and photoinhibited (Kirk 1994).

Light can drive respiration through processes including photorespiration, the Mehler-peroxidase reaction, and photolytic O_2 consumption . Photorespiration is the light-induced uptake of O_2 in glycolate metabolism. Photorespiration has been proven to occur in all oxygen producing photosynthetic organisms (Bauwe et al. 2010). This photorespiratory pathway is linked to stress protection in high O_2 environments, or when photosynthesis by is inhibited by drought, high salt concentrations and high light intensities. It serves as an energy sink providing metabolites for other metabolic processes, e.g., glycine for the synthesis of glutathione (Wingler et al. 2000). Hysteresis is considered an indication of the presence of the photorespiration in aquatic ecosystems (Levy et al. 2004). It is difficult to distinguish the portion of O_2 consumption by photorespiration from other respiration in most experimental methods and models. However, modeling results show that 30% or more of O_2 consumed in the light may be by photorespiration, meaning that gross photosynthesis and respiration are greatly underestimated (Gerbaud and Andre 1987, Parkhill and Gulliver 1998). Another main O_2-consuming reaction in the light is the Mehler-peroxidase (MP) reaction. Photochemical consumption of dissolved organic matter (DOM) may greatly decrease O_2 concentrations in aquatic ecosystems (Amon and Benner 1996, Graneli et al. 1996, Molot and Dillon 1997, Andrews et al. 2000, Bertilsson and Tranvik 2000, Gennings et al. 2001). A few studies in streams and rivers demonstrate the important role of this process, particularly in shallow aquatic systems with high DOC (Chomicki and Schiff 2008). However, quantification of its contribution to O_2 consumption is absent.

Temperature

Temperature is an important regulator of a series of metabolic processes including growth, development, predation, etc. (Staehr and Sand-Jensen 2006, Yvon-Durocher et al. 2010, Rasmussen et al. 2011, Velazquez et al. 2011, Yvon-Durocher et al. 2011, Bouletreau et al. 2012). Temperature usually has a positive effect on both primary production and respiration, but to different degrees. Colder temperatures appear to reduce respiration more than primary production and significantly increase P/R in periphyton

metabolism (Uehlinger and Brock 2005). Naimo et al. (1988) found that temperature explained most of the variation in NDM (net daily metabolism) in two rivers, Tombigbee (68%) and Buttahatchie (75%). Respiration is considered to be temperature dependent theoretically and empirically (Brown et al. 2004, Sand-Jensen et al. 2007, Acuna et al. 2008, Perkins et al. 2012, Regaudie-de-Gioux and Duarte 2012). Benthic respiration is often closely correlated with water temperature (Rees et al. 2005).

On a daily scale, both light and temperature, are important factors governing the shape of *P-I* curves. Temperature may regulate the photosynthetic response at saturating and inhibiting irradiances, but not at low irradiance (Davison 1991). Low temperature can even shift photosynthesis of river phytoplankton from light dependence to temperature dependence by lowering I_k values (Rae and Vincent 1998). Temperature and light are subject to strong seasonal variation, especially at middle and high latitudes. When flow variability is moderate, they often account for much of the temporal variability in primary production and ecosystem respiration (ER) in streams and rivers, whether in middle and high latitudes (Servais et al. 1984, Fleituch 1998) or in low latitudes (Hunt et al. 2012). In a wet-dry tropical river in Australia, temperature explained up to 52% of temporal variation of ER (Hunt et al. 2012). In River Stradomka, Southern Poland, water temperature and incident light accounted for 56% of the variability in gross photosynthesis (Fleituch 1998).

Nutrients

Nitrogen and phosphorus may have significant influences on ecosystem metabolism by limiting the rate and extent of plant growth in streams and rivers. It has been widely observed that significant increases in plant biomass (i.e., chlorophyll *a* or biomass of algae, periphyton, macrophytes) and ecosystem metabolism (i.e., NDPP, GDPP, and ER) occur in streams and rivers with the anthropogenic addition of bioavailable nitrogen and phosphorus (Guasch et al. 1995, Mulholland et al. 2001, Uehlinger and Brock 2005, O'Hare et al. 2010, Wassenaar et al. 2010).

The GPP and ER can be boosted to different degrees in streams that receive WTTP effluents. Extra nutrients from WTTP effluents may have more effect on the ER than on the GPP, because the GPP rates could be limited by light availability due to self-shading of stimulated nuisance macrophytes patches (Gucker et al. 2006). However, extra nutrient inputs can still enhance the ER by increasing community respiration from decaying aquatic plants, heterotrophic microbial biomass, BOD and COD from sewages (e.g., the portion of geochemical oxygen consumption processes such as nitrification), etc. In some small streams, a heavy canopy can also limit the further effects of nutrients on the GPP, but not on the ER (Sanchez-Perez et al. 2009). Hence, the ratios of GPP: ER of these streams and rivers will decrease from upstream to downstream locations.

Flow

Flow is another variable that affects ecosystem metabolism in streams and rivers (Young and Huryn 1996, Biggs et al. 1999, Acuna et al. 2004, Colangelo 2007). In many streams, flow variability is high, ranging from zero to channel-modifying floods with significant variability at several time scales from distinct seasonal cycles (i.e., spring freshet, summer base flow, autumn flood and winter snowcover or low flow) to events driven by weather, e.g., summer storms (Poff and Ward 1989, Molles and Dahm 1990). Flow can severely affect ecosystem metabolism through altering the composition and biomass of primary producers by moving bed sediments and scouring autotrophic communities and heterotrophic biofilm (Fisher et al. 1982, Uehlinger and Naegeli 1998, Uehlinger 2000, Vilches and Giorgi 2010), and reducing organic matter accumulations on the stream bed (Acuna et al. 2004), depressing metabolic activities due to increased turbidity and lowered light availability (Young and Huryn 1996).

In oceanic climate regions, such as New Zealand, river discharge with high temporal variation (within and between years) is a critical factor shaping longitudinal patterns of river metabolism. Low discharge periods tend to lead to longer autotrophic river reaches because GPP is controlled by fluctuations of water depth and turbidity (Young and Huryn 1996). In the study of a 6th order river, the River Thur, Switzerland,

average reductions of GPP and ER by spates are 37-53% and 14-24%, respectively, which make the ecosystem metabolism pattern shift to heterotrophy following spates (Uehlinger and Naegeli 1998). In a large flood-prone river, spates reduce primary production by 49% and ecosystem respiration by 19% (Uehlinger 2006). The effects of floods or spates on ecosystem metabolism in streams and rivers are dependent on the degree of disturbance and the resilience of the dominant communities, and are often ecosystem specific. In a forested headwater stream with episodic storms, GPP can be depressed for several days in spring, but may increase in autumn because of enhanced light availability by removing leaves shading the streambed. ER can be depressed initially, but then stimulated to 2-3 times pre-disturbance levels for several days, which may result from the increase of the lateral transfer of allochthonous organic matter by flooding (Roberts et al. 2007). In most cases, metabolic rates may rapidly return to pre-disturbance levels, but this postspate recovery is often dependent on season (Uehlinger and Naegeli 1998, Uehlinger et al. 2003, Uehlinger 2006). Disturbance caused by frequent bed-moving spates and subsequent recovery leads to episodic but stochastic variation in primary production and respiration, which is apart from the seasonality in light and temperature (Uehlinger and Naegeli 1998, Uehlinger 2006).

Other factors

Substrata and sediment stability also play an important role in controlling stream and river metabolism (Biggs et al. 1999, Parkhill and Gulliver 2002, Uehlinger et al. 2002, Atkinson et al. 2008). Instability of substrata and sediment is often the result of high discharge or riparian soil erosion due to land use or natural events which damage or eliminate primary producers and lower light availability in water. Organic matter supply is very important for fueling bacterial respiration, especially in headwater streams which are often heterotrophic (Meyer and Edwards 1990, Whitledge and Rabeni 2000, Crenshaw et al. 2002). A recent study examined the effects of a toxic pesticide and salinity on stream metabolism (Schafer et al. 2012), although the impacts of these pollutants on GPP and ER were not fully disentangled from the role of nutrients.

2.4.2 Contributors to river metabolism

Production contributors

Photosynthetic organisms producing DO in river ecosystems include three main types: macrophytes; phytoplankton; and periphyton. However, oxygen consumers doing respiration include also the bacteria, Archaea, fungi and animals of the river community. Oxygen consumption also occurs through abiotic oxidation of reduced species, such as Fe^{2+}, NH^{4+}, S, and is also defined as part of aquatic community respiration (CR) or ecosystem respiration (ER). Studies of river metabolism often focus on the community P and R, and/or one of the contributors of photosynthesis and respiration, due to the limitations of measurement techniques as well as the cost of time and labor. However, a broader understanding of ecosystem patterns and processes requires further knowledge of roles of different contributors to metabolism. Knowing the different contributors can help us to understand how human impacts change the ecosystem.

Aquatic plants are usually distributed according to environmental factors such as light, flow, nutrients, sediment, etc. (Vannote et al. 1980, Allan and Castillo 2007). Periphyton and bryophytes are found in all parts of a river, but often predominate in headwaters where low light availability due to shading by riparian vegetation underscores the competence of these plants at low-light. Vascular macrophytes occur mainly in middle-sized rivers and along the margins of larger rivers. The open channels of middle-sized rivers are often considered as light sufficient as the river is still shallow, but wide and thus less shaded by riparian vegetation. In large lowland sections, the underwater light climate shifts back to progressive shading because of attenuation of light by phytoplankton biomass and dissolved organic materials, sediment particles, etc. Phytoplankton populations can benefit from slow flow and therefore may substantially develop in large lower rivers (Allan and Castillo 2007).

A considerable body of studies on ecosystem metabolism has concentrated on streams and rivers, where macrophytes and periphyton determine autotrophic activity (Odum 1957b, Edwards and Owens 1962, Fisher and Carpenter 1976, Minshall 1978, Kelly et al. 1983, Bott et al. 1985, Naimo et al. 1988, Bowden et al. 1992, Elosegui and

Pozo 1998, Whitledge and Rabeni 2000, Uehlinger et al. 2003, Velasco et al. 2003, Fellows et al. 2009, Vilches and Giorgi 2010). Macrophytes affect ecosystem metabolism processes and oxygen dynamics in different ways. Macrophytes are main contributors of O_2 production and diel oxygen dynamics during their growing season from late spring to late summer. In the late summer or fall, the decomposition of macrophytes can also consume large amounts of oxygen (Servais et al. 1984) and plant decay can result in high ecosystem respiration rates (Servais et al. 1984, Kaenel et al. 2000). Reaeration rates may be reduced due to modified hydraulic roughness and lowered current velocity by prolific growth of macrophytes. Roles of macrophytes vary in different aquatic ecosystems. For example, the study by Fisher (1976) in the Fort River showed that macrophytes are minor primary producers and represent a short-lived, minor detrital input. The major role of macrophytes is not only in terms of energetics, but also in terms of spatial structuring of the stream ecosystem during the biologically active summer period.

In most situations, periphyton make a greater contribution to biomass and metabolic activity than phytoplankton in stream and river energy budgets. Periphyton production in streams and rivers is generally estimated from the change in O_2 or CO_2 content of a stream segment, or by enclosing a particular stream community in a test chamber measuring ^{14}C uptake or O_2 with microelectrodes (Bott et al. 1997). In addition to light, temperature, flow, and sediment stability, enhanced nutrient input from agriculture runoff and sewage effluents are major determinants of periphyton growth. Uehlinger (2005) found that periphyton respond to nutrient enrichment from a point source with a significant increase in biomass and metabolism under favorable light and temperature conditions prevailing during summer in a desert river. As discussed in previous section, flow, and in particular floods, have a critical influence on periphyton contributing to ecosystem metabolism.

There are few estimates of GPP and ER in lowland large rivers where phytoplankton dominate the autotrophic part of the community (Wissmar et al. 1981, Oliver and Merrick 2006). In general, with increasing nutrient concentration, phytoplankton contribution to primary production will increase more than macrophytes,

and so that phytoplankton makes a major contribution to GPP in eutrophic rivers (Oliver and Merrick 2006).

Respiration contributors

Compared to photosynthesis, it is more difficult to disentangle components of respiration. Ecosystem respiration not only involves autotrophic organisms, but also heterotrophic organisms and even surrounding environments, such as the hyporheic zone. Furthermore, some processes, such as photorespiration and the Mehler-peroxidase reaction in photoautotrophs, cannot be detected easily using conventional incubation methods or whole-system methods. Routine incubation methods are capable of quantifying respiration of community components, but not all components, and so results cannot be summed to ER. Whole-stream methods can obtain an integrated ER, but may only partly include hyporheic sediments.

Mounting evidence provides strong support for inclusion of the hyporheic zone (HZ) in metabolic measurements (Grimm and Fisher 1984, Pusch and Schwoerbel 1994, Jones et al. 1995, Pusch 1996, Mulholland et al. 1997, Naegeli and Uehlinger 1997, McCutchan et al. 1998, Uzarski et al. 2001, McCutchan et al. 2002, Uzarski et al. 2004, Hall and Tank 2005). Grimm and Fisher (1984) were one of the first to suggest that the HZ may be an important and overlooked component in estimates of lotic metabolism. The HZ can contribute more than 70% of whole system respiration (Fuss and Smock 1996, Naegeli and Uehlinger 1997). The hyporheic zone contributes a substantial proportion of whole-stream R in montane streams, even high up to 93% (Fellows et al. 2001). Similar results have been reported by Naegeli (1997) that 76-96% of ecosystem respiration is provided by the HZ in a pre-alpine gravel-bed river. These findings overturn our traditional view of trophic balance of streams and rivers, and suggest that systems traditionally considered autotrophic may, in fact, be heterotrophic if the ecosystem is defined as including the HZ (Mulholland et al. 1999, Uzarski et al. 2001, Uzarski et al. 2004).

The significance of hyporheic zone to ecosystem metabolism depends on the types and rates of metabolic processes occurring in the HZ, the proportion of discharge travelling through the HZ, and its hydrologic residence time in the HZ (Fellows et al. 2001). Suitable measurement technique has been a challenge in the study of HZ metabolism in lotic ecosystems. Uzarski (2001, 2004) designed a flow-through system to address limitations of the microcosm approach to estimating lotic metabolism. This chamber integrates two important facets typical of an open system: (1) improved approximation of ambient surface and interstitial water conditions; (2) at least partial inclusion of HZ respiration.

2.4.3 Temporal-spatial patterns

River ecosystem metabolism exhibits clear temporal-spatial patterns as a result of corresponding patterns of drivers, controlling factors and sometimes external perturbations. The main temporal-spatial patterns studied are day to day, seasonal, annual, episodic (storm-related) and longitudinal. Daily rates and ratios are provided in most metabolism studies.

Light and temperature are more likely to determine diel cycles on most days, while episodic high discharge events can determine ecosystem metabolism on other days. Seasonal patterns of ecosystem metabolism in streams and rivers are shaped by the seasonal dynamics of biological communities both in the water body and in the riparian zone and hyporheic zones, and as a result of natural seasonal rhythms of abiotic factors such as light, temperature and flow. For example, the GPP of headwater streams in middle and high latitude regions often exhibits a discernible seasonal pattern that follows the phenology of aquatic plants and riparian vegetation. Leaf phenology and productivity of the deciduous riparian forest largely determines light availability, and therefore controls the primary production (Roberts et al. 2007). Seasonal variation of ER is not likely to be the same as that of GPP because it is less controlled by light. The degradation of allochthonous organic matter can continue in winter even without significant GPP (Servais et al. 1984). In the summer, ER variations are likely to be parallel to those of

GPP because a large portion of respiration will be of recent primary production. A peak of respiration is often observed in autumn in some streams and rivers under the condition of low discharge (Servais et al. 1984). Decaying primary producers are no longer contributors to GPP, whereas they still contribute to ER. Leaf fall also provides extra organic matter fueling respiration.

The seasonal trajectory of ecosystem metabolism is often interrupted by episodic storm events (i.e., bed-moving spates), which modify ecosystem metabolism. The modification of river ecosystem metabolism depends on the frequency and severity of the hydrological events, and is often ecosystem specific (Uehlinger and Naegeli 1998, Uehlinger 2000, 2006). Some rivers are totally subject to hydrological control, for example rivers in marine climate regions (Young and Huryn 1996). A few studies using continuous multiple-year monitoring data to extract metabolism are able to demonstrate the role of climate factors on the inter-annual pattern of river ecosystem metabolism (Wilcock et al. 1998, Uehlinger 2006).

Spatial heterogeneity in light, nutrients and watershed/channel parameters co-determine the spatial pattern of metabolism of a river ecosystem. For example, GPP often exhibits longitudinal patterns according to spatial variability of controlling factors and the physical environment. The general longitudinal pattern of river ecosystem metabolism described by the River Continuum Concept (Vannote et al. 1980) provides a basic model of how metabolism changes as water travels from headwater streams to larger rivers. It predicts a change from P<R in the headwaters, to P>R in the middle reaches, then a return to P<R in the lower reaches owing to influences both within and outside of the river, such as shifts in primary producer communities (i.e., moss, macrophytes), nutrients, physical factors such as flow and light availability, and temperature. This general pattern predicted by the RCC has been tested in streams around the world and, for the most part, its principles have been supported.

A study by Mctammany (2003) on the longitudinal patterns of ecosystem metabolism in Little Tennessee River (LTR), North Carolina, showed that the LTR changes from heterotrophic to autotrophic along this stretch of river and that

autochthonous C sources become more important for respiration and secondary production at downstream sites. Young (1996) proposed a conceptual model explaining how hydrological variability may control longitudinal patterns of river metabolism. Patterns of gross primary production are controlled by fluctuations in water depth and turbidity that determine light availability. In regions with oceanic climates, river discharge varies widely within and between years. In such regions, autotrophic river reaches should extend downstream during low-discharge periods, and retreat during high discharge periods.

2.4.4 Coupling of nutrient cycling

Oxygen cycling is tightly coupled with nutrient cycling through metabolic processes. Uptake of inorganic nutrients is positively associated with carbon fixation via stoichiometry, which provides us a way to link nutrient demands and metabolic rates. Higher rates of gross primary production and respiration are associated with greater uptake of inorganic nitrogen (Hall and Tank 2003, Meyer et al. 2005, Fellows et al. 2006b). Streams that have high primary production exhibit high NO_3^- uptake rates (Hall and Tank 2003). Respiration has relatively weak relationship with dissolved nitrogen uptake rates (Fellows et al. 2006b). At the ecosystem level, dissimilative nitrogen utilization (i.e., nitrification and denitrification) is also an important pathway that leads to inorganic nitrogen: phosphorus uptake ratios different from Redfield ratios (Potter et al. 2010).

Ecosystem metabolism and the availability of associated metabolic substrates (e.g., nutrients, DO, autochthonous and allochthonous sources of organic matter) mainly co-determine the temporal and spatial variability in nutrient uptake in a river ecosystem, but the details are still largely unknown (Hall and Tank 2003, Fellows et al. 2006b, Gucker and Pusch 2006, Mulholland et al. 2006, Hoellein et al. 2009). Dissolved inorganic nitrogen (e.g., NO_3^+) usually shows higher uptake during the day than at night because of photoautotrophic nitrogen demand during photosynthesis (Fellows et al. 2006b). Nutrient retention, storage, and exports in a river network exhibit different

patterns in headwater streams and large rivers (Alexander et al. 2000, Hall 2003, Hall and Tank 2003, Fellows et al. 2006b, Dodds et al. 2008). Watershed/channel parameters play roles in nutrient cycling as well as in ecosystem metabolism. Headwater streams and small rivers can retain substantial nitrogen (Alexander et al. 2000, Darracq and Destouni 2005). Benthic metabolism often dominates nutrient uptake processes in small headwater streams; however, macrophytes may dominate in middle reaches of a river, and plankton in large lowland rivers. In an 8th order Kansas River, heterotrophic processes mainly determined the rates of nitrogen cycling (Dodds et al. 2008).

Recent studies on eutrophic rivers show that nutrient uptake rates are usually high, but nutrient uptake capacities may be overwhelmed by high nutrient loads (Gucker and Pusch 2006, Ruggiero et al. 2006). Low DO due to high nutrient loads can limit N_2O production because there is a strong negative correlation between N_2O concentration and daily minimum DO concentration (Rosamond et al. 2011).

2.4.5 Metabolic responses to human activities

Responses of ecosystems to a variety of disturbances have been core studies in ecology. This is also the case in studies of lotic ecosystem metabolism in response to natural or anthropogenic disturbance (Young and Huryn 1996, Uehlinger et al. 2003, Acuna et al. 2004, Houser et al. 2005, Mulholland et al. 2005, Uehlinger and Brock 2005, Bernot et al. 2010, Stanley et al. 2010, Burford et al. 2011, Demars et al. 2011). Responses of river ecosystem metabolism to disturbance depend on the characteristics of disturbance such as type, intensity, frequency and temporal-spatial scale. In general, river ecosystem metabolic dynamics integrate episodic perturbation such as spring floods and summer storms. It is believed that river ecosystems are able to adjust to this kind of natural disturbance. Natural disturbances are often viewed as part of natural ecosystem dynamics. However, human activities can alter environmental parameters beyond the natural range, and produce changes in the ecosystem (Burford et al. 2011).

Anthropogenic disturbances influencing river ecosystem metabolism often occur at the watershed/channel level, including land use (Houser et al. 2005, Mulholland et al. 2005, Bott et al. 2006a, McTammany et al. 2007, Von Schiller et al. 2008, Gucker et al. 2009, Bernot et al. 2010), external nutrient loading from WTTPs (Hornberger et al. 1977, Gucker et al. 2006, Ruggiero et al. 2006, Sanchez-Perez et al. 2009, Wassenaar et al. 2010), flow/discharge control, i.e., channelization, dams and irrigation, etc., (Young and Huryn 1996, Young and Huryn 1999, Uehlinger et al. 2003, Vink et al. 2005, Colangelo 2007, Burford et al. 2011, Griffiths et al. 2012), channel restoration (Colangelo 2007, Atkinson et al. 2008) and aquatic plant management (Kaenel et al. 2000).

Land use change usually occurs at watershed scales and results in a cascade of alteration in physical, chemical and biological parameters in river networks, leading to nonlinear influences on stream structure and function (Von Schiller et al. 2008). In general, whole-stream GPP and ER would be enhanced in agricultural and urbanized streams due to increased light, nutrients, and temperature because of loss of riparian cover, nutrient loading from non-point and point sources, and associated changing of biotic assemblages (Von Schiller et al. 2008, Gucker et al. 2009). Changes in biomass and species of aquatic plants follow, and are strongly related to disturbance characteristics (i.e., degree, history of agricultural development). However, land use impacts may be confounded by channel structure and riparian vegetation (Bott et al. 2006a). Whole-stream GPP and ER in a Mediterranean catchment were observed to be positively correlated and increased with algal biomass along an agricultural development gradient (Von Schiller et al. 2008). In-stream primary producers shifted from palatable unicellular algae to prolific filamentous green algae and macrophytes in forest streams supposed to be heterotrophic, resulting in a substantial increase in activity of phototrophs (GPP exceeded ER) but a decrease in their quality as forage for grazers (Bunn et al. 1999). However, with restoration efforts in disturbed watersheds, such as reforestation, river ecosystems show a certain recovery capability and improvement can occur. Shade-tolerant algal communities dominate again and shading due to recovery of riparian trees can limit stream GPP (McTammany et al. 2007).

Anthropogenic alterations in channel morphology and structure are common. Straightened channels lead to less variability in channel morphology and are associated with smaller channel cross-sectional areas and riparian zones, smaller transient storage zones and higher current velocities. Consequent soil erosion will further result in increased sedimentation and turbidity in streams (Gucker et al. 2009). Increased flow and sedimentation override the role of light and nutrients, and become major factors determining the rates and locations of ecosystem metabolism. In general, they depress stream GPP (Mulholland et al. 2005, Atkinson et al. 2008). Stream metabolism responds to natural flow variations relatively quickly and often can return to previous levels in a short time (Uehlinger et al. 2003). In the Kissimmee River, a tropical, low gradient, black-water River in central Florida, USA, river ecosystem metabolism parameters changed to be similar to other reference systems in the southeast U.S.A. after river flow was artificially restored (Colangelo 2007).

Increased metabolic rates and nuisance macrophyte growth are often observed in channels receiving effluents from agriculture, industry and urban WTTPs (Gucker et al. 2006, Wassenaar et al. 2010). However, in some nutrient-enriched rivers, ER increases more than GPP due to increased chemical oxidation processes such as nitrification. Effluents from WTTPs include not only inorganic and organic nutrients, but also toxic contaminants such as heavy metals, pesticides, herbicides, microbes, etc. (Crossey and Lapoint 1988, Baldwin and Fraser 2009). Growth of aquatic plants could be depressed by these toxic contaminants, leading to “dead zones” in rivers. Relevant studies on the effects of toxic pollutants on ecosystem metabolism have not been widely carried on in rivers. Only one recent study has examined the effects of a pesticide and salinity on stream metabolism (Schafer et al. 2012). Less information is known about the long term impacts of these toxic pollutants accumulated in sediments.

Overall, human activities have complex influences on river ecosystems. Being an integrated measure of function, river ecosystem metabolism has proven to be a good indicator for river health under a variety of human disturbance (Lorenz et al. 1997, Bunn et al. 1999, Meyer et al. 2005, Young 2006, Young et al. 2008, Clapcott et al. 2012).

– Chapter 3 –

Study area and methods

3.1 The Grand River Watershed and Grand River Network

3.1.1 Nature of the GRW

The Grand River Watershed (GRW) is the largest watershed in southern Ontario, Canada, with a drainage area of 6965 km^2, and an altitude differential of about 360 m, dropping from 535 m ASL (above sea level) the north to 175 m ASL in the south near Lake Erie (Figure 3.1).

Climate

The GRW belongs to humid continental climate zone primarily affected by the warm, humid tropical air masses from the Gulf of Mexico which provide around 75% of the precipitation in the watershed (USGS 2006). The climate of the GRW is also regionally moderated by the nearby Great Lakes which can generate lake-effect local precipitation. The climate in the GRW is highly variable and can be next divided into four sub-climate zones based on the average frost-free period (GRCA, 2012). There are distinct seasons in the GRW. January and February are the coldest and driest months of the year. In contrast, July and August are the warmest and wettest months of the year. The average annual temperature is 6.5℃, but varying from 6 ℃ in the headwaters to 9℃ at Lake Erie (Mayer and Delos 1996). The annual average precipitation is 750-1000 mm and includes precipitation falling as snow. Rainfall accounts for 80% of the precipitations (Stadnyk-Falcone 2008). The snowmelt often results in spring freshets in April.

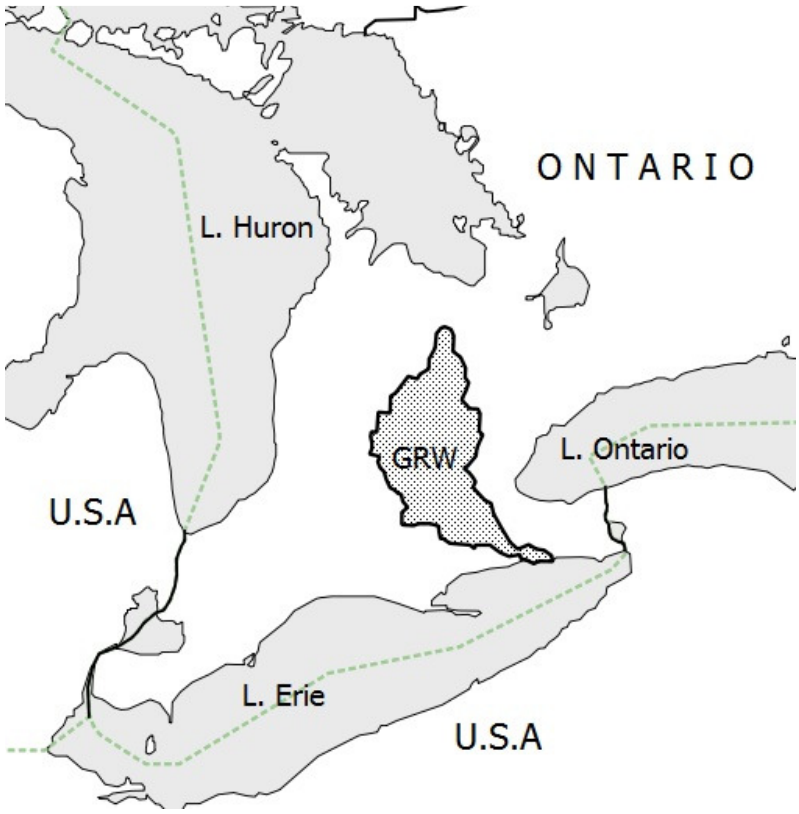

Figure 3.1 Geographic position of the Grand River Watershed.

Soil and topography

The GRW has a wide variety of soils and topography due to its glacial history, especially the last glacial retreat (ca. 12,000 B.P.). The central area of the GRW has moderately high relief and is characterized by many aquifers because of high permeability sand and gravel kame moraines that facilitate groundwater recharge. Both northern and southern regions of the GRW are low permeability areas. The northern portion is marked by undulating ground moraine, and consists of till plains with varying surface relief. This poorly drained surficial geology has many natural wetlands. The south portion is comprised of glacial lacustrine clay plains with low topographic relief, e.g., old raised glacial shorelines and lake bottoms (Holysh et al. 2000, Nelson et al. 2003).

Natural habitats

The relatively large area with varied topography supports a diversity of plants and animals in the GRW. The whole watershed falls within the mixed-wood plain ecozone, and involves two forest zones, Alleghenian forest in the north and Carolinian forest in the south. The dividing line approximately crosses southern Guelph, central Cambridge and northern Paris (GRCA 2012b). The watershed is also occupied by large wetlands such as Luther Marsh at the headwaters and Dunville Marsh near the mouth of the Grand. Luther Marsh is an artificial wetland created by the construction of a dam on Black Creek in 1952. It is called "the largest and most valuable inland marsh in Southern Ontario" with an area of 4000 hectares (GRCA 2012a). Alleghenian forest can be found in the area of Luther Marsh, with sub-boreal plant species such as black spruce, pitcher plant, royal fern and sphagnum moss (GRCA 2004). The most southern Dunville Marsh preserves undisturbed river shoreline Carolinian forests including various species of ash, oak, hickory, butternut, chestnut, birch, walnut, tulip and mulberry trees (GRCA 2004). Besides these notable natural habitats, a variety of fragmented forest patches, coniferous plantations, upland hardwood and small swamps are dotted throughout the watershed.

A growing highly-developed watershed

The GRW is mostly agricultural and urban, providing a home to 925,000 people. The total basin is 76% agricultural land, 17% scattered wooded areas, and 5% urban region. Agricultural land is mainly in the upper and lower portions of the basin with areas of intensive livestock farming, tobacco production, croplands and rural non-farm communities. The urbanized central portion of the watershed includes the cities of Waterloo, Kitchener, Guelph and Brantford. Over 80% of the people live in these cities and other small towns dispersed within the watershed. As part of the provincial government's "Places to Grow" plan for population growth in Southern Ontario, the GRW will further increase about 30% in population and grow to 1.2 million people in next 20 years (OMI 2006). The growing population means increasing demands on local

ecological services, including water resources. However, the damaged Grand River is already in need of restoration.

3.1.2 The GRN: the focus linking disturbance, development, management and restoration

Grand River Network

The largest river in the GRW is the Grand River. It runs approximately 300 km beginning from Dundalk in the highlands of Dufferin County, receiving numerous tributaries, and finally flowing into Lake Erie at Port Maitland. The four largest tributaries of the Grand are Speed River, Eramosa River, Conestogo River and Nith River, totalling another approximately 300 km of waterways. The 6th order Speed River and the 5th order Eramosa River drain the eastern portion of the basin. The Eramosa River enters the Speed at the city of Guelph and the Speed River joins the Grand River in Cambridge. Both the Conestogo River and the Nith River are 6th order, draining the western section of the watershed and flowing into the Grand at Conestogo and Paris, respectively.

The Grand River is also the largest Canadian tributary to eastern Lake Erie (Ongley 1976). The discharge of the Grand River to Lake Erie is highly seasonal, ranging from a minimum of 6 m^3 s^{-1} in the winter to a maximum of 1800 m^3 s^{-1} in the spring with an average annual discharge of 55 m^3 s^{-1} (WSC 2001). Water temperature in the Grand generally varies annually from 0 to 25 °C.

The Grand River Network (GRN) sums up to about 11,329 km of stream habitat, supporting the biodiversity of the watershed including some rare species (Sawyer et al. 2005). For example, as a result of significant ground water inputs, cold-water streams are commonly found in the central part of the watershed serving cold-water fishes such as brook trout.

The Grand River provides water for municipalities (e.g., approximately 70% of the total water use), agriculture (e.g., for livestock and irrigation), industry, recreation

and other uses (Disch 2010). However, to date, rapid urbanisation and agricultural intensification have greatly altered the structure and function of the GRN. These changes include persistent water quality issues, shifts in aquatic plant species composition, reduction in fishes and other wildlife (Ivey 2002, Brown 2010, Brown et al. 2011). The Grand River is considered to be a eutrophic, heavily impacted river (Mayer and Delos 1996, Barlow-Busch et al. 2006). It is representative of many municipally and agriculturally impacted surface waters, with particularly with regard to sediment and nutrient concentrations. Restoring the natural ecological structure and function of the Grand River network may be the only way of facing the persistent water quality issues and stresses from the growth of population in the watershed.

Agricultural practices

Early documents showed that some original vegetation such as white pine stands had been cut and burned by native farmers in aboriginal agricultural activities in the GRW since the 1400's (Pollock-Ellwand 1997). However, original vegetation was still predominant with mature coniferous and deciduous forest, interspersed with wetlands, meadows and oak savannas, until the coming of Europeans in the late 1700s (Wood 1961, Moss and Davis 1994). Significant portions of the watershed were considered unsuitable for farming by early settlers because of they were wild and swampy. With the railroad connection to the area and rapid increase of European settlers in the watershed since the 19th century, deforestation was accelerated and original marshes and wetlands were drained to meet the demands of agriculture. Since the 1930s, about 75% - 90% original wetlands have been changed into either agricultural or urban land use (Detenbeck et al. 1999). Large areas of original forests are no longer found in the watershed. The remaining forest patches are often the riparian forests (e.g., Dumfries Forest) associated with marshes (e.g., Luther Marsh).

Up to 90% of the watershed is considered rural (Jyrkama and Sykes 2007). Land use changes led to degradation of aquatic ecosystems in the watershed. A number of headwaters disappeared and small streams shrunk following the destruction of riparian

wetlands. Increasing sediment loading further altered benthic habitats and brought associated non-point pollutants such as phosphate and bacteria (Mayer and Delos 1996). Suspended sediment and nutrients have made a significant impact on water quality in the watershed, and are the most serious contaminant issues in the watershed (Cooke 2006). After 1850, the recorded sediment deposit rate of small lakes in southern Ontario is up to 100 cm/century, compared to just 2 cm/century prior to the coming of European settlers in areas (Campbell and Campbell 1994). Moreover, the water retention capacity of the GRN has been greatly damaged resulting in annual floods in 1930s, agricultural drought, and degraded water quality. As a solution, watershed-scale management was prompted through a cooperative strategic approach among the Province, watershed municipalities, local communities, stakeholders and scientists.

The Grand River Conservation Commission (GRCC, the predecessor of GRCA) was formed in 1938, managing the GRN to provide sufficient water of good quality to municipalities and residents in the watershed. Although early work of the GRCA succeeded in flood control and water provision by means of artificial dams, such as the Shand Dam near Fergus in 1942, Luther Marsh Dam in 1954 and the Conestogo Dam in 1958, the adverse effects of the blockage of the river network emerged consequently and things have become worse over time. The approach of restoring natural habitats has drawn more attention in recent years. The “Watershed Forest Plan” is one of the important plans operated by GRCA. This plan entails restoration of woodland coverage to almost 30% of the watershed area. It is considered that 30% forest coverage in a watershed is capable of self-organizing and self-sustaining (Gilbert and Anderson 1998).

WWTPs

Wastewater effluents from urbanized areas contain nutrients (e.g., phosphorous, nitrogen), toxics, bacteria and suspended solids. They have caused impacts on the Grand River ecosystems superimposed on the impacts of agriculture. As a solution, wastewater

treatment plants (WWTPs) are often built to treat effluents before discharge. So far, there are 28 WWTPs located in the watershed, including 15 advanced tertiary treatment plants, 9 secondary treatment plants and 4 lagoons on the GRW. However, effluent loading compared to the assimilative capacity of river ecosystem is a serious concern regarding river ecosystem health and the near-future development of the watershed. For example, the effluents released from the WWTPs cannot be diluted sufficiently due to the low discharge of the Speed River downstream the city of Guelph. The Grand River may also have the same problem in summer. The WWTPs in Waterloo Region may need to be increased and updated to meet the rapidly increasing population.

The river downstream of WWTPs can be considered part of the sewage treatment and assimilation process. Hotspots of poor water quality cover stretches of the Nith and Conestogo Rivers, the Speed River downstream of the City of Guelph, and the Grand River between the confluence with the Conestogo River and Glen Morris. The poorest water quality reach is in the middle, more urbanized portion of the Grand River Watershed. Low DO levels are of particular concern in these reaches. High nutrients levels stimulate the prolific nuisance growth of aquatic plants leading to high biomass of benthic algae and macrophytes (e.g., *Cladophora glomerata*, *Stuckenia pectinata*, *Myriophyllum spicatum*) and resultant DO problems. Excessive aquatic plants produce high DO during daytime, but tissues and decomposers consume oxygen during the night. These factors result in strong daily oxygen fluctuations in these reaches (>10 mg L^{-1} during the growing season). Concentrations may fall to less than 1 mg L^{-1} at Blair in midsummer, threatening the survival of sensitive species, including fish. Also, O_2 concentration are linked to the retention and transformations of inorganic nitrogen (DIN; NO_3^-, NO_2^- and NH_3/NH_4^+) that are a significant threat to drinking water and wildlife, especially fish and amphibians. Furthermore, export of nutrients and contaminants from the Grand is an important facet of Lake Erie ecosystem health, particularly for the adjacent coastal areas and fisheries in the lower Grand/Lake Erie.

Artificial dams and reservoirs

There are 7 large multipurpose reservoirs, 25 smaller dams, and nearly 100 privately owned dams in the Grand River basin. The large reservoirs are used for managing the flow of the river for flood control and flow augmentation (Shantz et al. 2004). These dams lead to alterations in river ecosystem structure and function. The three largest three artificial reservoirs on the Grand River, Belwood Lake above Fergus, Conestogo Lake on the Conestogo River below Drayton, and Guelph Lake on the Speed River, have a total storage capacity of approximately 150 million m^3. They are lakes with increased water depth, decreased flow velocity, sediment accumulation, altered thermal regime, and altered light and oxygen profile (Spence and Hynes 1971). Physical and chemical alterations lead to corresponding changes in biota both upstream and downstream. Eutrophication of reservoirs caused by excessive nutrients presents a potential threat to the composition of the downstream benthic community (Spence and Hynes 1971). The degree of impact depends on the dam type and drawdown. One obvious impact is that cold and deoxygenated water runs out of deep-release dams (Shand dam, Conestogo dam and Guelph dam) in summer, whereas surface-release dams (Shade's mills dam, Laurel creek dam) release warm and well-oxygenated surface water. Usually, reservoirs are seasonally drawn down either slowly in the summer or quickly in the fall. denHeyer (2007) indicated that current management strategies in the Grand River (e.g., release position, reservoir drawdown) were negative influences to downstream benthic macroinvertebrate communities resulting in decreased abundance and diversity of benthic macroinvertebrate fauna. This is contrary to other studies on the Grand River (Spence and Hynes 1971) and on other rivers (Al-Lami et al. 1998, Lessard and Hayes 2003). Deep release reservoirs impact benthic macroinvertebrate abundance more than surface release reservoirs in the Grand River watershed (denHeyer 2007).

3.2 Study Sites

14 sampling sites were chosen in this study, from 2nd order streams sites on the Speed and Eramosa Rivers to 7th order sites along the main channel of the Grand in the central portion of the watershed (Figure 3.2). The location, elevation, stream size, and basic information (e.g., riparian zone, downstream of dams, WWTPs and confluences) of these sites are summarized in Table 3.1.

Table 3.1 Study sites in the Grand River Watershed.

Sites	Location	Elevation (m)	Stream order	Shaded	Notes
2F	43º44´04.44" -80º05´14.41"	385	2	mostly closed	
2NF	43º42´52.93" -80º05´18.80"	396	2	open	
3F	43º43´44.04" -80º07´38.80"	381	3	semi-closed	
3NF	43º41´59.69" -80º06´45.76"	380	3	open	
4F	43º42´20.63" -80º07´31.34"	379	4	mostly closed	
4NF	43º42´28.40" -80º16´12.10"	397	4	open	
5F	43º38´24.23" -80º16´11.36"	354	5	semi-closed	
5NF	43º39´59.86" -80º08´22.65"	370	5	open	
SPa	43º32´04.44" -80º15´04.07"		6	open	100 m downstream of a small top-draw reservoir dam
SPb	43º29´03.25" -80º16´54.03"		6	semi-closed	~2 km downstream of Guelph WWTP
WM	43º03´08" -80º28´53. 6"	323	6	open	
BP	43º28´54.7" -80º28´ 53.6"	302	7	open	~10 km downstream of Conestogo R. confluence
BL	43º23´09.8" -80º02´9.1"	274	7	open	5 km downstream of Kitchener WWTP
GM	43º16´38.02" -80º20´40.17"	265	7	open	9 km downstream of Galt WWTP, and ~16 km downstream of Speed R. confluence

Both site 2F and 2NF are located on small 2nd order streams that are tributaries of the Eramosa River. The position of site 2F is about 50 m east of Wellington Rd 124, at the intersection with Sixth Line. Site 2F is almost totally shaded by coniferous trees of over 8 m in height. Site 2NF is on Side Road 10, near Fifth Line and Wellington Rd 124. Site 2NF is quite open without trees and shrubs and the stream runs through a pasture (Figure 3.3).

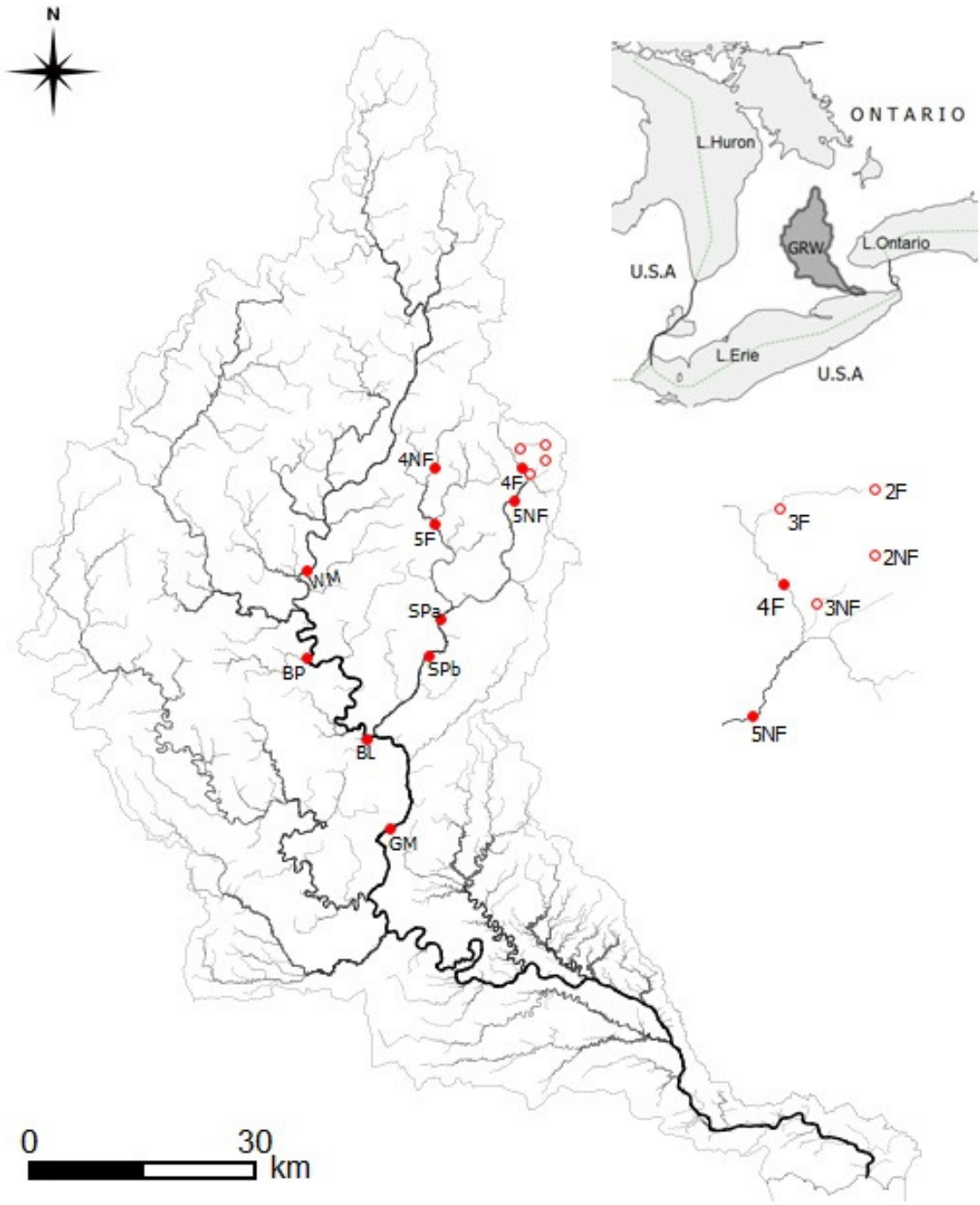

Figure 3.2 The surficial boundary of the Grand River Watershed, river network exhibited in stream orders, and study sites chosen in this study. Not all tributary streams in the watershed are shown.

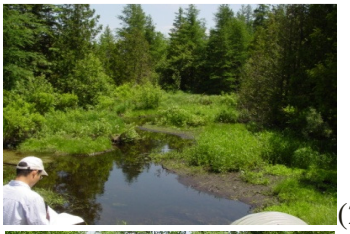
(2F)

(2NF)

(3F)

(3NF)

(4F)

(4NF)

(5F)

(5NF)

(WM)

(BP)

(BL)

(GM)

Figure 3.3 12 study sites, 2F, 2NF, 3F, 3NF, 4F, 4NF, 5F, 5NF, WM, BP, BL and GM.

Both site 3F and 3NF are located on 3rd order streams that are tributaries of the Eramosa River. The site 3F is on Fourth Line, about 2 km west of Wellington Rd 124. Site 3F has a deep and wide channel compared to site 2F, 2NF and 3NF. Site 3F is over 50% shaded by secondary broadleaf trees and shrubs. Site 3NF is on the Third Line, about 500 m east of Wellington Rd 124. It is located on a narrow stream with an average width of 2.2 m. It runs through a pasture and joins the Eramosa River nearby. Site 3NF is partly shaded by grasses and sparse shrubs (Figure 3.3).

Site 4F is located on main body of the Eramosa River with relatively mature forested riparian wetlands. The site is near the bridge crossing Wellington Rd 124 at Ospringe. It is a fourth-order stream about 6 m wide and 0.4 m in depth. The water is shaded most of day except a few hours around noon. Site 4NF has the same order and is about 4 m wide and 0.2 - 0.3 m deep, but is located within the headwaters of the Speed River. The sampling site is on Fifth Line near Side Road 30. It flows through a pasture with a few trees (Figure 3.3).

Site 5NF is about 10km downstream of site 4F, but without a forest buffer zone along the river channel, just low shrubs and wild grasses. Site 5NF is on the Eramosa-Erin Town Line (Rd 26) where the Eramosa River is 5th order. Site 5F is about 15 km downstream of site 4NF and located on the Speed River on Jones Baseline, near Side Road 20 and Mill Rd. Site 5F has a well-preserved riparian buffer zone with mature coniferous and broadleaf trees (Figure 3.3). The channel is wide and shallow, and full of gravel and pebbles.

Site SPa is artificially channelized and in a large urban area, about 100 m downstream of a top-draw reservoir and dam. Site SPb is 1.5-2 km downstream of the Guelph WWTP.

Sampling sites WM (West Montrose), BP (Bridgeport), BL (Blair) and GM (Glen Morris) are all located along the main channel of the central Grand (Figure 3.3). They are 7th order reaches except the site WM which is 6th order. Site WM is located in an agricultural landscape and is approximately 20 km upstream of the cities of Waterloo and Kitchener. The site is quite open with a hill east of the watercourse. Site BP is

downstream of site WM, and below the Canagagigue Creek and the Conestogo River tributaries. The watercourse is quite open, and receives full sunlight except in early morning and close to dusk during the open-water season. Site BL is located within the area where the Grand flows into the city of Cambridge. Site BL is upstream of the confluence of the Speed River, but 5 km and 20 km downstream of the large Kitchener WWTP and Waterloo WWTP, respectively. Site GM is about 16 km downstream of the Speed River confluence and 19 km downstream of site BL. There is a small WWTP, Galt WWTP, about 9 km upstream of site GM.

3.3 Sample collection and analysis

This section introduces the procedures of field sampling and data analysis common to more than one chapter. Specific methods will be explained in the relevant Chapter.

Diels and diurnal samplings were carried out several times at selected sites during the open water season (April to October) from 2006 to 2009. Dissolved O_2 and δ^{18}O-DO samples were collected at mid-depth near mid-channel at about 1.5-h intervals for 17~20 samplings in diel sampling or 5~7 samplings in diurnal sampling (Appendix A). At each sampling time, water temperature, pH, and salinity were recorded with a YSI sonde as well. DO samples were collected using 300-mL BOD bottles. For the δ^{18}O-DO samples, I used 160-ml serum bottles. The serum bottles were prepared by adding 0.4 g of NaN_3 as a bactericide and crimp sealed with blue butyl stoppers. These bottles were then evacuated to near vacuum (< 0.001 atm) with a rotary vacuum pump. To avoid contamination with air while collecting water samples, the stoppers were punctured underwater by an 18-gauge needle; the needle was first tapped a few times to get rid of air before piercing the septum to let water in. When no vacuum remained, the needle was removed and the bottle was taken out. Samples were stored in a cooler with ice for transfer to the laboratory. In addition, a water sample was collected into a 20 ml plastic bottle once during the diel sampling period. This sample was also kept cold and sent to lab for measuring δ^{18}O-H_2O. Irradiance reaching the water surface was directly recorded

at 5-min intervals in situ using a HOBO light meter with a LI-COR LI-190SA quantum sensor.

DO samples were analyzed by Winkler titration with a precision 0.2 mg L^{-1} (APHA 1995). δ^{18}O-DO samples were analyzed in the Stable Isotope Lab at the Earth and Environmental Science Department, University of Waterloo. Prior to analysis, samples were prepared by injecting 5 ml of helium into the bottles, simultaneously extruding about 4 to 5 ml of water, and then putting them on a shaker for at least 1.5 h to equilibrate the headspace. A gas sample was drawn from the headspace for the analysis of δ^{18}O-DO. It was measured via continuous flow IRMS using a Micromass Optima-EA spectrometer following the method of Wassenaar and Koehler (1999) with a precision of 0.5‰. The δ^{18}O-H_2O was analyzed by CO_2 equilibration method (Horita and Kendall 2004). Isotopic ratios are expressed in δ notation and referenced to VSMOW with units of per mill (‰).

At each diurnal sampling, 1L water samples were also collected 3 times (at the beginning, middle time, and the end of sampling period) using 1L plastic acid-washed bottles for phosphorus (SRP, TDP and TP) and chlorophyll *a* analysis. Samples were stored in a cooler with ice for transfer to the laboratory. Water samples were next divided into three parts in the lab: filtered samples for SRP and TDP using inline 0.2 μm polycarbonate filters; unfiltered samples for TP; and 47 mm GF/F filters for chlorophyll *a*. Filtered samples were frozen if they were not analyzed immediately. The molybdate colorimetric test was used for PO_4^+ analysis using a CARY 100 Bio UV-Visible Spectrophotometer.

3.4 Ecosystem metabolism

Sampled diel DO and δ^{18}O-DO time series were analysed using a new transient model, ROM-TM, to reconstruct the diel DO and δ^{18}O-DO time series and to calculate the daily photosynthesis, respiration and gas exchange rates. Chapter 4 introduces the development and application of ROM-TM in detail.

3.5 Data from other sources:

In addition to the data I collected, another important data source was GRCA. GRCA has established continuous O_2 data collection (e.g., at West Montrose, Bridgeport, Glen Morris, and Blair on the Grand River, 3 sites in the Speed River and at other locations within the watershed to provide as broad a range as possible of environmental conditions and metabolic rates. Discharge data at relevant sites were used. This study also was supported by the GRCA with GIS data for the Grand River watershed.

– Chapter 4 –

Inverse modeling of dissolved O_2 and δ^{18}O-DO to estimate aquatic metabolism, reaeration and respiration isotopic fractionation: effects of variable light regimes and input uncertainties

4.1 Introduction

Dissolved O_2 (DO) is vital for higher aquatic life in water (Davis 1975, Seibel 2011) and aquatic ecosystem health (Bunn et al. 1999, Brisbois et al. 2008, Young et al. 2008). Variation in DO in aquatic ecosystems is largely determined by biological processes including photosynthesis and respiration. Since the middle of the 20th century, oxygen metabolism has been one of the key measures used to gain insight into the structure and function of ecosystems (Fisher and Likens 1973, Duncan and Brusven 1985), carbon processing (Wissmar et al. 1981, Meyer and Edwards 1990, Howarth et al. 1992, Biddanda et al. 1994, Baker et al. 2000, Cole and Caraco 2001, Tank et al. 2010), nutrient cycling (Grimm and Fisher 1984, Lehman and Naumoski 1986), and food web structure (Thorp and Delong 2002, Maixandeau et al. 2005, Sobczak et al. 2005, Spivak et al. 2009). Understanding aquatic ecosystem metabolism contributes to the theoretical and conceptual foundations of ecology (Vannote et al. 1980, Ward et al. 2002), and guides the management and manipulation of stressed aquatic ecosystems (Kaenel et al. 2000, Caraco and Cole 2002, Cronin et al. 2007, Suren 2009).

Despite a long history of study (Odum 1956, Edwards and Owens 1962), our understanding of aquatic metabolism is still limited, particularly in lotic ecosystems

(Bayley 1995, Naegeli and Uehlinger 1997, Gomi et al. 2002, Del Giorgio and Williams 2005, Berman-Frank et al. 2009). The challenges mainly lie in four aspects: the complexity of river ecosystems; correct mathematical description (expression) of metabolic processes at the ecosystem level; the confounding effects of some hydraulic and physical processes on the variation of DO (e.g., ground water input with lower concentration of DO, gas exchange with atmosphere); and, more importantly, the lack of direct and efficient methods to tackle metabolic and physical processes (Bott et al. 1978, Marzolf et al. 1994, Mulholland et al. 1997, Dodds and Brock 1998, Uzarski et al. 2004, Warkentin et al. 2007).

The complexity of river ecosystems is related to high spatial heterogeneity, which limits the extrapolation of incubation approaches to the ecosystem scale (Townsend 1989, Reichert et al. 2009). Compared to ocean and lake ecosystems, river ecosystems have a relatively low ratio of water volume to benthic surface area. Gradually, recognition of river ecosystems as four-dimensional networks, with associated hyporheic zones and floodplain zones, has reformed our concept of river ecosystems. This knowledge has substantially increased our appreciation of the heterotrophic domain of river ecosystems, and led to more challenges for the measurement of metabolic balance in the field. Macrophytes and periphyton, rather than phytoplankton, tend to play a more important role in river ecosystems than in lakes and oceans. Macrophytes are thought to contribute significantly to variation in DO in the middle reaches of rivers (Rebsdorf et al. 1991, Allan and Castillo 2007), and even in some headwater streams under anthropogenic disturbance (Kaenel et al. 2000). Most submerged macrophytes root in the sediment, and macrophytes are highly heterogeneous temporally and spatially in rivers. Incubation of macrophytes in the field is much more problematic than incubation of phytoplankton in lakes and oceans. Microcosm incubation approaches, including the ^{14}C method and the O_2 light and dark bottle method in a variety of closed chambers, can provide estimates of metabolic processes. However, there are serious shortcomings of the incubation approach, for example, that measurements must be taken at the patch scale regardless of high heterogeneity at the reach scale and disturbances to incubated organisms are difficult to avoid, as are alterations to environment conditions. These lead to unreliable and

erroneous extrapolations to the reach scale (Marzolf et al. 1994, Mulholland et al. 1997). Therefore, so far, it is still difficult for us to directly obtain independent measurements of metabolic parameters at the ecosystem scale by means of field measurements.

Ecosystem-level mathematical expressions of metabolic processes still challenge ecosystem modelers. There is often a trade-off between the simplicity of models and the preciseness of metabolic estimates. Photosynthesis is driven by solar light and usually considered to be a function of photosynthetically active radiation (PAR). Light saturation is demonstrably present at the physiological level (Falkowski and Raven 2007). Whole-stream studies of the relationship between photosynthesis and irradiance demonstrate that light saturation occurs at the whole stream level but to different degrees, from no light saturation (Hornberger et al. 1976) to moderate light saturation (Duffer and Dorris 1966, Uehlinger et al. 2000), to complete light saturation (Young and Huryn 1996). However, some models still ignore light saturation for the purpose of simplicity of modeling (Venkiteswaran et al. 2007). This erroneous assumption leads to less accuracy in metabolism estimates (Holtgrieve et al. 2010).

Respiration also leads to additional challenges. Respiration at the ecosystem scale (often referred to as community respiration or ecosystem respiration) includes all O_2 consuming reactions, such as respiration by heterotrophs and autotrophs, photochemical consumption of O_2, nitrification, and all other kinds of biogeochemical oxidation. The magnitude of each pathway varies greatly within and among ecosystems. Another obstacle is photorespiration, which is driven by light in the day and occurs only in phototrophs. The extra O_2 consumption due to photorespiration has been found to be significant in several autotrophs (Jackson and Volk 1970, Gerbaud and Andre 1987, Sharkey 1988, Raghavendra et al. 1994, Xue et al. 1996, Ekelund 2000). Photorespiratory metabolism occurs in high-O_2 environments, possibly to decrease the toxic accumulation of glycolate (Bauwe et al. 2010, Maurino and Peterhansel 2010). Modeling results show that 30% more O_2 may be consumed during the daytime, which means photosynthesis and respiration rates are greatly underestimated by the usual assumption that dark and light respiration are equal (Gerbaud and Andre 1987, Parkhill

and Gulliver 1998). However, except for a few modeling studies, metabolic models tend to avoid this issue and consider ecosystem respiration to be equal to dark respiration.

Another challenge for using DO to estimate ecosystem metabolism is dealing with air-water gas exchange. The incubation approach can avoid this issue, but it cannot be used without solving the problem of scaling-up to the ecosystem level. Reaeration coefficients can be independently measured in the field using tracer compounds (Wilcock 1984, Murphy et al. 2001, Reid et al. 2007, Tobias et al. 2009), sound pressure (Morse et al. 2007) or other ways, however, sophisticated field equipments are required (Wilcock 1984, Kilpatrick 1989, Reid et al. 2007). Hence, air-water gas exchange tends to be estimated by various empirical models (Lau 1972, Rathbun 1977, Aristegi et al. 2009) and also it can be estimated from inverse modeling of ecosystem metabolism (Chapra and Ditoro 1991, Venkiteswaran et al. 2007, Holtgrieve et al. 2010).

Based on these challenges, we concluded that the whole-ecosystem approach is the only viable choice to obtain the estimates of metabolic balance at the ecosystem scale. However, it does not provide direct measurements of metabolism. Relevant metabolic parameters are abstracted from changes in DO (e.g., the DO diel curve) by fitting models with assumptions, such as: ecosystem respiration is equal to dark respiration in the nighttime regression method (Odum 1956); that photosynthesis can be adequately represented as a half-sinusoid function in the delta method (Chapra and Ditoro 1991); that best fit of oxygen data to inverse models provides correct estimates of parameters (Venkiteswaran et al. 2007, Holtgrieve et al. 2010). However, estimated parameters cannot be measured independently, except the reaeration coefficient. In addition, whole-ecosystem estimates cannot be truly replicated. Hence, it is a challenge to estimate the parameters and constrain the uncertainty of metabolism estimates.

In recent years, there is a growing interest in estimating aquatic whole-ecosystem metabolism using inverse modeling approaches (Vallino et al. 2005, Tobias et al. 2007, Van de Bogert et al. 2007, Venkiteswaran et al. 2007, Atkinson et al. 2008, Hanson et al. 2008, Holtgrieve et al. 2010). Some models can provide estimates not only of metabolic parameters, but also the gas exchange coefficient (Venkiteswaran et al. 2007, Holtgrieve

et al. 2010). This provides a practical way of avoiding the high costs and logistical problems of using field experimentation for extracting reaeration rates. The only concern is that inverse modeling approaches may result in a higher uncertainty for estimates of metabolic parameters. Minimizing uncertainty on parameter estimates (i.e., model parameters, GPP, ER, and *k*) is the priority of this kind of model. Possible solutions include uncertainty analysis to constrain the errors on parameter estimates and the addition of new variables that can be measured independently, such as isotopic composition of DO (δ^{18}O-DO diel curve).

Isotopic analysis of O_2 is not as time-consuming as it was due to the advent of continuous-flow isotope-ratio mass spectrometry (CF-IRMS), which has reduced the large sample requirements of conventional dual-inlet analysis by orders of magnitude with only a slight loss in precision over dual-inlet analysis (Wassenaar and Koehler 1999). Moreover, basic knowledge about oxygen isotopes has gradually accumulated and enriched our understanding of aquatic ecosystems. There is a growing trend for researchers to apply oxygen isotopes (mainly δ^{18}O) in metabolic balance research in a variety of aquatic ecosystems, not only in incubations but also for whole-ecosystem modeling of rivers, small lakes and the Great Lakes (Quay et al. 1995, Russ et al. 2004, Parker et al. 2005, Tobias et al. 2007, Venkiteswaran et al. 2007, Holtgrieve et al. 2010). The δ^{18}O approach provides an independent data set, a δ^{18}O-DO time series; on the other hand, it also introduces one more parameter, the respiration isotopic fractionation factor (a_R), which adds uncertainty to the estimates of conventional metabolic parameters, such as *GPP*, *R* and *G*. The dynamics of δ^{18}O-DO are tightly linked to those of the DO, but with different behaviors, so δ^{18}O can be treated as second oxygen budget to constrain the estimation of parameters. For instance, the dynamic equilibriums of DO and its isotopic composition $^{18}O^{16}O$ are not reached synchronously (Venkiteswaran et al. 2008). Currently, there are two models based on time-courses in both DO and δ^{18}O-DO. One is PoRGy (Venkiteswaran et al. 2007) and another one is BaMM (Holtgrieve et al. 2010). They were designed to estimate oxygen dynamics and metabolic balance in river ecosystems, providing unified daily estimates of metabolism parameters at the ecosystem

scale. However, they both use the same simplifying assumptions that make them less suitable for some circumstances.

PoRGy assumes no light saturation for photosynthesis, and it uses a theoretical light sub-model to calculate transient PAR as light input. This allows its application where light data are not available. However, using theoretical rather than real PAR when shading and cloud cover are present obviously limits the application of PoRGy, especially in heavily canopied headwater streams. Moreover, some issues related to light cannot be addressed in PoRGy, such as, production efficiency (a), light saturation (I_k); the effect of cloud cover on metabolic balance; and so on. The second model, BaMM, adopts a Bayesian optimization approach providing estimated parameters with probability distributions. Due to the inherent constraints of the Bayesian method, BaMM may have problems with prior information and computational costs.

To avoid these shortcomings and, more importantly, to promote the widespread application of oxygen isotope budgets in whole-ecosystem approaches, a transient model (hereafter referred to as "ROM-TM") has been developed to quantify river ecosystem metabolic rates and reaeration rates from field observations of diel dynamics in both DO and δ^{18}O-DO. The specific objectives of this paper are to: (1) present the new transient model, capable of teasing apart gas exchange and the two metabolic processes; photosynthesis and respiration; (2) test the possibility of integrating photorespiration into whole-ecosystem models using two oxygen budgets; (3) report the uncertainties of metabolism estimates resulting from two sources of error: errors in the DO time series and time series inputs with different resolution.

4.2 Materials and methods

4.2.1 Representation of O_2 and associated $\delta^{18}O$

The DO concentration is mainly controlled by three simultaneous processes: photosynthesis, respiration and reaeration with the atmospheric O_2 (Figure 4.1). Other

processes are neglected or included in these processes for the sake of simplicity in modeling.

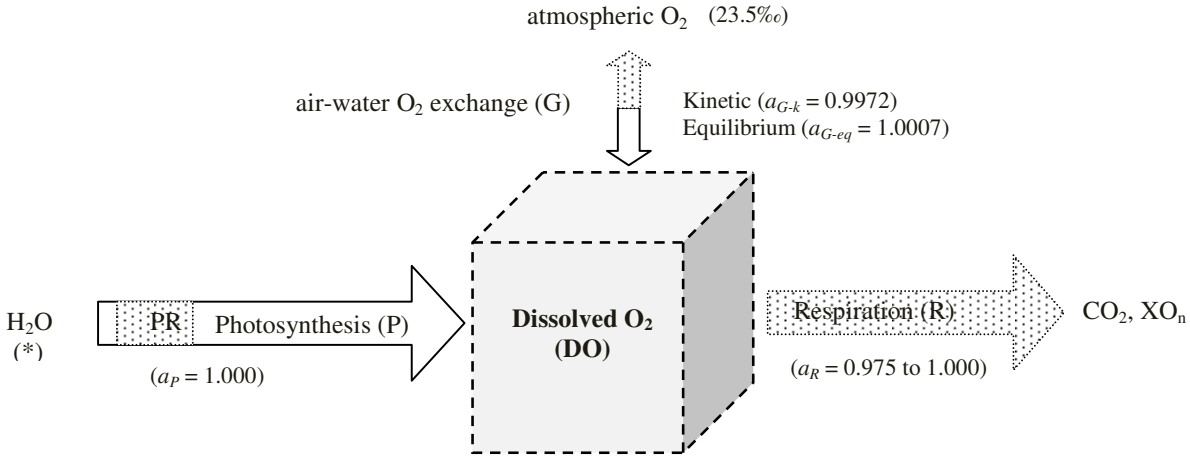

Figure 4.1 Conceptual model of ROM-TM considering three processes: photosynthesis (*P*), respiration (*R*), and gas exchange with atmospheric O_2 (*G*). Arrows represent O_2 flux. Solid arrows mean gaining and dotted arrows mean losing DO. PR stands for photorespiration. *H_2O represents the $\delta^{18}O$ value of water. Other numbers in parentheses are isotopic fractionation factors for each process. XO_n represents other oxides besides CO_2 (modified from Holtgrieve (2010)).

Following the law of mass balance, a differential equation including these three processes is commonly used to describe transient DO time series in the conventional oxygen budget (Equation 4.1):

$$\frac{dDO_t}{dt} = P - R + G(O_{2sat}, k) \tag{4.1}$$

Where, *DO* is the dissolved O_2 concentration in the units of mg L^{-1}; *P*, *R*, and *G* are instantaneous rates for photosynthesis, respiration, and gas-exchange, respectively. All of them are in the units of mg O_2 m^{-2} h^{-1}; O_{2sat} is the amount of O_2 dissolved in the water at saturation; *k* is the gas exchange coefficient in the unit of m h^{-1}.

The additional measurement of $\delta^{18}O$-DO provides us a second oxygen budget to quantify rates of biological processes and gas-exchange with atmospheric O_2

(Venkiteswaran et al. 2007, Holtgrieve et al. 2010). The molecule $^{18}O^{16}O$ is controlled by the same processes as $^{16}O^{16}O$ but must be adjusted for process-specific fractionation factors and the isotopic ratios of the given sources (Figure 4.1). Oxygen has three naturally occurring stable isotopes: ^{16}O, ^{17}O, and ^{18}O. The most abundant is ^{16}O (99.76%), next is ^{18}O with a much smaller abundance (0.2%), and the ^{17}O comprises only 0.04%. Oxygen isotope analysis via dual-inlet analysis only considers the ratio of ^{18}O to ^{16}O present in a sample, and is reported in δ per thousand notation. Isotope fractionation factors for different processes are denoted as α value ($\alpha = R_b / R_a$). R_a and R_b are the ^{18}O:^{16}O ratio of the reactant (a) and product (b) respectively. The $\delta^{18}O$-DO time series can be expressed using a similar differential equation to equation 4.1 by incorporating $\delta^{18}O$ values of source water and atmospheric O_2, and mass dependent fractionation factors for the three processes above (Equation 4.2):

$$\frac{\partial \frac{^{18}O}{^{16}O} \cdot DO_t}{\partial t} = P \bullet \alpha_p \bullet R_{H_2O} - R \bullet \alpha_R \bullet R_{sam(t)} + G(O_{2sat}, k, \alpha_{G-k}, \alpha_{G-eq}, R_{air}) \quad (4.2)$$

Where, a_P, a_R, $a_{G\text{-}k}$, $a_{G\text{-}eq}$ are isotopic fractionation factors for photosynthesis, respiration, gas-exchange kinetic, gas-exchange equilibrium; R_{sam} is the isotopic ratio of DO in water; R_{H2O} is the isotopic ratio of water; and R_{air} is the isotopic ratio of air, which is a constant 23.5‰. The a_P is a constant 1.000, which means photosynthesis does not discriminate between O isotopes (Helman et al. 2005).

4.2.2 ROM-TM model

ROM-TM is a transient model using the one-station method. An important modification is that ROM-TM allows for light effects on respiration as well as photosynthesis (Figure 4.1).

Photosynthesis – primary producers produce O_2 through photosynthesis by utilizing PAR, a fraction of solar energy (wavelengths: 400nm ~ 700 nm). The *P-I* curve describes the relationship of photosynthesis to irradiance. A complete *P-I* curve may include three typical photosynthesis-irradiance responses: light-limited, light-saturated and

photoinhibited. Light-limited photosynthesis occurs only at low intensity light where oxygen production rates are linearly proportional to light. If light increases beyond a certain level (i.e., onset of saturation), oxygen production rates still increase but with gradually decelerating rate to a saturation level, P_m. Very high light intensity can cause photoinhibition of production rates (Falkowski and Raven 2007). A number of empirical equations have been used to describe the relationship of photosynthesis to irradiance (Chalker 1980, Iwakuma and Yasuno 1983, Peterson et al. 1987), among which a hyperbolic tangent curve is often the best fit (Falkowski and Raven 2007). Whole-ecosystem studies have shown that light-saturated photosynthesis may be common at the ecosystem level (Binzer et al. 2006), therefore, photosynthesis in ROM-TM is defined as a hyperbolic tangent function of irradiance (Equation 4.3).

$$P_t = P_m \bullet \tanh[a(\frac{I_t}{P_m})] \tag{4.3}$$

There are two parameters in this equation, P_m and a. P_m is the maximum production rate (mg O_2 m^{-2} h^{-1}); a is the production efficiency (mg O_2 s (µmol photons $h)^{-1}$) and is the slope of the *P-I* curve at low light intensity (Jassby and Platt 1976). I_t represents the instantaneous PAR (µmol photons m^{-2} s^{-1}). a will be converted and reported in the unit of mol O_2 (mol photon)$^{-1}$ in the result section.

Respiration – Respiration is treated as a single temperature-weighted rate integrating all possible O_2 consuming pathways. While daily variation of respiration is affected by water temperature, light and DO concentration, respiration is usually considered constant during the diel cycle or only a function of water temperature. The conventional van't Hoff-Arrhenius equation expressed in exponential form is often used in DO modeling:

$$R_t = R_{20} \bullet 1.047^{T-20} \tag{4.4}$$

Where, R_{20} is the normalized respiration rate at 20℃; number *1.047* is an empirical constant used to correct the effect of temperature on respiration rate (Bowie et al. 1985); T represents the water temperature in Celsius.

In addition to the conventional approach, ROM-TM provides one more option; including an increase in respiration driven by light. ROM-TM adopts the equation developed by Parkhill to include a photorespiration term in the respiration sub-model (Parkhill and Gulliver 1999):

$$R_t = (R_{20} + \beta_R \bullet \bar{I}_t) \bullet 1.047^{T-20} \tag{4.5}$$

Where, β_R is the photorespiration coefficient (mg O_2 s (µmol photons h)$^{-1}$); $\bar{I}_t$ is the average photosynthetic photon flux density for the previous t hours (µmol photons m^{-2} s^{-1}). β_R will be converted and reported in the unit of mol O_2 (mol photon)$^{-1}$ in the result section.

The $^{18}O^{16}O$ equation also contains a_R and the isotopic ratio of DO in water (R_{sam} in Equation 4.2). Theoretically, a_R can be measured by means of incubations, but it requires careful experimental design. The values of a_R for a variety of respiration pathways generally fall in a narrow range from 0.975 to 1.000 (Quay et al. 1995, Brandes and Devol 1997, Buchwald and Casciotti 2010). ROM-TM treats a_R as single value.

Gas exchange – the air-water O_2 exchange is generally described using a standard flux equation (Equation 4.6). The difference between saturation O_2 and DO drives the O_2 into or out of the system.

$$G_t = k \bullet (O_{2sat} - O_2) \tag{4.6}$$

The key parameter of this process is *k*, the gas exchange coefficient (m h^{-1} in Equation 4.6). This parameter is mainly influenced by surface turbulence in rivers and wind effects in lakes. ROM-TM treats *K* as an estimated parameter and uses the modeling approach to obtain it. O_{2sat}, the amount of O_2 dissolved in the water at saturated level, is a function of water temperature, salinity and atmospheric pressure (Weiss 1970, Wilde et al. 1998). An empirical equation is used to calculate the O_2 concentration in ml L^{-1}(Equation 4.7):

$$ln(DO) = -173.4292 + 249.6339 * 100 / T + 143.3483 * ln(T / 100) - 21.8492 * T / 100 + S * [-0.033096 + 0.014259 * T / 100 + -0.001700 * (T / 100)^2] \quad (4.7)$$

Where, T is the temperature in Kelvins; S is the salinity in unit of g kg^{-1}. The calculated DO is converted from ml L^{-1} to mg L^{-1} by multiplying by (P/T)*0.5130, where P is the pressure in mmHg.

As for the ^{18}O equation, the difference between the saturated concentration and the co-instantaneous concentration forces the dissolved O_2 isotopologue $^{18}O^{16}O$ into or out of the system. This process is additionally controlled by two isotopic fractionation processes during gas exchange with atmospheric O_2: kinetic ($a_{G\text{-}k}$) and equilibrium ($a_{G\text{-}eq}$). Hence, they need to be incorporated into the flux equation (Equation 4.8). They are 0.9972 and 1.0007, respectively.

$$G_{^{18}O^{16}O} = k \bullet \alpha_{G-k} (O_{2sat} \bullet \frac{^{18}O}{^{16}O_{air}} \bullet \alpha_{G-eq} - O_2 \bullet \frac{^{18}O}{^{16}O}) \quad (4.8)$$

4.2.3 Parameters and computational implementation of ROM-TM

ROM-TM employs an inverse modeling approach to reconstruct both the DO and $\delta^{18}O$-DO time series. The first important step is to obtain reasonable estimates for each parameter. Each parameter is treated as a single value for each set of two diel curves. There are six basic parameters to be estimated in ROM-TM. They are maximum production rate (P_m), production efficiency parameter (a), respiration rate at 20℃ (R_{20}), gas exchange coefficient (k), and isotopic fractionation factor for respiration (a_R) and photorespiration coefficient (β_R) (Table 4.1).

ROM-TM is programmed using MATLAB. The *fminsearch* function of MATLAB, which adopts *Nelder-Mead* multidimensional search algorithm, is used to find the best combination of modeled parameters by minimizing the sum of square errors (*SSE*) between the field-observed points and the corresponding fitted points by means of adjusting the modeled parameters. The observed points and the fitted points for both DO and $\delta^{18}O$-DO time series are normalized to their maximum values, which ensures equal

statistical weight in the calculation of *SSE*. Initial starting points for all parameters in the fitting function can be provided by either experience or pre-fitting the DO diel curve only.

Table 4.1 Environment variables, fitted parameters, and basic outputs of ROM-TM

Environmental Variables & measured diel data	**Fitted Parameters**	**Basic Output**
Sampling date and time (d/h/m)	P_m (mg O_2 m^{-2} h^{-1})	fitted DO (mg L^{-1})
Depth (m)	α (mg O_2 s (µmol photons $h)^{-1}$)	fitted δ^{18}O-DO (‰ vs. SMOW)
Elevation (m)	R_{20} (mg O_2 m^{-2} h^{-1})	*P* rate (mg O_2 m^{-2} h^{-1})
PAR irradiance (µmol photons m^{-2} s^{-1})	α_R	*R* rate (mg O_2 m^{-2} h^{-1})
Water Temperature (℃)	k (m h^{-1})	*G* rate (mg O_2 m^{-2} h^{-1})
pH	β_R (mg O_2 s (µmol photons $h)^{-1}$)	pR rate (mg O_2 m^{-2} h^{-1})
Salinity (g kg^{-1})		GPP (g O_2 m^{-2} day^{-1})
O_2 concentration (mg L^{-1})		ER (g O_2 m^{-2} day^{-1})
δ^{18}O-DO (‰ vs. SMOW)		G (g O_2 m^{-2} day^{-1})
δ^{18}O-H_2O (‰ vs. SMOW)		I_k (µmol photons m^{-2} s^{-1})

On achieving the best combination of estimates for all parameters, ROM-TM simultaneously obtains DO and δ^{18}O-DO for each time step, and transient *P*, *R* and *G* rates. *P* is calculated using equation 4.3 with input PAR and fitted parameters P_m and *a*. *R* is calculated using equation 4.4 with input water temperature and the fitted R_{20}. *G* is calculated using equation 4.6 with input water temperature, salinity and the estimated parameter *k*. Consequently, ROM-TM provides daily average estimates for *P*, *R* and *G* rates by integrating 24 h transient rates of *P*, *R* and *G*. These daily average values are gross primary production (*GPP*), ecosystem respiration (*ER*), and total absolute flux of O_2 via gas exchange (*G*). The latter is the mean of absolute rates of O_2 invasion and evasion. The saturation onset parameter I_k (the ratio of P_m to *a*) is calculated, providing the irradiance level that saturates photosynthesis at the ecosystem level. In addition, the *P-I* curve can be plotted using the instantaneous *P* rate against the corresponding irradiance for each diel data set.

4.2.4 Model performance and uncertainty analysis

A model with good performance is more likely to be accepted and widely used. There are various quantitive performance measures providing different information about model behaviors, such as the coefficient of determination (R^2), normalized absolute mean error, confidence interval test (CIT), ratio of scatter, and others (Alewell and Manderscheid 1998). The commonly-used coefficient of determination (R^2) between field DO and δ^{18}O-DO data and model fitted data was chosen to assess the performance of ROM-TM (Equation 4.9). As for individual processes, because photosynthesis and respiration cannot be measured independantly at the ecosystem level, checks for each single sub-model cannot undertaken. In general, the model is considered to have a good performance if R^2 is greater than 0.9.

$$R^2 = 1 - \frac{\sum_{i=1}^{n}(P_i - O_i)^2}{\sum_{i=1}^{n}(O_i - \bar{O})^2} \tag{4.9}$$

Where, n is the number of sampling points; P_i is the predicted value for the ith corresponding sampling point; O_i is the observed value of the ith sampling point; $\bar{O}$ is the average value of all observed points.

Because metabolism parameters cannot be independently measured at the ecosystem level, whole-ecosystem models cannot be validated through independent data. This does not mean that these models are not capable of representing the actual processes occurring in a river ecosystem. The reliability of modeled results is greatly dependent on the analysis of errors and uncertainties from model structures, inputs, and parameters. In this paper, we analyzed the effects of error in input data on parameter estimates in two ways:

1) Resampling and re-assigning the residuals of observed DO time series;
2) Using time series with different resolution; the delete-m Jackknife technique was used to estimate the bias and variance of every parameter. The number of sampling points deleted varied from 1 to m (N-m $\geq$ 5, the number of total estimated parameters. N is the total number of sampling points for each diel).

In addition, we addressed the effects of photorespiration in the respiration sub-models.

ROM-TM is available from the authors.

4.2.5 Application of ROM-TM to field data

We applied ROM-TM to field data from two very different sites in the Grand River basin, the largest drainage basin (6965 km^2) in southern Ontario, Canada. The Grand River basin is mixed agricultural and urban land use; a good site to address impacts of anthropogenic activities on river oxygen metabolic balance. One site, 4F (43º42´20.63"N, 80º7´31.34"W) is a 4^{th} order stream about 6 m wide and 5 km in length located within the headwater system of the Eramosa River, a tributary of the Grand River. The elevation of site 4F is 379 m. It is a small narrow stream with a forested riparian zone (Figure 4.2). The water was shaded most of day except for a few hours at noon. The other site is Bridgeport (BP), a 7^{th} order reach along the main channel of the Grand River at 43º28´54.48"N, 80º28´52.60"W. Site BP is quite open and has an elevation of 302 m. Except during early morning and close to dusk, the watercourse receives full sunlight (Figure 4.2).

Figure 4.2 Site 4F (left) and site BP (right).

Diel samplings for dissolved O_2 and δ^{18}O-DO were conducted from August 09 to 10, 2006 at site BP and from July 22 to 23, 2007 at site 4F. Temperature, pH and salinity were recorded with a YSI sonde at each sampling time. During the sampling periods, irradiance reaching the water surface was also recorded at 5-min intervals in situ using a HOBO light meter with a LI-COR LI-190SA quantum sensor. Sampling procedures and lab analysis in detail refer to Chapter 3.

4.3 Results

4.3.1 Partitioning and quantifying P, R and G

Site 4F was a shallow stream with an average depth of 0.38 m. The average depth of site BP was 0.40 m. The salinity was 0.27 g/L at site 4F and 0.21 g/L at site BP. Site 4F and BP had a similar δ^{18}O-H_2O, -9.98‰ at site 4F and -9.85‰ at site BP. At site 4F, the pH varied from 8.0 to 8.5 and water temperature varied from 14.5 to 20.7 ℃ during the sampling period. At site BP, the pH varied from 8.2 to 8.9 and water temperature varied from 22.5 to 25.6 ℃ during the time of sampling.

ROM-TM successfully estimated mean metabolic parameters (Table 4.2) and reconstructed DO and δ^{18}O-DO diel curves for both sites (Figures 4.3, 4.4, 4.5 & 4.6). Four fitting scenarios were used: fitting the DO diel curve alone using the respiration sub-model without photorespiration (S1-pR); fitting the DO diel curve alone using the respiration sub-model with photorespiration (S1+pR); fitting both DO and δ^{18}O-DO diel curves using the respiration sub-model without photorespiration (S2-pR); and fitting both DO and δ^{18}O-DO diel curves using the respiration sub-model with photorespiration (S2+pR). For all cases, the coefficients of determination (R^2) for both DO and δ^{18}O-DO were greater than 0.90 (Table 4.2), indicating that ROM-TM performed well for both sites with all fitting scenarios.

Both sites appeared to be net heterotrophic at the time of sampling, which was consistent for all fitting scenarios. Site 4F exhibited a relatively small diel change in both DO and δ^{18}O-DO. The measured DO ranged from 7.76 to 9.41mg L^{-1} and the δ^{18}O-DO

ranged from 21.00 to 26.80‰. The DO was below atmospheric saturation most of time (Figure 4.5). When both DO and δ^{18}O-DO are modeled, ROM-TM yielded a *P*: *R* ratio of 0.42 and a *P*: *R*: *G* ratio of 0.72:1.72:1 at site 4F. Daily average rates of *P*, *R* and *G* are 1.42, 3.41 and 1.98 mg O_2 m^{-2} day^{-1}, respectively. In contrast, site BP showed strong diel cycles in both DO and δ^{18}O-DO, with a change of DO from 5.18 to 12.37 mg L^{-1} and δ^{18}O-DO from 11.46 to 26.61‰. ROM-TM yielded a *P*: *R* ratio of 0.88 and a *P*: *R*: *G* ratio of 2.30:2.62:1 at site BP, with daily average rates of *P*, *R* and *G* of 5.18, 5.90 and 2.25 mg O_2 m^{-2} day^{-1}, respectively. Compared to site 4F, the higher *P* rate at site BP resulted in lower δ^{18}O-DO by adding O_2 with δ^{18}O-H_2O of -9.85‰.

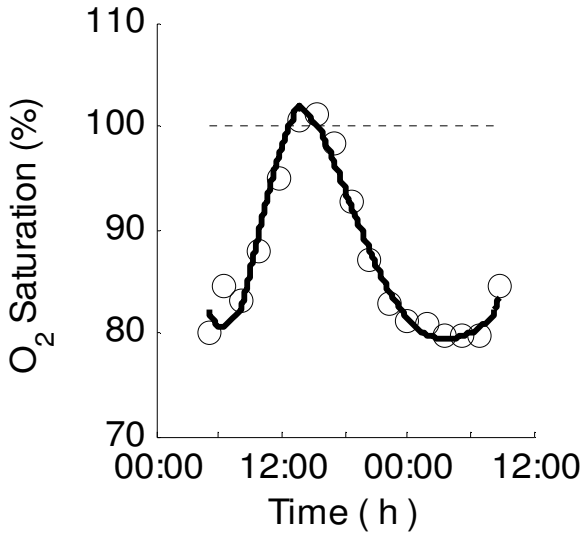

Figure 4.3 Field DO data (circles) and the reconstructed diel curve (black line) using ROM-TM from site 4F, July 22 to 23, 2007, with the fitting scenario S1-pR (fitting dissolved O_2 alone and respiration sub-model without photorespiration). The horizontal dashed line shows DO saturation.

Table 4.2 Estimated parameters and the coefficient of determination (R^2) for both sites with four fitting scenarios.

Site	Scenario	P_m (mg O_2 m^{-2} h^{-1})	a (mol O_2 (mol photon)$^{-1}$)	R_{20} (mg O_2 m^{-2} h^{-1})	K (m h^{-1})	a_R	β_R (mol O_2 (mol photon)$^{-1}$)	R^2	
								DO	$\delta^{18}O$-*DO*
4F	S1-pR	167.2	0.0017	140.6	0.18		-	0.96	
	S1+pR	167.2	0.0017	140.6	0.18		0.0000033	0.96	
	S2-pR	174.8	0.0033	159.6	0.19	0.9839	-	0.93	0.91
	S2+pR	174.8	0.0033	159.6	0.19	0.9840	0.000013	0.93	0.91
BP	S1-pR	676	0.0074	224	0.16		-	0.98	
	S1+pR	824	0.0126	204	0.081		0.0019	0.99	
	S2-pR	604	0.0070	204	0.13	0.9865	-	0.97	0.95
	S2+pR	636	0.0074	200	0.12	0.9856	0.0003	0.98	0.94

Table 4.2 Extended.

GPP (mg O_2 m^{-2} day^{-1})	***ER***(mg O_2 m^{-2} day^{-1})	G_t(mg O_2 m^{-2} day^{-1})	G_n(mg O_2 m^{-2} day^{-1})	***P:R***	***P:R:G$_t$***	I_k(µmol photons m^{-2} s^{-1})
1.09	2.99	1.88	1.85	0.37	0.58:1.59:1	830.2
1.10	2.99	1.88	1.84	0.37	0.58:1.59:1	830.2
1.42	3.41	1.98	1.92	0.42	0.72:1.72:1	460.0
1.42	3.40	1.96	1.90	0.42	0.72:1.73:1	460.0
5.62	6.43	2.94	-0.44	0.88	1.92:2.19:1	804.8
7.88	8.77	1.47	-0.24	0.90	5.37:5.98:1	572.2
5.18	5.90	2.25	-0.34	0.88	2.30:2.62:1	755.0
5.52	6.25	2.14	-0.34	0.88	2.59:2.93:1	757.1

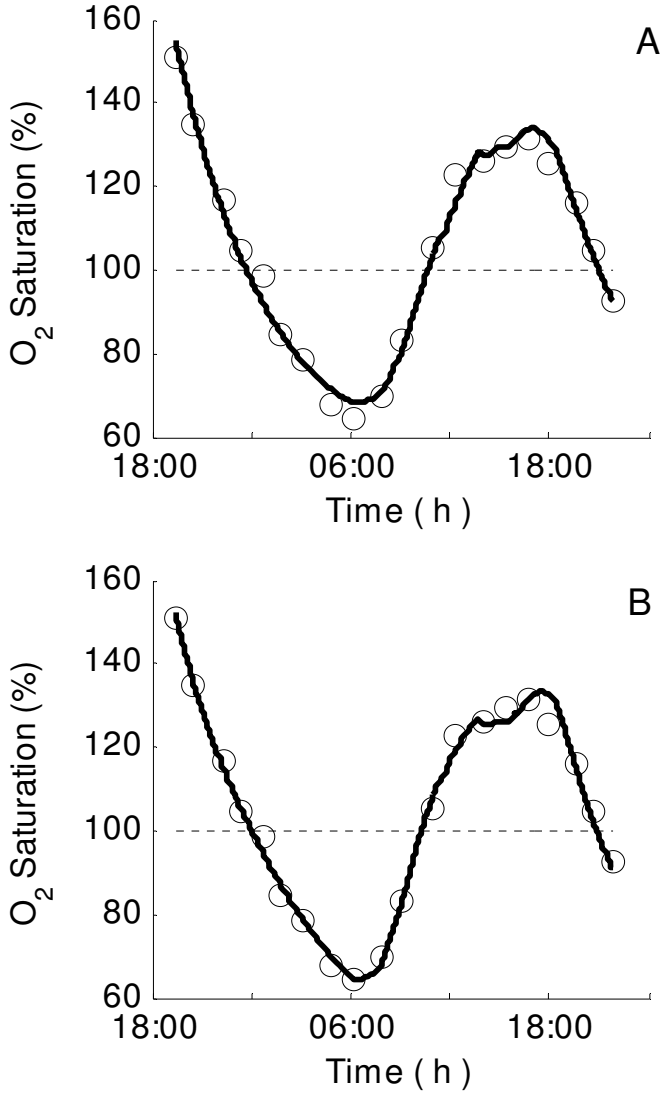

Figure 4.4 Field dissolved O_2 data (circles) and the reconstructed DO diel curve (black line) using ROM-TM from site BP, August 09 to 10, 2006. (A) with the fitting scenario S1-pR (fitting dissolved O_2 alone and respiration sub-model without photorespiration), and (B) with the fitting scenario S1+pR (fitting dissolved O_2 alone and respiration sub-model with photorespiration). The horizontal dashed line shows DO saturation.

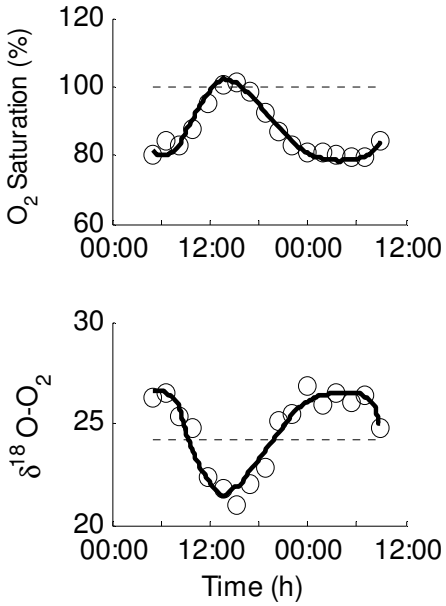

Figure 4.5 Field dissolved O_2 and δ^{18}O-DO data (circles) and the reconstructed DO and δ^{18}O-DO diel curves (black lines) using ROM-TM from site 4F, July 22 to 23, 2007. Horizontal dashed lines show the equilibrium saturation level. The respiration sub-model is without photorespiration.

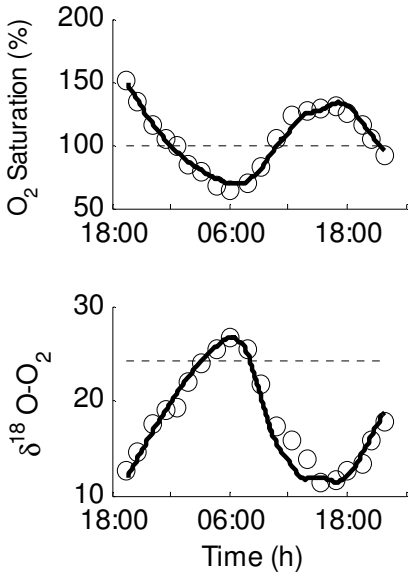

Figure 4.6 Field dissolved O_2 and δ^{18}O-DO data (circles) and the reconstructed DO and δ^{18}O-DO diel curves (black lines) using ROM-TM from site BP, August 09 to 10, 2006. Horizontal dashed lines show the equilibrium saturation level. The respiration sub-model is without photorespiration.

Besides obtaining metabolism parameters, one of the advantages of whole-ecosystem modeling using the isotope approach is that it is capable of providing estimates of a_R and k. Estimated values of a_R for the two sites were within a narrow range from 0.9839 to 0.9856. Average estimates of k varied from 1.94 to 4.56 (m day^{-1}).

4.3.2 The inclusion of photorespiration term β_R

Whether using DO only or using both DO and δ^{18}O-DO diel curves, the inclusion of photorespiration (β_R) causes little changes for site 4F. All estimated parameters and metabolism parameters are almost the same (Table 4.2), and the estimates of β_R are small. We did not see any improvement for the coefficient of determination (R^2). For site BP, the inclusion of β_R, significantly increased the P and R rates, whether fitting the DO curve only (S1+pR) or fitting both oxygen curves (S2+pR). The fitting scenario S1+pR estimated that β_R is 0.0019 mol O_2 (mol photon)$^{-1}$, and enhanced the P rate almost 40.2% (from 5.62 to 7.88 mg O_2 m^{-2} day^{-1}), and the R rate 36.4% (from 6.43 to 8.77 mg O_2 m^{-2} day^{-1}), but decreased the G rate from 2.94 to 1.47 mg O_2 m^{-2} day^{-1}. The fitting scenario S2+pR yielded β_R = 0.0003 mol O_2 (mol photon)$^{-1}$, and enhanced the P and R rates about 6%. The P rate changed from 5.18 to 5.52 mg O_2 m^{-2} day^{-1} and the R rate changed from 5.90 to 6.25 mg O_2 m^{-2} day^{-1}. The G rate was slightly decreased.

4.3.3 Light saturation occurring at the ecosystem level

An important application of ROM-TM is to address light saturation at the ecosystem level (Figure 4.7). For site 4F, we estimated P_m as 167.2 mg O_2 m^{-2} h^{-1} by fitting the DO diel curve alone and 174.8 mg O_2 m^{-2} h^{-1} by fitting both DO and δ^{18}O-DO diel curves. Correspondingly, the estimation of a varied from 0.0017 to 0.0033 mol O_2 (mol photon)$^{-1}$. We calculated a value of I_k (=P_m/a) 830.2 µmol photons m^{-2} s^{-1} fitting the DO diel curve alone, and 460 µmol photons m^{-2} s^{-1} fitting both DO and δ^{18}O-DO diel curves. For site BP with 4 fitting scenarios, S1-pR, S1+pR, S2-pR and S2+pR, the P_m was 676, 824, 604, and 636 mg O_2 m^{-2} h^{-1}, respectively, and the a was 0.0074, 0.0126, 0.0070, and 0.0074

mol O_2 (mol photon)$^{-1}$ respectively. The I_k ranged from 755-805 µmol photons m^{-2} s^{-1} except using S1+pR at site BP.

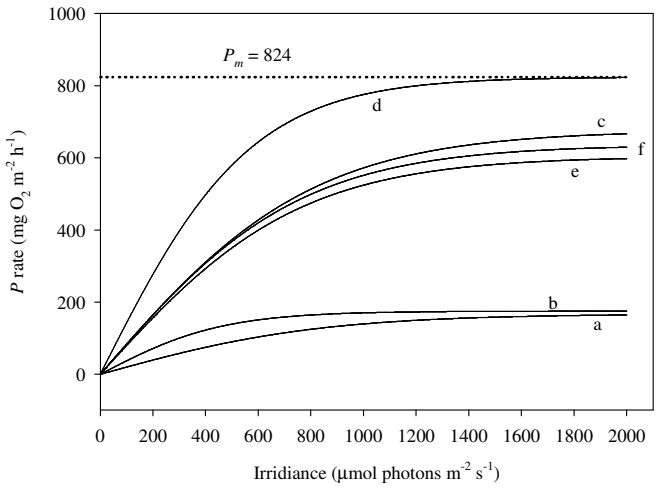

Figure 4.7 Photosynthesis-irradiance relationships for site 4F (curves a, b) and BP (curves c-f) under different fitting scenarios each. Scenarios as below: a) Site 4F, S1-pR & S1+pR; b) Site 4F, S2-pR & S2+pR; c) Site BP, S1-pR; d) Site BP, S1+pR; e) Site BP, S2-pR; and f) Site BP, S2+pR. The dotted horizontal line shows the maximum *P* rate for *P-I* curve d.

4.3.4 The effect of cloud cover

It was a partly cloudy day on August 10, 2006, at site BP. There were cloudy periods in the late morning and heavy cloud cover in the afternoon, reducing light below the saturation level (Figure 4.8). We used ROM-TM to model the effect of cloud cover on the metabolic balance (Figure 4.9). The corrected cloud-free daily rate of *P* was 5.94 g O_2 m^{-2} day^{-1}, which increased 14.7% (from 5.18 to 5.94 mg O_2 L^{-1} day^{-1}). The *P*: *R* ratio correspondingly changed from 0.88 to 1.01, so trophic status changed from heterotrophic to balanced.

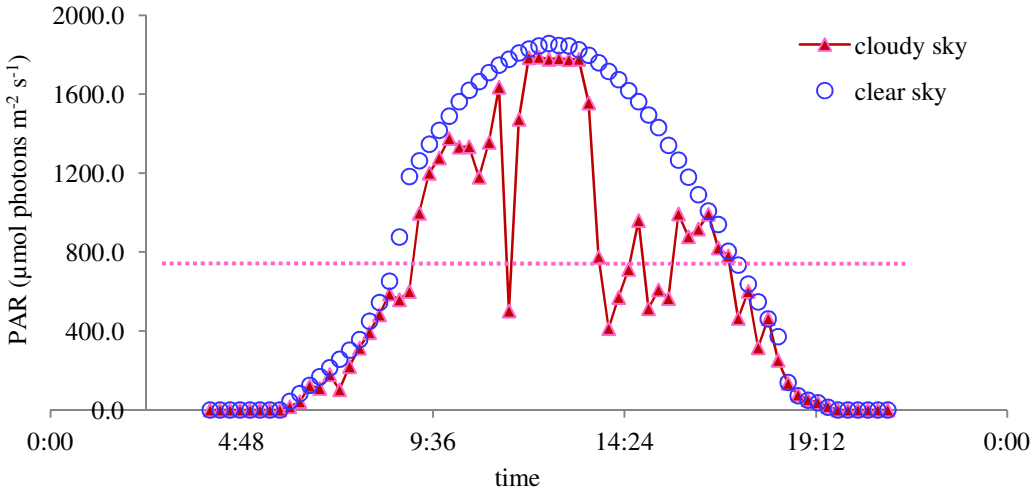

Figure 4.8 Measured light at site BP. Triangles represent the PAR during the sampling day, August 10, 2006. Circles are the PAR in the next day with a clear sky. The dotted horizontal line indicates the light level for saturated photosynthesis at that day.

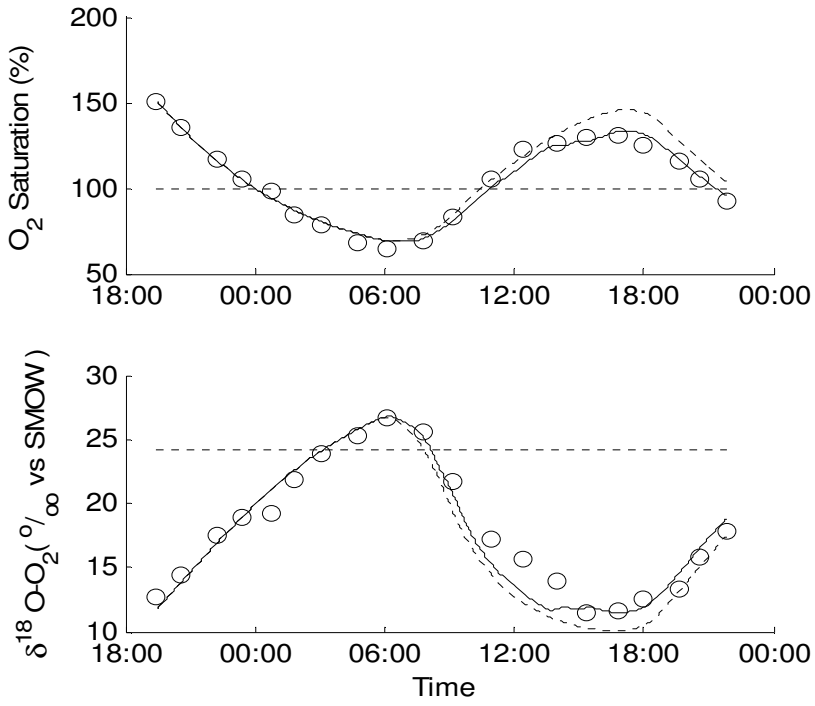

Figure 4.9 Field dissolved O_2 and δ^{18}O-DO data (circles), the reconstructed DO and δ^{18}O-DO diel curves (black solid lines), and corrected DO and δ^{18}O-DO diel curves (black dashed lines) using the theoretical lights under a clear sky. Data from the site BP with fitting scenario S2-pR. Horizontal dashed lines show the equilibrium saturation level.

4.3.5 Uncertainty analysis and error analysis

We analyzed the effect of measurement error of DO time series data on five estimated parameters, *GPP*, *ER*, and *G*, using the measured data from site BP with fitting scenario S2-pR. After running the model with the measured data, ROM-TM obtained fitted DO, δ^{18}O-DO and their residuals. The residuals of DO time series were retained and resampled randomly with bootstrapping techniques 1000 times. The model was then run repeatedly to provide 1000 combinations of estimated parameters (Figure 4.10). The parameter P_m, *GPP*, *R* and *G* were fitted using generalized extreme value distribution (GEV), other parameters using the normal distribution (Figure 4.10). The means (the highest density) of each parameter were fairly close to the values from the single run with the original data (fitting scenario: S2-pR, Table 4.2), which demonstrates ROM-TM was robust and stable for the random errors of DO time series.

We ran the data from BP with fitting scenario S2-pR and tested the combined effects of data resolution and sampling structure on all estimates. Best values for each parameter came from fitting with all 20 sampling points for both DO and δ^{18}O-DO diel cycle over a 28-h sampling period. Then sampling points were deleted so that the sampling interval increased from 1.5 h (20 samples) to 5 h (5 samples). We observed that parameters P_m and a are more sensitive than other parameters to few data (Figure 4.11). The mean of P_m had obvious bias at low sampling intensities. Other estimates had a trend of decreasing variance but no bias. When the number of sampling points was greater than 10, at data intervals of $\leq$ 3 h, all parameter and metabolism estimates appeared to have a similar behavior in that they converged symmetrically with a decreasing variance.

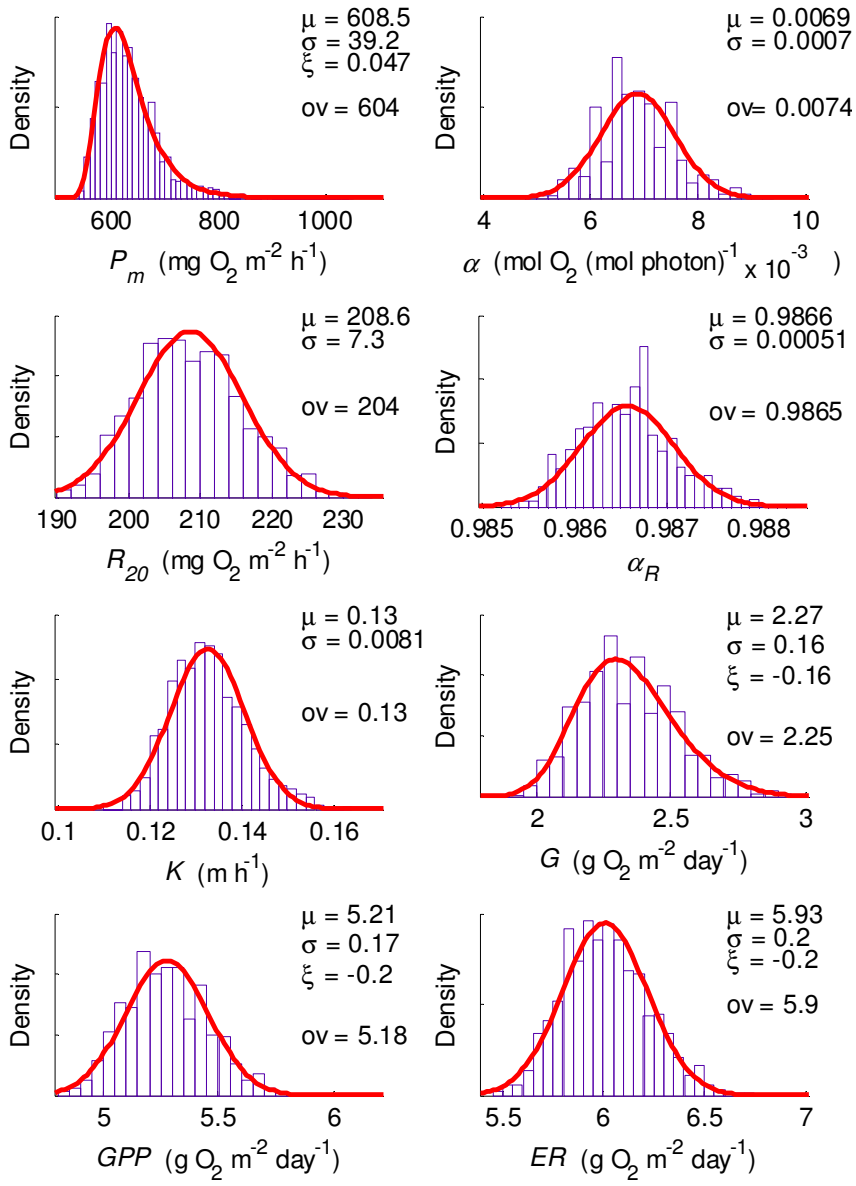

Figure 4.10 Results from 1000 re-samples using randomly assigned residuals of dissolved O_2 time series for site BP (fitting scenario: S2-pR). μ is the mean, σ is the standard deviation and ξ is the skewness. The ov represents the original fitted value with raw data. Solid lines are density distribution fitting curves.

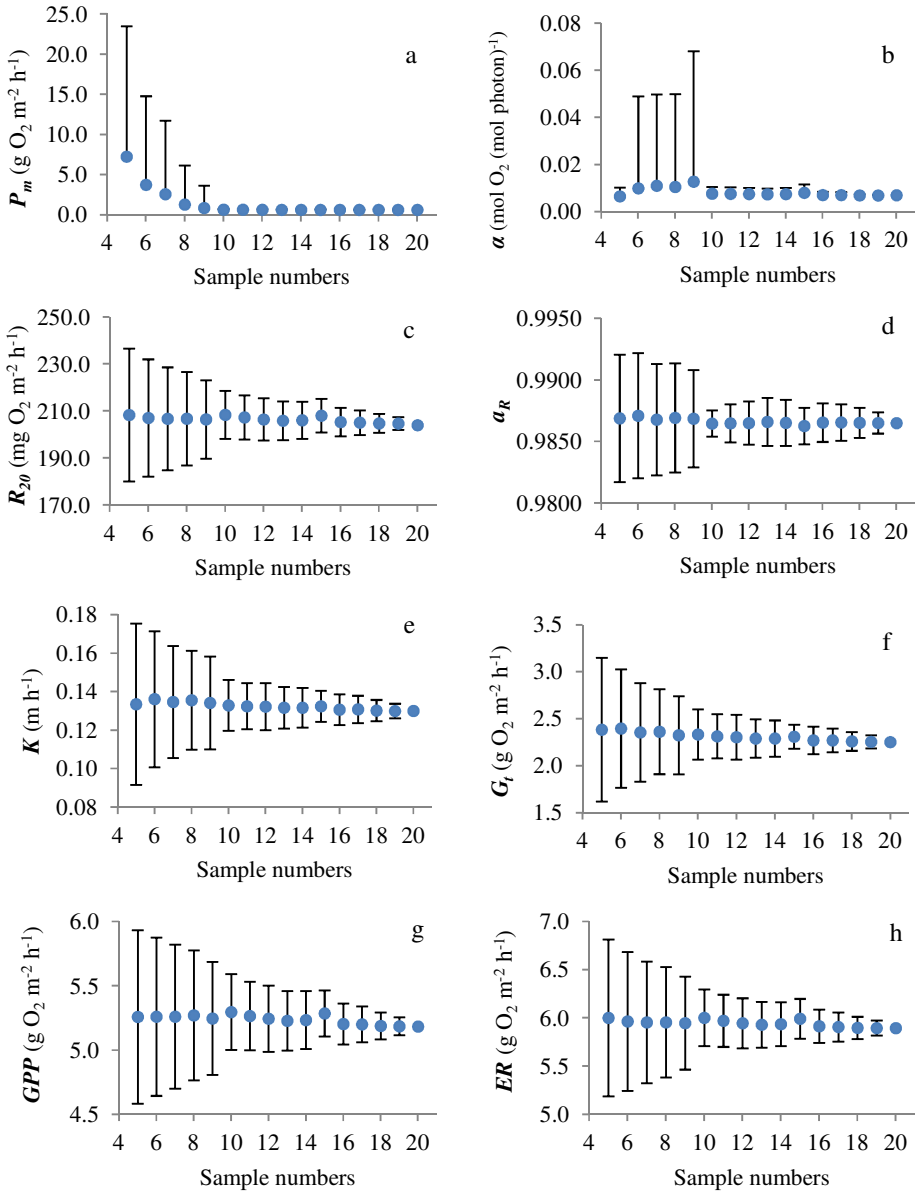

Figure 4.11 The bias and variance of five estimated parameters P_m (a), a (b), R_{20} (c), a_R (d), and $\boldsymbol{k}$ (e), G_t (f), GPP (g) and ER (h) and through jackknifing sampling density. Data from BP (fitting scenario: S2-pR). Solid circles are the mean of each estimate and error bars are standard deviation (5 to 17 sample points run 1000 times, 18 sample point run all 342 times, 19 sample point run all 20 times, 20 sample point no replicate run.).

Finding the best combination of estimated parameters by means of the *fminsearch* function of MATLAB to minimize the *SSE* should be questioned, because *fminsearch* is meant to achieve a local minimum, rather than guaranteed to find a global minimum. To test the *fminsearch* function in ROM-TM, we ran the same raw data with 6 different initial parameters (Table 4.3). These values were in the range of one-tenth to five times of the original estimated value. These initial values created 7776 five-parameter arrays in total. ROM-TM was then run 7776 times and yielded 7597 sets of estimates, excluding 179 sets of estimates having negative R^2 (Figure 4.12). All estimated parameters have more than 91% of results within the range of 95% to 105% of the original fitted value, which demonstrates that initial values have little impact on using *fminsearch* function. Initials from a wide range for each parameter lead to fairly close results. Only P_m and a showed signs of convergence away from the true values in a very small number of cases (Figure 4.12). There were 348 sets of estimates with $P_m > 800$ mg O_2 m^{-2} h^{-1}; 4.48% of the total 7776 sets. It is noteworthy that initial parameter values creating these cases did not show any obvious range. Hence, if estimated parameters do not make sense, it is worth running the model again with different combinations of initial values. Usually, one single fitting of ROM-TM only takes about 15s or even less.

Table 4.3 Six initial values of each fitted parameter.

Parameters	**Initial 1**	**Initial 2**	**Initial 3**	**Initial 4**	**Initial 5**	**Initial 6**
P_m **(mg O_2 m^{-2} h^{-1})**	67.6	270.8	473.6	1578.8	2480.8	3383.2
R_{20} **(mg O_2 m^{-2} h^{-1})**	22.4	89.2	156	520.4	818	1115.6
K **(m h^{-1})**	0.016	0.065	0.114	0.380	0.597	0.814
a **(mol O_2 (mol photon)$^{-1}$)**	0.00074	0.00287	0.00504	0.01677	0.02632	0.03591
a_R	0.9657	0.9714	0.9771	0.9828	0.9885	0.9942

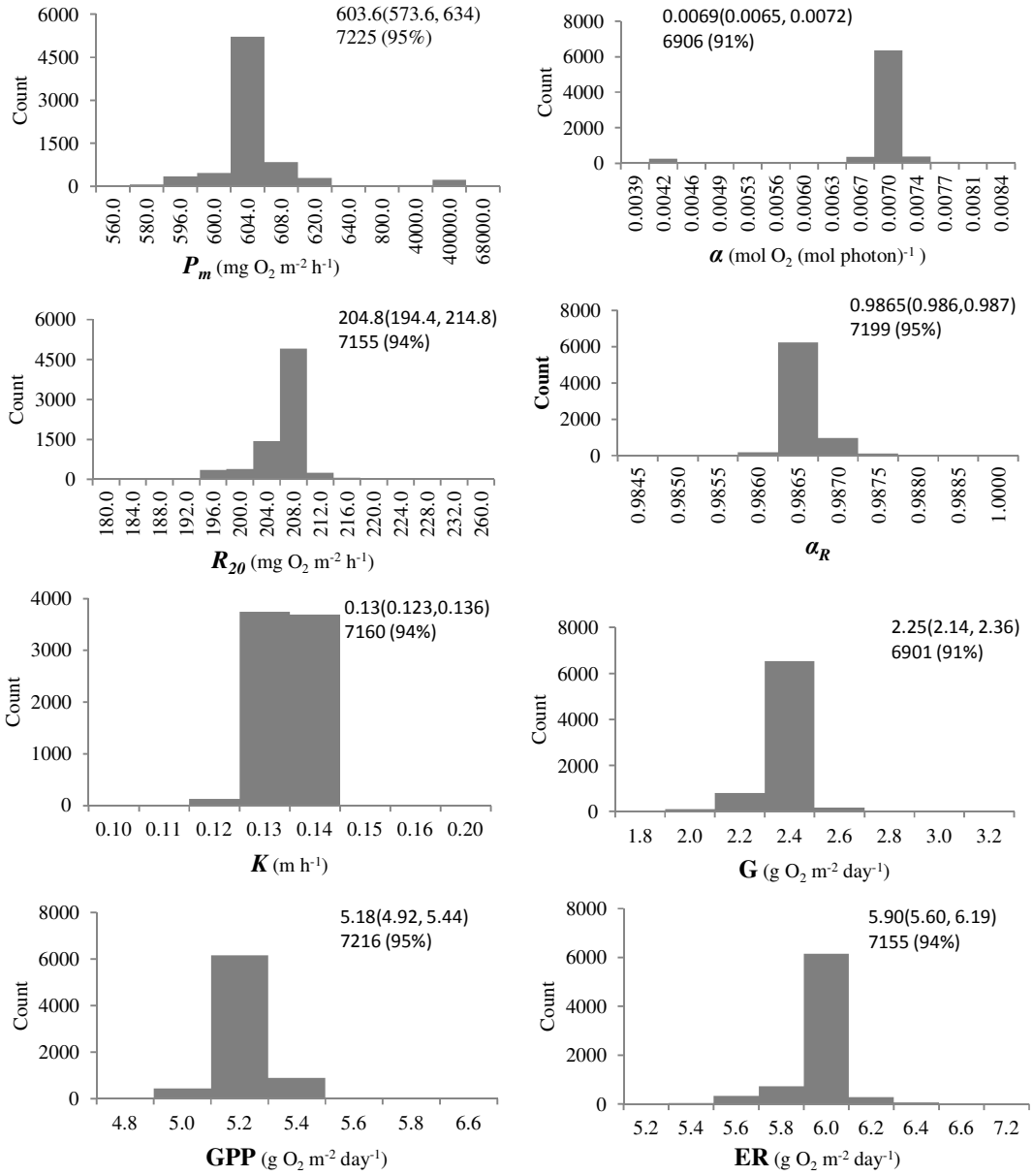

Figure 4.12 Results from 7776 times repeated runs of ROM-TM starting with different initial value combination of five main estimated parameters for *fminsearch* function. Data from site BP with fitting scenario (S2-pR). The numbers in the first row are the original fitted values with a range of 95% to 105% given in the parenthesis for each estimated parameter except the a_R. The a_R gives a more narrow range from 0.9860 to 0.9870. The second row includes the counts and ratios of each parameter falling into the above range of the original fitted value.

4.4 Discussion

Most whole-ecosystem metabolism methods based on DO serve a variety of research purposes, but mainly focus on the rates of *P* and *R*, and the ratio of *P*: *R*. ROM-TM provides estimates of these metabolic rates, but also gas exchange and relevant metabolic parameters (i.e., P_m, a, R_{20} and a_R). Standardized estimates of metabolic parameters (e.g., R_{20}, P_m and a) facilitate direct cross-system comparisons. The fact that all estimated parameters are obtained from the same model allows more systematic and consistent comparisons than if they were derived from different methods.

The addition of δ^{18}O-DO provides an estimate of a_R at the ecosystem level. The values of this parameter ranged from 0.9839 to 0.9865, which is close to the median of reported range from 0.975 to 0.998 for a variety of aquatic organisms and communities (Quay et al. 1995, Brandes and Devol 1997, Tobias et al. 2007, Venkiteswaran et al. 2007). The estimation of a_R in this paper is reasonable, so the whole-ecosystem models provide a solution for measuring the respiration isotopic fractionation factor at the ecosystem level.

4.4.1 Validation of model estimates

Parameter estimates cannot be directly validated (Oreskes et al. 1994). The acceptance of whole-stream models lies in their fit to field data and the parameter estimates falling into a range that seems reasonable. The estimates should be questioned unless they can be tested independently. The diel dissolved O_2 curve is the result of several processes (e.g., photosynthesis, ecosystem respiration and gas exchange) and environmental variables (e.g., light, temperature). The same curve can be reproduced using different combinations of estimated parameters. Hence, whether the fitted model and abstracted parameters are in accord with the ecological interpretation of DO and δ^{18}O-DO diel curves provides one way to validate the model.

The location, scale and shape of DO and δ^{18}O-DO diel curves are ecologically informative, providing information on the aquatic ecosystem under study (Venkiteswaran

et al. 2008). The location of the DO diel curve is primarily determined by the ratio of *P*: *R*: *G*. Although site 4F and BP both are heterotrophic, the ratio of *P*: *R* at site 4F is only half of that at site BP, leading to the location of DO below the atmospheric equilibrium most of time. For the δ^{18}O-DO diel curve, not only the ratio of *P*: *R*, also *P* or *R* alone, the δ^{18}O-H_2O, and a_R, can significantly change its location (Venkiteswaran et al. 2008). The δ^{18}O-H_2O and a_R are similar at both sites (Table 4.2). Site 4F, compared to site BP, has a lower *P*: *G* ratio due to low *P* and relatively high *k*, resulting in the location of δ^{18}O-DO diel curve closer to the equilibrium state. The magnitude of *P* primarily controls the scale of both DO and δ^{18}O-DO diel curves. The δ^{18}O-H_2O signature can modify the amplitude of the δ^{18}O-DO diel curve; the more negative it is, the greater the amplitude. The impacts of *R* and *k* on the scale of both curves are dependent on the ratio of *P*: *R* and *P*: *G*. The a_R plays no role on the scale of DO diel curve and it only causes slight changes to the amplitude of δ^{18}O-DO diel curve. Hence, we can see that the higher *P* rate at site BP causes a larger amplitude of both the DO and δ^{18}O-DO diel curves (Figure 4.5 & Figure 4.6). The higher *k* also further constrains the amplitude of both curves at site 4F. The *k* greatly affects the shape of both DO and δ^{18}O-DO diel curves. The presence of a nighttime plateau at site 4F shows that the nighttime *R* and *k* reach a quasi steady state (Figure 4.5). However, the ratio of *R*: *G* at site BP is higher than that at site 4F leading to an obviously decreasing DO trend during the night (Figure 4.6).

4.4.2 Modeling the responses to light

Responses of photosynthesis to light – Based on fitted production parameters (e.g., P_m and *a*) and measured light, ROM-TM is capable of examining the response of photosynthesis to irradiance at the ecosystem level. The estimates of I_k for these two sites range from 460 to 830 μE m^{-2} s^{-1}(Table 2). According to the hyperbolic model ($P_t = P_m$ * tanh (PAR/I_k)) (Equation 4), the production rates can reach > 95% $\boldsymbol{P_m}$ at PAR of 1500 μmol photons m^{-2} s^{-1}, and > 98% $\boldsymbol{P_m}$ at maximum PAR of about 2000 μmol photons m^{-2} s^{-1}, even for the I_k of 830 μE m^{-2} s^{-1}. This means that substantial light saturation occurs at these two sites (Figure 4). At both sites, the production rate is substantially depressed

relative to a linear model of photosynthesis response to light (Figure 4). Hence, ecosystem-level responses of photosynthesis to light should be described using non-linear curves. Holtgrieve (2010) also demonstrated the need to adopt light-saturated photosynthesis in his Bayesian model (BaMM).

Sampling on a cloudy day – Another useful application of ROM-TM is to parse the effect of cloud cover on measurements of *P*. Typically, a day with a clear sky would be chosen for field sampling because of the adverse effect of cloud cover on PAR and thus photosynthesis. Usually, sunny days are easy to forecast, but cloudless days are less predictable and rarer. Correcting the *GPP* estimate for the cloud cover is needed to compare between sites and sampling periods. This study demonstrates that P/R could exceed 1 at site BP on sunny days (Figures 5 & 6). In addition, we can now use continuous PAR to estimate and sum the GPP for a long period.

The effect of light on respiration – A challenge for whole-ecosystem methods is accounting for the effect of light on respiration. Parkhill & Gulliver (1999) introduced the term β_R, and demonstrated that photorespiration could not be ignored in some DO diel curves. The data set from site BP showed that estimates of *GPP* and *R* increased with slightly better performance (higher R^2) when β_R was included. However, it is not clear that higher estimates of *P* and *R* rates were actually due to photorespiration, or just resulted from improved and different fit following the addition of one more parameter. Another data set (from site 4F in a smaller stream) did not show any improvement by adding the term β_R. Parkhill (1999) acknowledged this problem. Hysteresis is considered an indication of the presence of the photorespiration. However, it is usually demonstrated though incubation approaches rather than with modeling methods. More testing of this modification should be done using higher-resolution time series data.

4.4.3 Uncertainty and error analysis

A successful model depends on reasonable assumptions and model structures, mathematical expressions, inputs, and parameters. Errors and uncertainties of a model come from the extent to which these requirements are not met.

Homogeneous assumptions and model structure – A river reach is often spatially heterogeneous in environment variables and biotic communities, leading to spatial heterogeneity in primary production, respiration and reaeration rates (Reichert et al. 2009). ROM-TM applies the one-station method and provides weighted average estimates of metabolic rates and gas exchange for a river reach on a daily basis. While the weighting increases exponentially as water flows from upstream to the sampling location, spatial pattern of the upstream reach influences the estimates of metabolic rates. Therefore, the one-station requires that sampling locations are far enough downstream of subreaches with significantly different characteristics, such as reservoirs, dams, WWTPs, high groundwater inputs, tributaries, etc. The ideal situation would be a long homogeneous reach with uniformly distributed plants and no significant lateral flow (i.e., ground water and tributary) into the reach.

Reichert et al. (2009) suggested that whole-stream methods cannot work if subreaches with significantly different characteristics are within the distance of $0.4v/k$ (where $\boldsymbol{v}$ is flow velocity and $\boldsymbol{k}$ is the reaeration coefficient) upstream of the sampling location. In this case, ROM-TM would provide estimates of metabolic rates that are strongly affected by that subreach. Another mathematical guideline has been provided (Chapra and Ditoro 1991, Reichert et al. 2009) to judge the distance upstream that contributes to DO dynamics of the sampling station downstream. The length is about $3v/k$. This formula does not count the effect of metabolic processes contributing to DO turnover. So the real distance would be $< 3v/k$. Hence, ROM-TM should work well if the river is approximately homogenous or the variation is relatively fine in scale within the distance of $3v/k$ upstream of the sampling location.

If subreaches or tributaries with significantly different characteristics are within 0.4 to 3*v/k* upstream of the sampling location, the average estimates of metabolic rates using the one-station methods may be still useful but may be affected by those upstream heterogeneities. For example, ground water input with a lower concentration of DO would result in overestimated *R* but have little influence on *P* (McCutchan et al. 2002). ROM-TM currently does not account for other processes that may affect DO dynamics in rivers. However, the structure of ROM-TM is open to the addition of other processes, and it is not difficult to include other processes in the model if relevant field information is available. The effect of groundwater input on the estimates of metabolic rates can be addressed by adding an additive term, C_gQ_g (C_g is the concentration of O_2 in groundwater and Q_g is the rate of groundwater flux to the water parcel), on the right side of the Equation 4.1.

A more difficult issue to deal with is temporal heterogeneity, such as changing dam release and WWTP discharges with time; ROM-TM may not provide reliable estimates of metabolic rates under this situation. ROM-TM only provides one value for each process, and assumes that all processes except photosynthesis are independent of time.

The guidelines discussed above can help selecting appropriate sampling locations and making reasonable estimates of metabolic rates using the one-station method and ROM-TM. The distance range of 0.4 - 3*v/k* is about 0.9 - 7 km for site 4F, and 2 - 15 km for site BP. According to these ranges, site 4F can be studied as a shaded stream because riparian trees extend over 10 km upstream. The estimates of metabolic rates for site BP may include the effect of the Conestoga River, a big 6th order tributary of the Grand River and about 10 km upstream of site BP.

Accurate inputs - Improved precision of measurement of input variables can reduce the uncertainty of estimates of metabolic rates (McCutchan et al. 1998). Holtgrieve (2010) analyzed the effects of precision bias of DO and δ^{18}O-DO measurements on all parameter and metabolism estimates. He pointed out that production efficiency (***a***) tends to be more

sensitive than other parameters to precision errors, and also to data resolution. As for metabolism estimates, *ER* was more sensitive to accuracy errors than *GPP*, and *K* was almost immune to analytical errors in the DO measurements. We confirm that *a* was more sensitive than other parameters, but we also found that P_m was sensitive. When sampling intervals were of ≤ 3h, ROM-TM provides stable estimates for all parameters with the mean close to true value and with small variances that gradually decrease with sampling intensity. The analysis of the effect of random error from DO time series measurements in this paper supports the robustness of ROM-TM.

Parameters - Venkiteswaran (2007) analyzed the effect of varying estimated parameters on reconstructed DO and δ^{18}O-DO diel curves adopting a one-at-a-time (OAT) technique in the PoRGy model. Maximum and minimum of bias were chosen to provide a visualization of the confidence region. He called this a 'sensitivity cloud'. A combination of all estimated parameters will be validated as the best solution if the optimization requirement is met. A change to one parameter at a time must consequently cause instantaneous changes of other parameters while minimizing the *SSE* between the model fitted curve and the field data. We may need to consider the correlation among parameters when we use the one-at-a-time (OAT) technique to address the effect of varying parameter on the reconstructed DO and δ^{18}O-DO time series. Instead, it may be useful to address the impacts of one varying parameter on the others while reconstructing the same time series data.

Chapra demonstrated that errors in estimates of *k* would propagate to *P* and then *R* in the delta method (Chapra and Ditoro 1991). McCutchan (1998) demonstrated that under varying *k*, estimated *ER* rates were subject to greater uncertainty than the estimated *P* rates, especially in ecosystems with high *k* and low metabolic rates. Because *k* obtained from field measurement was not adjusted with other metabolism parameters, we are not sure whether McCutchan's study is true of whole-ecosystem models applying inverse modeling or not. ROM-TM estimates gas exchange by modeling rather than field experimentation, so is time and labor saving, and leads to reasonable estimates. Although

all parameters can be approximated simultaneously, this inevitably results in greater uncertainty. Hence, the further study of error propagation among parameters in ROM-TM is needed.

4.5 Chapter summary

ROM-TM applies the classic least-squares method rather than alternatives, such as evolutionary algorithms, Bayesian methods, etc. This paper supports the utilization of *fminsearch* in MATLAB in developing the whole-ecosystem model. ROM-TM is fast, with the time of one fitting ≤ 15s. MATLAB is a commonly used computational language, which guarantees that this model can be widely used.

ROM-TM is a robust whole-ecosystem model employing the one-station method. It is capable of teasing apart two metabolic processes and gas exchange, reconstructing both DO and δ^{18}O-DO time series, and then providing daily average estimates of metabolic parameters at the ecosystem level. Estimated parameters can be used further to address the issues related specifically to light, such as light saturation phenomena at the ecosystem level, photorespiration, effects of cloud cover and riparian shading on the metabolic balance. ROM-TM provides a solution estimating the gas exchange coefficient (k), and the isotopic fractionation factor of ecosystem respiration (a_R) by using the oxygen isotope budget (δ^{18}O-DO). Further analyses and applications of estimated parameters will benefit from this systematic modeling framework.

Reliable results from whole-ecosystem models are dependant not only on advanced modeling techniques, but also on understanding of the river ecosystem and its metabolic processes. To facilitate the application of whole-ecosystem model in aquatic ecosystem metabolism research, modelers should face the challenges and question their models because of the large gap between the complexity of aquatic ecosystems and the simplicity of models. They must constantly improve their models by incorporating new knowledge on aquatic ecosystem metabolism and new modeling techniques. Future work should address the following aspects: (1) Error and uncertainty propagation analysis

among estimated parameters (P_m, a, R_{20}, k, a_R) and results (e.g., metabolic parameters, gas coefficient, the ratios of P: R: G, etc.); (2) Using ROM-TM to abstract more ecological information from O_2 time series, for example, the graphical representations of O_2 time series (e.g., the location, scale, shape of O_2 curves). This kind of analysis will be helpful in comparing aquatic ecosystems; (3) Modifying and improving ROM-TM to deal with two-station sampling data, thereby, ROM-TM can address the effect of spatial heterogeneity and allow comparison of reaches with certain kind of different characteristics; (4) Comparing ROM-TM with other similar models (e.g., PoRGy and BaMM) to determine the effects of model construction on metabolic estimates and the uncertainty of results.

– Chapter 5 –

The responses of primary production to light at the ecosystem level in a temperate river network: effects of stream size and scale

5.1 Introduction

Light is one of major factors controlling production of an ecosystem (Uehlinger et al. 2000, Mulholland et al. 2001, Julian et al. 2011). The relationship between photosynthesis and light is therefore of considerable theoretical and practical interest. The photosynthesis-light response at the ecosystem level is not only fundamental for our understanding of aquatic ecosystem metabolism, it is critical to interpreting the role of other abiotic limiting factors (e.g., inorganic carbon, nutrients, temperature, etc.) on ecological processes (Sterner et al. 1997, Hill and Fanta 2008, Hill et al. 2009, Karlsson et al. 2009, Finlay et al. 2011). However, despite our knowledge of photosynthetic mechanisms and responses to light at molecular, organismal and assemblage/community levels, information at the ecosystem scale is still largely unknown for many ecosystems, including river ecosystems.

There are many studies of photosynthesis-light responses of plankton in lakes and oceans, but little research has focused on rivers, and most of this has occurred in small streams (Kelly et al. 1983, Vanderbijl et al. 1989, Guasch and Sabater 1995, Uehlinger et al. 2000, Laviale et al. 2009) rather than in middle-sized and large shallow rivers where vascular macrophytes usually dominate. There are a few reasons for this. First, there is more concern about nutrients controlling primary production than light. It is assumed that the low light utilization efficiency of primary producers indicates that light must be

sufficient at larger scales, or may not be as limiting as nutrients. This has been directly demonstrated through field manipulation of nutrients in open water ecosystems, e.g., lakes and oceans (Schindler 1977). Secondly, most aquatic ecosystem studies regarding primary production and light have been conducted in lakes and oceans. One reason may be the significant contribution of oceanic phytoplankton to the global carbon cycle. Almost 40% of the total global fixed carbon is produced annually by phytoplankton in oceans; however, the phytoplankton biomass only accounts for 1-2% of the total global plant carbon (Berger et al. 1989, Falkowski 1994). On the other hand, it is relatively easy to quantify light availability in these open water ecosystems because light intensity attenuates exponentially with water depth. In contrast, the underwater light availability is more spatially variable in rivers than in lakes and oceans. A great number of complex factors must be taken into consideration than the water depth and transparency (Julian et al. 2008). These factors include topography (e.g., boundary mountains, deep valleys, river banks), biota (riparian vegetation, aquatic plant communities), and hydrology (e.g., river channel direction and geometry, and hydrologic regime). Thirdly, because the shading of riparian vegetations leads to obvious light insufficiency in headwaters, greater attention has been paid to light in headwater streams rather than in middle-sized and large rivers that are relatively open to the sun.

A characteristic feature of river ecosystems is the presence of a longitudinal environmental gradient. In natural rivers, light availability largely controls the composition and distribution of primary producers that often exhibit longitudinal patterns from headwaters to lower reaches (Vannote et al. 1980). Light availability of aquatic plants *in situ* depends on the light intensity reaching the water surface and light penetration in the water column (Julian et al. 2008). Periphyton and bryophytes may be found in all parts of a river, but often predominate in headwaters and upper reaches where low light availability due to shading by riparian vegetation underscores the competitive advantage of these low-light adapted phototrophs. Vascular submersed macrophytes occur mainly in middle-sized rivers and along the margins of larger rivers. The open channels in middle-sized rivers may be light sufficient where the river is shallow and wide, and thus less shaded by riparian vegetation. In larger lowland sections,

the underwater light climate shifts back from self shading by prolific submersed angiosperms to progressive shading because of attenuation by phytoplankton biomass, dissolved organic matter, sediment particles, etc. Phytoplankton populations need time to develop, but can be substantial in large lowland rivers (Allan and Castillo 2007). From headwaters to downstream lowland reaches, longitudinal patterns of primary producers and light conditions in a river network shape patterns and processes in food webs, energy flow, and nutrient retention and cycling (Finlay et al. 2011). These functions highlight a river ecosystem as an important conduit, producer and transformer of organic matter between terrestrial ecosystems and lakes and oceans.

However, with increasing anthropogenic-induced disturbance (e.g., deforestation, agriculture and point-source effluents), environmental patterns of natural rivers, i.e., light, nutrients, temperature, etc., have been greatly altered. Removal of riparian trees usually leads directly to enhanced light availability and channel sedimentation in headwater streams. As a consequence, shifts in plant taxa occur in response to shade-sun acclimations and unstable substrates. The deficiency of natural rivers in nutrients (mainly nitrogen and phosphorus) is alleviated by exogenous nutrient inputs. On the other hand, nuisance growth of macrophytes stimulated by exogenous nutrients further decreases light availability by extensive self-shading. Anthropogenic activities lead to cascading alterations in structure and function of a river network. How photosynthesis-light relationships respond to these alterations is still poorly understood, which further limits our understanding of the rates of key in-channel processes of energy flow and nutrient cycling in a river network. Recent studies on macrophyte communities suggest that the photosynthesis-light response at the community level is more likely to be within the intermediate phase between light-limited to fully light saturated (Binzer et al. 2006). The original perception of light limitation of primary production of river ecosystems in headwaters and light saturation in middle-sized and larger rivers should be re-examined.

Photosynthesis-light responses can be described by an empirical model, the *P-I* curve. Primary parameters describing the hyperbolic *P-I* curve are the maximum photosynthetic rate ($\boldsymbol{P_m}$) and photosynthetic efficiency ($\boldsymbol{a}$). Derived parameters are onset

of light saturation ($\boldsymbol{I_k}$, the ratio of $\boldsymbol{P_m}$ to $\boldsymbol{a}$) and the compensation point ($\boldsymbol{E_c}$, the ratio of respiration to $\boldsymbol{a}$). Generally, a complete *P-I* curve involves three regions: light-limited, light-saturated and photoinhibited. Light-limited photosynthesis occurs at low intensity light where photosynthetic rates increase with light. If light increases beyond $\boldsymbol{I_k}$, photosynthetic rates reach a saturation level, $\boldsymbol{P_m}$. Very high light intensity may cause photoinhibition of photosynthetic rates (Falkowski and Raven 2007).

The *P-I* model can be applied at different scales, but it requires interpretation of relevant parameters at the corresponding scale (Binzer and Middelboe 2005, Binzer et al. 2006). With the level of organization increasing from the molecular (photosynthetic pigments, electron transport), to biological (photosynthetic tissues and organisms) to ecological (communities, ecosystems), the complexity of a photosynthetic system increases, with new phenomena and system behaviors. These include the photoadaptation of phytoplankton in space and time to light intensity (Prezelin and Matlick 1980), self-shading effects due to the thickness of benthic mats (Dodds et al. 1999), and the 3-dimensional structure of macroalgal and rooted macrophytes (Binzer and Sand-Jensen 2002, Middelboe and Binzer 2004). Photosynthetic characteristics of communities will reflect plant form, density, and light-absorption, and their influence on the distribution of light, which is different from photosynthetic behavior at small scales (Binzer and Middelboe 2005, Binzer et al. 2006). For example, photoinhibition has been often observed in the incubation of photoelements (e.g., thallus pieces) or biological systems (e.g., leaves and individual plant shoots), but rarely at the ecosystem level, perhaps because of the compensation of multiple layers of plants in a whole community (Binzer et al. 2006). Other environmental factors (e.g., nutrients, temperature, etc.) can complicate photosynthesis-light responses and play a role in shaping the *P-I* curve. Temperature regulates photosynthetic response at saturating and inhibiting irradiances, but not at low irradiance (Davison 1991). Low temperature can even shift photosynthesis of river phytoplankton from light dependence to temperature dependence by lowering $\boldsymbol{I_k}$ values (Rae and Vincent 1998). Hence, the *P-I* model synthesizes ecological information in terms of river ecosystem structure and function. Ecosystem-level parameters may be good indicators of the effects of human disturbance on environmental factors and

consequent changes of river structure and function. At the ecosystem scale, we are no longer meaning rate of photosynthesis, but rather the rate of photosynthetic production of dissolved oxygen. Hereafter, we will refer to this as primary production, or simply production.

The Grand River, located in an agricultural and urban mixed land-use watershed with a long history of anthropogenic activities, was chosen to demonstrate the patterns of ecosystem-level primary production versus light responses. 12 stream and river sites were chosen varying from 2nd order in headwaters to 7th order in the main channel. 8 low stream order streams were chosen in pairs with and without riparian trees. 4 large river sites were chosen with 2 located upstream and 2 located downstream of main WWTPs. The specific objectives of this study were (1) to systematically report how ecosystem-level production-light responses vary along the length of an impacted temperate river continuum, (2) to explore the effects of human disturbance (e.g., deforestation in headwater streams and WWTPs in main channels) on production-light responses, and (3) to address the effects of local reach characteristics on production-light responses and (4) to determine whether macrophyte-dominated, eutrophic river channels are light-saturated or light-limited.

5.2 Materials and methods

5.2.1 Study sites

For descriptions of each site and for water sampling procedures and lab analysis refer to Chapter 3.

5.2.2 Estimation of parameters

Relevant metabolic parameters, such as production rate ($\boldsymbol{P}$), maximum production rate ($\boldsymbol{P_m}$), production efficiency ($\boldsymbol{a}$), respiration rate ($\boldsymbol{R}$) and the normalized respiration rate at 20℃ ($\boldsymbol{R_{20}}$), etc., can be obtained by model fitting when dissolved oxygen time series are

used in a whole-system approach to quantifying the metabolic rates of streams (Uehlinger et al. 2000, Holtgrieve et al. 2010). In this study, diel/diurnal dissolved O_2 and δ^{18}O-DO data were analyzed by the transient model of river ecosystem oxygen metabolism introduced in Chapter 4, ROM-TM, to abstract relevant production parameters. In this model (Equation 5.1), photosynthesis is considered as a hyperbolic function of irradiance (Jassby and Platt 1976).

$$P_t = P_m \bullet \tanh[a(\frac{I_t}{P_m})] \tag{5.1}$$

$\boldsymbol{P_m}$ is the maximum production rate ($mg\ O_2\ m^{-2}\ h^{-1}$); $\boldsymbol{a}$ is the slope of the *P-I* curve at low light intensity. $\boldsymbol{a}$ is defined as the production efficiency (mg O_2 s (μmol photons h)$^{-1}$), and will be converted and reported in the unit of mol O_2 (mol photon)$^{-1}$ in the result section. $\boldsymbol{I_t}$ represents the instantaneous PAR (photosynthetically active radiation, $\mu mol\ photons$ m^{-2} s^{-1}).

5.2.3 Incoming PAR and underwater light profiles

A HOBO light meter with a LI-COR LI-190SA quantum sensor was deployed in the open channel to continuously record the irradiance reaching the water surface at 1-min intervals on August 17-20, 2011. Two Apogee amplified quantum sensors (SQ-200 series) were used to measure underwater light intensity at the same period. The sensors were randomly deployed at different depths, i.e., from water surface (around 1cm under the water surface) to near the sediment (around 75cm from the water surface). The measurement for each depth lasted about 20 minutes to obtain 15 to 20 recordings. The light intensity of each depth was calculated as the mean of those readings. The fraction of light intensity for each depth was expressed as the ratio of this mean value to the mean light intensity above the water.

5.2.4 Plant collection

The water depth at Blair ranged from 60 cm to 100 cm during low flow. *Stuckenia pectinata (*formerly *Potamogeton pectinatus)* stems reach the water surface in early summer, then progressively accumulate at the surface, and die back in fall. Maximum standing crop of macrophytes occurred in the middle of August, 2011. Most collected shoots were over 140 cm and some reached 180 cm. Stems were selected and collected in bunches. The form of each plant bunch was recorded before it was cut off. The measures included the portion floating on the water surface, the angle of plant in water, the length of each portion in water with depth, etc. This information was used to calculate the distribution of plant biomass with depth.

5.3 Results

5.3.1 Environmental parameters of all 12 sites

Environmental variables and major plant taxa were measured and recorded during sampling days for all 12 sites (Table 5.1). Hydrological variables, such as discharge, water depth and channel width, generally increased with stream size in the Grand River network (Table 5.1). Channel width spanned two orders of magnitude from 1.1 m to over 100 m. Mean depth varied from 0.21 m to 0.78 m. The average discharge ranged from 0.024 $m^3 s^{-1}$ at headwater site 2NF to 25.3 $m^3 s^{-1}$ at Grand River site GM (Table 5.1). Mean temperatures for sites were from 15.1 to 20.6 ℃ during sampling days, and mean pH ranged from 8.0 to 8.4 (Table 5.1).

The presence of riparian trees at headwater streams lowered the light availability. Headwater streams without riparian trees, e.g., 2NF, 3NF, 4NF and 5NF, received higher PAR than those sites with riparian trees, e.g., 2F, 3F, 4F and 5F (Figure 5.1). For these 4 pairs of streams, 2-way ANOVA demonstrated the effect of riparian trees on PAR ($P < 0.001$), but did not find an effect of stream order on PAR ($P = 0.34$) or a tree-order interaction ($P = 0.75$).

Table 5.1 Means of environmental variables at all 12 sites in the Grand River network in growing season (May - Oct): elevation (m), stream order, mean depth (m), mean width (m), mean water temperature (℃), mean discharges ($m^3 s^{-1}$), mean conductivity (μS), mean pH, mean soluble reactive phosphorus (μg L^{-1}), mean total phosphorus (μg L^{-1}), mean nitrogen content of ammonium (mg N L^{-1}), mean nitrogen content of nitrate (mg N L^{-1}), substrate types, stability of substrates, major plant taxa and amplitude of major plant species in growing season. Standard deviations for relevant variables are in parentheses.

Site:	**2F**	**2NF**	**3F**	**3NF**	**4F**	**4NF**	**5F**	**5NF**	**WM**	**BP**	**BL**	**GM**
Stream order	2	2	3	3	4	4	5	5	6	7	7	7
Elevation (m)	385	396	381	380	379	397	354	370	323	302	274	265
Depth (m)	0.27	0.21	0.50	0.29	0.37	0.21	0.28	0.65	0.41	0.41	0.57	0.78
	(0.03)	(0.05)	(0.05)	(0.04)	(0.04)	(0.04)	(0.1)	(0.09)	(0.05)	(0.07)	(0.09)	(0.06)
Width (m)	1.3	1.1	5	2.2	6.5	4.0	14	13.3	36	85	90	100
Temperature (℃)	15.1	15.6	17.5	18.1	17.2	18.6	19.5	18.1	19.5	20.6	20.5	19.0
	(0.3)	(0.6)	(0.4)	(0.8)	(2.5)	(2.3)	(2.8)	(2.8)	(4.7)	(4.1)	(4.7)	(5.8)
Discharge ($m^3 s^{-1}$)	0.064	0.024	0.136	0.068	0.14	0.10	0.41	0.23	7.6	12.9	18.1	25.3
	(0.037)	(0.014)	(0.078)	(0.039)	(0.13)	(0.094)	(0.43)	(0.25)	(1.6)	(6.3)	(7.2)	(14.5)
Conductivity (μS)	632	496	573	571	534	487	526	553	453	477	688	777
	(26.2)	(13.1)	(15.8)	(26.6)	(20.6)	(19.1)	(24.3)	(12.8)	(18.5)	(27.0)	(48.4)	(47.6)
pH	8.1	8.2	8.0	8.1	8.3	8.3	8.4	8.3	8.3	8.4	8	8.3
	(0.2)	(0.2)	(0.1)	(0.03)	(0.1)	(0.1)	(0.1)	(0.1)	(0.09)	(0.3)	(0.2)	(0.2)
SRP (μg L^{-1})	6.5	5.2	5.8	5.4	5.1	3.8	5.2	3.7	2.4	3.3	16.3	9.7
	(1.5)	(0.5)	(1.2)	(3.0)	(1.0)	(3.2)	(2.8)	(1.0)	(1.2)	(1.7)	(4.3)	(1.4)
TP (μg L^{-1})	11	13.3	18.5	17.8	23.8	22.1	25	26.7	22.5	31.8	53.3	47.6
	(4)	(5.3)	(1.7)	(0.7)	(11.6)	(13.1)	(5)	(8.1)	(8.3)	(9.7)	(20.6)	(14.5)
NH_4^+-N (μg L^{-1})	89	108	159	111	18.5	25	35	31	59	27	412	68
	(121)	(150)	(237)	(160)	(4)	(12)			(48)	(13)	(229)	(61)
NO_3^--N (μg L^{-1})	1010	1110	1080	280	1033	510	1470	1230	1250	1670	2600	2850
	(230)	(880)	(260)	(220)	(260)	(310)	(520)	(210)	(640)	(840)	(1040)	(470)
Substrates	①⑥	①	②⑥	④	④⑤	④⑤	④⑤	④⑤	④⑤	④⑤	④⑤	④⑤
Plant taxa	Peri	Peri	Peri	Peri	Peri	Peri	Mo	C.G	Mixed	M.S. 95%	S.P. 95%	Mixed

Substrates: ①Sand; ②Gravel, ③Cobble, ④mixed gravel-cobble, ⑤with boulders, ⑥Organic debris
Plant taxa: Peri(periphyton), Mo (moss), C.G.(*Cladophora glomerata*), M.S.(M*yriophyllum spicatum*), S.P. (*Stuckenia pectinata*), Mixed (M*yriophyllum spicatum* and *Stuckenia pectinata*).

Daily incoming PAR on sampling days at large river sites was from 22.9 to 65.8 mol photons m^{-2} day^{-1}, and exhibited a declining trend from early summer to early fall for sampling periods from 2006 to 2008 (Figure 5.2).

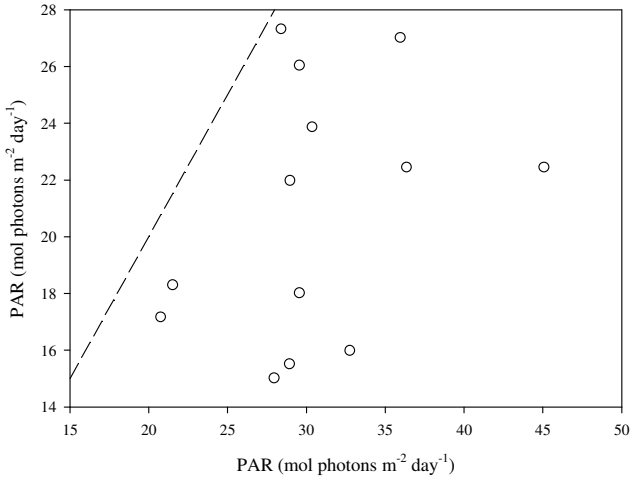

Figure 5.1 Daily incoming PAR (mol photons m^{-2} day^{-1}) at small streams in the Grand River network, with (y-axis) and without (x-axis) riparian trees. Dashed line is 1:1 line.

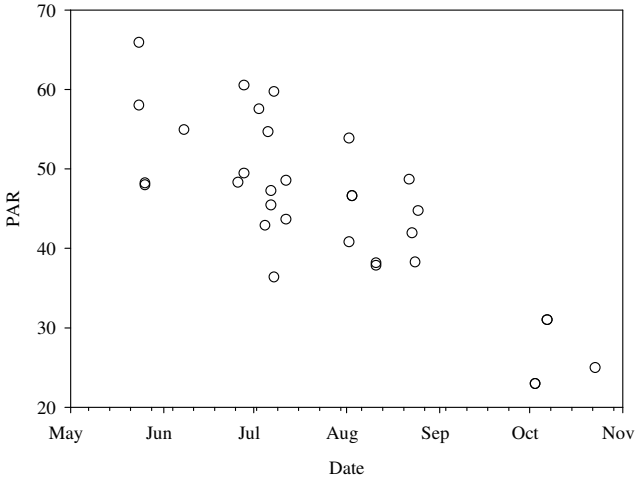

Figure 5.2 Incoming PAR (mol photons m^{-2} s^{-1}) at 4 Grand River sites (WM, BP, BL and GM) for sampling periods from 2006 to 2008.

Soluble reactive phosphorus (SRP) exhibited a slight declining trend from small streams to middle size streams, and then increased along the main channel of the Grand (Table 5.1). The highest mean level was 16.3 µg/L at site BL (Table 5.1). Site BL also had the highest mean level of total phosphorus (TP) of 53.3 µg/L and NO_3^- of 2.6 mg N/L, which marked this section of the Grand River as eutrophic (CCME 2007).

5.3.2 The effect of stream order and riparian trees on production parameters and compensation point

The maximum production rate ($\boldsymbol{P_m}$, $mg\ O_2\ m^{-2}\ h^{-1}$) for sites exhibited an apparent increasing trend with stream order (Figure 5.3). The two highest $\boldsymbol{P_m}$ values were at site BL, 2160 and 2677 mg O_2 m^{-2} h^{-1}. Other $\boldsymbol{P_m}$ fell in the range of 0~2000 mg O_2 m^{-2} h^{-1}. The $\boldsymbol{P_m}$ exhibited large variation at sites 3F, 3NF, 5F, 5NF and BL, but with similar coefficient of variation (0.3 to 0.5) except site 2F (0.7), 4F (0.2), and GM (0.1).

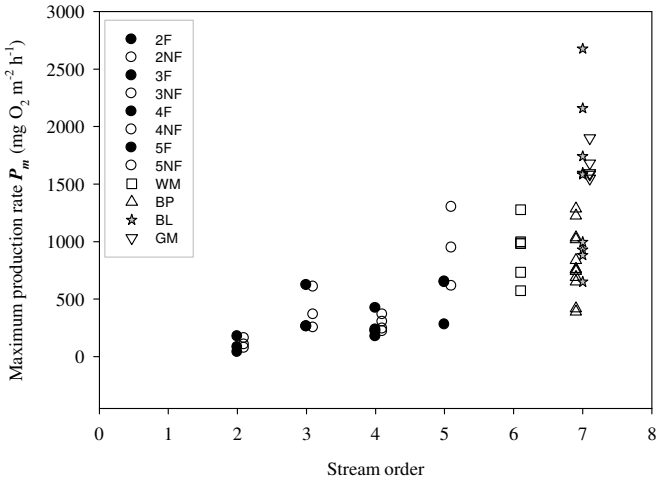

Figure 5.3 The maximum production rate ($\boldsymbol{P_m}$, $mg\ O_2\ m^{-2}\ h^{-1}$) against the stream order at multiple sites in Grand River network. The 12 sites from left to right in order are 2F, 2NF, 3F, 3NF, 4F, 4NF, 5F, 5NF, WM, BP, BL and GM.

The average P_m ranged from 98 mg O_2 m^{-2} h^{-1} at site 2F to 1663 mg O_2 m^{-2} h^{-1} at site GM, with an average of 667 mg O_2 m^{-2} h^{-1} for all sites (Table 5.2). All 12 sites could be roughly divided into four groups regarding the average level of P_m. Sites 2F and 2NF had lowest P_m level of less than a quarter of the average P_m value for all sites. The P_m levels at sites of 3rd and 4th order were close to half of the average P_m value, ranging from 263 to 408 mg O_2 m^{-2} h^{-1}. However, the two 3rd order sites were a little more productive than the two 4th order sites, one shaded and one non-shaded site (Table 5.2). Medium stream sites 5F and 5NF and river sites WM and BP showed high P_m ranging from 1.0 to 1.5 times the average P_m. The other two river sites, BL and GM, had a relatively high P_m level, double the average P_m, and even to a mean of 1663 mg O_2 m^{-2} h^{-1} at site GM (Table 5.2).

Table 5.2 The average level of production parameters and derived parameters (± SE), maximum production rate (P_m, *mg O_2 m^{-2} h^{-1}*), production efficiency (α, *mol O_2 (mol photon)$^{-1}$*), onset of saturation (I_k, *µmol photons m^{-2} s^{-1}*), compensation point (E_c, *µmol photons m^{-2} s^{-1}*), percent saturation at 2000 *µmol photons m^{-2} s^{-1}* for 12 sites in the Grand River network.

Sites		P_m	α	I_k	E_c	Saturation level
2F	*mean*	97.9	0.0116	67.8	103.9	100%
	SE (n)	± 40.4 (3)	± 0.0028 (3)	± 13.8 (3)	± 15.7 (3)	
2NF	*mean*	112.7	0.0039	266.8	356.2	100%
	SE (n)	± 25.2 (3)	± 0.0010 (3)	± 35.9 (3)	± 57.2 (3)	
3F	*mean*	381.3	0.0165	293.4	159.7	100%
	SE (n)	± 119.7 (3)	± 0.0100 (3)	± 83.6 (3)	± 43.8 (3)	
3NF	*mean*	407.6	0.0118	342.2	244.2	100%
	SE (n)	± 104.5 (3)	± 0.0038 (3)	± 76.3 (3)	± 44.5 (3)	
4F	*mean*	262.5	0.0126	245.6	175.0	100%
	SE (n)	± 54.8 (4)	± 0.0038 (4)	± 77.7 (4)	± 66.6 (4)	
4NF	*mean*	302.6	0.0076	395.3	212.6	100%
	SE (n)	± 30.9 (4)	± 0.0019 (4)	± 78.0 (4)	± 54.8 (4)	
5F	*mean*	604.6	0.0202	276.5	130.0	100%
	SE (n)	± 164.8 (3)	± 0.0069 (3)	± 28.8 (3)	± 14.0 (3)	
5NF	*mean*	952.9	0.0199	462.4	187.2	100%
	SE (n)	± 198.2 (3)	± 0.0059 (3)	± 115.9 (3)	± 45.8 (3)	
WM	*mean*	925.5	0.0107	786.2	299.2	98.8%
	SE (n)	± 99.5 (6)	± 0.0014 (6)	± 73.8 (6)	± 25.7 (6)	
BP	*mean*	818.4	0.0071	1024.8	311.4	95.7%
	SE (n)	± 81.4 (12)	± 0.0006 (12)	± 100.4 (12)	± 23.9 (12)	
BL	*mean*	1467.9	0.0124	1085.4	658.1	95%
	SE (n)	± 222.8 (9)	± 0.0020 (9)	± 115.6 (9)	± 57.6 (9)	
GM	*mean*	1663.0	0.0172	914.2	314.6	99.2%
	SE (n)	± 63.2 (5)	± 0.0025 (5)	± 132.6 (5)	± 17.8 (5)	
Total	**Average**	666.6	0.0126	513.4	262.7	

I used 4 pairs of streams with and without riparian trees (2F vs. 2NF, 3F vs. 3NF, 4F vs. 4NF, and 5F vs. 5NF) to demonstrate an effect of stream order on $\boldsymbol{P_m}$ (2-way ANOVA, $p < 0.001$), but did not find an effect of riparian trees ($p = 0.124$) or interaction ($p = 0.166$).

The production efficiency, ***a***, ranged from 0.004 mol O_2 (mol photon)$^{-1}$ at site 2NF to 0.02 mol O_2 (mol photon)$^{-1}$ at 5th order sites 5F and 5NF. The average ***a*** was 0.013 mol O_2 (mol photon)$^{-1}$ (Table 5.2). The production efficiency did not show any simple trend with stream size, but exhibited site to site differences. Sites 2NF and BP had low ***a***, sites 3F, 5F, 5NF and GM had much higher ***a*** levels, and other sites were close to the site average level (Table 5.2). Compared to other sites, sites 3F, 5F and 5NF exhibited high variations in ***a***. Two extreme high values of ***a*** were 0.037 at site 3F, and 0.031 at site 5NF (Figure 5.4).

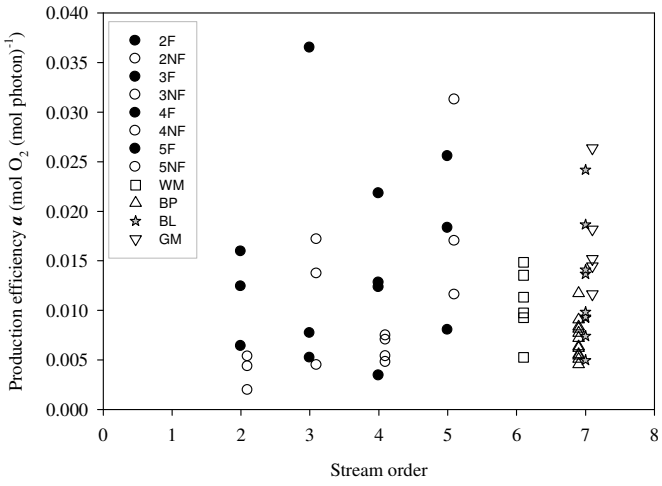

Figure 5.4 The production efficiency (***a***, *mol O_2 (mol photon)$^{-1}$*) against the stream order at multiple sites in Grand River network. The 12 sites from left to right in order are 2F, 2NF, 3F, 3NF, 4F, 4NF, 5F, 5NF, WM, BP, BL and GM.

I used 4 pairs of streams with and without riparian trees (2F vs. 2NF, 3F vs. 3NF, 4F vs. 4NF, and 5F vs. 5NF) to look for an effect of stream order on ***a*** but did not find

one (2-way ANOVA, p =0.176), nor did I find an effect of the presence or absence of riparian trees on $\boldsymbol{a}$ (p = 0.189) or order-tree interaction (p = 0.633).

The onset of saturation, $\boldsymbol{I_k}$, and compensation point, $\boldsymbol{E_c}$, were calculated for all sites (Figure 5.5, 5.6). Average values of these two parameters were also reported in Table 5.2.

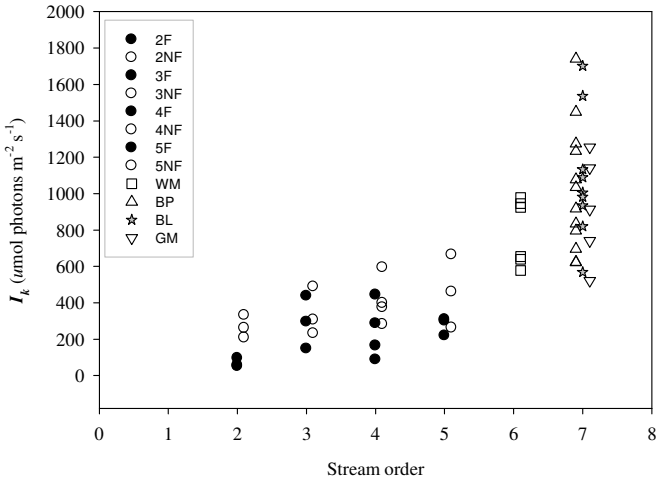

Figure 5.5 The onset of saturation ($\boldsymbol{I_k}$, *μmol photons m^{-2} s^{-1}*) against the stream order at multiple sites in the Grand River network. The 12 sites from left to right in order are 2F, 2NF, 3F, 3NF, 4F, 4NF, 5F, 5NF, WM, BP, BL and GM.

The $\boldsymbol{I_k}$ generally increased with stream order, varying from less than 100 μmol photons m^{-2} s^{-1} at headwater site 2F to around 1000 μmol photons m^{-2} s^{-1} at 7th order sites (Figure 5.5). For small and middle size streams, the $\boldsymbol{I_k}$ appeared to linearly increase with the stream order regardless of the presence of riparian trees. The maximum value of $\boldsymbol{I_k}$ could be over 600 μmol photons m^{-2} s^{-1} at site 5NF. For sites in the central Grand, WM, BP, BL and GM, the $\boldsymbol{I_k}$ varied broadly from 500 to 1800 μmol photons m^{-2} s^{-1}. I used 4 pairs of streams with and without riparian trees (2F vs. 2NF, 3F vs. 3NF, 4F vs. 4NF, and 5F vs. 5NF) to look for an effect of stream order on $\boldsymbol{I_k}$, but failed to do so (2-way ANOVA, p =0.066), but I did demonstrate an effect of riparian trees on $\boldsymbol{I_k}$ (p = 0.004). The interaction term was not significant (p = 0.584).

The compensation point, E_c, appeared to be independent of stream size except for site BL. The average level of all 12 sites could be roughly divided into three levels: 100 ~ 200 μmol photons m^{-2} s^{-1} to a little over 200 μmol photons m^{-2} s^{-1} (sites 2F, 3F, 3NF, 4F, 4NF, 5F and 5NF), around 300 ~ 400 μmol photons m^{-2} s^{-1} (sites 2NF, WM, BP and GM), and over 600 μmol photons m^{-2} s^{-1} at site BL only (Table 5.2 and Figure 5.6). High E_c at the site BL was due to high community respiration (Table 5.3).

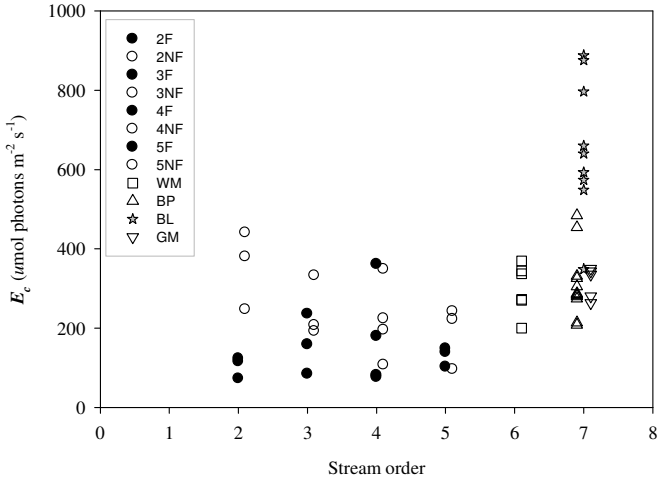

Figure 5.6 The compensation point (E_c, *μmol photons m^{-2} s^{-1}*) against the stream order at multiple sites in the Grand River network. The 12 sites from left to right in order are 2F, 2NF, 3F, 3NF, 4F, 4NF, 5F, 5NF, WM, BP, BL and GM.

I used 4 pairs of streams with and without riparian trees (2F vs. 2NF, 3F vs. 3NF, 4F vs. 4NF, and 5F vs. 5NF) to look for an effect of stream order on E_c, but did not find one (2-way ANOVA, p =0.366), but did find an effect of riparian trees on E_c (p = 0.001). The interaction term was not significant (p = 0.165).

Table 5.3 Ecosystem respiration (***ER***, *mg O_2 m^{-2} day^{-1}*) for 12 sites in the Grand River network.

Site	Ecosystem respiration (mg O_2 m^{-2} day^{-1})												Mean ER
2F	2.0	5.4	2.5										**3.3**
2NF	2.4	3.0	5.6										**3.7**
3F	3.4	8.5	3.4										**5.1**
3NF	4.1	9.1	7.9										**7.0**
4F	3.4	4.6	2.8	6.4									**4.3**
4NF	3.0	3.8	2.2	5.2									**3.6**
5F	7.1	7.2	3.3										**5.9**
5NF	10.5	8.3	7.8										**8.9**
WM	7.5	8.8	9.1	3.9	11.2	11.6							**8.7**
BP	6.9	6.8	6.4	3.5	6.5	7.8	3.1	5.7	5.1	5.1	7.0	7.5	**6.0**
BL	7.9	33	16.9	18.2	30.1	23.1	23.3	14.2	23.8				**21.2**
GM	13.4	19.2	14.1	14.4	11.3								**14.5**

5.3.3 Production-light response (*P-I* curves)

The sites demonstrated both light-limited and light-saturated oxygen production within the normal range of light availability (Figure 5.7 & Figure 5.8). All sites without riparian trees (2NF, 3NF, 4NF and 5NF) illustrated similar mean $\boldsymbol{P_m}$ and higher mean $\boldsymbol{I_k}$ than their counterparts with riparian trees (2F, 3F, 4F and 5F) (Figure 5.7). Much of variation about the average *P-I* curve is due to variation among sampling days.

The relationship of production with light at site WM, BP, BL and GM, shows less full light-saturation at the maximum level of light availability, > 2000 µmol photons m^{-2} s^{-1} (Figure 5.8).

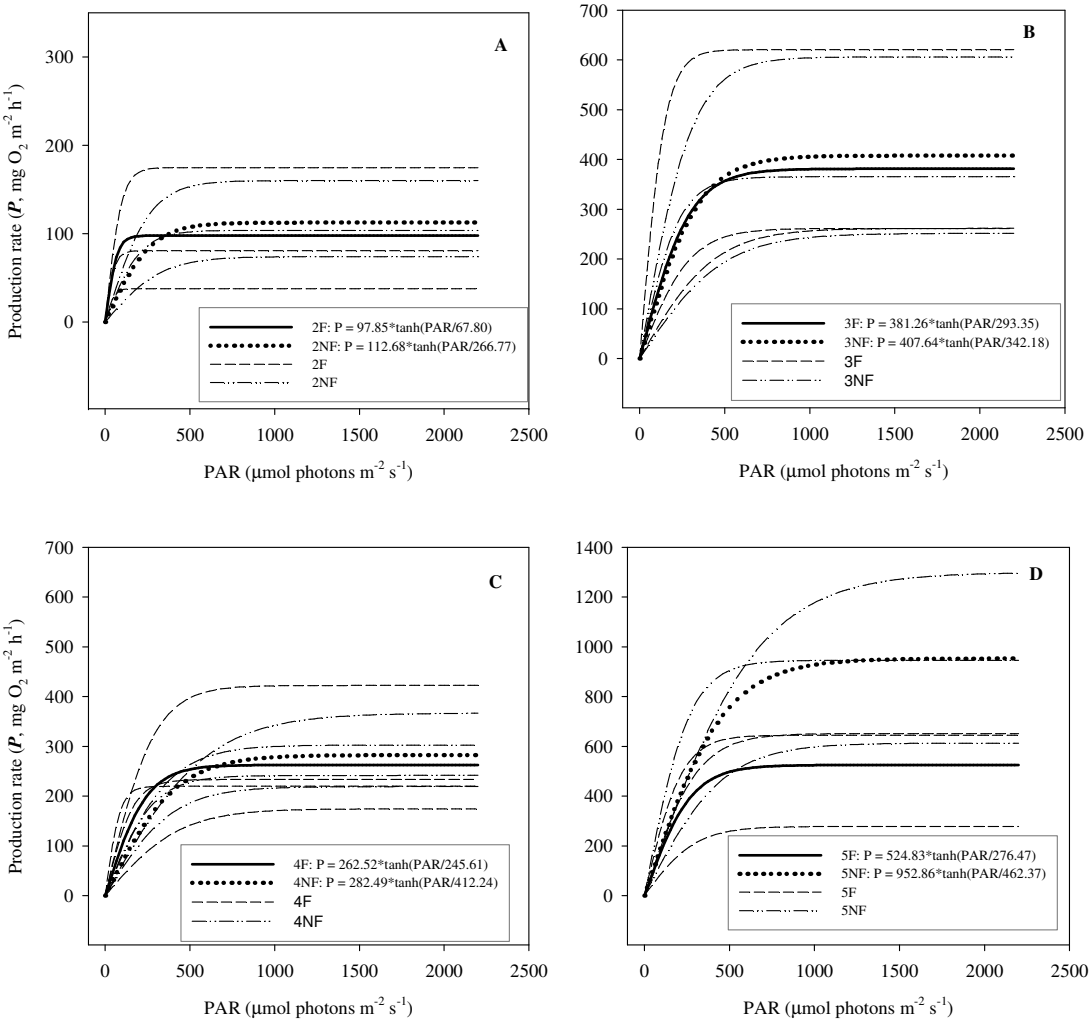

Figure 5.7 Plots of instantaneous production rate vs. incoming photosynthetically active radiation (PAR, *µmol photons* m^{-2} s^{-1}) for all sampling events for small and middle-sized stream sites in the Grand River network based on the parameters determined using ROM-TM. Subplot (A): site 2F and 2NF; (B): site 3F and 3NF; (C): site 4F and 4NF; and (D): site 5F and 5NF. The solid and dotted curves (*P-I* curves) describe the production-light responses for each site, using the average of the maximum production rate ($\boldsymbol{P_m}$, *mg* O_2 m^{-2} h^{-1}) and the production efficiency (***a***, *mol* O_2 *(mol photon)*$^{-1}$) of each site. The dashed and dash-dotted lines are for each sampling date. The solid and dashed curves are sites with riparian trees (sites 2F, 3F, 4F and 5F), and the dotted and dash-dotted curves are sites without riparian trees (sites 2NF, 3NF, 4NF and 5NF).

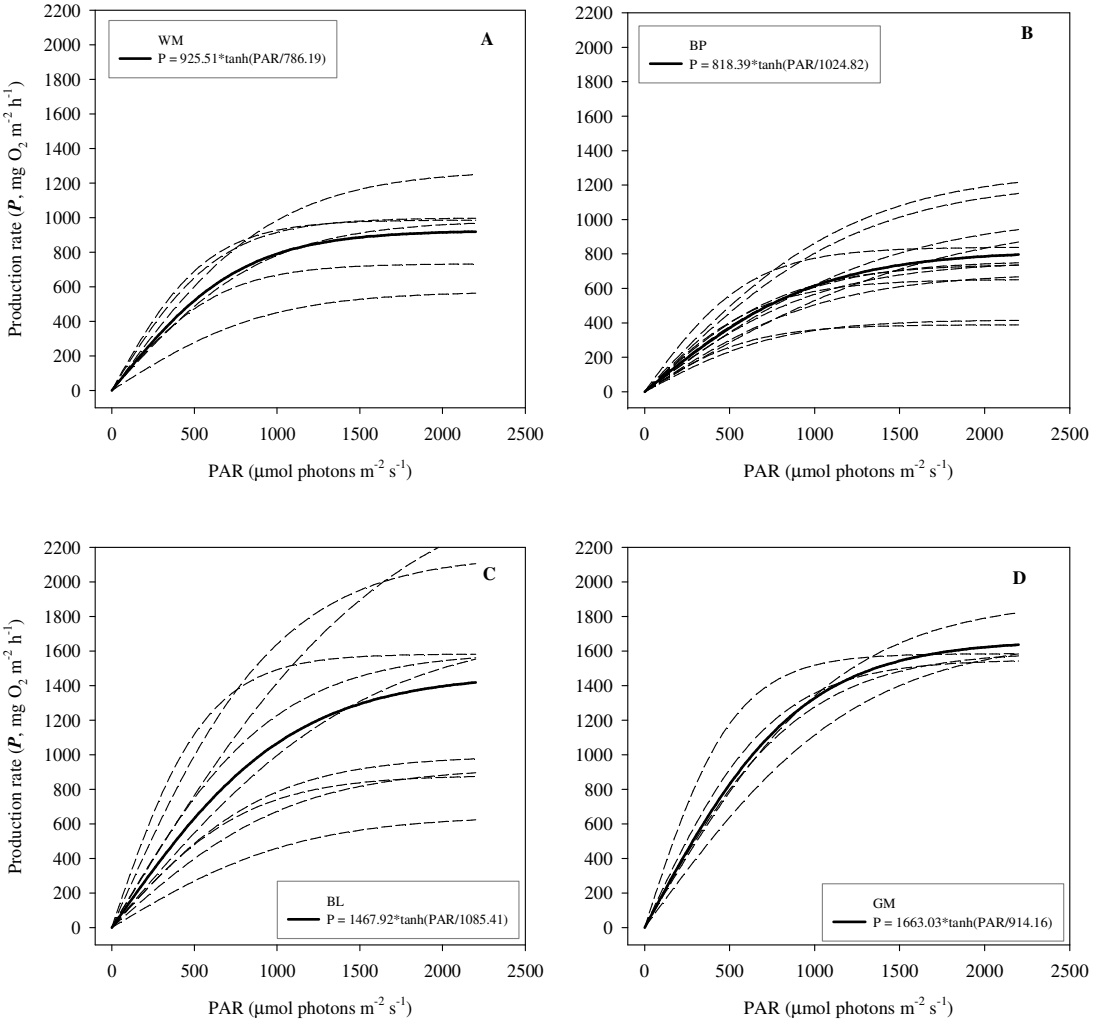

Figure 5.8 Plots of instantaneous production rate vs. incoming photosynthetically active radiation (PAR, *µmol photons* m^{-2} s^{-1}) for all sampling events for Grand River sites based on the parameters determined using ROM-TM. Subplot (A): site WM; (B): site BP; (C): site BL; and (D): site GM. The solid curves (*P-I* curves) describe the production-light responses for each site, using the average of the maximum production rate ($\boldsymbol{P_m}$, *mg* O_2 m^{-2} h^{-1}) and the production efficiency (***a***, *mol* O_2 *(mol photon)*$^{-1}$) of each site. The dash lines are for each sampling date.

5.3.4 Underwater light profiles

Underwater light profiles were measured at site BL on August 17-20, 2011. In open water where surrounding plant patches had been removed, they generally followed the Beer-Lambert Law; the intensity of incoming light exponentially decreased with depth. Approximately 90% incoming light penetrated the water surface, and over 30% of surface PAR could reach to 80 cm (Figure 5.9). However, heavy shading within *Stuckenia pectinata* patches (Figure 5.10), the dominant plant species at site BL, led to rapidly decreasing of light availability. In the situation of plant shading, the intensity of light exponentially decreased with depth. Only 30% of surface PAR could reach to a depth of 10 cm, and around 95% was attenuated at 40 cm (Figure 5.9).

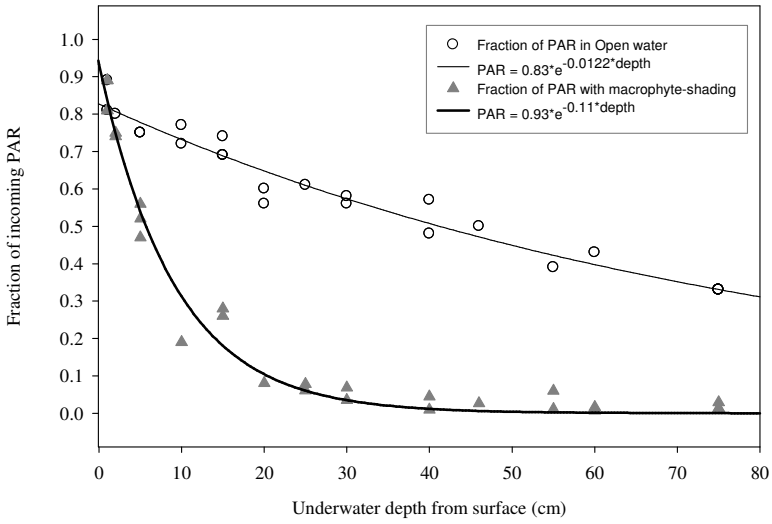

Figure 5.9 Underwater light profiles under the situation of open water and with macrophyte-shading at site BL in August 17-20, 2011. Solid lines are regression lines.

Figure 5.10 *Stuckenia pectinata* patches at site BL in the late August.

5.3.5 Depth profiles of *S. pectinata* biomass

The accumulated biomass of *S. pectinata* stands generally increased non-linearly with water depth (Figure 5.11A). The cumulative fraction of stand biomass (CFoSB) from water surface to river bed could be approximated as an exponential increase (CFoSB = $0.983*(1-e^{-0.0386*depth})$, R^2=92%; Figure 5.11B). A high fraction (30%) of stand biomass occurred within the first 10 cm of the water surface, and almost 50% of stand biomass was concentrated within the first 20 cm (Figure 5.11B).

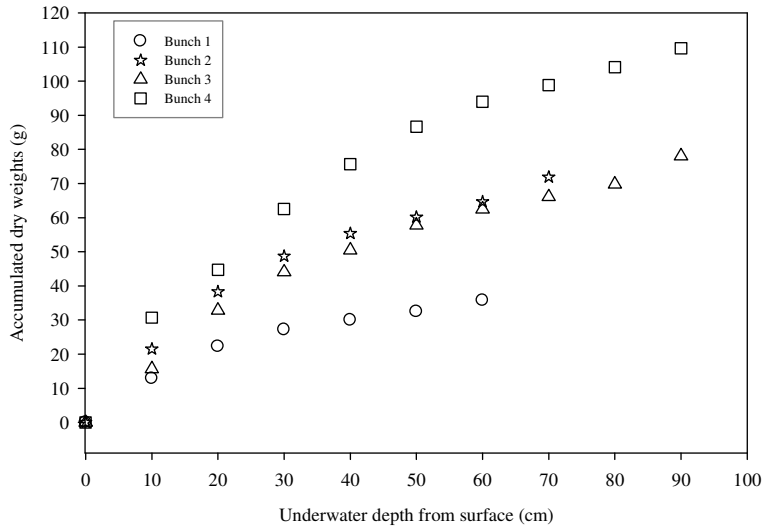

Figure 5.11A Depth profiles of accumulated dry weights of 4 *S. pectinata* stand bunches at site BL in August 17-20, 2011.

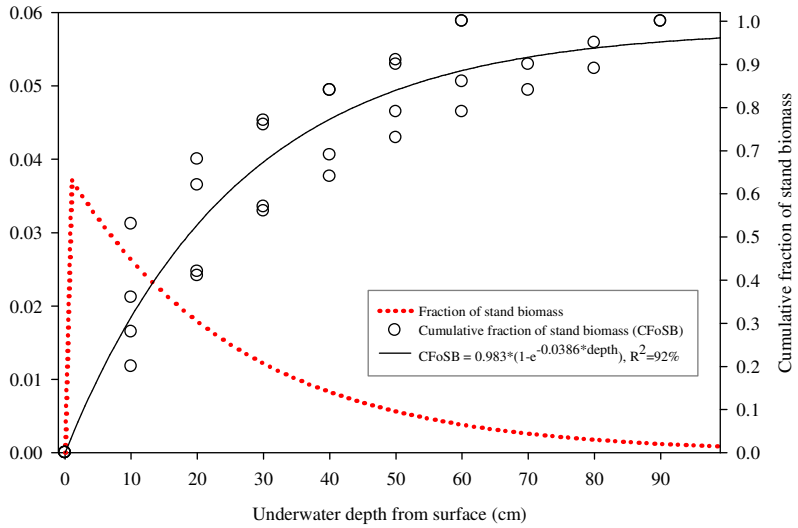

Figure 5.11B Fraction and accumulated fraction of total biomass of *S. pectinata* stands with depth (from water surface to river bed) at site BL in August 17-20, 2011.

I combined the depth profiles of light intensity and stand biomass in Figure 5.12, to illustrate how much light plants can receive with depth. For example, 30% of stand

biomass was within the first 10 cm at the water surface; these plants can receive >30% surface PAR (Figure 5.12). 20% of stand biomass was within 10 cm to 20 cm from the water surface. These plants only receive 10% to 30% surface PAR (Figure 5.12).

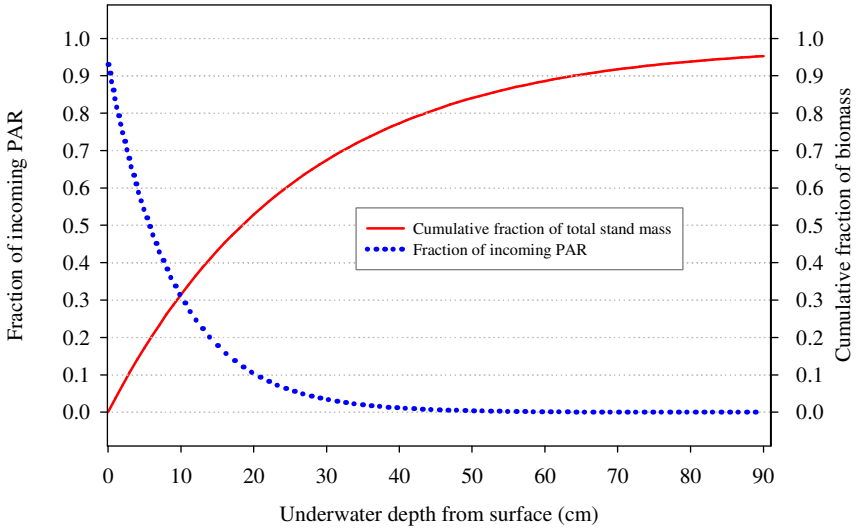

Figure 5.12 Depth profiles of light availability and accumulated fraction of biomass in *S. pectinata* stands at site BL in late August, 2011.

5.4 Discussion

This work is the first study to report patterns and characteristics of production parameters and production-light responses at the ecosystem level in a river network. A previous study of a New Zealand river at eight sites (Young and Huryn 1996) only reported the P-I relationships for gross primary production.

5.4.1 Production characteristics of a river ecosystem

The results demonstrate longitudinal gradients of production parameters $\boldsymbol{P_m}$, $\boldsymbol{a}$, and derived $\boldsymbol{I_k}$ and $\boldsymbol{E_c}$, in addition to site-specific variation due to local effects of environmental variables. In general, both $\boldsymbol{P_m}$ (38 to 2677 mg O_2 m^{-2} h^{-1}) and $\boldsymbol{I_k}$ (52 to 1740 μmol photons m^{-2} s^{-1}) exhibited increases with stream order (Figure 5.3 and Figure

5.5). However, the production efficiency, $\boldsymbol{a}$ (0.013 to 0.037 mol O_2 (mol photon)$^{-1}$) and the compensation point, $\boldsymbol{E_c}$ (73 to 888 μmol photons m^{-2} s^{-1}) did not exhibit a clear trend with stream order (Figure 5.4 and Figure 5.6). These patterns may be driven by the longitudinal patterns of light availability and plant community. With increasing stream size, the channels widened and received more incoming light. The consequent changes of plant communities might include increased abundance of sun-adapted plants, increased areal biomass of the aquatic plant community, multilayered structure, etc. These changes had positive effects on $\boldsymbol{P_m}$, but not apparently on $\boldsymbol{a}$, leading to different patterns among these two production parameters.

The increase of density and areal biomass of plant communities may be dominant contributing factors to $\boldsymbol{P_m}$ and $\boldsymbol{a}$ at and beyond the community level (Kelly et al. 1983, Binzer and Sand-Jensen 2002, Binzer et al. 2006). The density and biomass of communities naturally increase along the length of the river, likely due to increased light availability, nutrients, depth and width. I did not measure biomass at 2nd to 5th order sites. However, according to my visual inspection on sampling days, the density and biomass of periphyton were approximately 2nd order sites < 4th order sites < 3rd order sites < 5th order sites. There were no obvious plants at 2nd order sites, especially at site 2NF where sediments were unstable clays and fine sands. Maybe that is why site 2NF had the lowest $\boldsymbol{a}$ among all sites (Figure 5.4 & Table 5.2). My 4th order sites only had low density periphyton. Abundant periphyton occurred at site 3NF. Both periphyton and macrophyte patches were found at site 3F. There were prolific mosses and high density periphyton at site 5F, which is likely because of the mixed gravel-cobble substrate that is quite stable in shallow water. Site 5NF had dense moss and periphyton including macroalgae, *Cladophora glomerata,* probably favored by cold water and low speed current. Hence, the trend of $\boldsymbol{P_m}$ with stream size may be explained well in accordance with the trend of density and biomass at these sites. For example, 3rd order sites had higher $\boldsymbol{P_m}$ than 4th order sites.

Hood (2012) measured the macrophyte biomass at Grand River sites, WM, BP, BL and GM in August 2007 and 2009. The ranges of average biomass of macrophyte

community were around 30~40, 100~200, 200~300 g dry wt/m^2 at WM, BP, and BL and GM, respectively. These data also suggest that the trend of $\boldsymbol{P_m}$ in macrophyte-dominated reaches along the Grand follows the trend of macrophyte biomass. However, site WM had a higher average $\boldsymbol{P_m}$ than BP, which probably involves other mechanisms such as community composition and light utilization, and will be discussed later. A high $\boldsymbol{P_m}$ was reported by Kelly (1983), 580-900 mg O_2 m^{-2} h^{-1} in August in a small macrophyte-dominated river, Gryde River, Denmark. The Gryde River was only 2.9 m wide but had high macrophyte biomass, around 150 g dry wt/m^2, in August. Hence, this mass supports a $\boldsymbol{P_m}$ that is similar to my 7th order macrophyte-dominated site BP, but is still lower than other two 7th order sites, BL and GM (Table 5.4).

Significant effects of riparian trees on $\boldsymbol{I_k}$ and $\boldsymbol{E_c}$ were detected for 2nd-5th order stream sites. Non-shaded stream sites (2NF, 3NF, 4NF and 5NF) had higher levels of $\boldsymbol{I_k}$ and $\boldsymbol{E_c}$ (Table 5.2 & Figure 5.7), compared to their shaded counterparts (2F, 3F, 4F and 5F). Although both $\boldsymbol{P_m}$ and $\boldsymbol{a}$ were not statistically different between shaded and non-shaded streams, they also suggested a trend that high $\boldsymbol{P_m}$ and low $\boldsymbol{a}$ appear at open streams and low $\boldsymbol{P_m}$ and high $\boldsymbol{a}$ appear at shaded streams (Figure 5.7 & Table 5.2). This point may help understand why site 2NF still had higher $\boldsymbol{P_m}$ than site 2F, although site 2NF had very low plant biomass. These results may suggest that the effects of plant physiology, and shifting of shade-adaption plants/communities to sun-adaption plants/communities, can still extend to the ecosystem level. Studies on the photosynthesis-light responses of aquatic plants usually demonstrate that sun-adapted plants have higher $\boldsymbol{P_m}$ and higher light requirements, i.e., higher $\boldsymbol{E_c}$, $\boldsymbol{I_k}$, half-saturation constant and saturation point (Madsen et al. 1991, Kirk 1994), but lower $\boldsymbol{a}$ than shade-adapted plants due to fewer photosynthetic units (either in number or size, or both) or lower chlorophyll content (Kirk 1994). Incubation experiments on periphyton in small streams demonstrate that periphyton in open sites may have higher $\boldsymbol{P_m}$, $\boldsymbol{I_k}$, $\boldsymbol{E_c}$, and saturation point than shaded sites (Hill and Boston 1991, Guasch and Sabater 1995, Hill et al. 1995, Laviale et al. 2009). My study provides an example beyond the community level.

Table 5.4 Production parameters of aquatic plants, communities and rivers: maximum production rate ($\boldsymbol{P_m}$, *mg* O_2 m^{-2} h^{-1}), production efficiency ($\boldsymbol{a}$, *mol* O_2 *(mol photon)*$^{-1}$), compensation point ($\boldsymbol{E_c}$, *μmol photons* m^{-2} s^{-1}), onset of saturation ($\boldsymbol{I_k}$, *μmol photons* m^{-2} s^{-1}), irradiance required for half-maximal production rate ($\boldsymbol{K_m}$, *μmol photons* m^{-2} s^{-1}), and saturation point (*μmol photons* m^{-2} s^{-1}).

Aquatic plants & communities	P_m	a	E_c	I_k	K_m	Saturation point	Sources and notes
Autotrophs							
Diatoms				16~50			Cited in Kirk (1994), Table 10.1, P278, multiple sources
Phytoplankton				70-420			Cited in Coles & Jones (2000), mainly from tidal freshwater
Assemblages							
Algal biofilms	70-444		51-620	94-834			Dodds et al. (1999), 15 natural periphyton assemblages,
Biofilms	57~85		14 ~ 25	80 ~ 112			Guasch & Sabater (1995), Riera Major, undisturbed, 2nd order, **shaded**
	120~187		43 ~ 90	172 ~ 270			Guasch & Sabater (1995), La Solana, undisturbed, 2nd order, **open**
				352±17			Laviale et al. (2009), stream Sensée, **open**, 2W cultured in field
				453±221			Laviale et al. (2009), stream Sensée, **open**, 4W cultured in field
				670±153			Laviale et al. (2009), stream Sensée, **open**, 6W cultured in field
Stream periphyton	40~135	0.002~0.007		148~207			Hill & Boston (1991), site WOC 2.4, **dense canopy**, 8- to 58-d cultured in field, Lab incubation at ~ 20℃.
	17~220	0.0007~0.01		127~196			Hill & Boston (1991), site WOC 3.4, **moderate canopy**, 7- to 55-d cultured in field, Lab incubation at ~ 20℃.
	172~238	0.007~0.011		215~292			Hill & Boston (1991), Hinds Creek, **no canopy**, 17- to 66-d cultured in field, Lab incubation at ~ 20℃.
	15.4	0.0023		59		237	Hill et al. (1995), WOC, 2nd order stream, **shaded**, at ~ 17℃.
	11	0.001		113		445	Hill et al. (1995), WOC, 2nd order stream, **open**, at ~ 17℃.
Ecosystems							
Small streams						>200-500	Mulholland et al, (2001), two streams, stream width 2.4 m & 3.2 m
Small streams	38-175	0.002-0.016	73-441	52-332	0.55*$\boldsymbol{I_k}$	138-880	This study, 2nd order streams (2F & 2NF)
	252-621	0.005-0.037	85-333	148-488	0.55*$\boldsymbol{I_k}$	392-1293	This study, 3rd order streams (3F & 3NF)
Middle streams	175-422	0.003-0.022	77-362	88-595	0.55*$\boldsymbol{I_k}$	233-1577	This study, 4th order streams (4F & 4NF)
	278-1300	0.008-0.031	96-243	219-664	0.55*$\boldsymbol{I_k}$	580-1760	This study, 5th order streams (5F & 5NF)

Table 5.4 Extended.

Macrophytes							
C. caroliniana			55		160	700	Van et al (1976), apical section, Lab incubation at 30℃
C. demersum			35		145	700	Van et al (1976), apical section, Lab incubation at 30℃
C. glomerata			44~104*			345-1125*	Multiple sources cited in Lester (1988), temperature dependant
			43±32	189±124			Higgins et al. (2008), in vitro incubation, 15℃ ~ 20 ℃
E. canadensis			~ 12		~ 25		Madsen et al. (1991), apical/subapical section, Lab incubation at 20℃
H. verticillata			15		80	600	Van et al (1976), apical section, Lab incubation at 30℃
M. spicatum			~ 37		~ 92		Madsen et al. (1991), apical/subapical section, Lab incubation at 20℃
			35		120	600	Van et al (1976), apical section, Lab incubation at 30℃
			84±35	341±134			Harley & Findlay (1994), apical section, incubation in field
P. praelongus			~ 13		~ 22		Madsen et al. (1991), one/two leaves, Lab incubation at 20℃
P. amplifolius			~ 12		~ 31		Madsen et al. (1991), one/two leaves, Lab incubation at 20℃
P. gramineus			~ 22		~ 43		Madsen et al. (1991), one/two leaves, Lab incubation at 20℃
			10				Spencer & Ksander (2001), Lab growth & incubation at 25℃
P. perfoliatus			52±22	387±123			Harley & Findlay (1994), apical section, incubation in field
			25~30				Goldsborough & Kemp (1988)
P. robbinsii			~ 20		~ 37		Madsen et al. (1991), one/two leaves, Lab incubation at 20℃
S. pectinata			10~25			300~400	van Derbijl et al (1989), van Dijk and vanVierssen (1991)
			45				Spencer & Ksander (2001), Lab growth & incubation at 25℃
V. americana			30±36	179±77			Harley & Findlay (1994), apical section, incubation in field
			~ 10		~ 25		Madsen et al. (1991), one/two leaves, Lab incubation at 20℃
Macrophytes			0.2-55				Sondegaard (1988), multiple sources
Macrophyte phytoelements	1014(336-1567)	0.048(0.014-0.096)	22(5.0-52)	151(57-308)		337(82-700)	Binzer et al. (2006), summary of 31-151 studies on aquatic macrophyte phytoelements. Data form are average (5-95th percentiles).
Macrophyte communities	1636(363-2903)	0.036(0.007-0.076)	119(40-226)	455(203-795)		Not sat.	Binzer et al. (2006), summary of 190 studies on aquatic macrophyte communities. Data are average (5-95th percentiles).
Ecosystems							
Gryde river	580~900				94 ~ 210		Kelly (1983), small macrophyte dominated river, water width 2.9 m
Grand River	574-1277	0.005-0.015	200-370	577-978	$0.55*I_k$	>1530	This study, site WM (6^{th} order)
	390-1287	0.005-0.012	209-484	621-1740	$0.55*I_k$	>1640	This study, site BP (7^{th} order)
	649-2677	0.005-0.024	349-888	568-1700	$0.55*I_k$	>1500	This study, site BL (7^{th} order)
	1550-1900	0.012-0.026	264-350	522-1255	$0.55*I_k$	>1380	This study, site GM (7^{th} order)

Biomass and other factors may confound the effects of physiological characteristic of plant compositions beyond the community level. Hence, we did not see significantly different $\boldsymbol{P_m}$ and $\boldsymbol{a}$ between shaded and non-shaded streams. Possibly as a result of the combined effects of multiple factors, $\boldsymbol{a}$ was independent of stream size or light availability in the Grand River (Figure 5.4). Shifts from shade-adapted to light-adapted plants along the river may cause negative effects on $\boldsymbol{a}$. However, increased biomass and the more complex structure of plant community may offset this systematic, physiological-level loss of primary production capacity. This point may help understand the highest value for $\boldsymbol{a}$ in my study, 0.022 mol O_2 (mol photon)$^{-1}$ at site 5NF.

Multi-species communities may be able to utilize light more efficiently than single-species communities, leading to positive effects on $\boldsymbol{a}$ and then $\boldsymbol{P_m}$ (Middelboe and Binzer 2004, Binzer and Middelboe 2005). Possible mechanisms that enhance light use in multispecies communities include better horizontal space utilization, e.g., one species occupies where the other species cannot, and increased vertical space utilization, e.g., a blend of sun-adapted and understory shade-adapted species (Middelboe and Binzer 2004). The spatial effect mechanism may explain why site 5NF had the same $\boldsymbol{a}$, and higher $\boldsymbol{P_m}$, than site 5F. Although site 5NF was fully open and might be expected to have low $\boldsymbol{a}$ due to sun-adapted periphyton in summer, mixed *C. glomerata* and stream periphyton communities may have contributed to the high $\boldsymbol{a}$ and $\boldsymbol{P_m}$ of this stream. The spatial effect mechanism can be also applied to explain the differences among large river sites in this study. *M. spicatum* and *S. pectinata* are two macrophytes dominating in main channel of the Grand River. Madsen et al. (1991) demonstrated that *M. spicatum* is a high-light adapted macrophyte exhibiting high $\boldsymbol{P_m}$ and a high light requirement compared to many native species in the family *Potamogetonaceae*. *M. spicatum* in the Hudson River had a $\boldsymbol{P_m}$ of 9.3 (8.8 - 14.4) mg O_2 g^{-1} DW h^{-1}, an $\boldsymbol{I_k}$ of 341.1 (173.2 - 451.1) μmol photons m^{-2} s^{-1} and an $\boldsymbol{a}$ of 0.04 (0.02 - 0.06) mg O_2 g^{-1} DW h^{-1}/μmol photons m^{-2} s^{-1} in July and August (Harley and Findlay 1994). In contrast, *S. pectinata* in a Danish lowland stream had a $\boldsymbol{P_m}$ of 5.7 (4.8 - 7.4) mg O_2 g^{-1} DW h^{-1} and an $\boldsymbol{a}$ of 0.06 (0.05 - 0.08) mg O_2 g^{-1} DW h^{-1}/μmol photons m^{-2} s^{-1} in July and August (Vanderbijl et al, 1989, data estimated from their Figure 2). Hence, *M. spicatum* may have higher $\boldsymbol{P_m}$ but lower $\boldsymbol{a}$ than *S. pectinata*.

Site WM was 21 km upstream of site BP, and had similar environmental factors in terms of water depth, nutrients and light availability during sampling days. Site WM had a mixed plant community of these two macrophytes, but site BP was dominated only by *M. spicatum*. Site BP had higher macrophyte biomass than site WM (Hood 2012). However, the $\boldsymbol{P_m}$ of site BP was lower than site WM. This may be the result of enhanced $\boldsymbol{a}$ due to the mixed plant communities at site WM. The principle may also provide an explanation for the differences between site BL and GM in the study. Similarly, site GM was 19 km downstream site BL, and both of them were fully open and had similar levels of nutrients (Table 5.1) and macrophyte biomass (Hood 2012). Site GM had a mixed plant community of *M. spicatum* and *S. pectinata*, but *S. pectinata* dominated at site BL. However, site GM exhibited not only a higher $\boldsymbol{P_m}$, but also a higher $\boldsymbol{a}$ than site BL (Table 5.2).

Except site BL, the compensation point, $\boldsymbol{E_c}$, of sites in the Grand River seemed to be stream-size independent (Figure 5.6). This pattern resulted from the different effects of various factors. The $\boldsymbol{E_c}$ is determined not only by $\boldsymbol{a}$, but also by ecosystem respiration. Ecosystem respiration is dependent on temperature (Del Giorgio and Williams 2005), and is also affected by other factors such as nutrients (Gucker et al. 2009, Wassenaar et al. 2010), community abundance and biomass (Yvon-Durocher et al. 2012), and any COD from WWTP effluents etc. The highest $\boldsymbol{E_c}$ (658 μmol photons m^{-2} s^{-1}) occurred at site BL and was possibly driven by high nutrient inputs and the NH_4^+ load from upstream WWTPs. The details will be discussed in Chapter 6.

The effect of water depth should be taken into consideration in deep reaches. Increased water depth lowers underwater light availability at the substrate, but could support more plant biomass and alter the vertical structure of the plant community. *S. pectinata* can develop ~ 2 m shoots at site BL. Once the shoots are longer than the water depth, *S. pectinata* stands tend to concentrate plant biomass and productivity at the water surface, leading to self-shading.

Temperature may have important effects on photosynthetic production characteristics of a river ecosystem, at least if studies on the effects of temperature on P-I

relationships of phytoplankton (Rae and Vincent 1998, Coles and Jones 2000), macroalgae (Lester et al. 1988), and periphyton assemblages (Laviale et al. 2009) are relevant.

Overall, the production characteristics of a river ecosystem are a complex result of light availability, plant physiology, abundance, and community structure, as well as other abiotic factors that influence aquatic plants and their distribution, e.g., nutrients.

5.4.2 Scale effects: from individual to community, to ecosystem

This study provided ecosystem-level data on production parameters of streams with different sizes. The 2nd to 4th order sites and site 5F in this study were dominated by periphyton and lacked macrophytes. For two 2nd order sites, 2F and 2NF, both primary production parameters $\boldsymbol{P_m}$ (38 to 175 mg O_2 m^{-2} h^{-1}) and $\boldsymbol{a}$ (0.002 to 0.016 mol O_2 (mol photon)$^{-1}$), and the derived parameter $\boldsymbol{I_k}$ (52 to 332 μmol photons m^{-2} s^{-1}) and saturation point (138 to 880 μmol photons m^{-2} s^{-1}) had similar ranges to incubation studies on periphyton in small streams (Hill and Boston 1991, Guasch and Sabater 1995, Hill et al. 1995). Mulholland (2001) reported a similar range of the light demand for saturation (>200 to 500 μmol photons m^{-2} s^{-1}) in two small streams with widths of 2~3 m using the whole stream O_2 method.

The $\boldsymbol{P_m}$, $\boldsymbol{I_k}$, $\boldsymbol{E_c}$ and saturation point increased with stream size as discussed in the previous section. The periphyton-dominated, 3rd to 5th order sites in my study exhibited obviously higher levels of these parameters compared to incubation studies on periphyton in small streams (Table 5.4). It is not clear whether production parameters of periphyton living in small streams and middle-sized streams would be significantly different at the community level. Dodds et al. (1999) provided a broader range of $\boldsymbol{P_m}$ (70 - 444 mg O_2 m^{-2} h^{-1}), $\boldsymbol{E_c}$ (51 - 620 μmol photons m^{-2} s^{-1}) and $\boldsymbol{I_k}$ (94 - 834 μmol photons m^{-2} s^{-1}) for 15 natural periphyton assemblages/communities. They are comparable to periphyton dominated sites in my study (Table 5.4). Variation in production parameters of periphyton may be due to the differences in community composition and structure,

such as assemblage thickness (Dodds et al. 1999) and community development (Hill and Boston 1991, Laviale et al. 2009).

Binzer et al. (2006) provided comprehensive summaries of production parameters of aquatic macrophyte phytoelements and communities by compiling results from 190 studies of plant production vs. light at the individual and community level. I converted the data to the same units as in this study (Table 5.4). $\boldsymbol{P_m}$ increased from 1014 mg O_2 m^{-2} h^{-1} at the individual level to 1636 mg O_2 m^{-2} h^{-1} at the community level (Binzer et al. 2006), but this increase did not extend to the ecosystem level. My study had 4 large river sites dominated by macrophytes. The average $\boldsymbol{P_m}$ was 930 (range = 574 - 1277), 818 (range = 390 - 1287), 1468 (range = 649 - 2677) and 1663 (range = 1550 - 1900) mg O_2 m^{-2} h^{-1} at sites WM, BP, BL and GM, respectively. The $\boldsymbol{P_m}$ at sites WM and BP were much less than those in Binzer's study, both at the individual level and the community level. Sites BL and GM had comparable $\boldsymbol{P_m}$ to the community-level $\boldsymbol{P_m}$'s in Binzer et al (2006). These high $\boldsymbol{P_m}$'s at site BL and GM were supported by prolific growth of macrophytes, probably due to nutrients from upstream WWTPs. Hence, it appears that the ecosystem-level $\boldsymbol{P_m}$ of rivers is less than that the community level $\boldsymbol{P_m}$. This might be because river ecosystems include both productive areas (e.g., macrophyte patches) and non-productive areas (e.g., bare rocks, deep pools).

Individual aquatic macrophytes have higher production efficiency, $\boldsymbol{a}$, than entire macrophyte communities, which have previously recorded as 0.048 and 0.036 mol O_2 $(\text{mol photon})^{-1}$, respectively (Binzer et al. 2006). These values are higher than my data for the production efficiency at the ecosystem level. In summary, production efficiency appears to decrease from individual to community and to ecosystem.

Derived parameters ($\boldsymbol{I_k}$, $\boldsymbol{E_c}$, and saturation point) should increase from the individual level to the community level, and then to the ecosystem level. Binzer (2006) reported that the mean light compensation point, $\boldsymbol{E_c}$, for aquatic macrophyte phytoelements was 22 (range = 5.0-52) μmol photons m^{-2} s^{-1}, which was very close to the $\boldsymbol{E_c}$ of submersed aquatic macrophytes in Søndergaaard's study, 0.2 to 55 μmol photons m^{-2} s^{-1} (Søndergaaard 1988). A large number of tissue incubation studies, either in the lab

or in the field, have found E_c of aquatic macrophytes less than 55 μmol photons m^{-2} s^{-1} (Table 5.4), except two. Lester (1988) reviewed a broad range of the E_c for *C. glomerata*, 44-104 μmol photons m^{-2} s^{-1}, based on multiple sources. E_c for *M. spicatum* was up to 84 μmol photons m^{-2} s^{-1} in a field incubation experiment (Harley and Findlay 1994). The E_c of aquatic macrophyte communities was higher, ranging from 40 - 226 μmol photons m^{-2} s^{-1} with an average of 119 μmol photons m^{-2} s^{-1} (Binzer et al. 2006). My study in the Grand River yielded an average E_c of 300 (range = 200 - 370), 311 (range = 209 - 484), 658 (range = 349 - 888), and 315 (range = 264 - 350) μmol photons m^{-2} s^{-1} at site WM, BP, BL and GM, respectively (Table 5.2 & Table 5.4). Therefore, I conclude that E_c increases from the individual level to the community level, and to the ecosystem level.

I_k had the same trend as E_c as the scale increased. In incubation experiments at the individual level, the I_k of *C. glomerata* and *M. spicatum* were reported to be 189 and 341 μmol photons m^{-2} s^{-1}, respectively (Harley and Findlay 1994, Higgins et al. 2008). The average I_k of aquatic macrophyte phytoelements and communities reported by Binzer et al. were 151 (57 - 308) and 455 (203 - 795), respectively (Binzer et al. 2006) (Table 5.4). My study demonstrated a higher average level of the I_k at the ecosystem scale in the central portion of the Grand River; 786 (range = 577 - 978), 1025 (range = 621 - 1740), 1085 (range = 568 - 1700) and 914 (range = 522 - 1255) μmol photons m^{-2} s^{-1} at site WM, BP, BL and GM, respectively (Table5.2 & Table 5.4).

Three major macrophytes in the Grand River, *C. glomerata*, *M. spicatum* and *S. pectinata*, were reported as having saturation points of 345-1125 (Lester et al. 1988), 600 (Van et al. 1976) and 300-400 μmol photons m^{-2} s^{-1} (Vanderbijl et al. 1989, Vandijk and Vanvierssen 1991), respectively. These values are close to or slightly larger than the saturation point of aquatic macrophyte phytoelements, 337 (82 - 700) μmol photons m^{-2} s^{-1} (Binzer et al. 2006). Binzer (2006) found no sign of photosaturation or photoinhibition of aquatic macrophyte communities, even at highest irradiances of about 2000 μmol photons m^{-2} s^{-1}. My study had similar results for the Grand River. Extensive self-shading of macrophytes and high nutrients may be the major reasons, leading to light limitation at large river sites.

5.4.3 Primary production at high light intensity of the Grand River

Both light-limited and light-saturated O_2 production were observed at the ecosystem level in the Grand River. Young and Huryn (1996) found no ecosystem-level evidence of photoinhibition and no apparent saturation of production in most of instances in a New Zealand river.

Compensatory effects of multilayered macrophyte communities might explain why inhibition was not observed (Binzer et al. 2006). Although the channel in the central portion of the Grand River was wider and received less shading from riparian trees, self-shading from prolific growth of macrophytes occurred in summer. Self-shading occurred vertically so that only part of the community would experience photoinhibition. Also, river flow caused long plant shoots to keep swinging up and down, side to side, possibly reducing photoinhibition. Apical shoots did not always stay at the surface to experience high light intensities all the time.

The direct effect of macrophyte self-shading is to increase the $\boldsymbol{E_c}$ and $\boldsymbol{I_k}$ at the community level (Binzer et al. 2006). Studies on periphyton assemblages exhibited the same phenomenon (Dodds et al. 1999, Laviale et al. 2009). Higher $\boldsymbol{I_k}$ means that more light is required to reach $\boldsymbol{P_m}$. For the production rate to reach 95% $\boldsymbol{P_m}$, the light required for this would be 1.83 times $\boldsymbol{I_k}$ according to the hyperbolic model (PAR/$\boldsymbol{I_k}$ = ATANH (0.95$\boldsymbol{P_m}$/$\boldsymbol{P_m}$), Equation 5.1). In summer, maximum PAR was usually about 2000 μmol photons m^{-2} s^{-1}. Hence, an $\boldsymbol{I_k}$ $\geq$1090 μmol photons m^{-2} s^{-1} (=2000/1.83) means that full saturation might not be achievable even at the highest irradiances. In this study, the average $\boldsymbol{I_k}$ was 786, 1025, 1085 and 914 μmol photons m^{-2} s^{-1} for main channel sites WM, BP, BL and GM, respectively. These average values would allow these sites to reach 95%-99% $\boldsymbol{P_m}$ at maximum PAR in summer (Table 5.2). However, sites BP and BL on some sampling days had $\boldsymbol{I_k}$'s of close to 1800 μmol photons m^{-2} s^{-1} (Figure 5.5). Hence, full light-saturation might not even be reached on these days.

This study also provided evidence for light limitation of photosynthesis at site BL from measurement of underwater light and biomass profiles. At the maximum level of light intensity, 2000 μmol photons m^{-2} s^{-1}, over 50% of the leaf mass would not obtain

light $\geq I_k$ (Table 5.2 & Figure 5.12). One weakness of these data is the lack of measures of chlorophyll content of plant parts with depth. Vertical distribution of chlorophyll a can be used to weight the vertical profiles of leaf tissues with different photosynthetic production capacity. Nonetheless, it seems that the high plant biomass at BL generates self-shading. This may put a limit on the biomass response to nutrients.

– Chapter 6 –

Stream ecosystem metabolism in an impacted temperate river network: magnitude, variability and temporal-spatial patterns

6.1 Introduction

Ecosystem metabolism is related to many critical ecological processes such as diel cycles of oxygen and pH, nutrient cycling (Hall and Tank 2003, Dodds et al. 2008), energy flow (Odum 1957b, Rosenfeld and Mackay 1987) and community dynamics (Naiman et al. 1987, Taylor et al. 2006). The primary task when measuring metabolism usually is to obtain the magnitude and variability of primary production (P) and respiration (R). These are affected by plant communities and abiotic factors such as light, temperature, nutrients, river hydraulics (flow), substrata, etc. (Fisher et al., 1982; Bott et al., 1985; Uehlinger 2000a, 2000b, 2005; Mulholland 2001).

Anthropogenic activities have greatly changed stream ecosystems. Some features of impacted ecosystems may be more human-disturbance controlled than naturally controlled (e.g., by climate, geology and hydrology) as seen as in pristine or less disturbed streams. The assessment of disturbed river ecosystems has been the subject of many aquatic ecological studies. In recent years, measures of stream metabolism have been frequently used to quantify the impacts of human disturbance and indicate stream ecosystem health (Young 2006, McTammany et al. 2007, Bernot et al. 2010, Clapcott et al. 2010, Wassenaar et al. 2010).

Reliable ecosystem-level methods based on dissolved oxygen (DO) time series for measuring metabolism in streams have been available since Odum (1956) first

proposed the whole-stream approach, and many efforts to quantify stream metabolism have been made (Odum 1956, 1957a, Wright and Mills 1967, McDiffet et al. 1972, Fisher and Carpenter 1976, Bott et al. 1978, Chessman 1985, Naiman et al. 1987, Meyer and Edwards 1990, Wiley et al. 1990, Uehlinger 1993, Marzolf et al. 1994, Young and Huryn 1996, Bott et al. 2006b). Such work has contributed greatly to the development of aquatic ecology in both theory and application. In recent years, oxygen isotopes have expanded the suite of methods that can be used in the study of aquatic ecosystem metabolism (Quay et al. 1995, Tobias et al. 2007, Venkiteswaran et al. 2007, Holtgrieve et al. 2010, Quay et al. 2010, Karim et al. 2011, Luz and Barkan 2011).

The goal of this work was to explore the application of $\delta^{18}O$ to studies of ecosystem metabolism of impacted streams and rivers, and to examine the effects of human activities on ecosystem metabolism in an agricultural and urban impacted temperate river, Grand River, Ontario, Canada. Testable hypotheses included (1) the daily amplitude of dO_2 variation increases with stream size due to increasingly intense respiration and photosynthesis downstream, (2) gross primary production (GPP), ecosystem respiration and GPP/ER ratios will increase with stream size within Grand River catchment, (3) the ratio of GPP/ER from headwater to middle reaches is greater than 1.0 due to the deforested and open channel associated with loss of riparian vegetation and increased sunlight at headwater, (4) due to light availability, shaded sites in small and middle-sized streams have lower daily variation in dO_2 and ^{18}O-dO_2 than those open sites with otherwise similar reach conditions, (5) because of light availability and allochthonous organic matter inputs, shaded sites have less photosynthesis and respiration, and are more heterotrophic (have lower GPP/ER) than those open sites with otherwise similar reach conditions, and (6) WWTP effluents have strong positive effects on metabolic rates in the Grand River. To do this, I measured stream metabolism in multiple streams with different sizes in the Grand River basin using the whole-system one-station method with dual O_2 budgets (DO and $\delta^{18}O$-DO).

6.2 Materials and methods

6.2.1 Study sites

A total of 14 stream and river sites were chosen for study. These sites were distributed from headwater streams of the Speed River to the middle reaches of the Grand River, with the stream order varying from 2nd to 7th order. Eight stream sites (2F, 2NF, 3F, 3NF, 4F, 4NF, 5F and 5NF) and one large river site WM, are impacted by agriculture. The other 5 river sites (SPa, SPb, BP, BL and GM) are located in urban areas; and 3 sites (SPb, BL and GM) are downstream of large WWTPs. Descriptions of each site were provided in Chapter 3 (Figure 3.2), as were water sampling and lab analysis methods.

6.2.2 Data used and analysis

The model ROM-TM (Chapter 4) was used to model DO and δ^{18}O-DO and thereby obtain estimates of metabolic parameters and daily metabolic rates and ratios from each diel/diurnal sampling. Reconstructed diel DO and δ^{18}O-DO curves are in Appendix-A. Stream order of each site came from GIS data provided by GRCA. The total length of streams of each order was calculated from the same GIS data. Correlation analyses and regression were used to determine relationships between independent variables and metabolic rates and ratios (e.g., GPP, ER, NPP and GPP: ER). Two-way analysis of variance was used to examine the effect of stream order and riparian trees on metabolic rates (e.g., GPP, ER, NPP and GPP: ER) for streams from 2nd to 5th order.

6.3 Results

6.3.1 Environment parameters: physical variables and water chemistry

Environmental parameters were measured and recorded during each sampling day for all sites (Table 6.1A and Table 6.1B).

Hydrological variables such as discharge, water depth and channel width generally increased with stream order in the Grand River network (Table 6.1A & 6.1B).

Channel width spanned two orders of magnitude and from 1.1 to over 100 m (Table 6.1A & 6.1B). Mean depth varied from 0.15 m to 0.85 m from small streams to large river sites (Figure 6.1A). Discharge ranged from 0.008 $m^3 s^{-1}$ at site 2NF to around 50 $m^3 s^{-1}$ at Grand River site GM during sampling periods (Figure 6.1B). Mean daily temperature for sites were from 12.2 to 26.7 ℃ on sampling days, and mean daily pH ranged from 7.83 to 8.89 (Table 6.1A & 6.1B).

Table 6.1A Geomorphological, hydrological, physical, chemical and biological characteristics of 14 sampling sites in the Grand River network and at or near the time of metabolism measurements. Data are mean (±1SD, ranges and n).

Site	Date	Width	Depth	Discharge	Radiation	Temperature	pH	Salinity	Conductivity	$\delta^{18}O\text{-}H_2O$
		m	cm	$m^3\ s^{-1}$	mol m^{-2} day^{-1}	℃		PPT	µS	‰
2F	15-Jul-08	1.3	24.0	0.022	16.0	14.3±3.1(11.1~18.1,7)	7.96±0.08(7.84~8.12,7)		650.1±3.4(646~654,7)	-10.25
	19-Aug-08	1.3	30.0	0.093	15.0	14.8±1.1(13.5~16.1,8)	7.92±0.05(7.80~7.97,8)		643.9±2.3(641~647,8)	-9.51
	22-Jun-09	1.3	27.0	0.077	15.5	14.4±2.0(12.4~17.4,7)	8.37		602.0±2.0(599~605,7)	-10.01
2NF	15-Jul-08	1.1	15.0	0.008	32.8	15.4±3.3(11.8~19.4,7)	8.17±0.12(8.01~8.32,7)		502.6±6.2(493~508,7)	-10.28
	19-Aug-08	1.1	25.0	0.035	28.0	14.4±1.0(13.3~15.8,6)	8.04±0.08(7.92~8.14,6)		504.7±1.9(502~507,6)	-9.40
	22-Jun-09	1.1	23.0	0.029	29.0	15.6±2.2(13.3~18.7,7)	8.32		480.9±1.1(479~482,7)	-10.15
3F	15-Jul-08	5	45.0	0.048	27.0	17.1±2.3(14.7~20.3,8)	8.05±0.14(7.78~8.18,8)		589.5±1.6(587~592,8)	-9.95
	19-Aug-08	5	55.0	0.197	22.0	16.6±0.7(15.7~17.5,8)	8.02±0.13(7.78~8.16,8)		572.5±1.2(570~574,8)	-10.52
	22-Jun-09	5	50.0	0.163	23.9	17.0±1.5(15.6~19.4,7)	8.09		558.3±2.3(555~561,7)	-10.20
3NF	15-Jul-08	2.2	25.0	0.024	36.0	17.2±4.6(12.7~23.4,8)	8.10±0.25(7.56~8.31,8)		600.3±10.9(586~611,8)	-9.63
	19-Aug-08	2.2	32.0	0.099	29.0	16.4±1.3(15.0~18.3,7)	8.07±0.21(7.77~8.32,7)		565.1±2.5(562~568,7)	-9.61
	22-Jun-09	2.2	30.0	0.082	30.4	18.2±1.9(16.3~21.1,7)	8.04		548.3±2.3(546~553,7)	-9.60
4F	22-Jul-07	6.5	38.0	0.112	27.3	16.9±2.1(14.5~20.7,17)	8.19±0.12(8.03~8.39,17)	0.25	511.2±6.8(503~521,17)	-9.98
	27-Aug-07	6.5	35.0	0.063	18.0	17.6±1.7(16.0~20.3,7)	8.24±0.17(8.05~8.46,7)	0.27	549.1±3.4(544~553,7)	-10.26
	5-Oct-07	6.5	33.0	0.056	17.2	12.7±1.5(11.6~15.1,6)	8.17±0.18(7.94~8.44,6)	0.27	553.8±5.3(546~559,6)	-10.38
	23-Jun-09	6.5	42.0	0.330	22.4	18.5±1.8(16.9~21.1,5)	8.45		523.0±2.6(519~525,5)	-9.89
4NF	22-Jul-07	4.0	22.0	0.082	28.4	17.5±2.2(15.0~21.1,17)	8.29±0.18(8.03~8.58,17)	0.22	460.8±6.4(453~471,17)	-9.81
	27-Aug-07	4.0	20.0	0.046	29.6	19.3±2.8(16.5~22.9,7)	8.23±0.22(7.94~8.48,7)	0.23	483.4±2.9(480~489,7)	-9.71
	5-Oct-07	4.0	15.0	0.041	20.8	14.9±2.7(12.2~18.7,7)	8.19±0.27(7.77~8.49,7)	0.25	503.1±10.7(487~513,7)	-10.16
	23-Jun-09	4.0	25.0	0.240	36.4	20.1±2.8(17.3~24,6)	8.44		498.8±2.9(494~502,6)	-10.02
5F	27-Aug-07	14.0	25.0	0.170	22.4	20.2±2.4(17.7~23.3,7)	8.33±0.23(8.05~8.62,7)	0.24	504.0±11.0(487~514,7)	-9.56
	5-Oct-07	14.0	20.0	0.150	18.3	15.5±2.2(13.5~18.5,6)	8.27±0.21(8.03~8.48,6)	0.26	521.2±7.1(512~528,6)	-9.67
	23-Jun-09	14.0	40.0	0.900	26.0	20.4±2.1(18.3~24,7)	8.47		552.4±4.9(544~557,7)	-9.68
5NF	27-Aug-07	13.3	60.0	0.097	45.1	19.1±1.6(17.4~21.4,7)	8.37±0.20(8.11~8.61,7)	0.27	552.6±6.1(545~560,7)	-10.23
	5-Oct-07	13.3	60.0	0.086	21.6	13.8±1.4(12.7~16.1,6)	8.22±0.22(7.98~8.48,6)	0.28	566.5±4.1(560~570,6)	-10.34
	23-Jun-09	13.3	75.0	0.515	29.6	19.3±1.7(17.7~21.7,6)	8.40		541.4±5.2(534~546,5)	-9.85
SPA	19-Jun-06	N/D	25.0	N/D	47.3	24.4±1.0(23.2~26.3,20)	8.22±0.11(8.10~8.42,20)	0.30	619.8±7.8(606~631,20)	-9.24
	19-Jun-07	N/D	25.0	N/D	36.6	21.2±0.5(20.5~22.1,17)	8.47±0.11(8.31~8.63,17)	0.26	534.6±4.2(528~541,17)	-9.02
SPB	19-Jun-06	30.0	63.0	1.8	47.8	24.2±1.5(22.1~26.5,19)	8.24±0.27(7.89~8.63,18)	0.50	1014.8±51.9(923~1069,19)	-9.12
	19-Jun-07	30.0	65.0	2.3	36.6	21.2±0.8(19.8~22.1,17)	8.33±0.27(7.96~8.69,17)	0.48	969.4±66.2(847~1057,17)	-9.80

Table 6.1A Extended.

Site	SRP	TP	NH_4^+	NO_3^-	NO_2^-	DOC	Chlorophyll *a*
	(µg/L)			(mg N/L)		mg C/L	µg/L
2F	6.5±2.6(3.5~8.2,3)	10.7±0.7(10.1~11.5,3)	0.228±0.180(0.052~0.412,3)	1.26±0.04(1.23~1.30,3)	0.005	1.97±0.33(2.26~5.90,3)	0.78±0.17(0.61~0.94,3)
	5.0±3.2(2.9~8.7,3)	7.2	0.012±0.006(0.005~0.016,3)	0.96±0.03(0.92~0.98,3)	0.004	4.15±0.13(4.06~4.30,3)	0.77±0.19(0.58~0.95,3)
	7.9±0.2(7.8~8.1,2)	15.2±0.1(15.1~15.3,2)	0.026±0.001(0.025~0.026,2)	0.81±0.10(0.74~0.89,2)	0.000	4.07±0.24(3.90~4.24,2)	0.50±0.01(0.49~0.51,2)
2NF	4.6	12.3±0.9(13.3~36.8,3)	0.280±0.17(0.095~0.426,3)	2.11±0.05(2.06~2.15,3)	0.008	2.79±0.24(2.54~3.02,3)	1.20±0.27(0.90~1.43,3)
	5.7±2.9(3.1~8.8,3)	8.6±2.8(5.3~10.2,3)	0.009±0.004(0.005~0.012,3)	0.76±0.09(0.68~0.86,3)	0.001	5.79±0.33(5.60~6.17,3)	1.05±0.21(0.86~1.27,3)
	5.1±0.7(4.7~5.6,2)	19.0±0.1(18.9~19.1,2)	0.034±0.000(0.033~0.034,2)	0.47±0.03(0.45~0.49,2)	0.001	7.00±0.32(6.78~7.23,2)	1.13±0.07(1.08~1.18,2)
3F	6.7±2.6(4.6~9.7,3)	16.5±0.1(16.3~16.6,3)	0.432±0.158(0.305~0.609,3)	1.38±0.04(1.35~1.41,3)	0.011	3.55±0.30(3.34~3.90,3)	2.30±0.52(1.84~2.87,3)
	4.5±1.9(3.3~6.4,3)	19.9±2.8(17.0~22.7,3)	0.011±0.001(0.010~0.012,3)	0.88±0.10(0.80~1.00,3)	0.008	5.71±0.06(5.67~5.78,3)	3.66±2.13(2.19~6.10,3)
	6.1±0.1(6.1~6.2,2)	19.0±0.8(19.6~18.5,2)	0.034±0.008(0.029~0.040,2)	0.99±0.13(0.90~1.08,2)	0.002	5.47±0.17(5.34~5.59,2)	1.80±0.55(1.41~2.19,2)
3NF	8.7±2.8(5.9~11.4,3)	18.0±1.7(16.3~19.7,3)	0.296±0.046(0.246~0.335,3)	0.52±0.02(0.51~0.54,3)	0.004	5.64±0.18(5.47~5.83,3)	2.31±1.30(0.86~3.40,3)
	4.9±3.5(2.8~8.9,3)	18.3±1.5(17.2~19.3,2)	0.009±0.002(0.007~0.011,3)	0.23±0.15(0.12~0.40,3)	0.001	8.48±0.28(8.19~8.74,3)	1.39±0.58(0.88~2.02,3)
	2.7±1.2(1.9~3.6,2)	17.0±0.7(16.5~17.5,2)	0.029±0.004(0.026~0.032,2)	0.10±0.03(0.08~0.12,2)	0.000	7.53±1.84(6.22~8.83,2)	1.20±0.20(1.06~1.34,2)
4F	4.4±0.9(3.7~5.0,2)	11.8±2.5(10.1~13.6,2)	0.016±0.001(0.014~0.018,17)	0.73±0.09(0.59~0.88,17)		6.46±0.42(5.84~7.38,17)	0.46±0.46(0.14~0.79,2)
	5.8±0.3(5.6~6.0,2)	32.6±1.0(31.9~33.3,2)		1.19±0.01(1.18~1.20,2)	0.007		1.23±0.17(1.11~1.35,2)
	8.5±2.0(7.1~9.9,2)	34.8±11.9(26.3~43.2,2)					0.89±0.52(0.52~1.26,2)
	4.1±1.7(3.0~5.3,2)	16.0±0.3(15.7~16.2,2)	0.021±0.000(0.021~0.021,2)	1.18±0.06(1.13~1.22,2)	0.003	5.10±0.45(4.78~5.42,2)	1.65±0.16(1.54~1.76,2)
4NF	2.1±0.5(1.9~2.7,3)	9.1±0.7(8.6~10.0,3)	0.016±0.001(0.015~0.019,17)	0.18±0.04(0.14~0.25,17)		8.97±0.32(8.38~9.42,17)	0.57±0.41(0.12~0.91,3)
	3.7±1.6(2.6~4.9,2)	38.5±3.4(36.1~40.9,2)		0.8±0.1(0.73~0.87,2)	0.012		1.97
	8.3±0.1(8.2~8.4,2)	26.3±1.0(25.6~27.0,2)					0.37±0.13(0.28~0.46,2)
	0.9±0.2(0.8~1.1,2)	14.4±0.1(14.3~14.5,2)	0.033±0.008(0.028~0.039,2)	0.56±0.06(0.52~0.61,2)	0.004	5.85±0.03(5.83~5.87,2)	1.63±0.21(1.48~1.78,2)
5F	3.3±3.1(1.1~5.5,2)	30.3±1.2(29.5~31.1,2)		1.83±0.10(1.76~1.90,2)	0.009		1.59±0.62(1.15~2.03,2)
	8.4±1.4(7.4~9.4,2)	24.3±3.5(21.9~26.8,2)					0.61±0.36(0.35~0.86,2)
	3.8±0.3(3.6~4.0,2)	20.5±0.6(20.1~20.9,2)	0.035±0.002(0.033~0.036,2)	1.10±0.12(1.01~1.18,2)	0.003	6.77±0.16(6.66~6.89,2)	2.44±0.12(2.36~2.53,2)
5NF	2.8±0.2(2.6~3.0,2)	33.9±15.2(23.1~44.6,2)		1.37±0.04(1.34~1.40,2)	0.009		1.39±0.00(1.39~1.39,2)
	4.8±4.5(1.6~8.0,2)	28.3±1.8(27.0~29.6,2)					1.61±1.95(0.23~2.99,2)
	3.5±0.6(3.1~3.9,2)	17.8±0.9(17.2~18.5,2)	0.031±0.003(0.029~0.033,2)	1.08±0.02(1.06~1.09,2)	0.003	5.65±0.03(5.63~5.67,2)	1.94±0.25(1.76~2.12,2)
SPA	1.1±0.4(0.7~1.4,3)	36.4±1.9(34.4~38.2,3)	0.039±0.008(0.030~0.060,20)	0.75±0.06(0.62~0.84,20)		5.08	6.56±1.73(5.56~8.55,3)
	1.3±0.3(1.0~1.6,3)	13.4±1.5(11.8~14.4,3)	0.021±0.003(0.017~0.027,17)	0.53±0.02(0.49~0.56,17)		5.44±0.17(5.19~5.88,17)	2.87±0.48(2.37~3.34,3)
SPB	12.4±1.0(11.5~13.5,3)	59.5±2.6(56.7~61.9,3)	0.033±0.008(0.020~0.050,20)	4.36±0.38(3.55~4.80,20)		5.37	5.06±1.94(2.99~6.84,3)
	2.7±1.0(1.7~3.6,3)	12.3±5.9(5.5~15.8,3)	0.025±0.002(0.021~0.030,17)	4.46±0.85(2.99~5.74,17)		5.29±0.29(4.81~5.73,17)	4.86±0.38(4.56~5.28,3)

Table 6.1A Extended.

Site	DO_{min}	DO_{max}	R^2 (DO)	$\delta^{18}O$-DO_{min}	$\delta^{18}O$-DO_{max}	R^2 ($\delta^{18}O$-DO)	P_m	R_{20}	a	K	a_R	GPP	ER	G_t	G_n	NPP	P/R
	(mg/L)		(%)	(‰)		(%)	(mg O_2 m^{-2} h^{-1})		mol O_2 mol $photon^{-1}$	m h^{-1}		(g O_2 m^{-2} day^{-1})					
2F	7.3	8.6	97.7	22.9	25.9	68.1	37.9	107.1	0.0064	0.12	0.9920	0.38	2.04	1.58	1.58	-1.66	0.19
	6.3	8.5	99.9	19.8	26.6	95.8	174.8	279.6	0.0159	0.20	0.9904	1.51	5.43	3.87	3.87	-3.92	0.28
	7.1	8.3	98.9	20.9	26.0	92.7	80.8	129.9	0.0124	0.10	0.9883	0.93	2.50	1.52	1.52	-1.56	0.37
2NF	7.0	9.1	99.0	21.0	25.6	74.6	74.2	119.3	0.0019	0.26	0.9923	0.56	2.37	1.77	1.77	-1.81	0.24
	7.1	8.9	99.7	21.8	27.3	89.0	103.7	154.9	0.0043	0.16	0.9862	0.89	2.96	2.01	2.01	-2.07	0.30
	6.1	8.4	98.9	19.3	26.4	83.4	160.1	276.7	0.0053	0.29	0.9944	1.27	5.61	4.22	4.22	-4.34	0.23
3F	6.8	9.7	100.0	17.7	27.6	82.2	261.5	156.2	0.0077	0.11	0.9890	2.03	3.37	1.74	1.61	-1.34	0.60
	5.5	10.5	99.8	13.9	29.8	96.0	620.6	407.1	0.0365	0.12	0.9844	5.67	8.52	3.38	2.91	-2.85	0.67
	6.9	9.1	99.2	17.7	25.4	90.8	261.7	155.7	0.0052	0.07	0.9876	1.97	3.39	1.44	1.44	-1.42	0.58
3NF	6.2	9.8	99.7	17.0	26.1	76.2	251.5	184.0	0.0045	0.22	0.9912	1.82	4.11	2.70	2.26	-2.29	0.44
	5.6	11.1	100.0	14.8	28.5	84.4	606.0	430.3	0.0172	0.30	0.9873	4.86	9.13	5.52	4.18	-4.27	0.53
	3.9	8.2	99.6	12.3	25.4	85.5	365.4	342.8	0.0137	0.18	0.9951	3.20	7.85	4.68	4.68	-4.65	0.41
4F	7.7	9.5	93.3	21.4	26.6	91.2	174.6	160.1	0.0034	0.19	0.9839	1.42	3.41	1.98	1.92	-2.00	0.42
	7.2	9.3	96.9	19.5	26.4	91.4	219.7	208.4	0.0218	0.22	0.9877	2.27	4.62	2.31	2.22	-2.35	0.49
	8.7	11.3	99.3	18.8	25.71	96.5	233.3	154.4	0.0123	0.22	0.9866	2.00	2.78	1.93	0.87	-0.78	0.72
	6.8	9.8	99.9	17.2	25.9	94.7	422.4	270.5	0.0128	0.26	0.9923	3.00	6.37	3.73	3.11	-3.37	0.47
4NF	7.4	10.3	98.4	18.3	27.4	96.4	219.06	134.63	0.0048	0.25	0.9836	1.89	2.96	1.81	1.03	-1.07	0.64
	6.4	10.6	98.8	14.6	25.5	89.5	302.54	157.32	0.0070	0.31	0.9917	2.61	3.80	2.74	1.31	-1.19	0.69
	7.7	12.8	98.0	12.9	25.5	89.6	241.53	112.16	0.0074	0.22	0.9906	1.97	2.21	1.63	0.22	-0.24	0.89
	6.5	10.1	100.0	14.9	25.2	79.9	366.83	206.87	0.0054	0.37	0.9967	3.09	5.16	3.55	2.07	-2.07	0.60
5F	6.4	11.1	99.3	13.8	26.4	84.2	651.6	285.3	0.0183	0.52	0.9942	4.46	7.05	5.51	2.69	-2.58	0.63
	6.8	12.2	95.6	13.5	25.4	83.4	644.8	356.0	0.0255	0.62	0.9968	4.31	7.24	5.90	2.84	-2.94	0.59
	6.9	9.7	97.8	16.8	25.2	95.5	278.1	126.7	0.0080	0.15	0.9902	2.14	3.28	1.73	1.16	-1.15	0.65
5NF	6.3	15.0	99.6	9.1	29.2	89.5	1299.6	446.5	0.0170	0.15	0.9824	12.91	10.45	6.16	-2.62	2.46	1.24
	7.5	14.2	99.3	12.1	28.3	97.5	946.0	437.3	0.0312	0.14	0.9817	9.24	8.33	4.63	-0.92	0.91	1.11
	6.7	9.8	100.0	15.5	25.2	88.3	613.0	321.4	0.0116	0.14	0.9914	4.93	7.76	3.81	2.84	-2.83	0.64
SPA	6.6	8.1	83.7	20.5	29.2	98.3	1466.1	30.4	0.0005	0.05	0.9836	0.69	0.90	0.29	0.29	-0.21	0.77
	8.2	9.2	85.2	19.8	23.2	18.8	51.3	19.4	0.0007	0.00	0.9703	0.50	0.50	0.00	0.00	0.00	1.00
SPB	4.1	12.9	97.8	7.6	42.9	65.4	7510.9	366.9	0.0071	0.03	0.9761	10.78	10.82	1.11	0.06	-0.04	1.00
	5.1	13.0	94.7	8.1	32.9	68.3	488679.1	366.3	0.0079	0.00	0.9736	9.10	9.10	0.00	0.00	0.00	1.00

Table 6.1B Geomorphological, hydrological, physical, chemical and biological characteristics of 14 sampling sites in the Grand River network and at or near the time of metabolism measurements. Data are mean (±1SD, ranges and n).

Site	Date	Width	Depth	Discharge	Radiation	Temperature	pH	Salinity	Conductivity	$\delta^{18}O\text{-}H_2O$
		m	cm	$m^3\ s^{-1}$	mol m^{-2} day^{-1}	℃		PPT	µS	‰
WM	24-May-06	36.0	40.0	8.1	47.9	14.6±2.6(10.6~18.4,20)	8.32±0.35(7.76~8.83,20)		471.3±21.9(435~496,20)	-10.63
	5-Jul-06	36.0	35.0	4.9	47.2	29.5±2.0(16.5~22.8,19)	8.28±0.15(8.13~8.53,7)	0.21	440.4±16.9(411~461,19)	-10.50
	9-Aug-06	36.0	40.0	7.8	37.8	22.9±2.0(19.6~25.7,20)	8.51±0.28(8.04~8.84,20)	0.20	423.7±37.3(390~547,20)	-10.04
	5-Oct-06	36.0	50.0	9.8	30.9	12.9±1.4(10.9~15.4,19)	8.35±0.21(8.09~8.70,19)	0.23	471.3±19.0(437~492,19)	-8.64
	10-Jul-07	36.0	40.0	7.7	48.5	21.7±1.1(20.3~23.0,5)	8.24±0.25(7.97~8.56,5)	0.22	460.2±8.0(448~468,5)	-10.15
	31-Jul-07	36.0	40.0	7.5	40.7	22.3±1.7(20.7~25.4,7)	8.33±0.24(8.09~8.68,7)	0.22	452.1±9.4(437~462,7)	-9.91
BP	24-May-06	85.0	45.0	*14.7*	48.1	15.5±2.0(12.1~17.6,20)	8.40±0.18(8.05~8.66,20)		513.1±5.5(506~525,20)	-10.86
	5-Jul-06	85.0	35.0	8.3	45.4	21.9±1.3(19.7~23.9,20)	8.35±0.12(8.22~8.54,7)	0.22	459.3±8.7(445~475,20)	-9.85
	9-Aug-06	85.0	40.0	10.9	38.1	24.1±1.0(22.5~25.6,20)	8.61±0.23(8.20~8.85,20)	0.21	444.6±6.9(436~456,20)	-9.94
	5-Oct-06	85.0	50.0	19.5	30.9	13.9±1.2(12.3~16.2,19)	8.24±0.14(8.06~8.46,19)	0.26	539.6±24.7(491~574,19)	-8.66
	26-Jun-07	85.0	35.0	7.7	60.4	26.8±1.2(25.1~28.6,13)	8.48±0.24(8.13~8.79,13)	0.22	461.4±9.6(449~476,13)	-10.95
	31-Jul-07	85.0	35.0	8.8	53.8	24.9±1.3(23.8~27.2,7)	8.47±0.27(8.21~8.89,7)	0.21	432.3±3.9(426~437,7)	-10.02
	21-Oct-07	85.0	30.0	4.3	24.9	13.1±1.1(12.3~15.0,6)	8.18±0.18(7.97~8.43,6)	0.24	494.7±4.3(488~499,6)	-8.56
	6-Jun-08	85.0	40.0	9.0	54.9	21.1±2.5(18.7~24.6,6)	7.83±0.19(7.59~8.12,6)		486.7±8.8(473~496,6)	-10.48
	24-Jun-08	85.0	45.0	14.9	48.2	20.0±1.8(18.5~23.1,8)	8.59±0.19(8.37~8.98,8)		466.0±22.3(444~493,5)	-10.48
	4-Jul-08	85.0	40.0	10.8	54.6	20.7±1.5(19.3~23.8,21)	8.82±0.5(8.19~9.82,21)		470.3±11.4(457~489,21)	-10.36
	20-Aug-08	85.0	50.0	25.2	48.6	19.8±1.3(18.5~22.3,15)	8.76±0.41(8.27~9.66,15)	0.24	513.8±23.2(474~546,15)	-8.94
	21-Aug-08	85.0	50.0	21	41.9	19.9±1.2(18.6~22.1,17)	8.44±0.24(8.17~9.04,17)	0.24	473.6±7.6(460~484,17)	-8.90
BL	22-May-06	90.0	70.0	32.7	65.8	12.2±1.8(9.2~14.4,19)	8.11±0.10(7.83~8.25,19)		662.4±18.0(634~693,19)	-10.21
	6-Jul-06	90.0	45.0	10.6	36.3	21.9±1.5(19.9~24.0,17)	7.95±0.45(7.51~9.00,15)	0.35	722.2±36.1(643~774,16)	-10.11
	1-Aug-06	90.0	50.0	11.5	46.5	23.1±1.7(20.7~25.5,19)	7.91±0.42(7.04~8.52,19)	0.34	692.8±31.9(639~745,19)	-9.85
	1-Oct-06	90.0	60.0	17.3	22.9	13.8±1.1(12.3~15.6,19)	7.83±0.14(7.35~8.01,19)	0.35	715.4±27.2(672~752,19)	-9.52
	26-Jun-07	90.0	43.0	9.8	49.4	26.8±1.6(24.6~29.4,14)	8.01±0.36(7.70~8.66,14)	0.37	791.1±62.4(678~858,14)	-10.53
	1-Jul-08	90.0	60.0	20.4	57.5	19.5±1.8(18.0~22.4,7)	7.92±0.29(7.47~8.23,7)		672.7±13.5(654~688,7)	-9.44
	3-Jul-08	90.0	60.0	17.3	42.8	21.7±0.9(20.8~23.4,16)	8.07±0.18(7.79~8.29,16)		657.3±13.8(640~678,16)	-9.96
	22-Aug-08	90.0	65.0	22.8	38.2	21.5±1.3(20.3~23.6,21)	8.43±0.31(7.90~8.77,21)	0.31	646.2±23.6(612~694,21)	-9.23
	23-Aug-08	90.0	63.0	20.7	44.7	22.7±1.4(21.4~25.0,16)	8.81±0.18(8.50~9.07,16)	0.32	658.8±13.1(638~681,16)	-9.49
GM	22-May-06	100.0	85.0	49.9	57.9	12.2±1.4(9.8~13.9,18)	8.08±0.13(7.68~8.21,17)		706.2±14.9(691~731,18)	-10.14
	6-Jul-06	100.0	70.0	14.9	59.7	21.5±2.1(18.8~24.4,18)	8.45±0.47(7.84~9.01,15)	0.38	787.9±57.0(712~892,18)	-9.49
	1-Aug-06	100.0	75.0	16	46.5	23.3±2.3(20.1~26.2,19)	8.47±0.41(7.91~8.98,19)	0.40	814.6±35.9(758~860,19)	-9.71
	1-Oct-06	100.0	80.0	26.5	22.9	13.6±0.9(12.6~15.3,18)	8.22±0.15(8.07~8.51,18)	0.37	754.8±13.3(704~763,18)	-9.65
	10-Jul-07	100.0	78.0	19	43.6	25.3±1.8(22.8~27.6,5)	8.33±0.39(7.84~8.76,5)	0.40	821.6±52.3(777~903,5)	-9.98

Table 6.1B Extended.

Site	SRP	TP	NH_4^+	NO_3^-	NO_2^-	DOC	Chlorophyll *a*
	(µg/L)			(mg N/L)		mg C/L	µg/L
WM	1.9±0.9(1.3~2.8,3)	20.0±0.4(19.5~20.4,3)	0.042±0.024(0.011~0.115,20)	2.48±0.09(2.37~2.66,20)			0.50±0.45(0.00~0.86,3)
	2.3±0.2(2.2~2.4,3)	19.2±1.7(17.4~20.7,3)	0.033±0.014(0.016~0.072,20)	1.15±0.07(0.96~1.28,20)		7.74±0.21(7.32~8.14,20)	2.64±0.49(2.35~3.21,3)
	1.5±0.7(0.9~2.4,4)	21.7±1.8(19.5~23.8,4)	0.029±0.004(0.022~0.035,20)	0.58±0.06(0.50~0.69,20)		7.95±0.28(7.56~8.47,20)	1.02±0.27(0.64~1.28,4)
	2.7±0.4(2.4~3.1,3)	33.0±6.8(28.6~40.8,3)	0.130±0.160(0.020~0.515,19)	1.21±0.25(0.87~1.55,19)			5.06±0.54(4.49~5.56,3)
	1.6±0.3(1.4~1.8,2)	10.3±0.4(10.0~10.6,2)		1.10			1.82±1.15(1.03~2.61,2)
	4.7±3.7(2.1~7.4,2)	30.6±3.5(28.1~33.0,2)		1.00		6.34	1.80±0.45(1.48~2.12,2)
BP	2.9±0.8(2.1~3.5,3)	23.4±2.6(20.6~25.7,3)	0.012±0.002(0.009~0.015,20)	3.49±0.06(3.41~3.65,20)			0.21±0.37(0.00~0.64,3)
	2.0±0.2(1.8~2.3,3)	28.2±3.2(25.3~31.7,3)	0.034±0.012(0.019~0.067,20)	1.60±0.05(1.52~1.72,20)		6.49±0.18(6.17~6.85,19)	2.99±1.11(1.71~3.64,3)
	3.0±0.8(1.9~3.8,4)	39.6±5.8(33.2~47.2,4)	0.026±0.004(0.021~0.034,20)	0.78±0.02(0.74~0.82,20)		6.79±0.81(3.47~7.36,20)	3.90±1.46(2.57~5.99,4)
	7.1±3.1(3.6~9.1,3)	56.8±22.0(31.4~70.5,3)	0.040±0.017(0.011~0.071,19)	1.76±0.47(1.07~2.90,19)			8.70±2.92(5.35~10.69,3)
	1.7±0.1(1.6~1.9,3)	31.1±8.0(23.5~39.4,3)		1.28±0.06(1.18~1.42,17)		6.54±0.54(5.57~7.24,17)	1.65±0.95(0.60~2.46,3)
	5.6±0.3(5.5~5.8,2)	29.3±9.3(22.7~35.9,2)		0.80		5.93	1.51±0.05(1.48~1.54,2)
	4.3±0.7(3.8~4.8,2)	34.7±4.7(31.3~38.0,2)	0.029±0.008(0.023~0.035,2)			7.14±0.033(7.12~7.16,2)	3.61±1.06(2.87~4.34,2)
	2.2±0.8(1.3~3.3,4)	23.0±3.9(19.5~28.5,4)	0.040±0.026(0.014~0.076,4)	2.08±0.27(1.69~2.30,4)	0.020	2.69±0.24(2.34~2.84,4)	1.98±1.21(1.01~3.72,4)
	2.4±0.9(1.4~3.4,4)	20.2±6.7(11.5~27.8,4)	0.018±0.004(0.013~0.021,3)	2.16±0.09(2.06~2.25,3)	0.018	2.74±0.10(2.59~2.81,4)	2.16±1.27(0.92~3.76,4)
	1.6	35.2	0.038±0.027(0.022~0.069,3)	2.44±0.12(2.33~2.57,3)	0.017	5.15±2.17(2.64~6.42,3)	1.70±0.40(1.28~2.07,3)
	3.3	33.8±2.8(30.7~36.5,4)	0.010±0.001(0.009~0.012,4)	1.03±0.14(0.85~1.15,4)	0.005	6.95±0.58(6.12~7.40,4)	3.56±1.04(2.38~4.53,4)
	3.6±3.4(1.2~6.0,2)	26.6±7.2(18.8~32.9,3)	0.017±0.013(0.009~0.032,3)	0.92±0.02(0.90~0.93,3)	0.008	7.08±0.02(7.06~7.09,2)	3.92±1.99(2.01~5.99,3)
BL	13.0±2.0(10.9~14.8,3)	49.4±1.8(48.2~51.5,3)	0.588±0.138(0.370~0.868,19)	3.59±0.12(3.41~3.80,19)			0.36±0.45(0.00~0.86,3)
	18.4±2.6(15.7~20.8,3)	50.1±2.1(47.9~52.1,3)	0.132±0.143(0.029~0.430,17)	2.89±0.33(2.40~3.29,17)		6.67±0.19(6.30~7.01,17)	4.60±1.84(1.92~5.99,4)
	17.9±1.8(15.9~19.1,3)	68.3±14.2(58.0~84.5,3)	0.054±0.016(0.028~0.085,19)	2.35±0.24(1.93~2.62,19)		7.01±0.22(6.61~7.45,19)	3.78±0.75(2.99~4.49,3)
	13.8±2.4(11.2~16.0,3)	77.6±3.8(73.9~81.4,3)	0.664±0.202(0.325~1.050,19)	2.19±0.10(2.07~2.40,19)			4.28±1.19(3.21~5.56,3)
	24.7±9.2(14.5~32.3,3)	86.9±10.3(77.5~97.8,3)	0.526±0.395(0.069~1.146,17)	2.00±0.43(1.40~2.70,17)		7.07±0.31(6.56~7.63,17)	1.53±0.56(0.90~1.95,3)
	18.1±5.4(12.1~22.5,3)	48.9±5.4(43.3~54.1,3)	0.587±0.060(0.519~0.632,3)	4.59±0.06(4.53~4.65,3)	0.340	6.40±0.22(6.24~6.65,3)	1.35±0.64(0.64~1.86,3)
	16.5±2.2(14.8~19.0,3)	40.2±22.9(24.0~56.5,2)	0.597±0.073(0.521~0.667,3)	2.99±0.05(2.95~3.05,3)	0.450	4.55±0.18(4.36~4.72,3)	1.45±0.22(1.20~1.58,3)
	14.8	25.8±13.8(16.0~35.6,2)	0.282±0.040(0.236~0.312,3)	1.30±0.29(1.11~1.63,3)	0.180	6.72±0.60(6.20~7.38,3)	1.37±0.43(1.09~1.86,3)
	9.5±2.5(6.8~11.7,3)	31.8±3.1(28.7~35.0,3)	0.275±0.036(0.233~0.298,3)	1.53±0.06(1.46~1.57,3)	0.200	2.51±0.28(2.19~2.68,3)	1.39±0.38(0.95~1.63,3)
GM	8.4±1.3(7.3~9.8,3)	54.1±4.8(49.1~58.6,3)	0.120±0.045(0.056~0.211,18)	3.58±0.17(3.33~3.83,18)			0.86±0.77(0.00~1.50,3)
	10.0±0.4(9.6~10.5,5)	42.5±5.2(37.8~51.3,5)	0.009±0.006(0.00~0.022,18)	2.92±0.25(2.48~3.20,18)		6.16±0.27(5.79~6.45,4)	5.05±1.65(2.57~6.84,5)
	11.6±0.5(11.0~12.0,3)	58.7±7.4(53.1~67.1,3)	0.025±0.006(0.018~0.040,19)	2.77±0.34(2.25~3.22,19)		6.81±0.31(6.21~7.41,19)	5.84±3.06(3.21~9.20,3)
	8.2±0.5(7.7~8.8,3)	58.3±2.6(55.3~59.9,3)	0.121±0.021(0.087~0.167,19)	2.68±0.07(2.54~2.82,19)			2.35±1.11(1.07~2.99,3)
	10.3±2.9(8.3~12.3,2)	24.5±3.7(21.9~27.2,2)		2.30			1.44±0.23(1.28~1.60,2)

Table 6.1B Extended.

Site	DO_{min}	DO_{max}	R^2 (DO)	$\delta^{18}O$-DO_{min}	$\delta^{18}O$-DO_{max}	R^2 ($\delta^{18}O$-DO)	P_m	R_{20}	a	K	a_R	GPP	ER	G_t	G_n	NPP	P/R
	(mg/L)		(%)	(‰)		(%)	(mg O_2 m^{-2} h^{-1})		mol O_2 mol photon^{-1}	m h^{-1}		(g O_2 m^{-2} day^{-1})					
WM	7.1	16.7	98.7	11.1	31.3	70.0	998.7	394.5	0.0135	0.18	0.9763	10.14	7.49	5.96	-3.06	2.65	1.35
	6.8	12.1	94.3	16.1	31.5	92.4	983.8	366.7	0.0092	0.41	0.9707	8.55	8.81	6.67	-0.14	-0.26	0.97
	5.4	12.5	97.0	11.5	27.3	97.3	733.4	336.7	0.0097	0.23	0.9896	5.92	9.08	4.82	1.90	-3.17	0.65
	8.1	12.6	99.3	16.5	26.8	99.0	573.6	229.8	0.0053	0.14	0.9830	3.77	3.94	3.41	1.92	-0.18	0.96
	5.2	11.5	99.3	11.4	28.0	98.1	986.7	393.6	0.0148	0.33	0.9891	10.74	11.21	7.89	0.57	-0.47	0.96
	4.9	12.1	99.0	11.3	28.1	92.0	1277.0	405.7	0.0113	0.36	0.9878	10.11	11.58	8.93	1.65	-1.47	0.87
BP	7.2	16.5	99.1	10.7	30.7	75.2	839.4	355.2	0.0117	0.09	0.9763	8.65	6.94	3.19	-2.45	1.70	1.25
	6.2	11.5	95.1	14.7	28.8	57.0	1019.5	256.8	0.0051	0.33	0.9793	6.07	6.81	4.92	0.92	-0.74	0.89
	5.9	12.7	94.0	11.3	26.3	95.8	652.7	221.4	0.0081	0.18	0.9896	5.69	6.38	3.10	-0.34	-0.68	0.89
	7.7	11.7	98.4	17.2	26.7	98.7	418.3	191.9	0.0046	0.12	0.9837	2.98	3.46	2.83	2.24	-0.48	0.86
	5.2	12.7	99.2	9.6	29.5	88.8	742.7	203.1	0.0077	0.20	0.9833	8.03	6.52	4.47	-1.55	1.51	1.23
	5.2	12.5	99.9	9.6	27.7	97.2	1036.9	250.0	0.0062	0.27	0.9883	8.05	7.80	5.59	-0.24	0.25	1.03
	8.4	12.5	99.4	15.8	25.8	98.6	389.5	169.1	0.0054	0.19	0.9877	2.74	3.13	2.14	0.40	-0.39	0.88
	7.2	12.6	99.9	11.7	26.8	96.4	761.3	214.5	0.0072	0.22	0.9837	7.94	5.69	4.69	-2.23	2.25	1.40
	6.8	12.4	99.0	12.6	28.7	89.9	690.3	203.5	0.0056	0.12	0.9781	5.83	5.10	2.58	-0.67	0.73	1.14
	7.3	13.2	99.0	12.0	26.9	96.4	757.0	198.4	0.0064	0.20	0.9818	7.59	5.06	4.33	-2.52	2.53	1.50
	6.8	14.5	98.6	12.4	30.3	87.1	1286.9	281.8	0.0091	0.22	0.9739	10.23	7.02	6.95	-3.09	3.21	1.46
	6.0	13.8	99.6	8.8	28.2	97.8	1226.1	303.0	0.0084	0.12	0.9848	8.45	7.54	3.74	-0.91	0.90	1.12
BL	8.5	12.2	99.1	18.2	26.8	71.1	649.4	469.2	0.0050	0.20	0.9835	6.67	7.89	4.00	0.11	-1.22	0.85
	1.1	9.6	84.3	12.4	37.7	40.8	2159.0	1263.6	0.0186	0.37	0.9842	16.90	33.00	16.62	16.03	-16.10	0.51
	3.1	9.2	85.8	12.6	31.1	95.9	994.1	615.4	0.0092	0.23	0.9877	8.72	16.85	8.31	7.73	-8.13	0.52
	5.3	8.2	91.5	18.6	28.5	93.7	927.9	1022.3	0.0074	0.23	0.9889	4.70	18.16	13.73	13.73	-13.46	0.26
	0.9	11.0	99.5	8.4	33.7	96.9	2677.4	922.1	0.0137	0.39	0.9882	18.02	30.10	17.43	12.14	-12.08	0.60
	4.5	10.8	99.9	13.5	30.3	98.8	1596.8	943.9	0.0141	0.33	0.9855	15.65	23.14	12.92	7.68	-7.49	0.68
	2.9	11.3	99.9	10.3	33.1	93.2	1583.0	877.2	0.0242	0.22	0.9859	18.64	23.31	9.80	4.76	-4.67	0.80
	5.2	9.1	99.4	15.8	28.2	93.3	882.4	538.2	0.0093	0.23	0.9877	7.65	14.16	7.20	6.60	-6.51	0.54
	4.4	9.2	100.0	14.3	28.4	92.1	1741.3	849.8	0.0098	0.37	0.9892	11.52	23.81	13.76	12.19	-12.28	0.48
GM	8.8	14.2	99.0	16.1	28.3	80.4	1900.5	799.8	0.0145	0.36	0.9743	17.56	13.43	13.70	-5.08	4.14	1.31
	5.2	12.4	96.4	15.7	37.3	-366.2	1584.9	740.9	0.0264	0.23	0.9708	19.88	19.21	10.53	-0.93	0.67	1.03
	5.7	12.8	98.0	10.8	29.2	96.4	1550.4	514.9	0.0182	0.19	0.9837	14.74	14.10	8.81	-0.45	0.64	1.05
	8.2	11.8	96.7	16.6	26.5	76.1	1597.5	812.3	0.0152	0.30	0.9875	9.17	14.42	9.08	5.07	-5.24	0.64
	4.3	12.2	97.8	8.1	34.5	81.1	1681.9	369.4	0.0116	0.05	0.9763	12.70	11.27	2.38	-0.50	1.43	1.13

The presence of riparian trees at small and middle-sized streams lowered the light availability. The streams without riparian trees, 2NF, 3NF, 4NF and 5NF received higher incoming radiation than their counterparts with riparian trees, 2F, 3F, 4F and 5F (Figure 6.2A). Daily incoming radiation on sampling days at large river sites was from 22.9 to 65.8 mol photons m^{-2} day^{-1} (Table 6.1B), and exhibited a declining trend from early summer to early fall for sampling periods from 2006 to 2008 (Figure 6.2B).

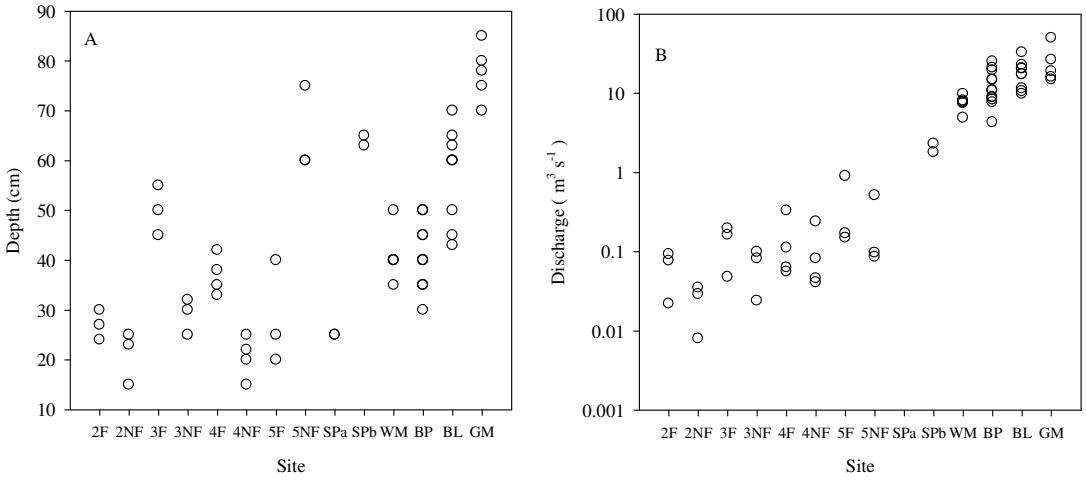

Figure 6.1 Water depth (A) and discharge (B) at 14 sites for sampling periods from 2006 to 2008 in the Grand River network.

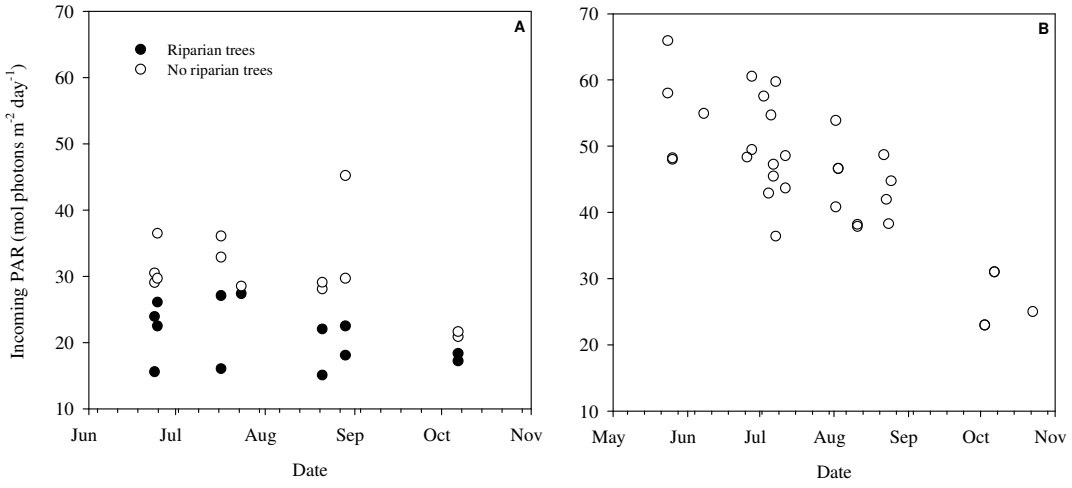

Figure 6.2 Daily incoming PAR (mol photons m^{-2} day^{-1}) at (A) small and middle-sized streams (2^{nd}-5^{th} order), and (B) 4 Grand River sites (WM, BP, BL and GM) for sampling periods from 2006 to 2008 in the Grand River network.

The highest means of salinity, 0.5 g/kg, and conductivity, 1000 µS, were observed at site SPb, about 2 km downstream of Guelph WWTP. Two other urban impacted sites, BL and GM, also had relatively high mean salinity of 0.36 g/kg and mean conductivity of 760 µS. Other sites had lower salinity of 0.2-0.3 g/kg and lower conductivity of 400-600 µS except site 2F, which had a high conductivity of 600-700 µS. The two upstream Grand River sites, WM and BP, had low mean salinity of 0.22 g/kg and conductivity of about 470 µS (Figure 6.3).

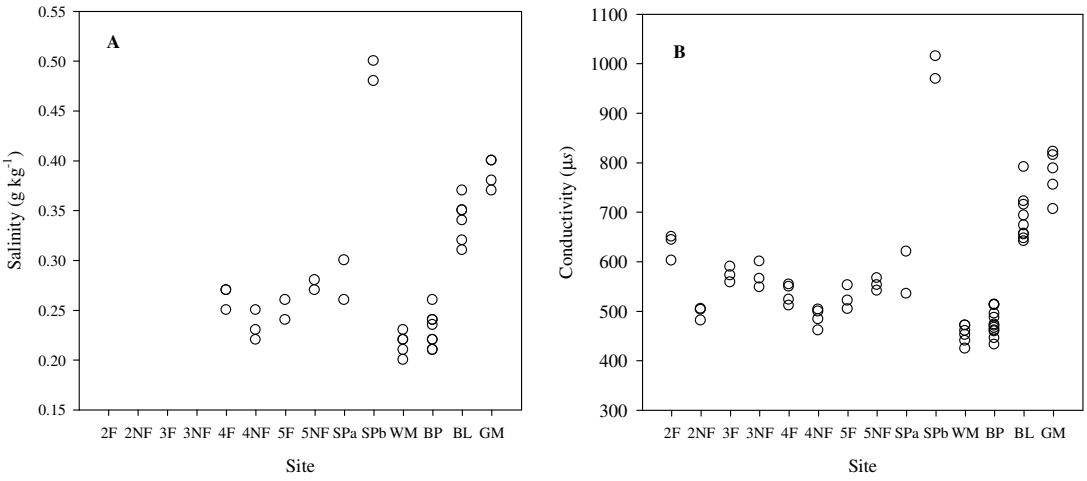

Figure 6.3 Salinity (g kg $^{-1}$) (A) and conductivity (µS) (B) at 14 sites for sampling periods from 2006 to 2008, in the Grand River network.

Soluble reactive phosphorus (SRP) exhibited a slight decline from small streams to middle-sized streams, and then increased along the main channel of the Grand (Figure 6.4A). The highest mean SRP was 25 µg/L at site BL. Site BL also had the highest level of total phosphorus (TP) with a mean of 53 µg/L. In general, TP increased with stream size (Figure 6.4B). According to the trophic ranges of TP (ultra-oligotrophic < 4 µg/L; oligotrophic 4-10 µg/L; mesotrophic 10-20 µg/L; meso-eutrophic 20-35 µg/L; eutrophic 35-100 µg/L and hyper-eutrophic >100 µg/L) suggested by the Canadian Council of Ministers of the Environment (CCME 2007), the small streams (2F, 2NF, 3F and 3NF) were mesotrophic, the middle-sized streams (4F, 4NF, 5F, 5NF, WM and SPb) and one

large 7th order river site, BP, were mesoeutrophic, and the two large river sites, BL and GM in the main channel of the Grand, were eutrophic.

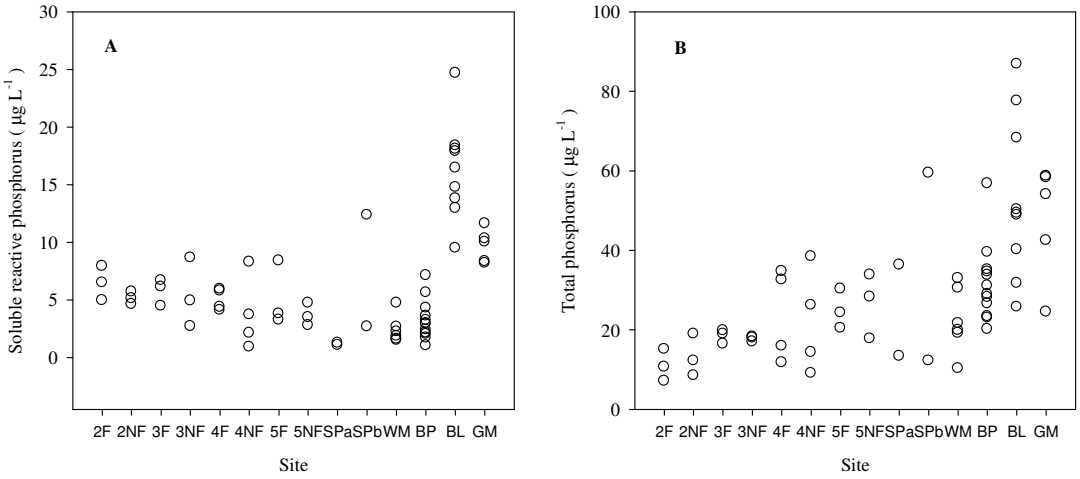

Figure 6.4 Soluble reactive phosphorus (SRP) (µg L^{-1}) (A) and total phosphorus (TP) (µg L^{-1}) (B) at 14 sites for sampling periods from 2006 to 2008 in the Grand River network.

Site BL had a large variation of NH_3/NH_4^+, ranging from 0.05 to 0.67 mg N/L, during 2006 to 2008. The NH_3/NH_4^+ for other sites were low and mainly ranged from 0.01 to 0.05 mg N/L. High levels of NH_3/NH_4^+ were observed at small streams on July 15, 2008, under conditions of low discharge (Table 6.1A & Figure 6.5A). The nitrate for all sites ranged from 0.1 to 4.6 mg N/L. The Grand River sites, BP, BL and GM, had relatively higher levels of nitrate than small and middle-sized sites (Table 6.1A, 6.1B & Figure 6.5B).

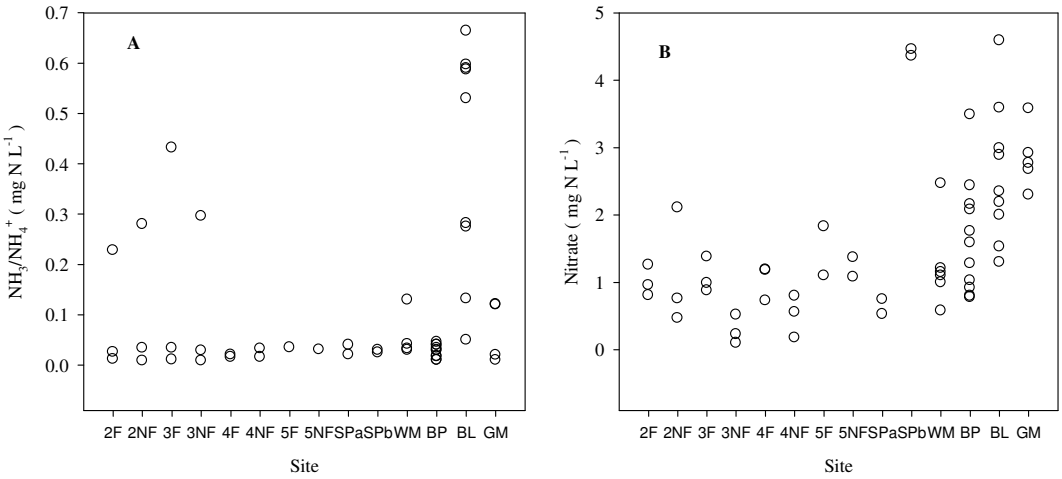

Figure 6.5 NH_3/NH_4^+ (mg N L^{-1}) (A) and nitrate (mg N L^{-1}) (B) at 14 sites for sampling periods from 2006 to 2008 in the Grand River network.

DOC exhibited an increasing trend from 2nd order streams to 4th order streams (Figure 6.6). The middle-sized streams and the large river sites had a level of around 6 mg L^{-1} (Figure 6.6).

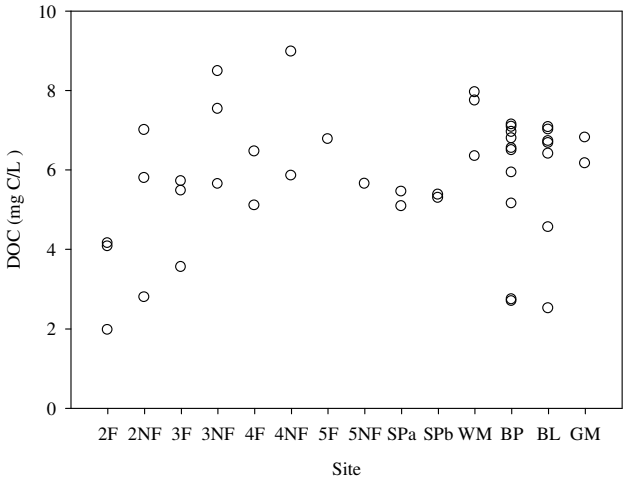

Figure 6.6 Dissolved organic carbon (mg C L^{-1}) at 14 sites for sampling periods from 2006 to 2008 in the Grand River network.

The chlorophyll ***a*** of seston for all sites ranged from 0.2 to 8.7 µg/L and exhibited a slightly increasing trend with stream size (Figure 6.7). There was no obvious increasing or decreasing temporal pattern observed for all 14 sites (Figure 6.8A), but there was an increasing seasonal trend for the 4 Grand River sites (Figure 6.8B).

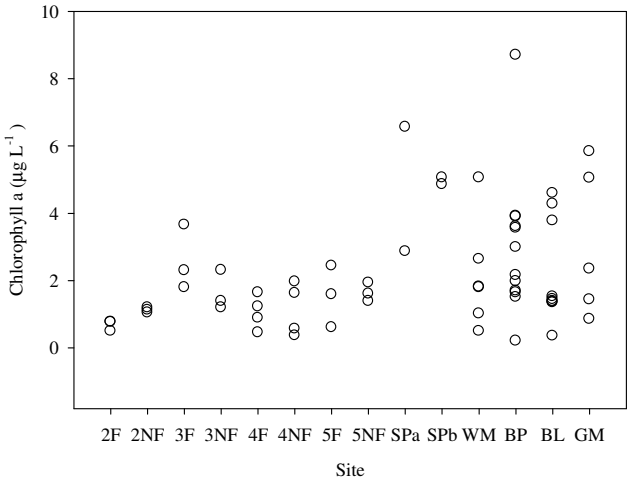

Figure 6.7 Chlorophyll ***a*** (µg L^{-1}) at 14 sites for sampling periods from 2006 to 2008 in the Grand River network.

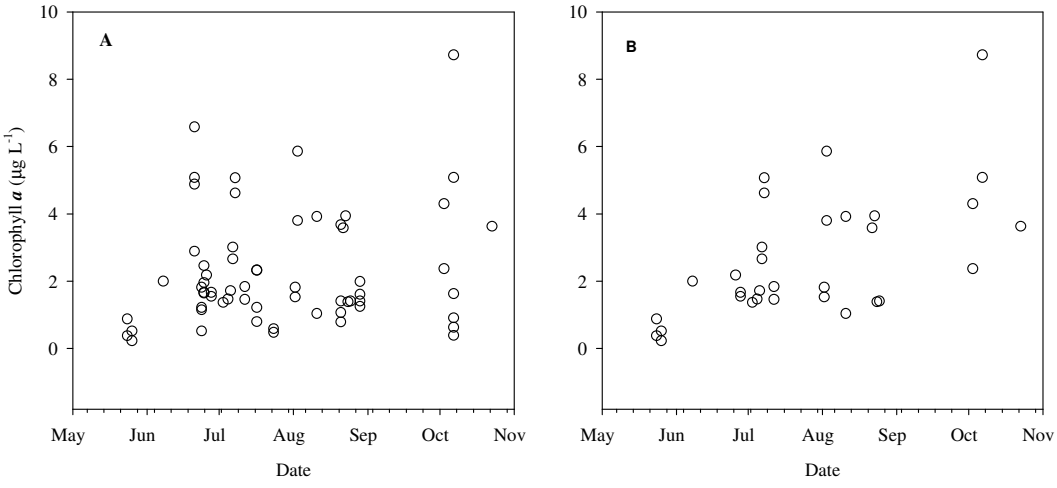

Figure 6.8 Seasonal pattern of chlorophyll a (µg L^{-1}) for all sites (**A**) and only for 4 Grand River sites, WM, BP, BL and GM (**B**) from 2006 to 2008 in the Grand River network.

The $\delta^{18}O\text{-}H_2O$ value for all sites ranged from -11 to -8.5 per mill (Figure 6.9, 6.10A). There was no site specificity observed (Figure 6.9, 6.10A), but there was a seasonal increasing trend for the Grand River sites (Figure 6.10B).

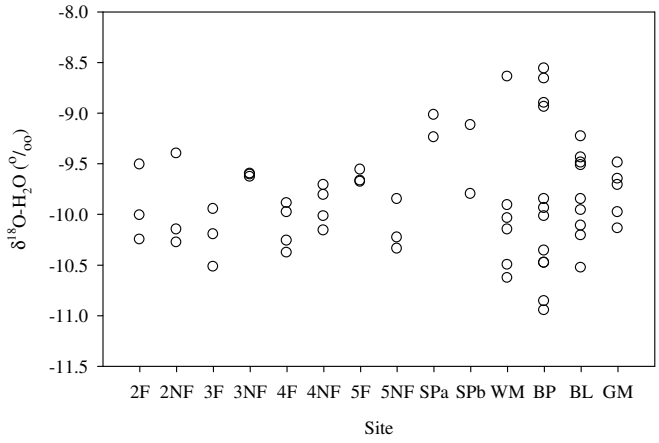

Figure 6.9 $\delta^{18}O\text{-}H_2O$ (‰) at 14 sites for sampling periods from 2006 to 2008 in the Grand River network.

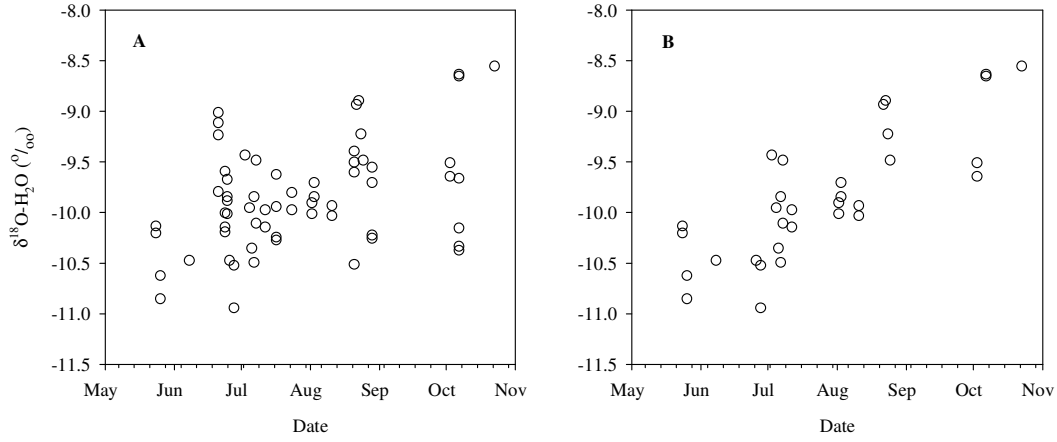

Figure 6.10 Seasonal pattern of $\delta^{18}O\text{-}H_2O$ (‰) for all sites (**A**) and only for 4 Grand River sites, WM, BP, BL and GM (**B**) from 2006 to 2008.

6.3.2 Observed and reconstructed DO and δ^{18}O-DO profiles

The DO concentration and δ^{18}O-DO signature varied inversely. The maximum DO concentration for each diel was usually observed in the mid afternoon, and the minimum DO concentration appeared just before sun rise. The DO concentrations for all sampling events ranged from 0.9 mg/L at site BL to 16.7 mg/L at site WM, while the δ^{18}O-DO varied between 7.6 and 43 ‰ (Table 6.1). Both observed and modelled DO and δ^{18}O-DO curves are illustrated in Appendix-A, as well as the cross plots of DO saturation and δ^{18}O-DO. The coefficients of determination (R^2) for all fittings of DO curves were ≥ 84% with an average of 97.5%, while R^2 for δ^{18}O-DO curve fitting were generally ≥ 70% but with an average of 87% (Table 6.1).

Cross plots of DO saturation and δ^{18}O-DO for all samples and all sites are provided in Figure 6.11. According to the 95% confidence ellipses, the diel DO and δ^{18}O-DO data of small stream sites 2F, 2NF and 3F are distributed within the range of site 3NF. The range of site 5NF covers other middle-sized streams, 4F, 4NF and 5F. The large river site SPb distributes towards the left, but site WM exhibits a balanced pattern, as well as two 7th order sites, BP and GM (Figure 6.11). Site BL has the diel DO and δ^{18}O-DO data trend towards the upper left quadrant, compared to upstream site BP and downstream site GM in the Grand River (Figure 6.11).

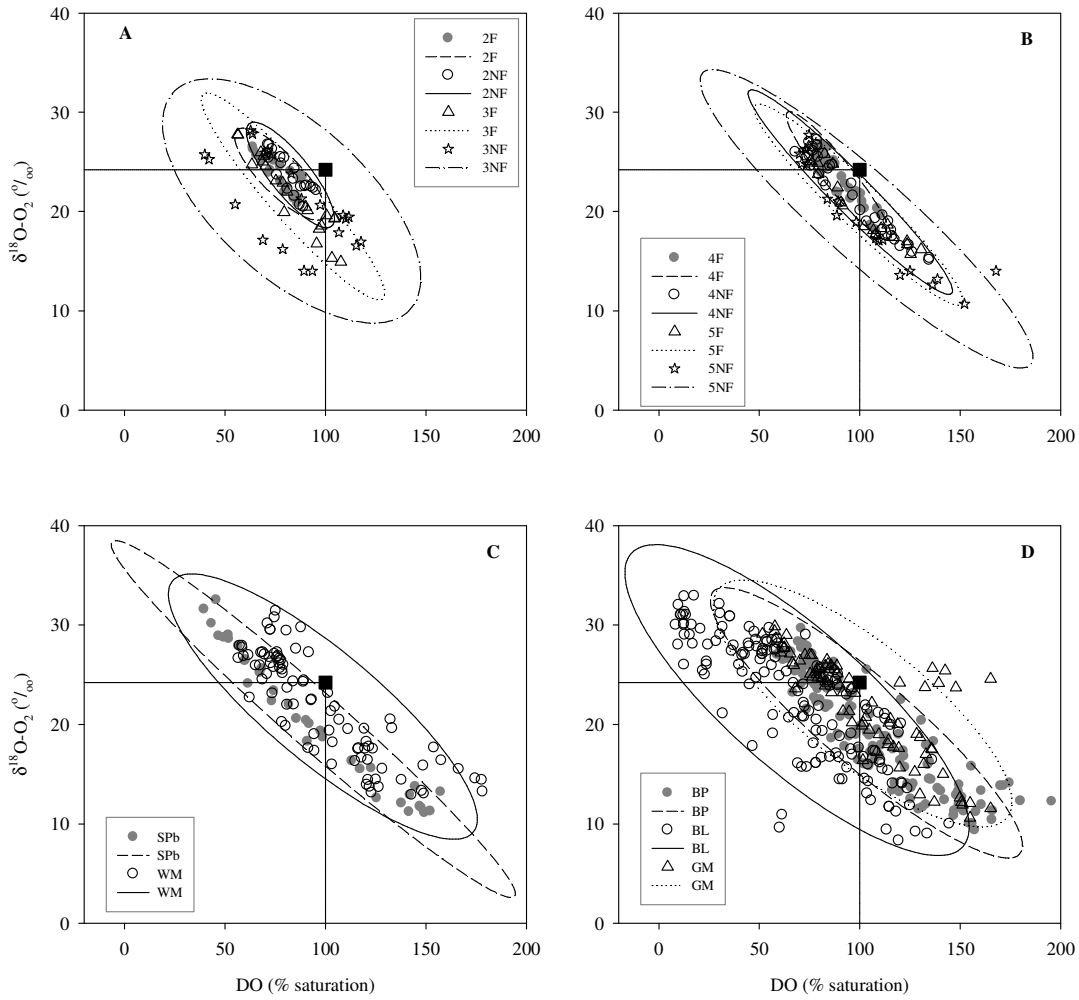

Figure 6.11 Cross plots of DO saturation and δ^{18}O-DO data obtained from all samples for 13 sites in the Grand River network. The black square indicates the equilibrium where both DO and δ^{18}O-DO are at atmospheric equilibrium (DO = 100% saturation and δ^{18}O-DO = 24.2‰). The 95% confidence ellipse is shown for each site.

6.3.3 Ecosystem metabolism

The GPP for the sites ranged from 0.4 g O_2 m^{-2} day^{-1} at site 2F to 20 g O_2 m^{-2} day^{-1} at site GM (Figure 6.12). The two 3rd order sites (3F and 3NF) had mean GPP of 3.2 and 3.3 g

O_2 m^{-2} day^{-1}, higher than the 2nd order sites with mean of 0.9 g O_2 m^{-2} day^{-1}. These 3rd order sites also had higher GPP than two 4th order sites, with means of 2.2 and 2.4 g O_2 m^{-2} day^{-1} (Table 6.1A & Figure 6.12). Site 5NF had higher GPP, 9.0 g O_2 m^{-2} day^{-1}, than its counterpart site 5F, 3.6 g O_2 m^{-2} day^{-1} (Table 6.1A & Figure 6.12). Relatively high variation in GPP were observed at sites 5NF, BL and GM (Figure 6.12).

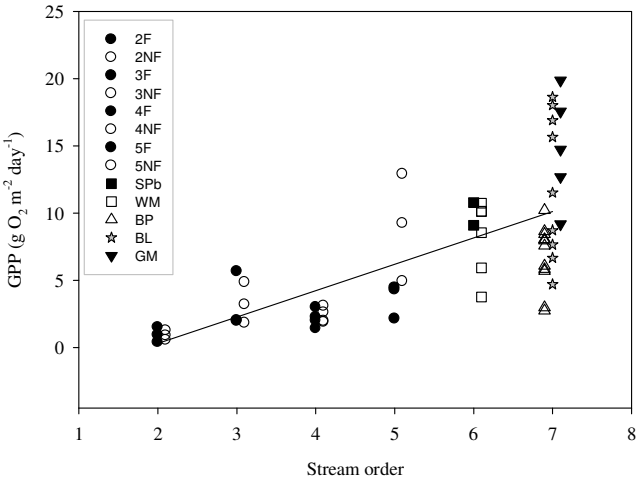

Figure 6.12 Gross primary production (***GPP***, *g O_2 m^{-2} day^{-1}*) against stream order at multiple sites in the Grand River network. The 13 sites from left to right in order are 2F, 2NF, 3F, 3NF, 4F, 4NF, 5F, 5NF, SPb, WM, BP, BL and GM. Statistically significant relationship was detected between GPP and stream order. GPP = 1.96 (stream order) – 3.60, $F_{1, 59} = 52.42$, adjusted R^2 = 46.6%, $P < 0.0001$.

GPP exhibited an increasing trend with stream order (Figure 6.12), as did channel geomorphology and hydrologic parameters such as width, depth, width/depth and discharge (Figure 6.13). The width, log (width) and log (discharge) are the better predictors of GPP among them, and are as good as the stream order with $R^2 \geq 45\%$ (Figure 6.12 & Figure 6.13).

I used 4 pairs of streams with and without riparian trees (2F vs. 2NF, 3F vs. 3NF, 4F vs. 4NF, and 5F vs. 5NF) to look for an effect of riparian trees, However, I only succeeded in demonstrating an effect of stream order on GPP (2-way ANOVA, $p < 0.001$). Only at the 5th order sites did riparian trees appear to reduce GPP (Figure 6.12 & Table 6.1A).

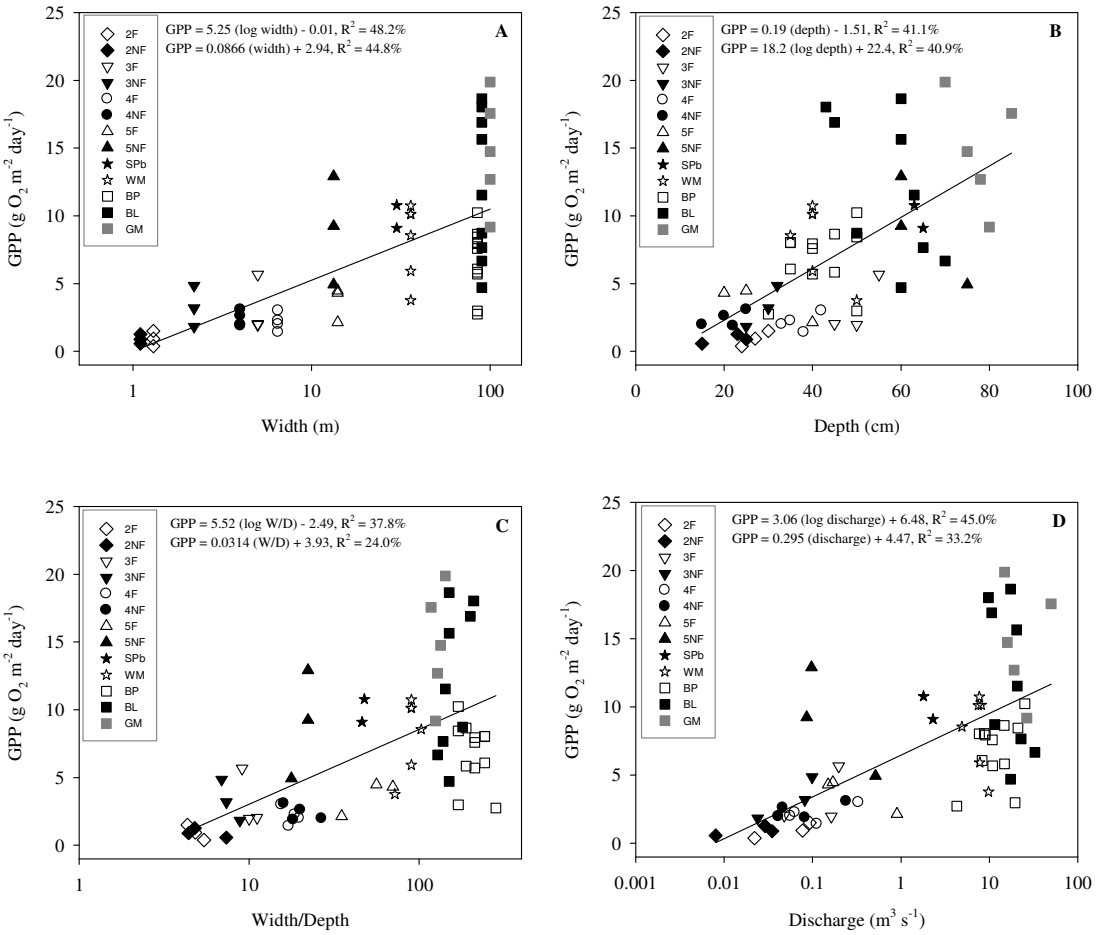

Figure 6.13 GPP for streams in the Grand River network, plotted vs. channel geomorphology and hydrologic parameters (width, depth, width/depth & discharge) as measures of stream ecosystem size. Statistically significant relationships were detected between GPP and these parameters as well as their logarithmic values ($P < 0.0001$). Regression equations associated with adjusted R^2 are provided in plots.

A weak but statistically significant relationship was detected between GPP and incoming PAR for the Grand River sites overall. The regression is GPP = 0.178 (PAR) + 1.82, $F_{1,31} = 5.97$, adjusted $R^2 = 13.8\%$, $P = 0.002$ (Figure 6.14A). By site, a statistically significant relationship was detected between GPP and light at site WM ($P = 0.02$), BP ($P = 0.003$) and GM ($P = 0.007$), but not at site BL ($P = 0.14$) (Figure 6.14B). Significant differences in intercept were detected between sites BL and BP (ANCOVA, $P < 0.001$)

as well as between sites BL and WM (ANCOVA, P = 0.004); however, no significant difference was detected among these sites in slope (ANCOVA, P > 0.3) (Figure 6.14B).

Combining all data points at 4 Grand River sites (WM, BP, BL and GM) from 2006 to 2008, there was a decline in GPP from May to October (Figure 6.15A). However, this was mostly due to lower rates in October (Table 6.1B & Figure 6.15). Considering the data from 2006 only, apparent decreasing trends were observed at site WM and BP. Low GPP at site BL in May, 2006, was associated with a high discharge event (Table 6.1B & Figure 6.15B).

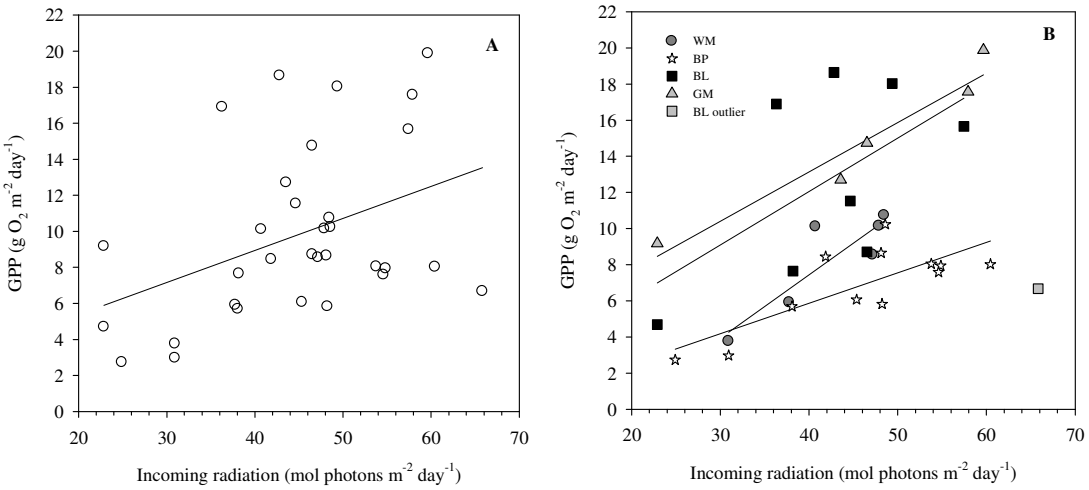

Figure 6.14 Gross primary production (***GPP***, *g O_2 m^{-2} day^{-1}*) regressed with incoming PAR (mol photons m^{-2} day^{-1}) for 4 Grand River sites (WM, BP, BL and GM) for sampling periods from 2006 to 2008.

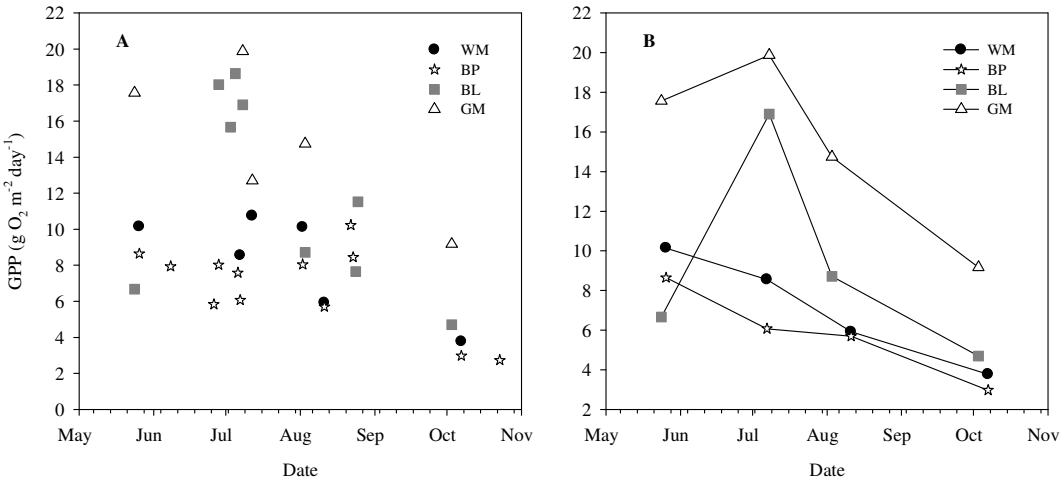

Figure 6.15 Seasonal trends of gross primary production (***GPP***, *g O_2 m^{-2} day^{-1}*) for 4 Grand River sites (WM, BP, BL and GM). Data for the whole sampling period from 2006 to 2008 were used for (A), while only 2006 data were used for (B).

ER ranged from 2.0 g O_2 m^{-2} day^{-1} at site 2F to 33 g O_2 m^{-2} day^{-1} at site BL (Figure 6.16). Relatively high ER, and high variation in ER, was found at site BL from 7.9 to 33 g O_2 m^{-2} day^{-1} in summer (Figure 6.16). This site is 5 km downstream of Kitchener WWTP. ER also exhibited an increase with stream order (Figure 6.16), and channel geomorphology and hydrologic parameters (width, depth, width/depth and discharge) as well (Figure 6.17). Among them, the width, log (width) and log (discharge) are the better predictors of ER, and are as good as the stream order with $R^2 \geq 26\%$ (Figure 6.16 & Figure 6.17).

I used 4 pairs of streams with and without riparian trees (2F vs. 2NF, 3F vs. 3NF, 4F vs. 4NF, and 5F vs. 5NF) to demonstrate an effect of stream order on ER (2-way ANOVA, p = 0.02), but did not find an effect of riparian trees on ER (p = 0.214) or interaction (p = 0.411).

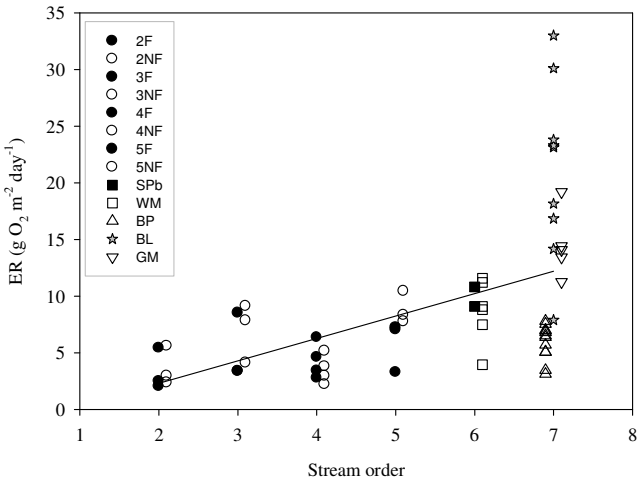

Figure 6.16 Ecosystem respiration (***ER***, $g\ O_2\ m^{-2}\ day^{-1}$) against stream order at multiple sites in the Grand River network. The 13 sites from left to right in order are 2F, 2NF, 3F, 3NF, 4F, 4NF, 5F, 5NF, SPb, WM, BP, BL and GM. The relationship between ER and stream order is: ER = 1.98 (stream order) – 1.65, $F_{1, 59} = 13.8$, adjusted $R^2 = 26\%$, $P < 0.0001$.

There was no relationship between ER and temperature for the Grand River overall (ER = 0.469 (Temperature) + 2.62, $F_{1,31} = 2.38$, adjusted $R^2 = 4.3\%$, $P = 0.133$) (Figure 6.18A). Some of the variation is due to differences among sites. By site, a statistically significant relationship was detected between ER and temperature for site WM (P = 0.006) and BP (P = 0.023), but not for BL (P = 0.056) and GM (P = 0.973) (Figure 6.18B). Site BL has significant different intercept than sites WM (ANCOVA, P < 0.001), BP (ANCOVA, P < 0.001) and GM (ANCOVA, P =0.014), and a significantly different slope from site BP (ANCOVA, P = 0.04) and site GM (ANCOVA, P = 0.016) (Figure 6.18B).

For 4 Grand River sites (WM, BP, BL and GM), there were no obvious seasonal trend in ER, except that some high ER estimates occurred in July and ER was lower in October at same sites (Figure 6.19).

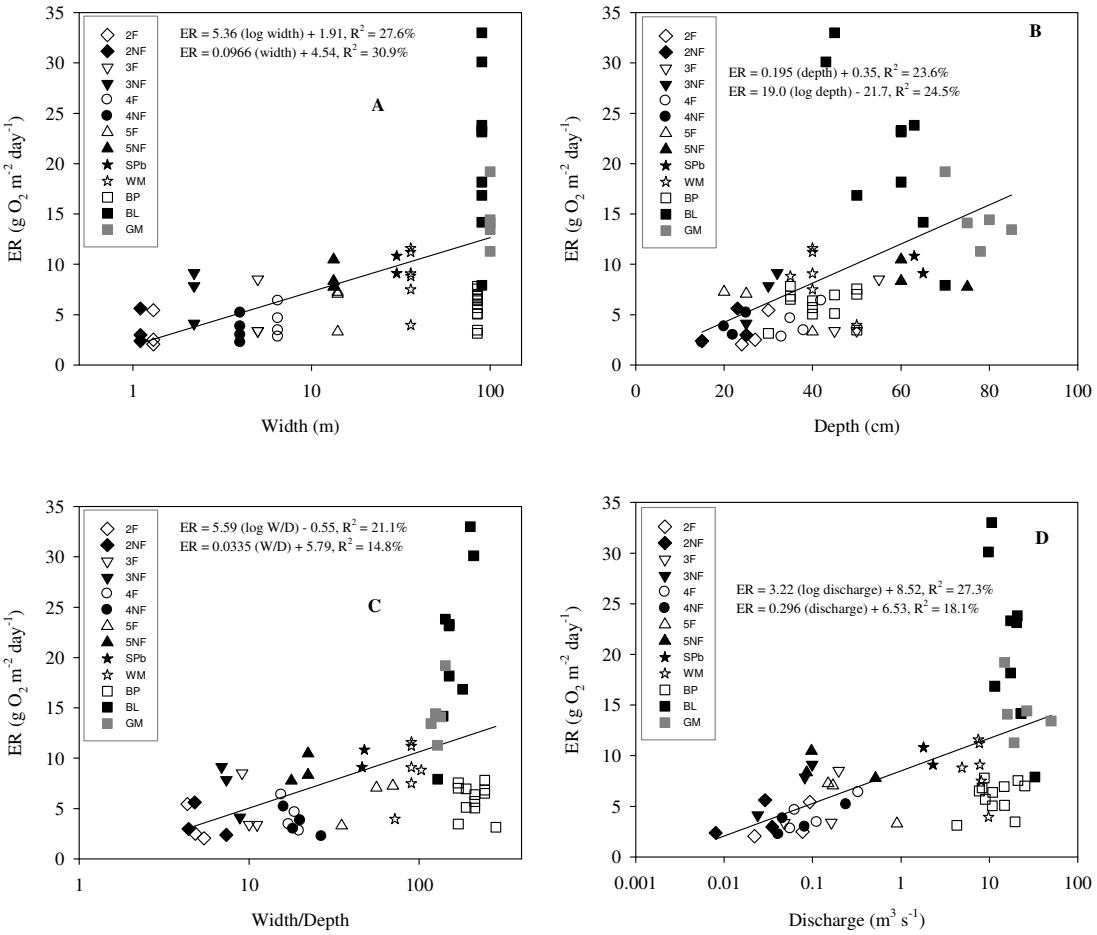

Figure 6.17 ER for streams in the Grand River network, plotted vs. channel geomorphology and hydrologic parameters (width, depth, width/depth & discharge) as measures of stream ecosystem size. Statistically significant relationships were detected between GPP and these parameters as well as their logarithmic values ($P \leq 0.001$). Regression equations associated with adjusted R^2 are provided in plots.

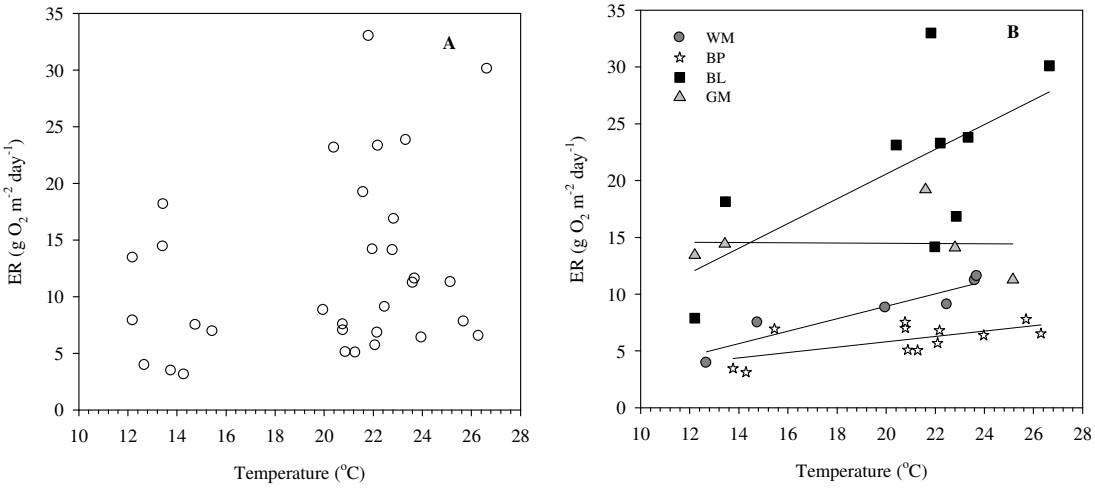

Figure 6.18 Ecosystem respiration (***ER***, *g O_2 m^{-2} day^{-1}*) regressed with temperature (℃) at 4 Grand River sites (WM, BP, BL and GM) for sampling periods from 2006 to 2008.

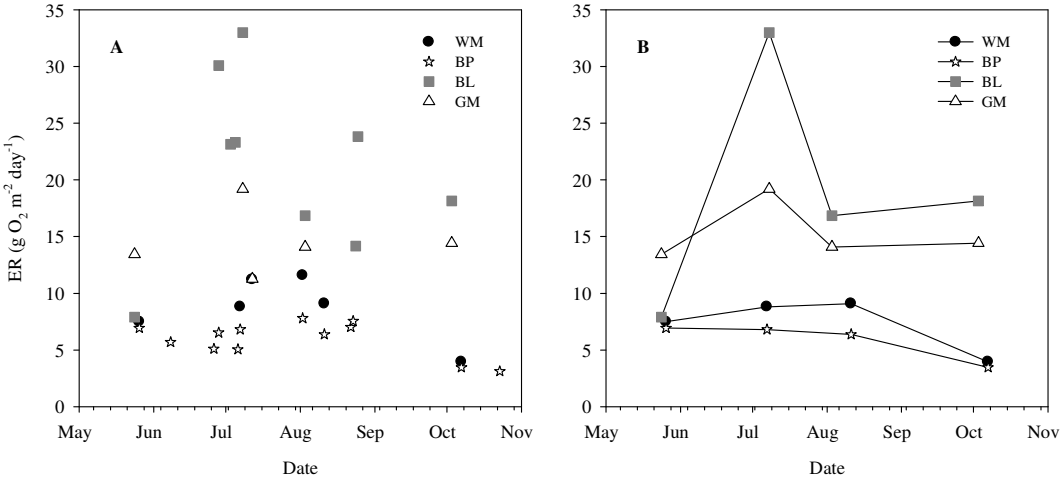

Figure 6.19 Seasonal trends of ecosystem respiration (***ER***, *g O_2 m^{-2} day^{-1}*) for 4 Grand River sites (WM, BP, BL and GM). Data are for the whole sampling period from 2006 to 2008 (A) and in 2006 only (B).

Sites 2F, 2NF, 3F, 3NF, 4F, 4NF and 5F and one large river site, BL, had negative NPP on all dates, ranging from -0.24 g O_2 m^{-2} day^{-1} at site 4NF to -16.1 g O_2 m^{-2} day^{-1} at site BL (Table 6.1B & Figure 6.20). The 6th order site, SPb, consistently had NPP

of close to 0 g O_2 m^{-2} day^{-1}. Non-shaded site 5NF and three large river sites, WM, BP and GM, had either positive or negative NPP in summer, with the maximum range of from -5.2 to 4.1 g O_2 m^{-2} day^{-1} at site GM (Table 6.1 & Figure 6.20). The NPP for 4 Grand River sites exhibited a decreasing trend with season (Figure 6.21).

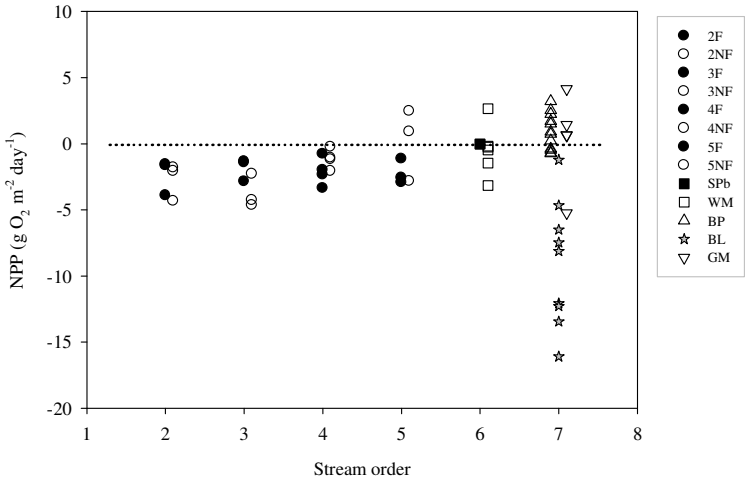

Figure 6.20 Net primary production (***NPP***, *g O_2 m^{-2} day^{-1}*) against stream order at multiple sites in the Grand River network. The 13 sites from left to right in order are 2F, 2NF, 3F, 3NF, 4F, 4NF, 5F, 5NF, SPb, WM, BP, BL and GM. The dotted line represents balance with NPP = 0.

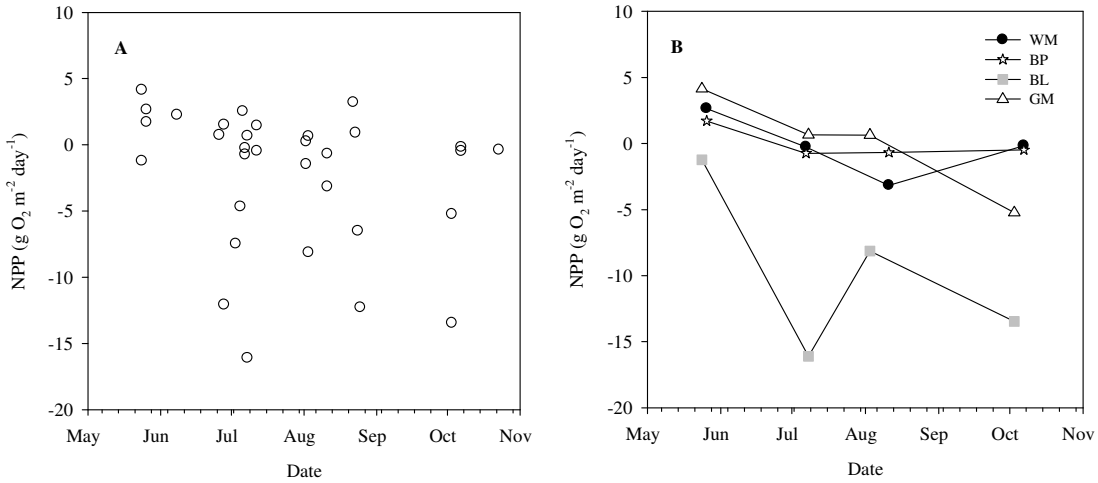

Figure 6.21 Seasonal trends of net primary production (***NPP***, *g O_2 m^{-2} day^{-1}*) for 4 Grand River sites (WM, BP, BL and GM). Data are for the whole sampling period from 2006 to 2008 (A) and in 2006 only (B).

I used 4 pairs of streams with and without riparian trees (2F vs. 2NF, 3F vs. 3NF, 4F vs. 4NF, and 5F vs. 5NF) to look for an effect of stream order on NPP but did not find one (2-way ANOVA, p = 0.167), nor did I find an effect of riparian trees on NPP (p = 0.627) or an order-tree interaction (p = 0.108).

Ratios of GPP: ER increased with stream order excluding site BL. The *GPP*: *ER* ratios of site BL were consistently less than 1 with an average level of 0.58 (Table 6.1B & Figure 6.22). Small stream sites (2nd to 4th order) were apparently heterotrophic. The transition from heterotrophic to autotrophic on some occasions occurred at 5th and 6th order sites. 7th order sites BP and GM had average *GPP*: *ER* ratios of 1.14 and 1.03, respectively (Table 6.1B & Figure 6.22).

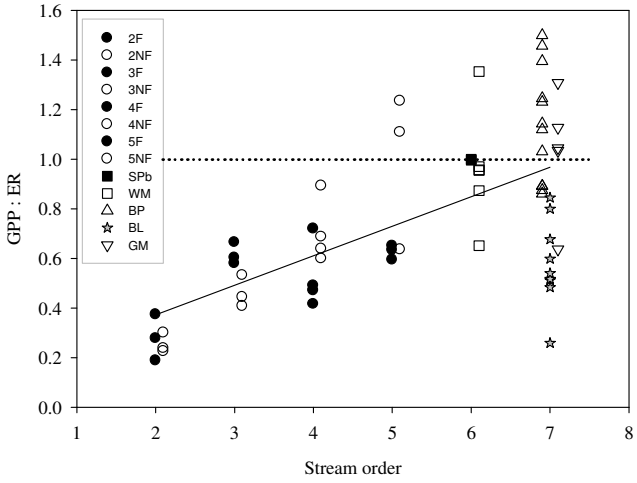

Figure 6.22 *GPP*: *ER* ratios against stream order at multiple sites in the Grand River network. The 13 sites from left to right in order are 2F, 2NF, 3F, 3NF, 4F, 4NF, 5F, 5NF, SPb, WM, BP, BL and GM. The dotted line represents balance with GPP: ER = 1. Statistically significant relationship was detected between GPP: ER and stream order. GPP/ER = 0.119 (stream order) + 0.135, $F_{1, 59} = 39.65$, adjusted $R^2 = 39.6\%$, $P < 0.0001$.

Linear regressions were significant between GPP: ER and stream order and channel geomorphology and hydrologic parameters (width, depth, width/depth and discharge) (P < 0.0001), indicating they are good predictors for the ratio of GPP: ER in the Grand River (Figure 6.22 & Figure 6.23).

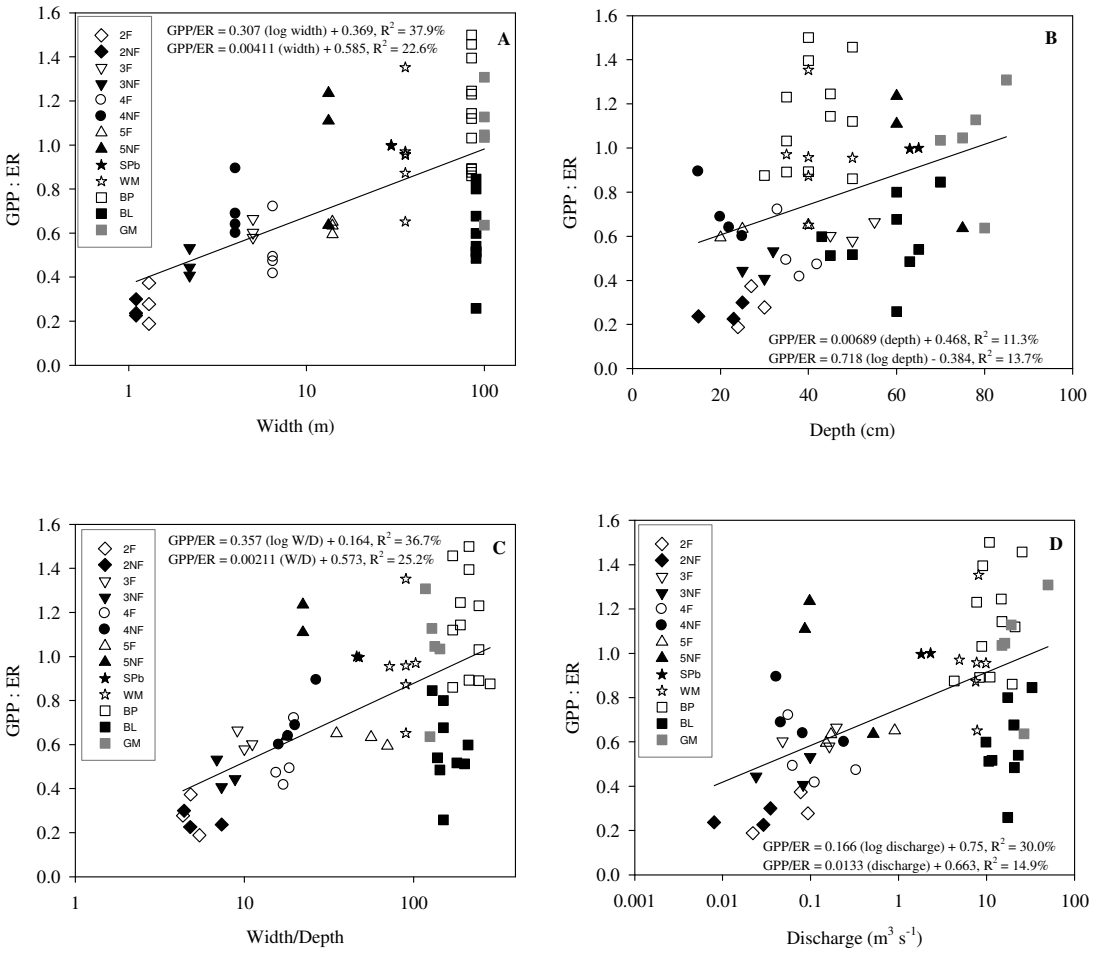

Figure 6.23 GPP/ER for streams in the Grand River network, plotted vs. channel geomorphology and hydrologic parameters (width, depth, width/depth & discharge) as measures of stream ecosystem size. Statistically significant relationships were detected between GPP and these parameters as well as their logarithmic values ($P \leq 0.005$). Regression equations associated with adjusted R^2 are provided in plots.

In comparison, stream order is the best predictor of GPP/ER among all of these parameters. The R^2 for the regression is 39.6%. The next are the log (width), log (width/depth) and log (discharge). They have the $R^2 \geq 30\%$ for the regressions.

I used 4 forested/non-forested pairs sites (2F vs. 2NF, 3F vs. 3NF, 4F vs. 4NF, and 5F vs. 5NF) to demonstrate an effect of stream order on the ratio of GPP: ER (2-way ANOVA, $p < 0.001$). The interaction of order and riparian trees on the ratio of GPP: ER

was significant (p = 0.025), but the effect of riparian trees on the ratio of GPP: ER was not (p = 0.136).

The ratios of GPP: ER for 4 Grand River sites decreased with season (Figure 6.24).

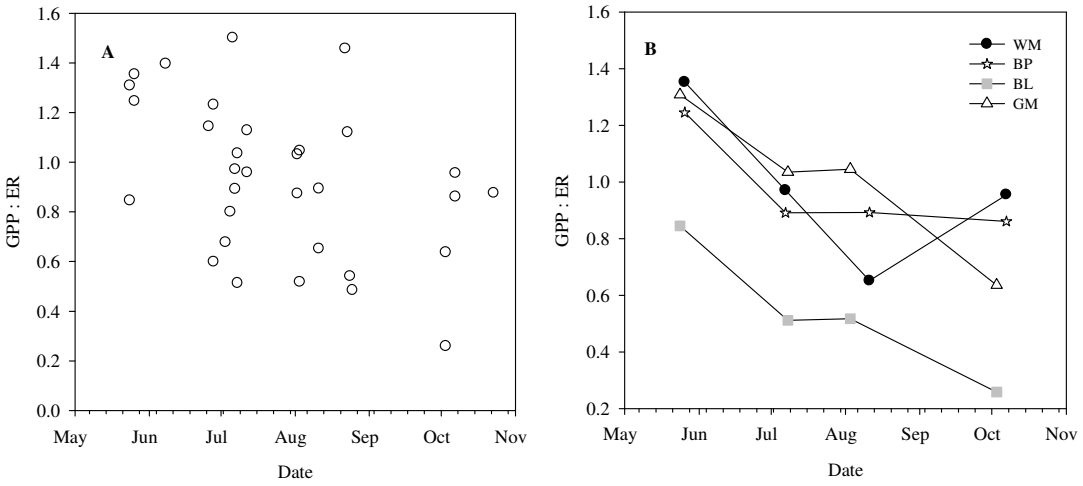

Figure 6.24 Seasonal trends of *GPP: ER* ratios for 4 Grand River sites (WM, BP, BL and GM). Data are for the whole sampling periods from 2006 to 2008 (A) and in 2006 only (B).

6.3.4 Gas exchange pattern in the Grand River

The average of daily total absolute O_2 flux of stream sites 2F, 2NF, 3F, 3NF, 4F, 4NF, 5F, 5NF and large river site BP, ranged from 2.2 to 4.9 g O_2 m^{-2} d^{-1}. Two Speed river sites (SPa and SPb) only had average rates of total absolute gas flux of 0.15 and 0.55 g O_2 m^{-2} d^{-1}, respectively (Table 6.1). Two Grand River sites, WM and GM, showed a range of total absolute gas flux of 6.3 to 8.9 g O_2 m^{-2} day^{-1}. Site BL had the highest daily rate of total absolute gas flux, 11.5 g O_2 m^{-2} d^{-1} (Table 6.1 & Figure 6.25).

The average gas exchange coefficients for sites ranged from 0.1 to 0.3 m h^{-1} except site 5F (Figure 6.26). Site 5F showed two extreme high gas exchange coefficients, 0.52 m h^{-1} in August-27 and 0.62 m h^{-1} in October-05, 2007, respectively, and the highest average of gas exchange coefficient, 0.43 m h^{-1} (Table 6.1 & Figure 6.26).

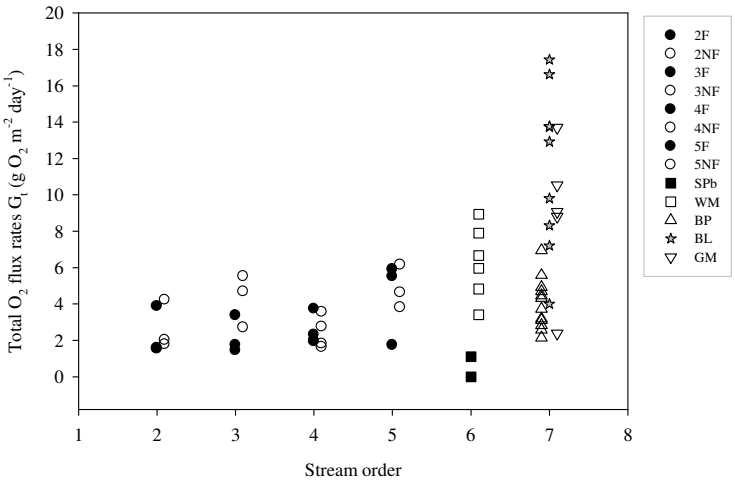

Figure 6.25 Daily rates of total absolute gas flux (***G*****$_t$**, *g O_2 m^{-2} day^{-1}*) against stream order at multiple sites in the Grand River network. The 13 sites from left to right in order are 2F, 2NF, 3F, 3NF, 4F, 4NF, 5F, 5NF, SPb, WM, BP, BL and GM.

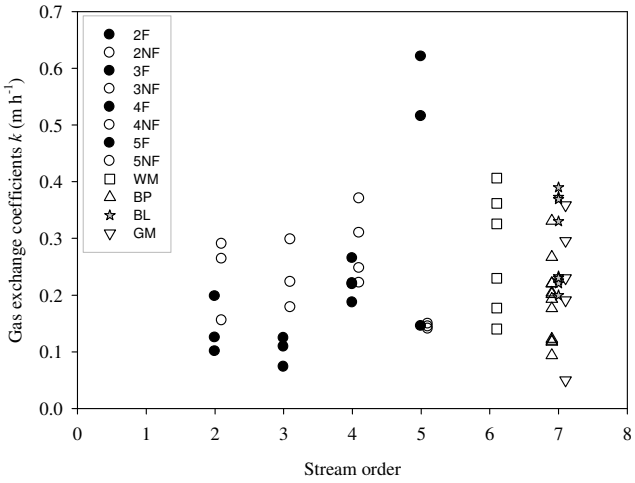

Figure 6.26 Gas exchange coefficients (***k***, *m h^{-1}*) against stream order at multiple sites in 4 Grand River network. The 12 sites from left to right in order are 2F, 2NF, 3F, 3NF, 4F, 4NF, 5F, 5NF, WM, BP, BL and GM.

6.3.5 Respiration isotopic fractionation factors in the Grand River

Respiration isotopic fractionation factors ranged from 0.9707 to 0.9968, and exhibited a declining pattern from small streams to large river sites (Table 6.1 & Figure 6.27). The average value of respiration isotopic fractionation factors at small stream sites (2F, 2NF, 3NF, 4NF and 5F) was above 0.9900. The highest average occurred at site 5F, 0.9937. Respiration isotopic fractionation factor averaged from 0.9867 to 0.9748 among 6^{th}-7^{th} order sites (Table 6.1).

Respiration isotopic fractionation factor exhibited no obvious seasonal patterns (Figure 6.28).

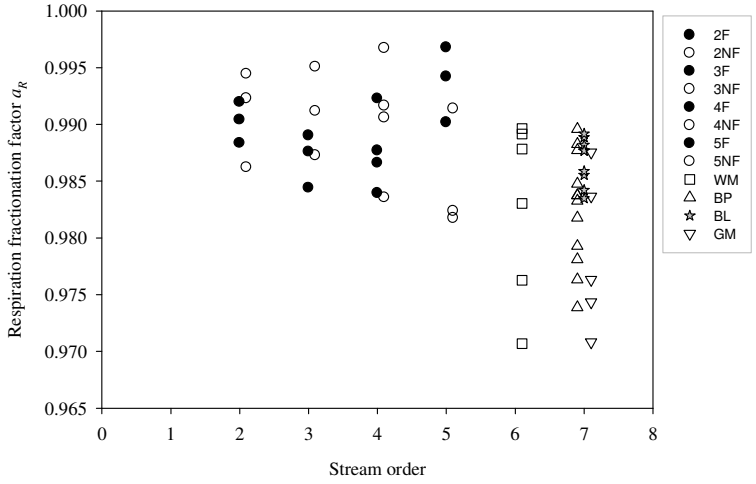

Figure 6.27 Respiration isotopic fractionation factor ($\boldsymbol{a_R}$) against stream order at multiple sites in the Grand River network. The total 12 sites from left to right in order are 2F, 2NF, 3F, 3NF, 4F, 4NF, 5F, 5NF, WM, BP, BL and GM.

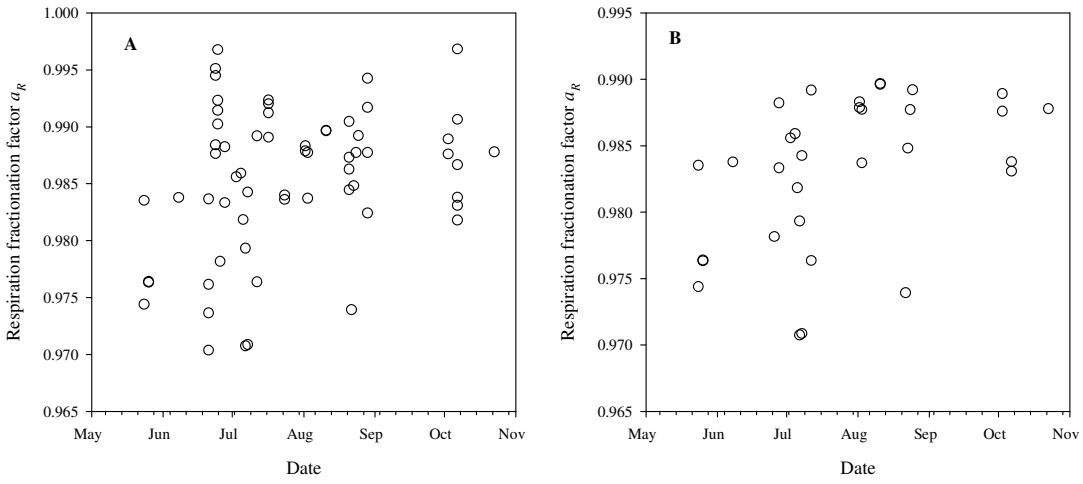

Figure 6.28 Seasonal trends of respiration isotopic fractionation factor ($\boldsymbol{a_R}$) for all 14 sites (A) and only for 4 Grand River sites (WM, BP, BL and GM) (B) in the Grand River network for sampling periods from 2006 to 2008.

6.3.6 River ecosystem metabolism for the entire Grand River Network

The length of stream channel in the GRW totals almost 11330 km, which includes 5504 km of 1st order streams, 2673 km of 2nd order streams, 1410 km of 3rd order streams, 830 km of 4th order streams, 466 km of 5th order streams, 255 km of 6th order streams and 192 km of 7th order streams (Table 6.2). The large river channel from site WM to the outlet to Lake Erie is almost 200 km. In order to scale up site estimates, the relationships of metabolic rates (both *GPP* and *ER*) to stream order were described using quadratic equations, whereas the stream width appeared to follow an exponential form with increasing stream order (Figure 6.29).

The total water coverage areas of streams for each order were calculated, increasing from 2.9 to 15.6 km^2 with stream order (Table 6.2). The total GPP and ER of streams with the same order were calculated by summing up daily GPP and ER of streams with the same order (Figure 6.30 & Table 6.2). The total gross primary production of the entire Grand River network was summed as 3.3×10^8 g O_2 day^{-1}and the total ecosystem respiration of the whole Grand River network was 4.2×10^8 g O_2 day^{-1}.

Hence, the Grand River network was a net heterotrophic system, and consumed O_2 around 0.9×10^8 g O_2 day^{-1} from May to October (Table 6.2 & Figure 6.30).

Table 6.2 Channel geomorphologic parameters and ecosystem metabolism parameters of streams grouped by stream order (from 1st to 7th): Total channel length (km), water coverage area (km^2), daily P and R rates (in g O_2 m^{-2} day^{-1}), daily gross primary production, daily ecosystem respiration and net primary production (in $\times 10^6$ g O_2 day^{-1}).

Stream Order	1	2	3	4	5	6	7	SUM
Length(km)	5503.9	2672.9	1410.2	830.0	465.5	255.1	191.6	**11330**
width(m)	0.52	1.21	2.81	6.53	15.15	35.16	81.58	
Area(km^2)	2.86	3.23	3.96	5.42	7.05	8.97	15.63	**47.1**
P rates	0.56	1.14	2.22	3.81	5.89	8.48	11.57	
R rates	5.2	4.25	4.23	5.15	7.01	9.81	13.55	
GPP	1.6	3.7	8.8	20.7	41.5	76.0	180.8	**333.1**
ER	14.9	13.7	16.8	27.9	49.4	88.0	211.8	**422.5**
NPP	-13.3	-10.1	-8.0	-7.3	-7.9	-11.9	-30.9	**-89.3**

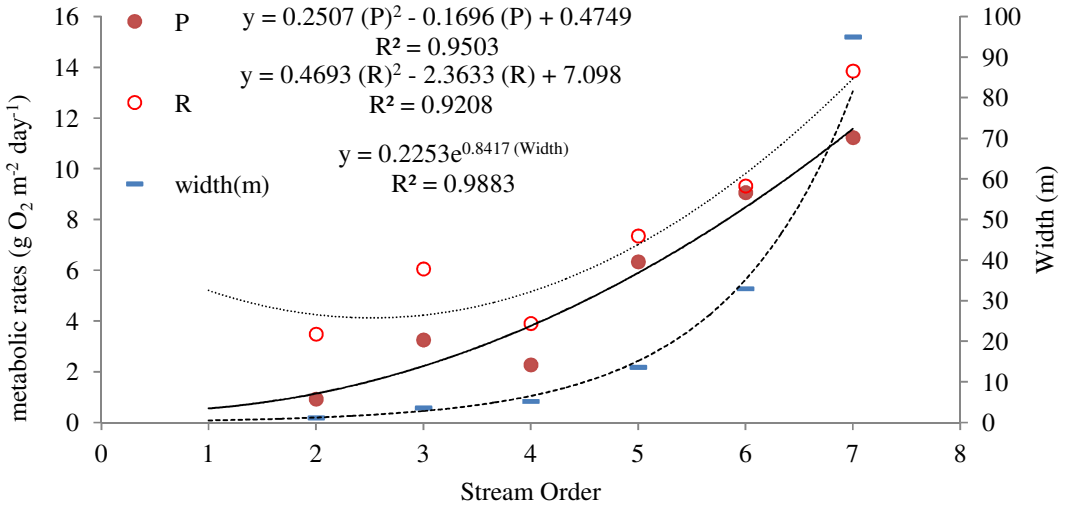

Figure 6.29 The relationship of ecosystem metabolic rates (***GPP*** and ***ER***, in g O_2 m^{-2} day^{-1}), and channel width (m) with stream order in the Grand River network.

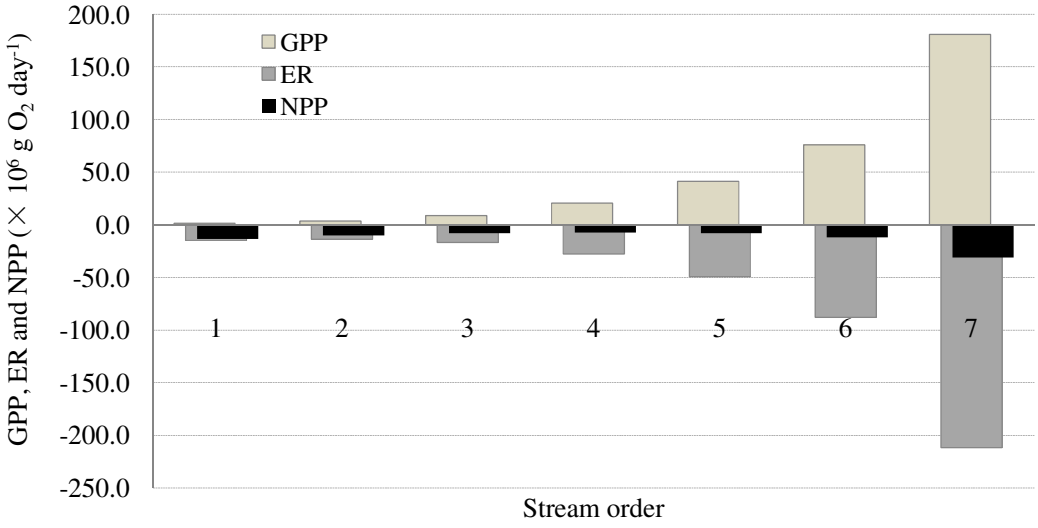

Figure 6.30 Total daily ecosystem GPP, ER and NPP (in ($\times 10^6$ g O_2 day^{-1}) of streams in each order (from 1st to 7th) in the Grand River network.

6.4 Discussion

Grand River network has a broad range of the metabolic rates (GPP = 0.4 to 20 and ER = 2 to 33 g O_2 m^{-2} day^{-1}), and much of this range was associated with stream size and human disturbance. The Grand River network is located in a highly developed agricultural and urban mixed land use watershed. It was not possible to find pristine streams that could be treated as 'reference' streams. All my study sites were subject to human disturbance to some extent. The SPb and BL were two urban-influenced sites within 2 and 5 km of large WWTPs. Site GM was just 19 km downstream of site BL. These three sites were eutrophic according to their average total phosphorus concentrations, 36-54 µg/L (CCME 2007). Other sites were mainly impacted by agriculture, and their trophic states ranged from mesotrophic (2F, 2NF, 3F and 3NF, their TP 11-18.5 µg/L) to mesoeutrophic (4F, 4NF, 5F, 5NF, WM and BP, their TP 22-32 µg/L) (CCME 2007). Deforestation was also a common disturbance to streams and rivers in the Grand River watershed, especially in riparian zones of small streams. Bank erosion was often seen in small streams in agricultural areas.

6.4.1 The effect of riparian trees on ecosystem metabolism in small and middle-sized streams

The small streams in my study were similar in water chemistry, e.g., pH, SRP, TP, nitrate and DIN (Table 6.1, Figure 6.5 & 6.6). Although the presence of riparian trees resulted in differences in light availability between shaded sites (2F, 3F, 4F, 5F) and non-shaded sites (2NF, 3NF, 4NF and 5NF), I did not find an effect of riparian trees on GPP and ER. There were similar metabolic rates in each of the paired shaded/non-shaded sites with stream orders 2 to 4, except at site 5F and 5NF (Figures 6.12 & 6.16). Different geomorphologic and hydrologic parameters between paired shaded/non-shaded streams might provide explanations. In 2^{nd} to 4^{th} order streams, non-shaded sites were shallow and narrow, with less discharge compared to their shaded counterparts with the same stream order. In addition, shading from stream banks and riparian grasses, and unstable sediments resulting from agricultural activities, might also counteract the positive effect of open canopy on stream GPP. I noticed that all non-shaded sites (2NF, 3NF, 4NF and 5NF) had high banks. The sediments at site 2NF were clays and fine sands with little periphyton, and this site had low production efficiency (discussed in Chapter 5). Abundant periphyton at site 3NF and macrophytes patches at site 3F may be responsible for higher GPP at sites 3F and 3NF than their counterparts of 4^{th} order. It was not clear why few macrophytes grew at 4F and site 4NF. As for 5^{th} order sites, 5F and 5NF, they had similar width and abundant aquatic plants. Site 5F was shallow with dense riparian trees, but it was still open in the middle part of the channel. The mixed gravel, cobbles and boulder substrate may be stable in shallow water, which may have favoured the growth of its prolific moss community. 5NF was fully open and was deeper than 5F. *Cladophora glomerata* were abundant at site 5NF. These factors may have led to high GPP at site 5NF, reaching to 12.9 g O_2 m^{-2} day^{-1} in summer, which was much higher than that at site 5F (Figure 6.12).

6.4.2 The effect of WWTPs on ecosystem metabolism in the Grand River

Impacts of human disturbance on the metabolic rates were more obvious at three urban impacted sites affected by WWTP discharges, i.e., SPa in the Speed River, and sites BL and GM in the Grand River, than the two agriculture impacted sites (e.g., WM and BP).

The GPP and ER in the Grand River were stimulated by WWTP effluents, but to different extents. Comparing sites BP (20 km upstream of Kitchener WWTP) and BL (5 km downstream of Kitchener WWTP) in the middle section of the Grand River, average GPP was nearly doubled from BP (6.9 g O_2 m^{-2} day^{-1}) to BL (12.1 g O_2 m^{-2} day^{-1}), however, ER was more than tripled between these two sites (6.0 g O_2 m^{-2} day^{-1} at BP to 21.2 g O_2 m^{-2} day^{-1} at BL). One of important reasons that the ER was stimulated more than GPP is that the site BP already had high concentration of nutrients (Table 6.1). Although the biomass of macrophytes is stimulated below WWTPs in the Grand (Hood 2012), GPP may be constrained due to self-shading. However, WWTPs inputs can enhance the ER by increasing heterotrophic microbial respiration and nitrification, especially if nitrogen is released in the form of NH_4^+ (Rosamond et al. 2011).

The highest ER rate I observed was in July, 2006, at site BL, 33 g O_2 m^{-2} day^{-1}. The reasons for high ER at site BL in the Grand River are still not clear. The Kitchener WWTP 5 km upstream usually discharges effluents with high ammonia (Rosamond et al. 2011). Strong nitrification occurs in the reach downstream of the Kitchener WWTP to site BL (Thuss 2008), and oxidation of NH_4^+ of WWTP discharge was estimated to consume 2.7 g DO m^{-2} day^{-1} (Jamieson 2010). Therefore this process may contribute significantly to ER, but is not the whole reason for elevated ER at site BL. Jamieson (2010) suggested that organic matter degradation and oxygen demand of sediment and benthic deposits might be the main reasons for apparently elevated DO consumption upstream of site BL. The DOC concentrations at site BL are similar to other Grand River sites (Figure 6.7). It is likely that bacterial oxidation of organic matter is more important to increased ER. In addition, macrophyte communities with high biomass at site BL may also be an important contributor of ER.

Increased metabolism rates of streams receiving WWTP inputs have been observed in many studies, and these studies found comparable metabolic rates to the Grand River, regardless of stream size (Flemer 1970, Hornberger et al. 1977, Chessman 1985, Gucker et al. 2006, Ruggiero et al. 2006, Uehlinger 2006, Sanchez-Perez et al. 2009, Young and Collier 2009, Wassenaar et al. 2010). Examples with high ER rates due to WWTP outfalls are also found in small streams. Sanchez-Perez (2009) observed an average ER rate high to 37.6 g O_2 m^{-2} day^{-1} in a 3rd order stream receiving WWTP discharges, Toulouse, France. Ruggiero (2006) also found that average ER rate increased from 4.6 to 35.1 g O_2 m^{-2} day^{-1} in a 3rd order Mediterranean stream due to the effect of WWTP discharges. A 3rd order urban stream in Berlin, the Erpe, exhibiting high ER rates upstream still displayed increased ER rates downstream of a WWTP. The ER rates increased from 28 to 38 g O_2 m^{-2} day^{-1} in a tributary, Demnitzer Mill Brook (1st order) and from 32 to 59 g O_2 m^{-2} day^{-1} in the Erpe from upstream to downstream of the WWTPs (Gucker et al. 2006).

Overall, the river channels downstream of WWTPs in the Grand River network are experiencing strong effects from human activities. Wastewater effluents from urbanized areas have caused impacts on the Grand River ecosystem superimposed on the impacts of agriculture. No strong effects of human activities on metabolic rates were detected in small streams as seen as in large rivers. The main reason may be that these streams are in a forested area of the Speed River sub-basin and some of them are protected by riparian trees. These streams may not be fair representatives of small streams in the Grand River basin. Small agriculture impacted streams in upper and lower sections of the basin may be strongly impacted by human activities.

6.4.3 The effect of stream order on ecosystem metabolism in the Grand River network

The metabolic parameters (GPP, ER and GPP: ER) exhibited positive relationships with stream order (Figure 6.12, Figure 6.16 & Figure 6.22). Stream order, width, depth, discharge and drainage basin size are all measures of stream size, and all related to these

parameters (Table 6.2). Among them, stream order and log width demonstrated the highest R^2 (Figure 6.13, Figure 6.17 & Figure 6.23).

The metabolic rates (both GPP and ER) and the ratio of GPP: ER of streams in the Grand River increased with stream size. However, this relationship may not extend to the lower Grand River where the water is turbid, the water depth is up to 3 m, and there is a lack of submersed macrophytes except close to the shore (Kuntz 2008). Kuntz (2008) measured the whole river metabolism at 10 sites along the last 35 km section of the lower Grand in summer (June-August), 2006-2007 (Table 6.3). The average GPP was 8.8 (2 - 13.9) g O_2 m^{-2} day^{-1}, the ER was 5.7 (2.8 - 9.1) g O_2 m^{-2} day^{-1}, and the ratio of GPP: ER was 1.6 (0.5 - 3.1). Both GPP and ER of the lower Grand were similar to those at WM and BP. However, they were lower than the corresponding metabolic parameters at BL and GM in the middle section of the Grand River. The average ratio of GPP: ER in the lower Grand was high, up to 1.6.

Table 6.3 Ecosystem metabolism rates (P and R in g O_2 m^{-2} day^{-1}) and ratios of the P/R at 10 sampling sites in the last 35 km section of the lower Grand River (from Cayuga to Lake Erie), in summer, 2006-2007. Data are from Figure 3.2 and 3.3 in Kuntz (2008).

		site1	site2	site3	site4	site5	site6	site7	site8	site9	site10	average	
P	2006	2.0	3.9	9.3	12.9	11.4	8.5	5.0	7.5	7.8	7.6	7.6	
	2007	5.8	7.8	11.5	13.9	13.7	7.2	5.7	11.2	12.4	11.3	10.1	8.8
R	2006	3.8	5.2	6.2	8.5	5.3	3.1	9.1	6.0	6.3	7.0	6.1	
	2007	3.7	5.5	5.8	7.0	4.4	2.8	7.9	5.0	5.6	6.2	5.4	5.7
P/R	2006	0.5	0.8	1.5	1.5	2.2	2.7	0.6	1.3	1.2	1.1	1.3	
	2007	1.6	1.4	2.0	2.0	3.1	2.6	0.7	2.3	2.2	1.8	2.0	1.6

Notes: A low-head dam is located between sites 6 and 7. The Channel becomes obviously wider right below site 4, with fringing wetlands. The summer average flow was 34.8 and 25.9 m^3/s in 2006 and 2007, respectively.

6.4.4 Spatial distribution patterns of ecosystem metabolism of the whole network

I examined the spatial distribution of stream metabolism within the Grand River watershed by stream order grouping (Table 6.2), and conclude that the higher order streams dominate ecosystem metabolism, both GPP and ER (Table 6.2 & Figure 6.30).

This distribution pattern resulted from increasing trends of water surface area, P rates and R rates with the stream order (Table 6.2 & Figure 6.30). Hence, the 7th order river reaches are responsible for most of the ecosystem metabolism (both GPP and ER) in the Grand River network (Figure 6.30). The small streams make minor contributions to whole basin metabolism. This general spatial distribution pattern is in agreement with an analysis of a similar-sized basin in a subtropical region (Meyer and Edwards 1990) and a boreal forest watershed (Naiman 1983) (Table 6.4).

As discussed in the previous section, the Grand River shows a simple increasing trend in both GPP and ER with the stream order. The GPP of a 6th order blackwater river in the Ogeechee River (Georgia, USA) basin also exhibited a simple increasing trend, but with less slope than ER (Meyer and Edwards 1990). The ER sharply increases from 3rd to 4th order streams in the Ogeechee River basin due to wide floodplains and riparian swamps. Compared to an undisturbed 9th order boreal forested river system, the Moisie River in eastern Quebec, Canada, the Grand River examined in this study exhibits a very similar spatial pattern (Table 6.4). The only apparent difference between these two river systems is that small streams contribute less to both GPP and ER in the Grand River relative to the Moisie River. In the Moisie River, the FPOM contributes 37 to 64% of GPP and ER in the whole ecosystem metabolism within all three stream-size groups (small size, middle size and large size). Both GPP and ER are of similar magnitude within the three size groups of streams. However, GPP in the Grand River varies two orders of the magnitude and ER varies just one order of the magnitude from smallest streams to largest rivers (Table 6.1). Increased light and nutrients along the length of the Grand River are likely responsible for this distribution pattern, as discussed in the previous section.

Table 6.4 Spatial distribution of total steam metabolism within watersheds by stream order grouping. Small streams are the 1st to 3rd order streams, middle-sized streams are the 4th to 6th order streams, large rivers are the 7th and above order rivers.

Watershed (stream order)	Climate zone	Drainage area (km^2)	Total channel surfaced area (km^2)		Small streams (1st – 3rd)	Middle-sized streams (4th – 6th)	Large rivers (7th -)
Grand River (7th)	Temperate	~7000	46.5	Area%	20.6% (31.2%)	45.4% (68.8%)	34%
				GPP	4% (8.6%)	42% (91.4%)	54%
				ER	10.5% (20.8%)	40.1% (79.2%)	49.4%
				NDM*	< 0	< 0	< 0
Moisie River (9th)	Temperate (boreal)	19871	204.9	Area%	23.2% (36%)	41% (64%)	34.8%
				GPP	13.6% (25.7%)	39.6% (74.3%)	46.8%
				ER	15.5% (26.6%)	42.7% (73.4%)	41.8%
				NDM*	< 0	> 0	> 0
Ogeechee River (6th)	Subtropics	6800		Area%	(32%)	(68%)	-
				GPP	(4%)	(96%)	-
				ER	(9%)	(91%)	-
				NDM*	< 0	< 0	-

Grand River: agricultural and urbanized, receiving effluents from WWTPs.
Ogeechee River: Primarily agricultural, unpolluted, little municipal and industrial effluents.
Moisie River: Undisturbed boreal forest watershed in eastern Quebec, Canada.
*: NDM – Net daily metabolism.
Numbers in parenthesis indicate the recalculated percentage of each variable if only considering 1st to 6th order streams in the Grand River and the Moisie River, for the sake of comparison with Ogeechee River.

6.4.5 Temporal patterns of ecosystem metabolism in the Grand River

The main channel of the Grand River was sampled mainly in summer, with most samples collected in July and August (Table 6.1 & Figure 6.15). This sampling bias may influence the following analyses of temporal patterns. GPP generally declined from May to October (Figure 6.15). Highest GPP occurred in June and July at site BL (Figure 6.15). No samples were early enough to catch the spring increase.

Light has been used to explain variation in GPP (Naiman 1983, Servais et al. 1984, Bott et al. 1985, Uehlinger et al. 2000, Mulholland et al. 2001) along with other abiotic factors, e.g., temperature, water depth, nutrients, DOC concentrations, etc. However, I found light intensity to be useful in explaining daily and seasonal patterns of GPP, but not for explaining month to month variation of stream GPP, especially in the main growth season from May to August in the Grand River. Light varies seasonally, and the maximum daily PAR ($\geq$ 60 mol photons m^{-2} day^{-1}) occurs in June (Figure 6.31). Light also has daily variations due to weather conditions (Figure 6.39). However, the daily PAR can have a high level, >50 mol photons m^{-2} day^{-1}, from the middle of the April to September in Waterloo region, although with wide daily variations (Figure 6.31).

Sunny days were chosen for field work; therefore light intensity was not an important factor determining the monthly variation I observed in GPP during the summer. The relationships were not strong between GPP and incoming radiation (Figure 6.14). The month to month variation of GPP during the main growing season is more affected by another critical determinant of GPP, the light utilization efficiency as addressed in Chapter 5. GPP can be considered to be a function of ecosystem efficiency (light utilization) and light availability at the ecosystem level.

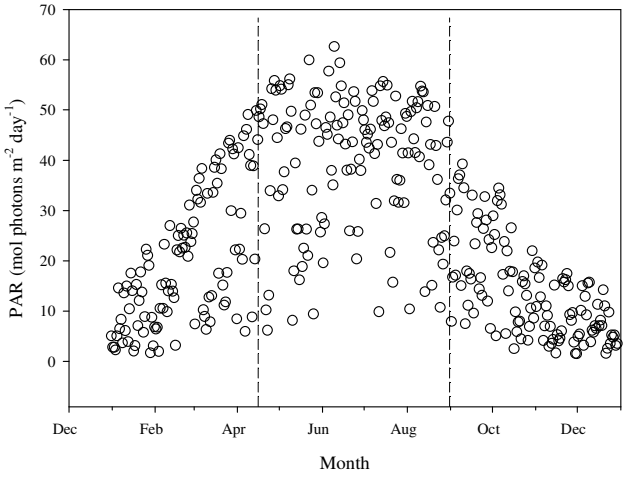

Figure 6.31 Seasonal patterns of the daily incoming radiations (mol photons m^{-2} day^{-1}) in 2006 in Waterloo, Ontario, Canada. Two dashed lines indicate the main growth period from the middle of April to the end of August. Data were provided by the weather station at University of Waterloo.

The ecosystem efficiency is a combined result of plant biomass, species composition, community structure, physiological status, etc. Biomass is often used in explaining variation in GPP. However, the temporal patterns of GPP at Grand River sites, e.g., the peak GPP in early July at site BL, and multiple peaks in early June and August at site BP (Figure 6.15), indicate that the GPP was not completely parallel with the growth of macrophytes. The macrophyte communities develop a peak biomass in August in the Grand River (Hood 2012). Hence, the developmental stage of primary producer communities may also determine the monthly patterns of GPP in the growing season in the Grand River. Different temporal patterns of GPP are expected to be seen due to different plant communities at different sites in the Grand River.

6.4.6 Heterotrophy of Grand River network

Stream heterotrophy in the Grand River network can be examined at various temporal scales. DO was consistently undersaturated with respect to atmospheric equilibrium at sites 2F and 2NF at all sampling periods. Heterotrophic metabolism exceeding photosynthesis consistently can be seen often in small headwater forested streams (Hamilton et al. 2001).

The ratios of GPP: ER at small and middle-sized streams (e.g., 2F, 2NF, 3F, 3NF, 4F, 4NF and 5F) were consistently below 1.0 on all sampling days, exhibiting consistent net O_2 consumption on a daily basis (Figure 6.32). Although we did not sample in the period from fall to early spring, low biomass of aquatic plants and low light availability and water temperature lead to low GPP: ER ratios in fall and winter, which is supported by a few studies from temperate and subarctic regions (Fisher and Carpenter 1976, Young and Huryn 1999, Bott et al. 2006b, Uehlinger 2006, Atkinson et al. 2008). Hence, it is likely that these small and middle-sized streams in my study are heterotrophic on an annual basis.

The large river sites, SPb, WM, BP and GM, exhibited a more balanced pattern of GPP vs. ER (Figure 6.32). Although site BL had consistently GPP: ER ratios <1 on

sampling days, site GM demonstrated a recovery of GPP: ER ratios from the effects of upstream WWTP effluents. The large river sites, except site BL, had either net production of O_2 in sunny days with normal flow or net heterotrophic metabolism on cloudy or high discharge days in spring and summer (Table 6.1). On an annual basis, these sites are heterotrophic. A few sampling days in early Oct at these sites suggest this (Table 6.1). Kuntz (2008) pointed out that the lower Grand River was autotrophic during the two successive summers, but was either balanced or net heterotrophic in October.

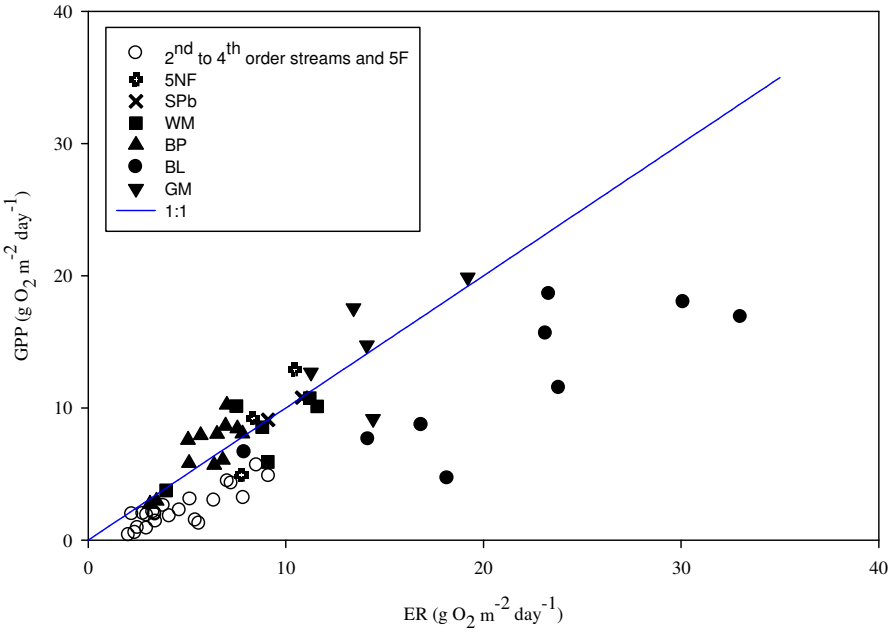

Figure 6.32 Plot of areal GPP vs. ER for all 13 sites for sampling periods from 2006 to 2008 in the Grand River network.

6.4.7 The value of using $\delta^{18}O$ in river ecosystem metabolism studies

$\delta^{18}O$-DO, used as the second oxygen budget, fulfilled several important roles. First, this study estimates metabolic rates in small streams, middle-sized streams and large rivers using a non-steady $\delta^{18}O$-DO modeling approach, which suggests $\delta^{18}O$ can be used in streams regardless of stream size. Secondly, field sampling can benefit from low temporal frequency but high spatial frequency while using both DO and $\delta^{18}O$-DO

budgets, rather than DO only, in small streams. I adopted a diurnal sampling strategy with 2 h intervals for small stream sites. I usually sampled four 2nd and 3rd order streams or four 4th and 5th order steams in one day to lower the time and labor costs, and to avoid including day to day variation in metabolism as much as possible when comparing sites.

Thirdly, although the dynamics of δ^{18}O-DO are tightly linked to those of the DO, they have different behaviors and are measured differently. The δ^{18}O-DO time series data can provide independent constraint on parameter estimation compared to using DO only. For example, the dynamic equilibria for DO and its isotopic composition are not reached simultaneously.

Fourthly, the best fit results for diel samplings demonstrated that fitting DO time series usually yielded less deviation from observed data (higher R^2) than δ^{18}O-DO time series (Table 6.1). Possible reasons for the greater uncertainty in δ^{18}O-DO than DO may include complex sampling and analysis procedures for δ^{18}O-DO, uncertainty propagation from the estimated parameter, respiration isotopic fractionation factor ($\boldsymbol{a_R}$), etc.

Fifthly, the addition of δ^{18}O-DO and thereby using two oxygen budgets to quantify metabolic rates provides another way to indicate trophic status of an aquatic ecosystem, by plotting δ^{18}O-DO against fraction of DO saturation in the water column (Quay et al. 1995). A cross plot of DO saturation and δ^{18}O-DO on a diel basis forms an elliptical shape (Figure 6.11 & Appendix-A). The cross plot is ecologically informative, providing information and a means of comparing streams through the size, range and location of their ellipses (Quay et al. 1995, Venkiteswaran et al. 2008). Streams with less metabolic activity distribute within a smaller range, such as sites 2F and 2NF compared to sites 3F and 3NF (Figure 6.11A), and sites 4F and 4NF compared to sites 5F and 5NF (Figure 6.11B). Quay et al. (1995) proposed that lower GPP: ER systems have ellipses that distribute towards the upper left quadrant and higher GPP: ER systems move towards the bottom right hand quadrant. In my study of the Grand River, site BL had all diels with GPP: ER < 1 and the diel DO and δ^{18}O-DO data trend towards the upper left quadrant as indicated for lower GPP: ER systems by Quay et al (1995), compared to upstream site BP and downstream site GM with high GPP: ER (Figure 6.11D).

In addition, the isotope approach provides a way to obtain estimates of $\boldsymbol{a_R}$ at the ecosystem level. The $\boldsymbol{a_R}$ is assumed to be constant on a daily basis like other parameters, e.g., $\boldsymbol{k}$, $\boldsymbol{R_{20}}$, $\boldsymbol{P_m}$ and $\boldsymbol{a}$. This value in the Grand River network ranged from 0.9707 to 0.9968 (Table 6.1), which basically fell into the scope from field and incubation experimentations for various river systems. Published values have been reported from 0.975 to 0.998 for a variety of aquatic organisms and communities. The estimation of $\boldsymbol{a_R}$ in this paper was reasonable. It supports that whole-ecosystem models using dual oxygen mass balance can provide a solution for measuring respiration isotopic fractionation factor at the ecosystem level.

– Chapter 7 –

A global perspective on ecosystem metabolism in streams and rivers

7.1 Introduction

There has been a long history of studies on stream ecosystem metabolism. These studies involve a diversity of streams and rivers and contribute to river ecosystem science as well as provide a scientific foundation for managing and restoring impacted steam and river ecosystems. However, there has been no review of the accumulated data to provide a whole picture of the general pattern of stream ecosystem metabolism. It is difficult to understand the main generalities of stream metabolism based on limited information over a small range, especially while facing the challenge of human disturbance, climate change, etc. There is a need for a global database to discover the generalities and peculiarities of stream ecosystem metabolism, which may facilitate broad cross-region and cross-biome comparison studies.

In this study, I made such an effort. I built a global dataset of stream ecosystem metabolism using whole-system methods. This dataset provides an overall perspective about metabolic rates and ratios across climate gradients, the effects of stream size on metabolic rates, and the effects of human disturbance on metabolic rates and ratios. I hypothesized that (1) river ecosystems are net heterotrophic systems globally and (2) globally, metabolic rates and GPP: ER ratios increase from small streams to middle-sized streams and then decrease from middle-sized streams to large rivers. I hypothesized that the Grand River had patterns of metabolic rates and ratios that differed from general global patterns due to human activities.

7.2 Materials and methods

A meta-dataset of stream ecosystem metabolism was collected from more than 110 studies during last sixty years, using either one-station or two-station methods. Dependent variables included mean magnitude and range of GPP, ER, NPP, and the ratio of GPP: ER. Independent variables belonged to three categories: geological and climatic; watershed and channel; and resources. Geological and climatic variables included geographic regions, coordinates (latitude, altitude and elevation), climate zone (based on Köppen-Geiger classification), vegetation, temperature and precipitation. Watershed and channel variables included drainage area, stream size (width, depth, length, and order), hydrological parameters (velocity, discharge and gradient), reach characteristics (e.g., disturbance, location relative to confluences, dams, and reservoirs), land use, riparian cover, substrate type and major autotrophs. Resource variables included light intensity and nutrients (NO_2^--N, NH_4^+-N, NO_3^--N, DON, TP, SRP, TDP, dissolved organic matter, etc.). In addition, water quality variables were also collected, if possible, such as pH, suspended solids, conductivity, alkalinity, turbidity and dissolved oxygen.

This chapter mainly illustrates the relationships between metabolism parameters and independent variables such as latitude, climate zone, stream order and discharge. I divided the study sites into 5 main climate zones according to the Köppen-Geiger climate classification system with a series of sub-climate types: tropical (e.g., tropical rainforest, wet/dry, savannah), dry lands (arid and semi-arid), subtropical (Mediterranean and humid subtropical), temperate (humid continental, oceanic and warm summer continental), and Polar (subarctic, alpine and highland). I combined subarctic, polar, alpine and highland because there were few studies in these groups.

In this chapter, I only report values measured in summer season (e.g., May-September in Northern hemisphere and Dec-April in Southern hemisphere) for the global dataset and the Grand River as well. If repeated measures through the season at the same site were available, the average value was calculated and used.

7.3 Results

7.3.1 Geographic and climate zone distribution of ecosystem metabolism studies

Most studies of ecosystem metabolism have been conducted within the region 30° - 50° from the equator. Another geographic region, 10° - 20° from the equator, also contributes a small amount of data (Figure 7.1). One study occurs at very low latitude region, an Andean piedmont river located in the Orinoco basin (9.2°N), Venezuela (Taylor et al. 2006). There is one study at very high latitude region, streams in the Caribou-Poker Creeks Research Watershed in the boreal forest of interior Alaska (65.2°N), USA (Betts and Jones 2009). The latitude of the Grand River watershed is around 43.7°N.

The GPP for streams and rivers in the global dataset is mostly in the range from 0 to 20 g O_2 m^{-2} day^{-1}, with a few between 20 and 30 g O_2 m^{-2} day^{-1} (Figure 7.1). There are three extreme high values. The highest one comes from the relatively undisturbed, middle-sized river (3^{rd} order) Blue River, where a large biomass of benthic producers growing on granite contributed this high primary productivity (Duffer and Dorris 1966). The other two also come from a middle-sized (4^{th} order) river, an agricultural prairie river system in central Illinois. Extreme high nutrients (DIN and SRP) and sufficient light condition are main reasons for its high primary productivity (Wiley et al. 1990). The ER for streams and rivers in this global dataset vary widely from 0 to about 40 g O_2 m^{-2} day^{-1}. Only one estimate exceeded 40 g O_2 m^{-2} day^{-1}, also from Wiley et al. (1990). Most GPP: ER data are < 1, supporting the generalization that streams and rivers are heterotrophic ecosystems (Duarte and Prairie 2005). Ecosystem GPP, ER and GPP: ER ratios in the Grand River fall within the range of the global dataset (Figure 7.1A & B).

On the whole, although results from relevant studies in the tropics (Mulholland et al. 2001, Ortiz-Zayas et al. 2005, Webster et al. 2005, Oliver and Merrick 2006, Taylor et al. 2006, Gucker et al. 2009, Bernot et al. 2010, Hunt et al. 2012), dry land areas (Fellows et al. 2001, Uehlinger et al. 2002, Hall and Tank 2003, Vink et al. 2005, Fellows et al. 2006b, Oliver and Merrick 2006, Gawne et al. 2007, Bernot et al. 2010), subtropics (Suarez and Vidal-Abarca 2001, McTammany et al. 2003, Acuna et al. 2004,

Meyer et al. 2005, Fellows et al. 2006b, Mulholland et al. 2006, Ruggiero et al. 2006, Colangelo 2007, McTammany et al. 2007, Roberts et al. 2007, Von Schiller et al. 2008, Bernot et al. 2010, Acuna et al. 2011), and subarctic zones (Naegeli and Uehlinger 1997, Kaenel et al. 2000, Uehlinger 2000, Uehlinger et al. 2003, Logue et al. 2004, Uehlinger 2006, Betts and Jones 2009, Reichert et al. 2009) have been published in recent years, there is still an obvious temperate zone bias to the sites (Figure 7.2). The Grand River is in the high latitude part of the temperate region (climate zone 4).

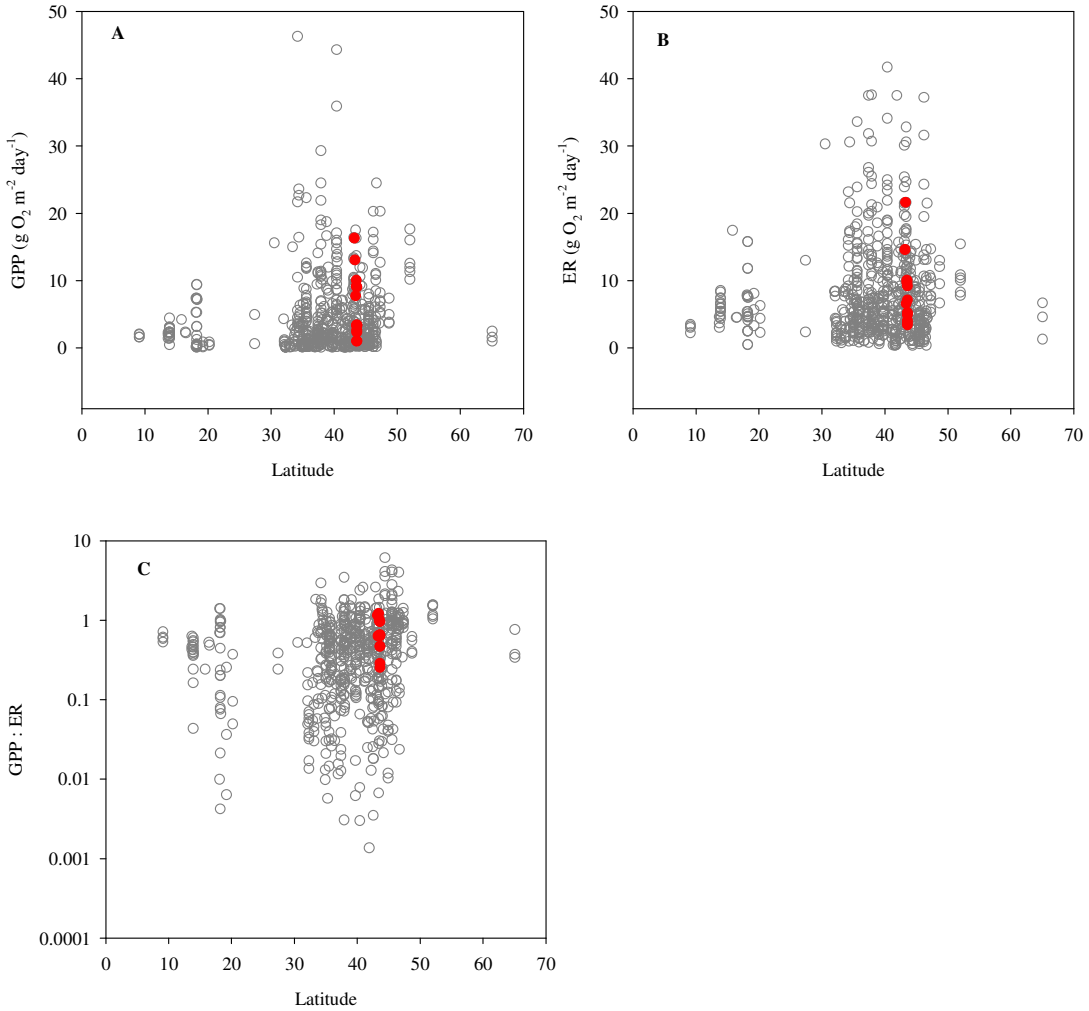

Figure 7.1 GPP (A), ER (B) and GPP: ER (C) for streams in the global dataset, plotted vs. latitude (in degree, regardless of orientation). Gray empty circles are global data points, and solid points are means for sites in this study of the Grand River network.

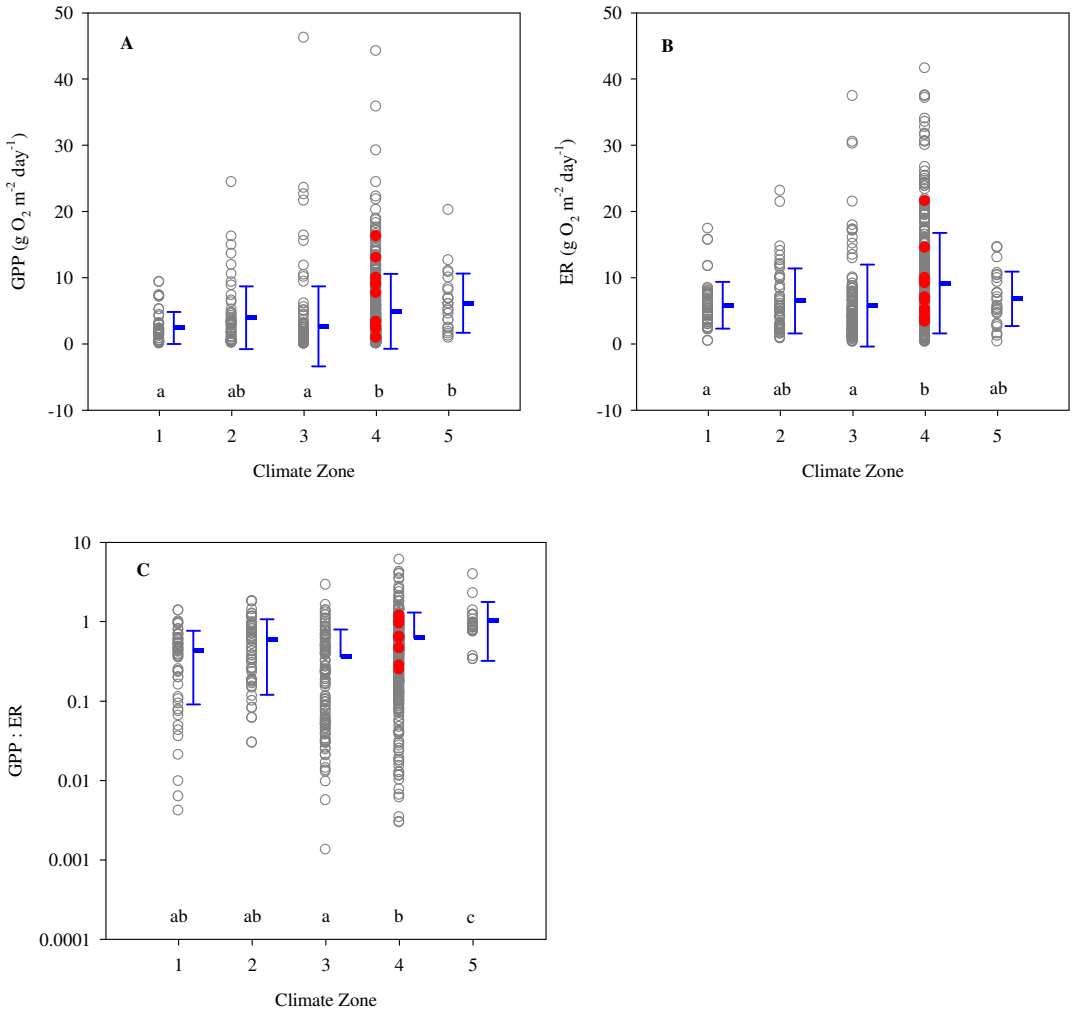

Figure 7.2 GPP (A), ER (B) and GPP: ER (C) for streams in the global dataset, plotted vs. climate zone. There are tropical (1), dry land (2), subtropical (3), temperate (4) and Polar (5). Gray empty circles are global data points, and solid points are means for sites in this study of the Grand River network. Mean and standard deviation for each climate zone are shown using the error bars. Significant differences of means among these groups are marked by different letters, a, b and c.

GPP and ER were related for climate zone 4, temperate zone (GPP = 0.433 * (ER) + 0.926, adjusted R^2 = 33.9%, $F_{1, 347}$ = 179.5, P < 0.0001) (Figure 7.3). The 2nd - 4th order sites and site 5F in the Grand River were below the balance line (GPP = ER), but around the regression line (Figure 7.3). All 6th-7th order sites and site 5NF in my study were

obviously above the regression line, but around the balance line except site BL (Figure 7.3).

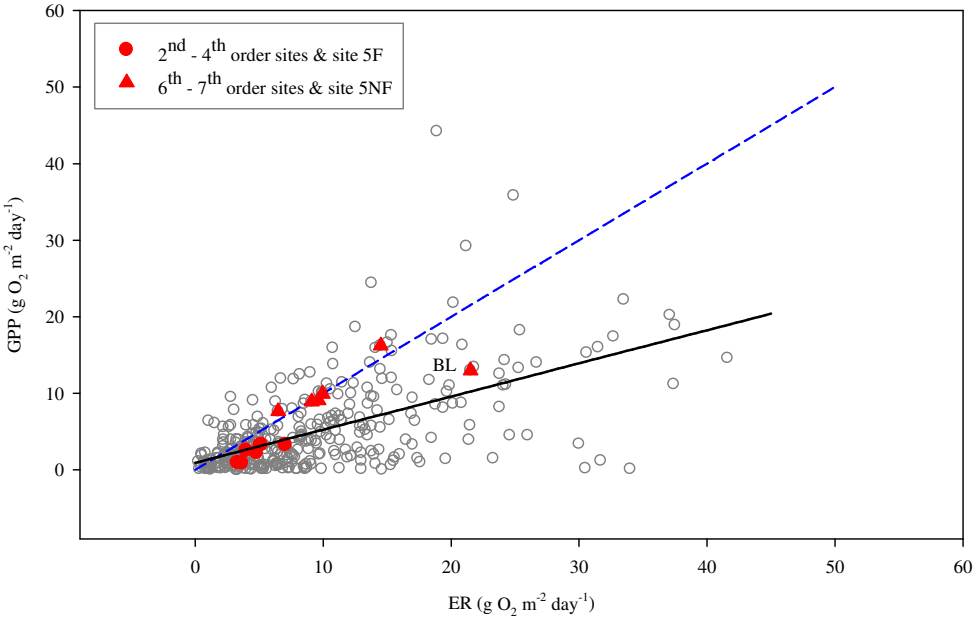

Figure 7.3 Plot of GPP vs. ER for all streams in the temperate zone (climate zone 4). Gray empty circles are global data points, and solid dotted points and triangles are streams in this study in the Grand River network. Site BL is specifically marked. The dashed line illustrates GPP = ER. The solid line is the regression line for global data. The equation is GPP = 0.433 * (ER) + 0.926, adjusted R^2 = 33.9%, $F_{1, 347}$ = 179.5, P < 0.0001.

7.3.2 The effects of stream size on ecosystem metabolism in global streams and rivers

All metabolic parameters (GPP, ER and GPP: ER) exhibit a similar pattern, i.e., increasing from small streams to middle-sized streams and then decreasing from middle-sized streams to large rivers (Figure 7.4 & Table 7.1). The maxima occur in 4th order streams for GPP and 5th order streams for ER and the ratio of GPP: ER. The minor violation of this pattern is that the mean GPP and ER in the 6th order streams are a little less than those in the 7th order streams (Figure 7.4). My study in the Grand River partly conforms to this general pattern but with a few peculiarities. The GPP and ER in 2nd to 4th order streams in the Grand River are lower than the averages in the global dataset,

especially in both two 4th order streams (4F and 4NF). A relatively well-protected riparian zone, low nutrient concentration and unstable sediment may account for these low GPP and ER in my study, although these two sites are in agricultural regions in the Grand River watershed. The other 6th and 7th order sites show a relatively high GPP and ER, especially site BL and GM. These two sites are downstream of 2 large WWTPs in the middle section of the Grand River.

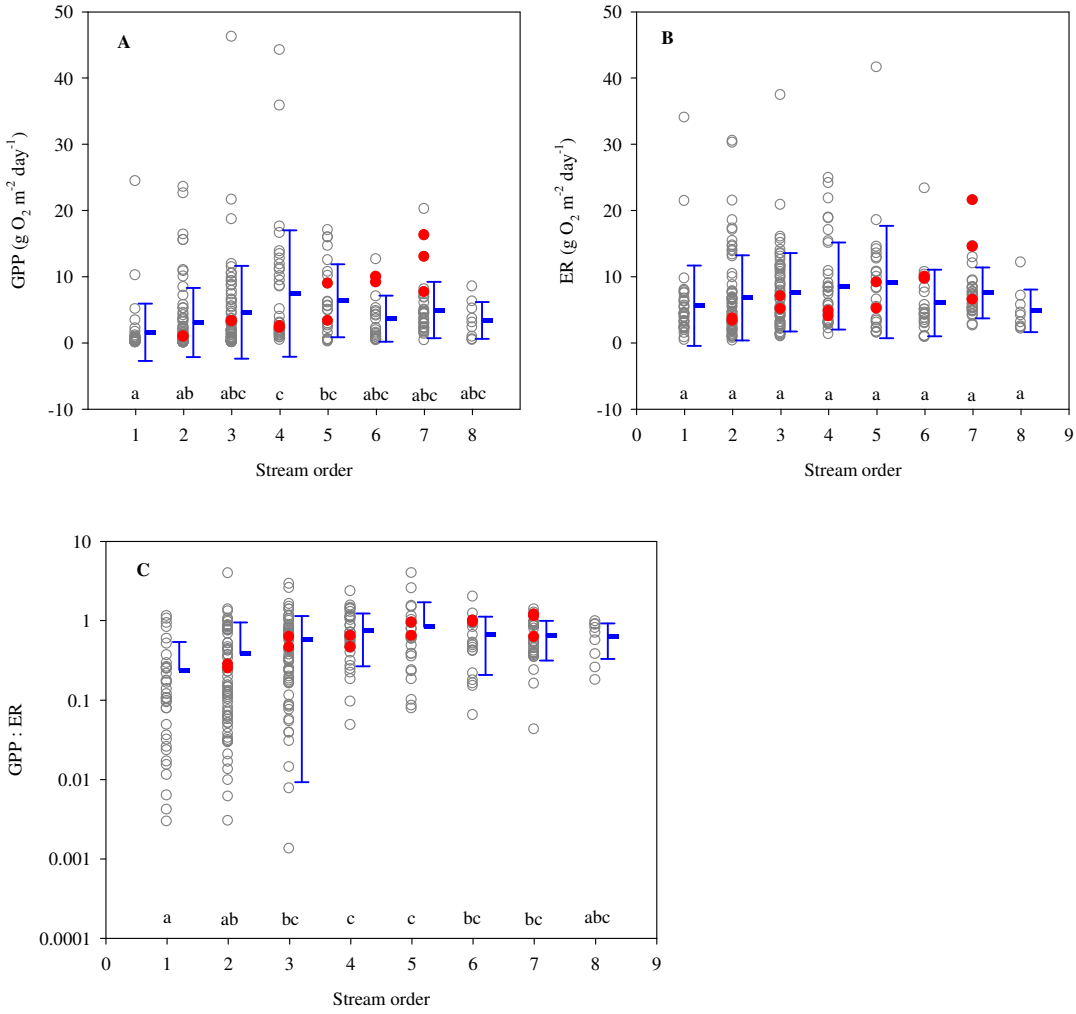

Figure 7.4 GPP (A), ER (B) and GPP: ER (C) for streams in the global dataset, plotted vs. stream order (1st - 8th). Empty circles are global data points, and solid points are means for sites in this study of the Grand River network. Error bars indicate the mean and standard deviation for each stream order. Significant differences of means among these groups are marked by different letters, a, b and c.

Table 7.1 Mean GPP, ER and GPP: ER for streams in each order in the global dataset. Data are mean ± standard errors and data points (n). The unit of GPP and ER is g O_2 m^{-2} day^{-1}.

Streams	1st order	2nd order	3rd order	4th order	5th order	6th order	7th order	8th order
GPP	1.6±1.0 (36)	3.1±0.7 (68)	4.6±0.8 (62)	7.5±1.0 (36)	6.5±1.2 (24)	3.4±1.3 (22)	4.9±1.0 (33)	3.4±2.0 (9)
ER	5.6±1.0 (36)	6.8±0.7 (68)	7.7±0.8 (62)	8.6±1.0 (36)	9.3±1.2 (24)	5.7±1.3 (22)	7.6±1.1 (33)	4.8±2.0 (9)
GPP/ER	0.24±0.09 (36)	0.38±0.064 (68)	0.58±0.067 (62)	0.75±0.09 (36)	0.84±0.11 (24)	0.67±0.11 (22)	0.65±0.09 (33)	0.63±0.18 (9)

Both metabolic rates and ratios of global streams increased first and then decreased in the plot of metabolic rates vs. discharge (Figures 7.5, 7.6 & 7.7). However, GPP and ER exhibited more similar trend than GPP: ER ratios (Figures 7.5, 7.6 & 7.7). The peak GPP and ER occurred in streams with discharge of about 0.3 and 0.4 m^3 s^{-1}, respectively. The 5th order streams, 5F and 5NF, in the Grand River had similar discharges. High GPP: ER ratio occurred in streams with discharge of from 3 to 8 m^3 s^{-1}. This discharge range appeared in 6th order rivers, SPb and WM, in the Grand River. The 2nd-5th order, shaded streams had lower GPP and ER than the global average, whereas non-shaded streams had GPP and ER that were close to the global average, except stream 4NF with ER below the global average line (Figure 7.6). All 6th and 7th river sites, SPb, WM, BP, BL, GM and lower Grand, stood out and had higher GPP than the global average. However, only two urban impacted sites, BL and GM, had higher ER than the global average, the other river sites stayed with the global average line (Figure 7.5). No site had GPP: ER ratio apparently out of the ordinary except the lower Grand (Figure 7.7).

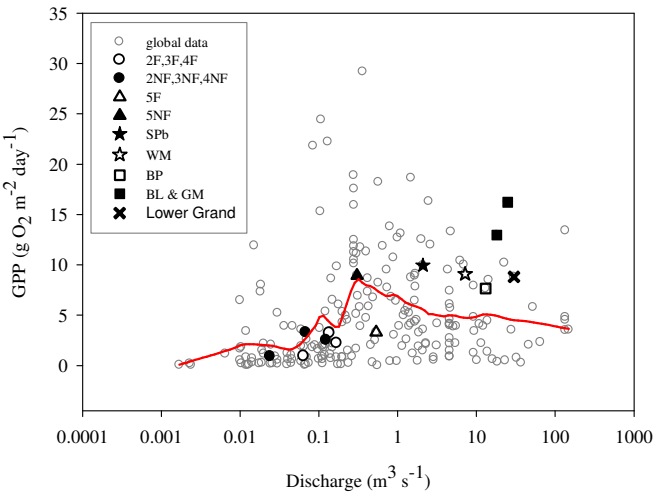

Figure 7.5 Plot of GPP vs. discharge for all streams in the temperate region (Climate zone 4). Gray empty circles are global data points. Other symbols represent sites in the Grand River network. The data point for the Lower Grand is from Kuntz (2008). The line is a lowess curve (weighted average smoothing).

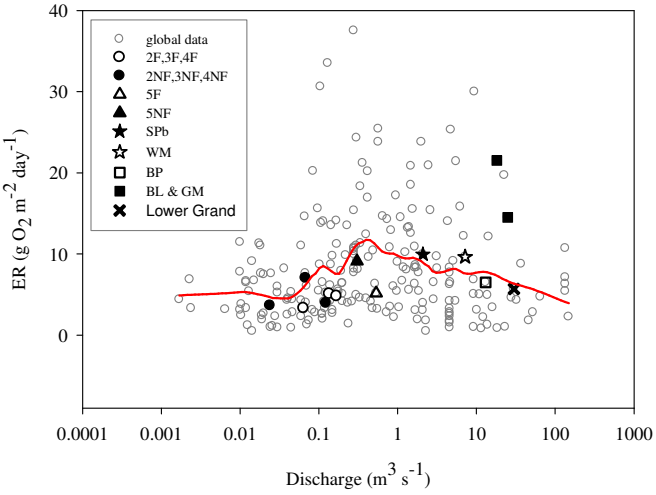

Figure 7.6 Plot of ER vs. discharge for all streams in the temperate region (Climate zone 4). Gray empty circles are global data points. Other symbols represent sites in the Grand River network. The data point for the Lower Grand is from Kuntz (2008). The line is a lowess curve (weighted average smoothing).

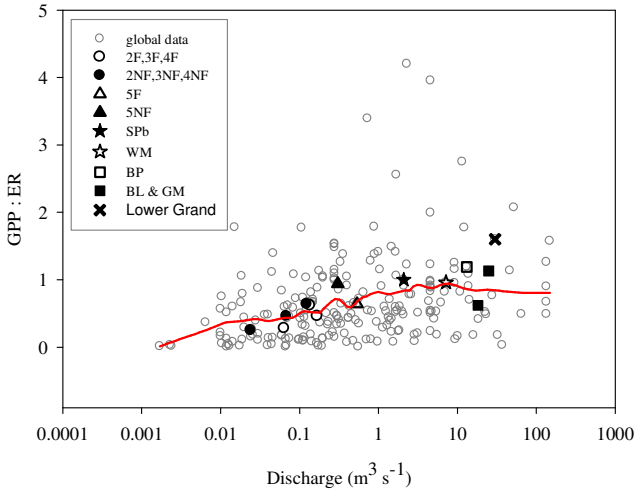

Figure 7.7 Plot of GPP: ER vs. discharge for all streams in the temperate region (Climate zone 4). Gray empty circles are global data points. Other symbols represent sites in the Grand River network. The data point for the Lower Grand is from Kuntz (2008). The line is a lowess curve (weighted average smoothing).

7.3.3 The effects of human disturbance on ecosystem metabolism of small streams in temperate regions

According to my review of the global dataset, there are 178 ecosystem metabolism studies of small streams (1st - 4th order) in the temperate zone with known stream order and human disturbance. Among them, 104 are from agriculturally impacted streams, including 32 sites in currently and formerly forested watersheds (hereafter, just called forested watersheds) and 72 sites in grassland/prairie watersheds. 24 are from urban impacted streams, 25 are from streams disturbed in other ways (mining, channelization, flow restoration, etc.), and only 25 are from pristine or less disturbed streams, including 21 sites in originally forested watersheds and only 4 sites in grassland/prairie watersheds.

GPP of 2F, 2NF, 3F, 3NF, 4F and 4NF in the Grand River network were from 0.4 to 5.7 g O_2 m^{-2} day^{-1} with an average of 2.2 g O_2 m^{-2} day^{-1} and ER were 2 to 9.1 g O_2 m^{-2} day^{-1} with an average of 4.6 g O_2 m^{-2} day^{-1} (Figure 7.8).

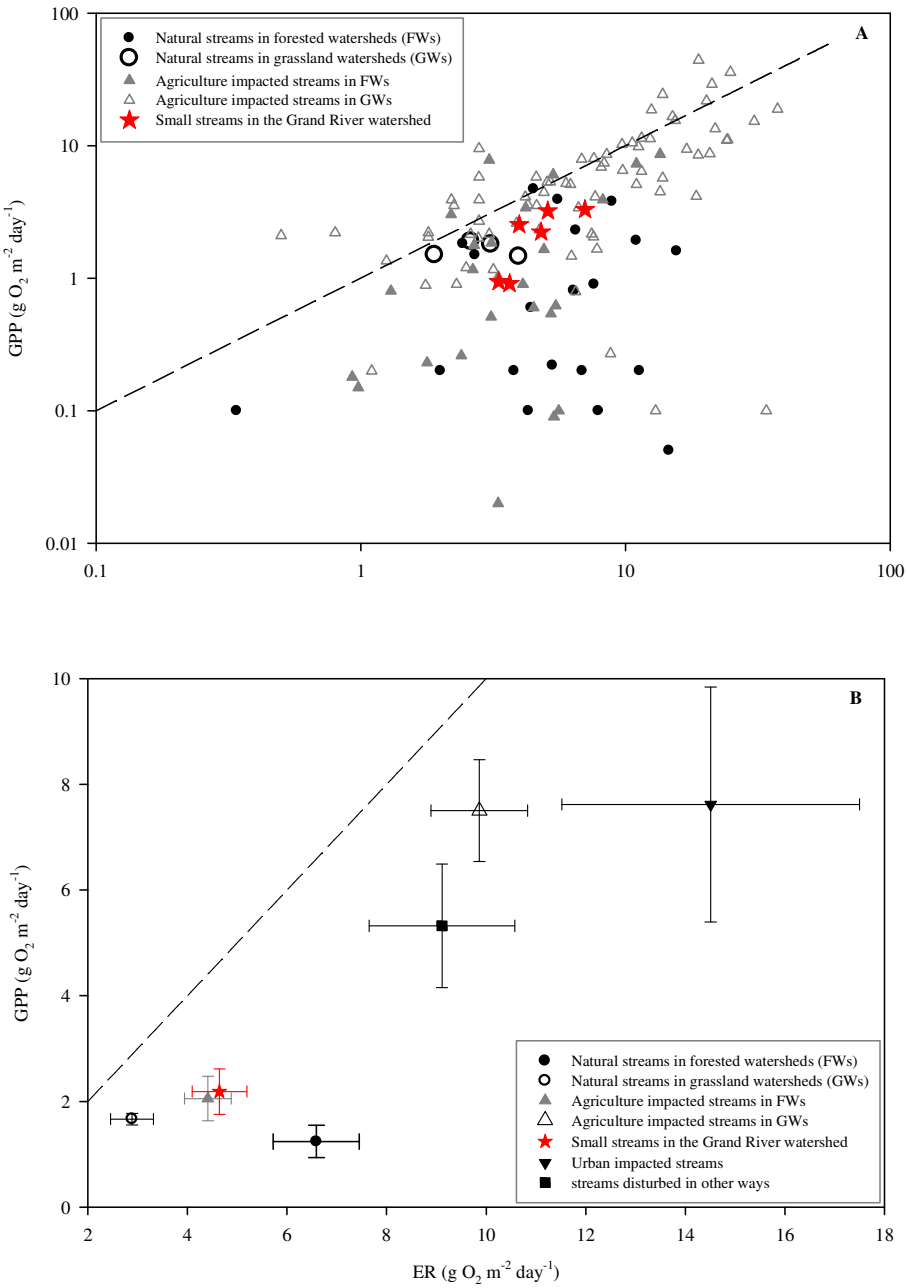

Figure 7.8 Metabolic rates (GPP and ER) of small streams (1st - 4th order) in Czone4 (temperate regions) and in the Grand River network. The dashed lines illustrate GPP=ER. These streams are grouped by disturbances and original vegetation characteristics of the watershed. The subplot (B) is means and standard errors of metabolic rates of each group.

GPP rates of 25 natural, small streams (1st to 4th order) without obvious human disturbance in the temperate region (Climate zone 4) ranged from 0.05 to 4.7 g O_2 m^{-2} day^{-1} with an average of 1.3 g O_2 m^{-2} day^{-1}. ER rates of these streams were from 0.3 to 15.6 with an average of 6 g O_2 m^{-2} day^{-1}. The average GPP and ER rates of 4 natural streams in grassland watersheds were 1.7 and 2.9 g O_2 m^{-2} day^{-1}, respectively (Figure 7.8). 21 natural streams in forested watersheds had average rates of GPP and ER, 1.2 and 6.6 g O_2 m^{-2} day^{-1}, respectively (Figure 7.8). Agriculture impacted streams in forested watersheds had an average GPP rate of 2.1 g O_2 m^{-2} day^{-1} and an average ER rate of 4.5 g O_2 m^{-2} day^{-1} (Figure 7.8). However, agriculture impacted streams in grassland watersheds had obviously high GPP and ER rates, 7.5 and 9.9 g O_2 m^{-2} day^{-1}, respectively (Figure 7.8). Urban impacted streams and impacted streams in other ways also had obvious high average rates of GPP and ER (Figure 7.8).

7.4 Discussion

7.4.1 A global perspective on the ratio of GPP: ER

The summer average ratios of the GPP: ER of streams in the world are below the balance line (GPP = ER) except a few streams in subarctic regions (Figure 7.9), supporting the generalization that streams are net heterotrophic ecosystems (Duarte and Prairie 2005). Small headwater forested streams and large lowland rivers in the northern-hemisphere are most likely to be heterotrophic (Vannote et al. 1980). It is possible for middle-sized rivers to have GPP > ER on days when light and temperature are favorable. However, from a global perspective, all streams and rivers are heterotrophic, although middle-sized streams are less so (i.e., have less negative NPP) (Figure 7.4C).

This study provides the possibility of viewing the river continuum concept (RCC) from multiple macroscopic scales. To my knowledge, it is the first comprehensive study addressing the RCC not only at local watershed scale, but also at the regional and global scales (Figure 7.9).

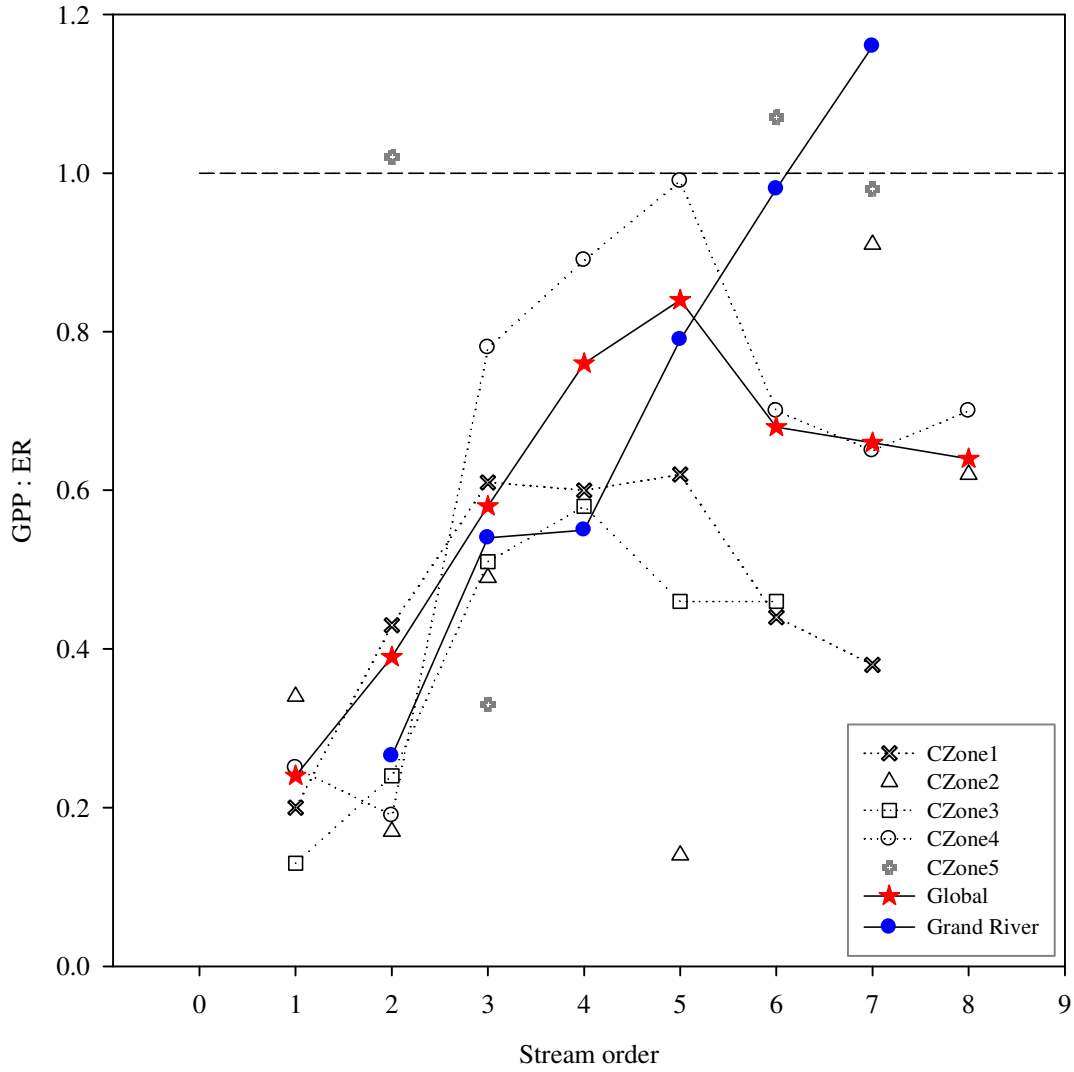

Figure 7.9 Patterns of mean summer ratios of GPP: ER against with stream order in 5 climate zones, the Grand River and globally. Climate zones are tropical (CZone1), dry land (CZone2), subtropical (CZone3), temperate (CZone4) and Polar (CZone5). Site BL in the Grand River is not included in the calculation of the average GPP: ER of the 7th order streams.

The RCC (Vannote et al. 1980) proposes a longitudinal trend of GPP: ER ratio in a river network. GPP: ER ratios are often < 1 in small headwater streams (1st to 3rd order) due to depressed autotrophic production by shading from riparian vegetation, and the ratios increase and can be >1 in middle-sized streams (4th to 6th order) as a result of

increased primary production due to increased light and autotrophy communities. However, the lower land rivers (> 6th order) turn to heterotrophic again with GPP: ER ratios <1 because primary production may often be limited in deep and cloudy water. The basic predictions of RCC on ecosystem metabolism have been supported by a large number of field observations and empirical data (Statzner and Higler 1985, Naiman et al. 1987).

My work examined the predictions of the RCC along a heavily impacted temperate river. The general trend of the GPP: ER ratio along the Grand partly conforms to the predictions of the RCC (Figure 7.9). The small streams (2nd-3rd) are heterotrophic with GPP: ER ratios < 1, and then the ratio gradually increases to reach the balance at 6th order river reaches (sites WM and SPb). However, the GPP: ER ratios continue to increase at 7th order sites BP (ranging 0.9 - 1.5 with an average of 1.2) and GM (ranging 1.0 - 1.3 with an average of 1.1). Site BL had significant different ratios of GPP: ER, 0.5 to 0.9 with an average of 0.6, due to the effects of WWTPs as discussed in Chapter 6. I do not know whether the GPP: ER would drop to < 1 downstream of site GM as a natural consequence of the river becoming deeper and more turbid. The influence of dams (e.g., Parkhill dam), and WWTPs in the lower Grand River should be major considerations. As discussed in the previous section, the last 35 km lower Grand had very high GPP: ER ratios (> 2 to 3) probably due to the effects of a dam (Kuntz 2008).

Mean summer GPP: ER ratios of the global dataset exhibit a clear pattern that is in accordance with the RCC regarding the longitudinal pattern of P/R ratios. However, the mean for any stream order in these compiled data is always <1 (Figure 7.9). The GPP: ER ratios in tropical (Czone1), subtropical (Czone 3) and temperate (Czone 4) climate zones exhibited patterns that are close to the global pattern (Figure 7.9). More studies are needed to determine whether the dry land (Czone2) and Polar (Czone5) climate zone conform to the general pattern.

The size of the streams where the peak ratio of GPP: ER occurs differs among climate zones. The peak of mean GPP: ER ratio appears at 3rd order in tropical streams (mean GPP/ER = 0.6), at 4th order in subtropical streams (mean GPP/ER = 0.58), at 5th

order streams in temperate streams (mean GPP/ER = 0.99), and at 6th order in Polar streams (mean GPP/ER = 1.07). Hence, I conclude that the maximum GPP: ER ratio is higher at higher latitude and occurs at higher order streams.

Many aspects of the RCC have been debated and challenged based on different river ecosystems, such as those in the New Zealand geo/climatic zone (Young and Huryn 1996), the black water river continuum (Meyer and Edwards 1990), non-forested grassland rivers (Young and Huryn 1996), and agricultural prairie rivers (Wiley et al. 1990). The application of RCC is subject to criticisms as a concept of worldwide applicability due to its genesis primarily based on unperturbed forested streams in North America (Winterbourn et al. 1981, Statzner and Higler 1985). However, these global data, and subsets of the data for each climate zone, still support the general ecosystem metabolism pattern of river longitudinal change, if not strictly on the point proposed in original concept of RCC that the maximum ratio of GPP: ER will be >1 in middle-sized streams (Vannote et al. 1980).

7.4.2 The effects of agricultural activities on ecosystem metabolism in temperate streams

Agricultural streams and rivers are influenced by cumulative, non-point source nutrient additions, loss of riparian zones and associated bank erosion. According to the effects of agricultural activities on metabolic rates of streams, small streams in temperate regions can be generally divided into three groups (Figure 7.8B).

(1) Streams with basal GPP and ER: the 21 natural, small streams (1st to 4th order) in forested watersheds without obvious human disturbance exhibit low metabolic rates (Figure 7.8). The natural streams in grassland watersheds may have even lower baseline. These streams have obviously lower ER than those in forested watersheds (Figure 7.8B). However, there are currently only 4 such streams in the global dataset.

(2) Streams with elevated GPP: increased GPP is supported by enhanced light and nutrient availability due to loss of riparian trees and non-point nutrient additions. However, this may be counteracted by the effects of increased erosion. Reduced inputs of riparian organic matter

may decrease the ER rates in these streams. The small streams (2F, 2NF, 3F, 3NF, 4F and 4NF) in the Grand River in my study fall into this category (Figure 7.8B).

(3) Streams with extremely high GPP and ER: Without canopy coverage from riparian trees, but ample nutrients and stable substrates, small and middle-sized streams in heavily agriculturalized, grassland or prairie watersheds often exhibit extremely high metabolic rates (Figure 7.8B). For example, the summer GPP rates in small headwater streams in the Taieri River located in a grassland watershed reached to 7 to 8 g O_2 m^{-2} day^{-1} in summer (Young and Huryn 1996). Wiley (1990) measured summer metabolic rates in the Vermilion river network in Illinois, USA. The GPP rates were 0.1 to10.2 g O_2 m^{-2} day^{-1} in 1st order streams, 5.7 to 15.5 g O_2 m^{-2} day^{-1} in 2nd order streams, 0.1 to 11.4 g O_2 m^{-2} day^{-1} in 3rd order streams and 8.5 to 44.2 g O_2 m^{-2} day^{-1} in 4th order streams. The ER rates were 6.2 to 34 g O_2 m^{-2} day^{-1} in 1st order streams, 13.8 to 15.4 g O_2 m^{-2} day^{-1} in 2nd order streams, 11.5 to 13 g O_2 m^{-2} day^{-1} in 3rd order streams and 17 to 24.9 g O_2 m^{-2} day^{-1} in 4th order streams. These streams had obviously higher GPP and ER rates than the streams with the same order in the Grand River network.

7.4.3 The effects of WWTPs on ecosystem metabolism in streams and rivers

There are about 10 relevant studies addressing the impacts of WWTPs on the metabolic rates of streams and rivers (Table 7.2). A few points can be summarized according to these studies.

First, streams and rivers receiving WWTP effluents have been often observed to have increased metabolic rates, either GPP or ER or both (Flemer 1970, Hornberger et al. 1977, Chessman 1985, Gucker et al. 2006, Ruggiero et al. 2006, Uehlinger 2006, Sanchez-Perez et al. 2009, Young and Collier 2009, Wassenaar et al. 2010). These streams exhibit comparable metabolic rates, regardless of stream size (Table 7.2).

Table 7.2 Summary of studies on the effects of wastewater treatment plants on stream ecosystem metabolism.

Study	Climate/Lat	Time	Sites	location*	Size			GPP	ER	GPP/ER
					SO	W/D (m)	Discharge ($m^3 s^{-1}$)	($g O_2 m^{-2} day^{-1}$)		
This study	temperate	2006-2008	Speed River @ SPb	2km DS	6	30/0.64	1.8-2.3	9.1-10.8	9.1-10.8	1
(ON, CA)	43.7° N	(Summer)	Grand River @ BP	20km US	7	85/0.40	4.3-25.2	2.7-10.2	3.1-7.5	0.9-1.5
			Grand River @ BL	5km DS	7	90/0.60	9.8-32.7	4.7-18.6	7.9-33	0.3-0.8
			Grand River @ GM	25km DS	7	100/0.75	14.9-49.9	9.2-19.9	11.3-19.2	0.6-1.3
Wassenaar	temperate	2004	Bow River	0.1km US	L#	70-100/	135	3.5	7.1	0.49
(2010)	51° N	(July)	(Calgary,CA)	3.2km DS	L#	70-100/	135	13.4	10.7	1.26
				24km DS	L#	70-100/	135	4.5	6.3	0.67
				47km DS	L#	70-100/	135	4.8	5.4	0.9
	subarctic	2004	S. Saskatchewan River	1.6km US	L#		62	4.1	6.9	0.59
	52.1° N	(July)	(Saskatoon,CA)	1.7km DS	L#		62	3.9	4.5	0.88
				19km DS	L#		62	10.4	8.9	1.17
				46km DS	L#		62	10.0	8.7	1.15
Chessman	temperate	1980-1981	La Trobe @ W	US	5		1-2.9	0.5(0.4-0.6)	6.0(5.4-6.5)	0.08
(1985)	38.1° S	(Summer)	La Trobe @ M	DS	6		5.4-11	3.1(2.2-4.1)	4.7(4.2-5.0)	0.64(0.5-0.8)
(Australia)										
Flemer (1970)	temperate	1962	NB of Raritan River @ s1	US	3/4	15/0.11	0.4	5.1(3-8.8)	4.5(3.7-5.4)	1.1(0.8-1.6)
(NJ, USA)	40.6° N	(Summer)	NB of Raritan River @ s2	DS	4	19/0.22	1	11.9(6-16.7)	8.3(3.2-13.2)	1.5(1.1-1.9)
			NB of Raritan River @ s3	DS	4	14/0.19	0.8	15.7(7.2-25.1)	10.8(7.5-19.4)	1.4(0.9-2.0)

*: US means upstream; DS means downstream;

L# : Large; M# : Middle; S# : Small;

Table 7.2 Extended.

Study	Climate/Lat	Time	Sites	location*	Size			GPP	ER	GPP/ER
					SO	W/D (m)	Discharge ($m^3 s^{-1}$)	($g O_2 m^{-2} day^{-1}$)		
Gucker 2006	temperate	2002	Demnitzer Mill Brook	US	1	/0.27	0.023	3	28	0.1
(Berlin)	52.5° N	August		DS	1	/0.25	0.022	3	38	0.02
			Erpe	US	3	/0..46	0.16	32	32	1
				DS	3	/0.77	0.51	47	59	0.8
Ruggiero 2006	subtropical	2002	Fosso Bagnatore @ DW	US	3		0.003	1.3(0.7-1.9)	4.6(2.1-7.1)	
(Rome, Italy)	42° N	(Apr-Jun)		DS	3		0.003	0.1	35.1(20-48)	
Sanchez-Perez 2009	temperate	2001	Rozeis stream @ Montegut	US	1-2	4.7/0.22	0.12	3.3±1.6	4.2±1.3	0.6±0.17
(Toulouse, France)	43.7° N	(all year)		DS	1-2	3.7/0.23	0.11	3.6±1.7	7.1±4.1	0.6±0.19
	temperate	2001	Leze stream @ Lezart	US	3	5.2/0.14	0.11	0±0.7	5.1±1.6	0.03±0.11
	43.5° N	(Summer)		DS	3	4.8/0.14	0.11	5.9±4.1	37.6±23.6	0.15±0.14
Young 2009	temperate	-	Mangaokewa @ S3	2km US	M#			1.6	11.9	0.13
(North Island, NZ)	39.1° S	-	Mangaokewa @ S4	0.5km DS	M#			3.9	16.5	0.24
			Mangaokewa @ S5	8km DS	M#			4.5	10.3	0.44
								annual rates		
Kanel 2000	temperate	1995	Muhlibach	0.2km DS	S#	3.2	0.38±0.28	12.5±4.5	8.9±6.84	1.07±0.08
(Switzerland)	47.7° N	(Summer)								
Hornberger 1977	subtropical	1974	South Fork Rivanna R.	US	M#	26/0.37	0.6	2.13±1.07	3.4±1.37	
(Virginia,USA)	38.5° N	(Summer)	Rivanna R.	DS	M#	36/0.33	2.4	2.11±1.17	5.13±3.34	

Secondly, the GPP and ER are often stimulated by WWTP effluents, but to different extent. This study in the Grand River is an example demonstrating this point in a large river. Similar phenomena have also been observed in small streams, where nutrient additions increase ER more than GPP, leading to decreased ratios of the GPP: ER if the streams are limited by light (Sanchez-Perez et al. 2009) or when the stream is in a eutrophic state both upstream and downstream of a WWTP (Gucker et al. 2006).

Thirdly, as water flows downstream, WWTP inputs are gradually diluted. Elevated GPP persists further than ER. The impacted reaches in some large rivers extend 50 km or more downstream (Wassenaar et al. 2010). Site GM is 19 km downstream of site BL, and 25 km downstream of the Kitchener WWTP in the Grand. It is still within the impacted zone below the WWTP. The average GPP of site GM (14.8 g O_2 m^{-2} day^{-1}) was higher than that at the site BL (12.1 g O_2 m^{-2} day^{-1}). However, the average ER of site GM (14.5 g O_2 m^{-2} day^{-1}) was lower compared to site BL (21.2 g O_2 m^{-2} day^{-1}), although it was still higher than upstream site BP (6.0 g O_2 m^{-2} day^{-1}). Three other studies of the effects of WWTPs on stream metabolism (Flemer 1970, Young and Collier 2009, Wassenaar et al. 2010) found similar phenomena (Table 7.2). These phenomena may indicate a recovery of ER from the effects of WWTP outfall.

In addition, besides generally stimulative effects on the metabolic rates as seen in almost all relevant case studies (Table 7.2). WWTP outfalls may also have inhibitory effects (e.g., toxicity from NH_4^+, Cl_2) on the growth of aquatic plants (Hood 2012) and may depress the metabolic rates of the downstream streams. Effluent chlorination was thought to be responsible for lower P and R rates immediately downstream of a WWTP in the South Saskatchewan River, Canada, compared to the metabolic rates upstream (Wassenaar et al. 2010).

7.4.4 Ecosystem metabolism in the Grand River network

The summer metabolic rates in the Grand River network (GPP = 0.4 to 20 and ER = 2 to 33 g O_2 m^{-2} day^{-1}) were within the broad range of the metabolic rates observed in

temperate regions (climate zone 4) regardless of stream size (Figure 7.2). Besides the different pattern of the GPP: ER ratios between the Grand River and the temperate regions (Figure 7.9), another two aspects of metabolism of the Grand River also differed from the general pattern for the temperate regions.

First, the Grand River had higher mean GPP (6.2 compared to 4.9 g O_2 m^{-2} day^{-1} overall) and lower mean ER (8.0 compared to 9.1 g O_2 m^{-2} day^{-1} overall), which may indicate that human activities in the Grand River watershed have stronger positive effects on the GPP than on the ER. More Grand River sites are above the mean for GPP vs. discharge (Figure 7.5) compared to the plot of ER vs. discharge (Figure 7.6), and most sites above the mean for GPP: ER vs. discharge (Figure 7.7) may also suggest the GPP is more affected than ER.

Secondly, the middle-sized to large river sites (5^{th}-7^{th} order) had greater influence than small to middle-sized streams (2^{nd}-5^{th} order) in the Grand River on overall GPP and ER. The plots of metabolic rates (both GPP and ER) in streams grouped by stream order support this conclusion (Figure 7.4). The site 5NF and the 6^{th}-7^{th} order sites had higher GPP, and other sites had lower GPP, than the average of the global data (Figure 7.4A). All of these sites and the lower Grand were above the average line on the plot of GPP vs. discharge, whereas 2^{nd}-5^{th} order sites basically distributed below the average line (Figure 7.5). Sufficient light and nutrients may be the main reasons supporting high GPP at these large sites. All 2^{nd}-5^{th} order sites had lower ER than the average level of global data, whereas the 6^{th}-7^{th} order sites, with the exception of site BP, did not (Figure 7.6).

7.5 Conclusions

The global dataset presented here provides an overview of stream ecosystem metabolism across gradients of climate, stream size and human disturbance. This dataset can serve as a resource for future research on the generalities and peculiarities of ecosystem metabolism, including large-scale inter-regional and inter-biome comparison studies, and examinations of current concepts and theories in ecology. This dataset can also be used

as a baseline to compare particular rivers to the broader pattern seen in other rivers, as I do here in the Grand River.

– Chapter 8 –

Summary, Conclusions and Recommendations

Streams and rivers are altered and stressed with increases in human population and associated land use change. Responses of stream metabolism to anthropogenic disturbance are key to understanding those alterations and to the scientific management and restoration of these important ecosystems. There is a growing body of studies using oxygen isotopes ($\delta^{18}O$) to measure aquatic ecosystem metabolism (Quay et al. 1995, Luz and Barkan 2000, Russ et al. 2004, Parker et al. 2005, Tobias et al. 2007, Venkiteswaran et al. 2007, Beardall et al. 2009, Holtgrieve et al. 2010, Quay et al. 2010, Viviani et al. 2011). However, thus far, little work has been done using the $\delta^{18}O$ approach in streams of differing sizes and degrees of anthropogenic stress, except a few pioneering studies on methods (Tobias et al. 2007, Venkiteswaran et al. 2007, Holtgrieve et al. 2010) or applications (Venkiteswaran et al. 2008, Wassenaar et al. 2010, Jamieson et al. 2012).

The goals of this thesis were to apply the $\delta^{18}O$ ecosystem metabolism approach to streams with a variety of sizes and to examine the effects of human disturbance including agriculture, deforestation and urban WWTPs. I began with the development of a transient model of river ecosystem oxygen metabolism, ROM-TM, which was designed to quantify river ecosystem metabolic rates, gas exchange, and respiration isotopic fractionation from time series of dissolved O_2 (DO) and $\delta^{18}O$-DO. Then, I addressed responses of photosynthesis to light at the ecosystem level using estimated metabolic parameters. Third, I compiled a global dataset of stream ecosystem metabolism from more than 110 studies in the last sixty years, using either the one-station or the two-station method to provide a framework for comparison of my measurements of

ecosystem metabolism in the Grand River basin. These data were examined from multiple aspects and scales to detect both basic patterns and the effects of human disturbance on streams and rivers.

8.1 ROM-TM: A Transient Model of River Oxygen Metabolism

This thesis presents a new, isotope-enabled, transient model of river ecosystem oxygen metabolism, ROM-TM that incorporates actual measured light in the field. It applies an inverse modeling approach and is programmed using MATLAB.

ROM-TM is capable of estimating river ecosystem metabolic rates, reaeration rates and oxygen isotopic fractionation factors from field observation of changes in DO and δ^{18}O-DO. Key parameters describing the main metabolic processes, gas exchange, and isotopic fractionation, such as maximum production rate ($\boldsymbol{P_m}$), production efficiency ($\boldsymbol{a}$), respiration rate at 20℃ ($\boldsymbol{R_{20}}$), gas exchange coefficient ($\boldsymbol{k}$), respiration isotopic fractionation factor ($\boldsymbol{a_R}$), and photorespiration coefficient ($\boldsymbol{\beta_R}$), can be abstracted by minimizing the error sum of squares between the fitted data and the observed field data. Then the DO and δ^{18}O-DO time series can be reconstructed using estimated parameters and input variables.

ROM-TM is capable of addressing issues related to variable light, such as responses of photosynthesis to light at the ecosystem level, the effect of cloud cover on the metabolic balance, and photorespiration. ROM-TM can be used to analyze error and for uncertainty propagation. I specifically addressed the effects of varied resolutions of DO and errors in DO inputs on estimated metabolic parameters and rates. I found that $\boldsymbol{a}$ was more sensitive than other parameters to precision errors, and also to data resolution, and $\boldsymbol{P_m}$ was also sensitive. As for metabolism estimates, *ER* was more sensitive to accuracy errors than *GPP*, and $\boldsymbol{k}$ was almost immune to analytical errors in the DO measurements. I confirmed that when sampling intervals were of ≤ 3 h, ROM-TM provided stable estimates for all parameters with the mean close to true value and with small variances that gradually decrease with sampling intensity. These results suggest

that the precision and resolution of the DO data I used in the Grand River are acceptable for the purpose of comparing the sites in the Grand River with the streams in other studies.

Remaining questions of interest

1. What are the effects of potential violations of the assumptions of homogeneity, either in space or in time, on estimated metabolic parameters while using ROM-TM? These would include pulsed or other inputs, such as WWTP effluents, tributaries and groundwater inputs, changes in riparian forest cover, macrophyte patches.
2. How reasonable it is to assume that respiratory rates are a function of temperature and not affected by light?
3. Can pH time-series, perhaps instead of δ^{18}O-DO, be incorporated into ROM-TM? Like DO and temperature, high resolution pH data are also easily obtained from monitoring stations.
4. Can the lack of discrimination against $\delta^{18}O\text{-}H_2O$ by phototrophs, that is typically assumed for photosynthesis, be confirmed?

8.2 The responses of primary production to light at the ecosystem level

This thesis addresses ecosystem-level responses of primary production to light in the Grand River, based on metabolic parameters; the maximum production rate ($\boldsymbol{P_m}$), production efficiency ($\boldsymbol{a}$) and respiration rate ($\boldsymbol{R}$). These parameters are calculated using ROM-TM from the DO and δ^{18}O-DO time series. To my knowledge, this work is the first study to make such efforts at the ecosystem level in a river network.

The longitudinal pattern of production parameters reflects longitudinal changes of a river network including hydrologic and geomorphologic variables, light availability, species distribution and abundance, and the effects of human disturbance. Production parameters $\boldsymbol{P_m}$ and $\boldsymbol{I_k}$ in the Grand River network exhibited distinct nonlinear increase with stream order, while $\boldsymbol{a}$ was independent of stream size. However, $\boldsymbol{a}$ did vary among and within sites.

Ecosystem-level production parameters are the combined result of the physiologic status of aquatic plants (e.g., sun adaption and shade adaption), plant communities (taxonomic composition, structure and abundance, etc.) and the effects of environmental factors. Comparing production parameters in shaded and non-shaded streams with same stream order, I found that increasing light availability in small and middle-sized streams due to loss of riparian trees consistently enhanced P_m, I_k and E_c, but lowered a. This result demonstrates the effects of environmental variables in the horizontal dimension.

Ecosystem-level P_m in both small periphyton-dominated streams and large macrophyte-dominated rivers in the Grand River basin were generally less than community-level P_m values from the literature. However, Grand River sites BL and GM had comparable P_m to literature-derived P_m due to the prolific growth of macrophytes supported by high nutrient effluents from upstream WWTPs. Ecosystem-level a in my study streams were less than those at the community level, indicating there was a declining trend of this parameter with scale, from individual, community to ecosystem. As a consequence, derived parameters (e.g., I_k, E_c, and saturation point) increased from the individual level to the community level, and then to the ecosystem level.

P-I curve methods are often used to address the relationship between photosynthesis and light at different scales. The responses of photosynthesis to light are not only dependent on the behavior of integrated aquatic plant communities but, more importantly, on the surrounding terrestrial and aquatic environment that is likely to be affected by human activity in the Grand River network. From small streams to the central Grand, 2 typical responses of production to light; light-limited and light-saturated, were commonly observed. Nuisance macrophyte biomass occurs during the summer because of WWTP effluents in the central urbanized regions. Extensive self-shading in plant patches results in some reaches along central Grand not reaching full light saturation in summer, although the channel is quite open and shallow.

Remaining questions of interest

1. The production efficiency, ***a***, is stream-size independent, but varies between and within sites. What is the seasonal trend of ***a***? What is the trend of ***a*** with developmental stage of plant communities after disturbance? Is ***a*** temperature or climate independent?
2. What are the photosynthetic responses of periphyton and other benthic phototrophs to shading by macrophytes?
3. What is the effect of self-shading and light-limited production on the accumulation of plant biomass in eutrophic sites such as Blair?
4. Can photorespiration and photoinhibition be distinguished by a modeling approach? Could photoinhibited production be directly proven to be present if it could be shown that the P rate for given light decreases at high light through a piece-wise fitting of high resolution DO time series data?

8.3 Stream ecosystem metabolism in an impacted temperate river network - magnitude, variability and temporal-spatial patterns

This study examined an agricultural and urban impacted temperate river from multiple aspects and scales. The results suggest that the Grand River network is experiencing effects of human disturbance, mostly downstream of the urban areas and least in small streams with remaining riparian forest. The main indications are:

1) Reach geomorphology controls spatial patterns of stream metabolism in the Grand River network; although the spatial patterns may be modulated by effects of human disturbance on riparian vegetation, nutrients and other factors. Stream order and channel width, as measures of stream size, are good predictors of metabolic rates and ratios of GPP: ER in the Grand River. Ecosystem metabolic rates and ratios generally increased with stream size, but with site specific variation, in the Grand River network.

2) The small and middle-sized streams (2^{nd} to 4^{th} order) without riparian trees in agriculture regions in the Grand River basin did not exhibit significantly different

GPP and ER than their counterparts with riparian trees. The stimulative effect of increased light availability due to open canopy on GPP in non-shaded streams may be offset by shading from stream banks and riparian grasses, and unstable sediments resulting from agricultural activities.

3) Large river sites receiving WWTP effluents on the Grand had significantly increased metabolic rates, GPP and ER, compared to two upstream sites impacted by agriculture only. This result suggests that urban areas have caused impacts on the Grand River that are superimposed on the impacts of agriculture.

4) I did not specifically address seasonal patterns of metabolic rates and ratios in the Grand River due to a shortage of information for spring and autumn. However, the succession of phototroph communities appears to be an important aspect to understanding the seasonal patterns of GPP in the Grand River, associated with light intensity and biomass.

5) This study suggests that the Grand River network is a net heterotrophic system and relies on terrestrial or human subsidies of organic matter. From May to early October, the average GPP for whole basin was 3.3e+08 g O_2 $day^{-1}$and ER was 4.2e+08 g O_2 day^{-1}. The Grand River network consumed 0.9e+08 g O_2 day^{-1}.

Remaining questions of interest

1. What are the effects of seasonal shift of plant communities from early spring to late fall on ecosystem metabolism in temperate rivers?
2. How do the temporal-spatial patterns of stream ecosystem metabolism in the Grand River network contribute to patterns in nutrient cycling (e.g., C, N, P, etc.) at the ecosystem level?
3. What are the direct and indirect effects of remaining forested buffer strips on stream ecosystem metabolism? How long and how wide a segment of forested buffer strip is enough for eliminating the effects of upstream and surrounding agriculture land use?
4. Can partitioning the contributors to photosynthesis and respiration help determine the causes of high ecosystem respiration at site Blair?

8.4 A global perspective on ecosystem metabolism in streams and rivers

This study presents a global dataset of stream ecosystem metabolism using whole-system methods. This dataset provides an overall perspective about metabolic rates and ratios across climate gradients, the effects of stream size and human disturbance on metabolic rates and ratios. The Grand River was also examined in this global dataset to highlight the differences in stream ecosystem metabolism pattern due to human activities. The main points are:

1) The region 30° - 50° from the equator contributes most studies of ecosystem metabolism and thus there is an obvious temperate zone bias to the sites.

2) GPP, ER and GPP: ER of global streams have a similar pattern. These metabolic parameters increase from small streams to middle-sized streams and then decrease from middle-sized streams to large rivers. Globally, ER is size independent.

3) The general trend of GPP: ER ratio in the tropical, subtropical, temperate, and global datasets, approximately conforms to the predictions of the River Continuum Concept (RCC). However, the maximum ratio of GPP: ER in mid-reaches of different river networks is not always >1 as proposed in the RCC. There is a latitude and stream size shift phenomenon regarding where the peak ratio of GPP: ER occurs in each climate zone. The maximum GPP: ER ratio is higher at higher latitudes and occurs at higher order streams. It appears at 3^{rd} order in tropical streams (GPP/ER = 0.6), at 4^{th} order in subtropical streams (GPP/ER = 0.58), at 5^{th} order streams in temperate streams (GPP/ER = 0.99), and at 6^{th} order in Polar streams (GPP/ER = 1.07).

4) Globally, most streams are heterotrophic systems except possibly in tropical regions.

5) For small streams (1^{st} to 4^{th} order), agriculture-impacted ones in forested watersheds, have higher GPP than pristine or less disturbed streams, probably due to enhanced light and nutrients, but have lower ER than natural streams, possibly due to reduced inputs or retention of riparian organic matter. However, agriculture impacted streams in grassland watersheds have obviously high GPP and high ER as well.

6) WWTP effluents can stimulate metabolic activities in streams, either GPP or ER or both, regardless of stream size. GPP and ER often obviously increase due to WWTP effluents, but to different extents. As water flows downstream, elevated GPP usually persists further than ER.

7) The summer metabolic rates in the Grand River network (GPP = 0.4 to 20 and ER = 2 to 33 g O_2 m^{-2} day^{-1}) were within the broad range of the metabolic rates occurring in the temperate zone, regardless of stream size. Three aspects of metabolism of the Grand River differ from the general pattern for the temperate regions: (1) the Grand River had a different longitudinal pattern of the GPP: ER ratios; an increasing trend of GPP: ER ratios with stream size from 2^{nd} to 7^{th} order; (2) compared to global average metabolic rates in the temperate zone, the Grand River had higher mean summer GPP and lower mean summer ER, indicating that human activities in the Grand River watershed had stronger positive effects on GPP than on ER; and (3) the middle-sized to large river sites (5^{th}-7^{th} order) had greater influence than small to middle-sized streams (2^{nd}-5^{th} order) in the Grand River on overall GPP and ER.

Remaining questions of interest

1. Is there a similar pattern of ecosystem metabolism in streams in high elevation areas at low latitudes and streams at high latitudes that have similar climate and vegetation conditions? What is the role of light availability in controlling ecosystem metabolism in these streams?
2. What causes the different patterns of stream metabolism in forested watersheds and grassland watersheds? Light availability? Nutrients? or other factors? What is the role of terrestrial vegetation and formerly forested soils?
3. What is the effect of stream size on the responses of ecosystem metabolism to environmental change?
4. Are there responses of ecosystem metabolism in streams similar in different climate zones for the same perturbation?

8.5 The role of δ^{18}O-DO budget in the current study

Studies of stream ecosystem metabolism can benefit from the addition of the second oxygen budget, δ^{18}O-DO, in four ways: 1) It is better to use both DO and δ^{18}O-DO budgets, rather than DO only, in sampling protocols with low temporal frequency; 2) The δ^{18}O-DO time series data can provide an independent constraint on parameter estimation; 3) The addition of the δ^{18}O-DO budget to quantify metabolic rates provides a way, the cross-plot of δ^{18}O-DO against fraction of DO saturation, to indicate trophic status of an aquatic ecosystem; and, in addition, 4) the addition of δ^{18}O-DO can provide an estimate of $\boldsymbol{a_R}$ at the ecosystem level that can be used to understand factors affecting respiration.

8.6 Future challenges and initiatives

There is an increasing need for scientific knowledge of ecosystem metabolism to provide scientific foundations for managing and restoring impacted stream and river ecosystems as well as contributing to river ecosystem science. Over sixty years of measurements of ecosystem metabolism in streams and rivers have not only provided us knowledge and understanding of metabolic processes, but also have highlighted the limitations of our efforts at larger scales. All efforts can be unified into one task, that of seeking both the generalities and peculiarities of river ecosystems at appropriate temporal-spatial scales (Lamberti and Steinman 1997). This task could guide us to science-based river management while facing emerging challenges from basin-scale water use, land use changes, and global-scale climate change. Some research areas in river ecosystem metabolism, discussed below, are emerging as promising new areas of research in ecosystem metabolism.

1) *Integrating multiple approaches and methods*:

There are advantages and disadvantages of different methods (e.g., incubation vs. whole-stream methods) for measuring stream and river ecosystem metabolism, and no single

method is adequate in all situations. A few comparative studies have addressed the issue of choosing appropriate methods by examining metabolic rates obtained from different methods (Bott et al. 1978, Kelly et al. 1983, Hickey 1988, Marzolf et al. 1994, Tobias et al. 2007) and various techniques (Paul et al. 1989, Aristegi et al. 2009). These studies highlight differences among methods and techniques, and can guide us in applying the best method in metabolism studies.

Benthic chambers are favored for streams where lateral or groundwater inflow and/or O_2 exchange across the air-water interface are expected to be high, compartmentalization of metabolism is desired, and an estimate of variance is required. The whole stream metabolism method is preferred where a broad range of habitat types need to be incorporated in the measurement and/or where artifacts are expected if closed chambers are used. However, incubation methods may be the only choice in some headwater streams with high reaeration and extensive groundwater (Clapcott and Barmuta 2010b). Oxygen isotope information can help us to understand metabolic processes through other associated geochemical, biological, and ecological processes such as food webs (Thorp et al. 1998), coupled nutrient cycling processes (Luz and Barkan 2005, Parker et al. 2005, Kool et al. 2009, Mandernack et al. 2009, Rosamond et al. 2011), and hydrologic processes (Kendall and Coplen 2001, Henderson and Shuman 2010). If metabolic rates of streams and rivers need to be scaled up to the watershed/region scale, GIS tools have to be incorporated into measuring processes as well as the analysis of parameters (Warnaars et al. 2007).

Future challenges come not only from making the best use of the advantages and avoiding the disadvantages of each method but also from integrating multiple approaches and methods to break through the constraints of scale, to achieve consistent and effective estimates of metabolic rates over space and time.

2) *Error, sensitivity and uncertainty analysis*:

The importance of error and uncertainty analysis has been increasingly recognized in the study of ecology when modeling ecological phenomena and extracting inferences (Cressie et al. 2009). However, most studies of stream and river metabolism have been interested in obtaining metabolic rates, but do not provide analysis of error and uncertainty. To date, only a few pioneer studies of stream and river metabolism have been specifically aimed at quantifying error and uncertainty using Monte Carlo simulation (Hornberger 1980, McCutchan et al. 1998) or Bayesian methods (Holtgrieve et al. 2010). Analysis of error and uncertainty could significantly improve our confidence in estimates of metabolic rates. In addition, error, sensitivity and uncertainty analysis can help us in developing effective field sampling protocols. They should assist in developing clear objectives for sampling frequency (Holtgrieve et al. 2010) and in choosing appropriate sites (Reichert et al. 2009). Such work will lower our time and labor costs in the long run. Future work should develop straightforward and effective protocols for quantifying error and uncertainty.

3) *Long term continuous monitoring*:

Monitoring stations can provide us with long-term, stable, continuous, and high frequency time-series of DO, DIC, temperature, pH, etc. Such data are good platforms to extract relevant information on river ecosystem metabolism at multiple scales of temporal variability (Roberts et al. 2007), and across systems and regions (Izagirre et al. 2008). Compared to most field studies, which are often sporadic and seasonally restricted, long-term data are able to provide more precise, large scale estimates of river ecosystem metabolism such as annual GPP and ER (Uehlinger 2006). These data can be used address relevant issues at varying temporal-spatial scales, especially at the global level, such as integrating energy flow and nutrient cycling models, and responses of ecosystem metabolism to climate change at the global level (Marcarelli et al. 2010).

4) *Challenges in a globally changing world*:

The mean surface temperature of the earth is likely to warm 2-4.5℃ by 2100 according to the prediction of IPCC (IPCC, 2007). Ontario, Canada, is facing similar scenarios (Disch 2010). Water temperatures are increasing with the increased air temperature. Annual mean water temperatures increased by 0.009-0.077 ℃ $year^{-1}$ in many streams and rivers throughout the US (Kaushal et al. 2010). Changes in flow regimes may be harder to predict than expected temperature changes due to human greenhouse gas emissions. Compared to a considerable amount of work on responses of river ecosystem metabolism to land use, WWTPs, channelization and river management, fewer studies have focused on the impacts of climate change on ecosystem metabolism in streams and rivers (Acuna et al. 2008, Marcarelli et al. 2010, Demars et al. 2011).

The potential effects of climate change on stream and river ecosystems are unlikely to be similar at different temporal-spatial scales or in the same way for all of systems. For example, headwater streams and large rivers in a river network may have different responses to the same temperature and hydrology changes. Rivers in high latitude regions may be more sensitive to temperature change than those in lower latitude regions. Locating key controlling factors in river ecosystems is a big challenge for future research given the lack of empirical or theoretical bases. One important way of building our confidence and grasping the potential influences of climate change on river metabolism is to conduct broad cross-region and cross-biome comparison studies. A global database in term of the generalities and specifics of river ecosystem metabolism should be a priority for future study. Work relevant to this task has already started with this thesis.

References

Acuna, V., A. Giorgi, I. Munoz, U. Uehlinger, and S. Sabater. 2004. Flow extremes and benthic organic matter shape the metabolism of a headwater Mediterranean stream. Freshwater Biology **49**:960-971.

Acuna, V., C. Vilches, and A. Giorgi. 2011. As productive and slow as a stream can be-the metabolism of a Pampean stream. Journal of the North American Benthological Society **30**:71-83.

Acuna, V., A. Wolf, U. Uehlinger, and K. Tockner. 2008. Temperature dependence of stream benthic respiration in an Alpine river network under global warming. Freshwater Biology **53**:2076-2088.

Al-Lami, A. A., H. J. Jaweir, and M. R. Nashaat. 1998. Benthic invertebrates community of the river Euphrates upstream and downstream sectors of Al-Qadisia dam, Iraq. Regulated Rivers-Research & Management **14**:383-390.

Alewell, C. and B. Manderscheid. 1998. Use of objective criteria for the assessment of biogeochemical ecosystem models. Ecological Modelling **107**:213-224.

Alexander, R. B., R. A. Smith, and G. E. Schwarz. 2000. Effect of stream channel size on the delivery of nitrogen to the Gulf of Mexico. Nature **403**:758-761.

Allan, J. D. and M. M. Castillo. 2007. Stream ecology: structure and function of running waters. 2nd edition. Springer, Dordrecht.

Amon, R. M. W. and R. Benner. 1996. Photochemical and microbial consumption of dissolved organic carbon and dissolved oxygen in the Amazon River system. Geochimica Et Cosmochimica Acta **60**:1783-1792.

Andrews, S. S., S. Caron, and O. C. Zafiriou. 2000. Photochemical oxygen consumption in marine waters: A major sink for colored dissolved organic matter? Limnology and Oceanography **45**:267-277.

APHA. 1995. Standard methods for the examination of water and wastewater. 19th ed. American Public Health Association (APHA). Inc., New York.

Aristegi, L., O. Izagirre, and A. Elosegi. 2009. Comparison of several methods to calculate reaeration in streams, and their effects on estimation of metabolism. Hydrobiologia **635**:113-124.

Arscott, D. B., W. B. Bowden, and J. C. Finlay. 2000. Effects of desiccation and temperature/irradiance on the metabolism of 2 arctic stream bryophyte taxa. Journal of the North American Benthological Society **19**:263-273.

Atkinson, B. L., M. R. Grace, B. T. Hart, and K. E. N. Vanderkruk. 2008. Sediment instability affects the rate and location of primary production and respiration in a sand-bed stream. Journal of the North American Benthological Society **27**:581-592.

Baker, M. A., C. N. Dahm, and H. M. Valett. 1999. Acetate retention and metabolism in the hyporheic zone of a mountain stream. Limnology and Oceanography **44**:1530-1539.

Baker, M. A., H. M. Valett, and C. N. Dahm. 2000. Organic carbon supply and metabolism in a shallow groundwater ecosystem. Ecology **81**:3133-3148.

Baldwin, D. S. and M. Fraser. 2009. Rehabilitation options for inland waterways impacted by sulfidic sediments - A synthesis. Journal of Environmental Management **91**:311-319.

Barlow-Busch, L., H. M. Baulch, and W. D. Taylor. 2006. Phosphate uptake by seston and epilithon in the Grand River, southern Ontario. Aquatic Sciences **68**:181-192.
Bauwe, H., M. Hagemann, and A. R. Fernie. 2010. Photorespiration: players, partners and origin. Trends in Plant Science **15**:330-336.
Bayley, P. B. 1995. Understanding large river floodplain ecosystems. Bioscience **45**:153-158.
Beardall, J., S. Ihnken, and A. Quigg. 2009. Gross and net primary production: closing the gap between concepts and measurements. Aquatic Microbial Ecology **56**:113-122.
Berger, W. H., V. S. Smetacek, G. Wefer, Stifterverband für die Deutsche Wissenschaft., Berlin (Germany : West). Senat., and Wilhelm Woort-Stiftung. 1989. Productivity of the ocean : present and past : report of the Dahlem Workshop on Productivity of the Ocean, Present and Past, Berlin 1988, April 24-29. Wiley, Chichester [England] ; New York.
Berman-Frank, I., T. Berman, and H. MacIntyre. 2009. Progress and perspectives in aquatic primary productivity: introduction. Aquatic Microbial Ecology **56**:109-111.
Bernot, M. J., D. J. Sobota, R. O. Hall, P. J. Mulholland, W. K. Dodds, J. R. Webster, J. L. Tank, L. R. Ashkenas, L. W. Cooper, C. N. Dahm, S. V. Gregory, N. B. Grimm, S. K. Hamilton, S. L. Johnson, W. H. McDowell, J. L. Meyer, B. Peterson, G. C. Poole, H. M. Valett, C. Arango, J. J. Beaulieu, A. J. Burgin, C. Crenshaw, A. M. Helton, L. Johnson, J. Merriam, B. R. Niederlehner, J. M. O'Brien, J. D. Potter, R. W. Sheibley, S. M. Thomas, and K. Wilson. 2010. Inter-regional comparison of land-use effects on stream metabolism. Freshwater Biology **55**:1874-1890.
Bertilsson, S. and L. J. Tranvik. 2000. Photochemical transformation of dissolved organic matter in lakes. Limnology and Oceanography **45**:753-762.
Betts, E. F. and J. B. Jones. 2009. Impact of wildfire on stream nutrient chemistry and ecosystem metabolism in boreal forest catchments of interior Alaska. Arctic Antarctic and Alpine Research **41**:407-417.
Biddanda, B., S. Opsahl, and R. Benner. 1994. Plankton respiration and carbon flux through bacterioplankton on the Louisiana shelf. Limnology and Oceanography **39**:1259-1275.
Biggs, B. J. F., R. A. Smith, and M. J. Duncan. 1999. Velocity and sediment disturbance of periphyton in headwater streams: biomass and metabolism. Journal of the North American Benthological Society **18**:222-241.
Binzer, T. and A. L. Middelboe. 2005. From thallus to communities: scale effects and photosynthetic performance in macroalgae communities. Marine Ecology-Progress Series **287**:65-75.
Binzer, T. and K. Sand-Jensen. 2002. Importance of structure and density of macroalgae communities (Fucus serratus) for photosynthetic production and light utilisation. Marine Ecology-Progress Series **235**:53-62.
Binzer, T., K. Sand-Jensen, and A. L. Middelboe. 2006. Community photosynthesis of aquatic macrophytes. Limnology and Oceanography **51**:2722-2733.
Bott, T. L., J. T. Brock, A. BaattrupPedersen, P. A. Chambers, W. K. Dodds, K. T. Himbeault, J. R. Lawrence, D. Planas, E. Snyder, and G. M. Wolfaardt. 1997. An evaluation of techniques for measuring periphyton metabolism in chambers. Canadian Journal of Fisheries and Aquatic Sciences **54**:715-725.
Bott, T. L., J. T. Brock, C. E. Cushing, S. V. Gregory, D. King, and R. C. Petersen. 1978. Comparison of methods for measuring primary productivity and community respiration in streams. Hydrobiologia **60**:3-12.
Bott, T. L., J. T. Brock, C. S. Dunn, R. J. Naiman, R. W. Ovink, and R. C. Petersen. 1985. Benthic community metabolism in 4 temperate stream systems: An inter-biome comparison and evaluation of the river continuum concept. Hydrobiologia **123**:3-45.

Bott, T. L., D. S. Montgomery, J. D. Newbold, D. B. Arscott, C. L. Dow, A. K. Aufdenkampe, J. K. Jackson, and L. A. Kaplan. 2006a. Ecosystem metabolism in streams of the Catskill Mountains (Delaware and Hudson River watersheds) and Lower Hudson Valley. Journal of the North American Benthological Society **25**:1018-1044.

Bott, T. L., J. D. Newbold, and D. B. Arscott. 2006b. Ecosystem metabolism in piedmont streams: Reach geomorphology modulates the influence of riparian vegetation. Ecosystems **9**:398-421.

Bouletreau, S., E. Salvo, E. Lyautey, S. Mastrorillo, and F. Garabetian. 2012. Temperature dependence of denitrification in phototrophic river biofilms. Science of the Total Environment **416**:323-328.

Bowden, W. B., B. J. Peterson, J. C. Finlay, and J. Tucker. 1992. Epilithic chlorophyll a, photosynthesis, and respiration in control and fertilized reaches of a tundra stream. Hydrobiologia **240**:121-131.

Bowie, G. L., Mills W.B., Porcella D.B., Campbell C.L., Pagenkopf J.R., Rupp G.L., Johnson K.M., Chan P.W.H., and Gherini S.A. 1985. Rates, constants, and kinetic formulations in surface water quality modelling, 2nd edn. EPA/600/3-85/040, USEPA, Athens.

Brandes, J. A. and A. H. Devol. 1997. Isotopic fractionation of oxygen and nitrogen in coastal marine sediments. Geochimica Et Cosmochimica Acta **61**:1793-1801.

Brisbois, M. C., R. Jamieson, R. Gordon, G. Stratton, and A. Madani. 2008. Stream ecosystem health in rural mixed land-use watersheds. Journal of Environmental Engineering and Science **7**:439-452.

Brown, C. J. M. 2010. Fish communities near municipal wastewater discharges in the Grand River Watershed. Master Dissertation. University of Waterloo, Waterloo, ON, Canada.

Brown, C. J. M., B. W. Knight, M. E. McMaster, K. R. Munkittrick, K. D. Oakes, G. R. Tetreault, and M. R. Servos. 2011. The effects of tertiary treated municipal wastewater on fish communities of a small river tributary in Southern Ontario, Canada. Environmental Pollution **159**:1923-1931.

Brown, J. H., J. F. Gillooly, A. P. Allen, V. M. Savage, and G. B. West. 2004. Toward a metabolic theory of ecology. Ecology **85**:1771-1789.

Buchwald, C. and K. L. Casciotti. 2010. Oxygen isotopic fractionation and exchange during bacterial nitrite oxidation. Limnology and Oceanography **55**:1064-1074.

Bunn, S. E., P. M. Davies, and T. D. Mosisch. 1999. Ecosystem measures of river health and their response to riparian and catchment degradation. Freshwater Biology **41**:333-345.

Burford, M. A., A. T. Revill, D. W. Palmer, L. Clementson, B. J. Robson, and I. T. Webster. 2011. River regulation alters drivers of primary productivity along a tropical river-estuary system. Marine and Freshwater Research **62**:141-151.

Campbell, I. D. and C. Campbell. 1994. The impact of late woodland land-use on the forest landscape of southern Ontario. The Great Lakes Geographer **1**:21-29.

Caraco, N. F. and J. J. Cole. 2002. Contrasting impacts of a native and alien macrophyte on dissolved oxygen in a large river. Ecological Applications **12**:1496-1509.

CCME. 2007. Canadian water quality guidelines for the protection of aquatic life: summary table. Updated December 2007. In: Canadian environmental quality guidelines, 1999, Canadian Council of Ministers of the Environment, Winnipeg.

Chalker, B. E. 1980. Modeling light saturation curves for photosynthesis - An exponential function. Journal of Theoretical Biology **84**:205-215.

Chapra, S. C. and D. M. Ditoro. 1991. Delta method for estimating primary production, respiration, and reaeration in streams. Journal of Environmental Engineering-Asce **117**:640-655.

Chessman, B. C. 1985. Estimates of ecosystem metabolism in the La-Trobe river, victoria. Australian Journal of Marine and Freshwater Research **36**:873-880.
Chomicki, K. M. and S. L. Schiff. 2008. Stable oxygen isotopic fractionation during photolytic O-2 consumption in stream waters. Science of the Total Environment **404**:236-244.
Churchill, M. A., H. L. Elmore, and R. A. Buckingham. 1962. The prediction of stream reaeration rates. International Journal of Air and Water Pollution **6**:467-504.
Clapcott, J. E. and L. A. Barmuta. 2010a. Forest clearance increases metabolism and organic matter processes in small headwater streams. Journal of the North American Benthological Society **29**:546-561.
Clapcott, J. E. and L. A. Barmuta. 2010b. Metabolic patch dynamics in small headwater streams: exploring spatial and temporal variability in benthic processes. Freshwater Biology **55**:806-824.
Clapcott, J. E., K. J. Collier, R. G. Death, E. O. Goodwin, J. S. Harding, D. Kelly, J. R. Leathwick, and R. G. Young. 2012. Quantifying relationships between land-use gradients and structural and functional indicators of stream ecological integrity. Freshwater Biology **57**:74-90.
Clapcott, J. E., R. G. Young, E. O. Goodwin, and J. R. Leathwick. 2010. Exploring the response of functional indicators of stream health to land-use gradients. Freshwater Biology **55**:2181-2199.
Colangelo, D. J. 2007. Response of river metabolism to restoration of flow in the Kissimmee River, Florida, USA. Freshwater Biology **52**:459-470.
Cole, J. J. and N. F. Caraco. 2001. Carbon in catchments: connecting terrestrial carbon losses with aquatic metabolism. Marine and Freshwater Research **52**:101-110.
Coles, J. F. and R. C. Jones. 2000. Effect of temperature on photosynthesis-light response and growth of four phytoplankton species isolated from a tidal freshwater river. Journal of Phycology **36**:7-16.
Cooke, S. 2006. Water quality in the Grand River: A summary of current conditions (2000-2004) and long term trends. Report. Grand River Conservation Authority, Cambridge, Ontario.
Crenshaw, C. L., H. M. Valett, and J. R. Webster. 2002. Effects of augmentation of coarse particulate organic matter on metabolism and nutrient retention in hyporheic sediments. Freshwater Biology **47**:1820-1831.
Cressie, N., C. A. Calder, J. S. Clark, J. M. V. Hoef, and C. K. Wikle. 2009. Accounting for uncertainty in ecological analysis: the strengths and limitations of hierarchical statistical modeling. Ecological Applications **19**:553-570.
Cronin, G., J. H. McCutchan, J. Pitlick, and W. M. Lewis. 2007. Use of Shields stress to reconstruct and forecast changes in river metabolism. Freshwater Biology **52**:1587-1601.
Crossey, M. J. and T. W. Lapoint. 1988. A comparison of periphyton community structural and functional responses to heavy metals. Hydrobiologia **162**:109-121.
Darracq, A. and G. Destouni. 2005. In-stream nitrogen attenuation: Model-aggregation effects and implications for coastal nitrogen impacts. Environmental Science & Technology **39**:3716-3722.
Davis, J. C. 1975. Minimal dissolved oxygen requirements of aquatic life with emphasis on Canadian species - a review. Journal of the Fisheries Research Board of Canada **32**:2295-2332.
Davison, I. R. 1991. Environmental effects on algal photosynthesis: temperature. Journal of Phycology **27**:2-8.
Del Giorgio, P. A. and P. J. l. Williams. 2005. Respiration in aquatic ecosystems. Oxford University Press, Oxford ; New York.

Demars, B. O. L., J. R. Manson, J. S. Olafsson, G. M. Gislason, R. Gudmundsdottir, G. Woodward, J. Reiss, D. E. Pichler, J. J. Rasmussen, and N. Friberg. 2011. Temperature and the metabolic balance of streams. Freshwater Biology **56**:1106-1121.

denHeyer, E. E. 2007. Assessing the effects of deep release and surface release reservoirs on downstream benthic macroinvertebrate communities in the Grand River Watershed: Implications for planning and management. Master Dissertation. University of Waterloo, Waterloo, ON, Canada.

Detenbeck, N. E., S. M. Galatowich, and H. Ball. 1999. Evaluating perturbations and developing restoration strategies for inland wetlands in the Great Lakes Basin. Wetlands **19**:789-820.

Disch, J. 2010. Assessing the resilience of Ontario's low water response plan under a changed climate scenario: An Ontario case study. Master Dissertation. University of Waterloo, Waterloo, ON, Canada.

Dodds, W. K., J. J. Beaulieu, J. J. Eichmiller, J. R. Fischer, N. R. Franssen, D. A. Gudder, A. S. Makinster, M. J. McCarthy, J. N. Murdock, J. M. O'Brien, J. L. Tank, and R. W. Sheibley. 2008. Nitrogen cycling and metabolism in the thalweg of a prairie river. Journal of Geophysical Research-Biogeosciences **113**:G04029 DOI:04010.01029/02008JG000696.

Dodds, W. K., B. J. F. Biggs, and R. L. Lowe. 1999. Photosynthesis-irradiance patterns in benthic microalgae: Variations as a function of assemblage thickness and community structure. Journal of Phycology **35**:42-53.

Dodds, W. K. and J. Brock. 1998. A portable flow chamber for in situ determination of benthic metabolism. Freshwater Biology **39**:49-59.

Duarte, C. M. and Y. T. Prairie. 2005. Prevalence of heterotrophy and atmospheric CO2 emissions from aquatic ecosystems. Ecosystems **8**:862-870.

Duffer, W. R. and T. C. Dorris. 1966. Primary productivity in a southern great plains stream. Limnology and Oceanography **11**:143-151.

Duncan, W. F. A. and M. A. Brusven. 1985. Energy dynamics of three low-order southeast Alaska streams: autochthonous production. Journal of Freshwater Ecology **3**:155-166.

Edwards, R. W. and M. Owens. 1962. The effects of plants on river conditions. 4. The oxygen balance of a chalk stream. Journal of Ecology **50**:207-220.

Ekelund, N. G. A. 2000. Interactions between photosynthesis and 'light-enhanced dark respiration' (LEDR) in the flagellate Euglena gracilis after irradiation with ultraviolet radiation. Journal of Photochemistry and Photobiology B-Biology **55**:63-69.

Elosegui, A. and J. Pozo. 1998. Epilithic biomass and metabolism in a north Iberian stream. Aquatic Sciences **60**:1-16.

Falkowski, P. G. 1994. The role of phytoplankton photosynthesis in global biogeochemical cycles. Photosynthesis Research **39**:235-258.

Falkowski, P. G. and J. A. Raven. 1997. Aquatic photosynthesis. Blackwell Science, Malden, Mass.

Falkowski, P. G. and J. A. Raven. 2007. Aquatic photosynthesis. 2nd edition. Princeton University Press, Princeton.

Fellows, C. S., S. E. Bunn, F. Sheldon, and N. J. Beard. 2009. Benthic metabolism in two turbid dryland rivers. Freshwater Biology **54**:236-253.

Fellows, C. S., J. E. Clapcott, J. W. Udy, S. E. Bunn, B. D. Harch, M. J. Smith, and P. M. Davies. 2006a. Benthic metabolism as an indicator of stream ecosystem health. Hydrobiologia **572**:71-87.

Fellows, C. S., H. M. Valett, and C. N. Dahm. 2001. Whole-stream metabolism in two montane streams: Contribution of the hyporheic zone. Limnology and Oceanography **46**:523-531.

Fellows, C. S., H. M. Valett, C. N. Dahm, P. J. Mulholland, and S. A. Thomas. 2006b. Coupling nutrient uptake and energy flow in headwater streams. Ecosystems **9**:788-804.
Finlay, J. C., J. M. Hood, M. P. Limm, M. E. Power, J. D. Schade, and J. R. Welter. 2011. Light-mediated thresholds in stream-water nutrient composition in a river network. Ecology **92**:140-150.
Fisher, S. G. and S. R. Carpenter. 1976. Ecosystem and macrophyte primary production of Fort river, Massachusetts. Hydrobiologia **49**:175-187.
Fisher, S. G., L. J. Gray, N. B. Grimm, and D. E. Busch. 1982. Temporal succession in a desert stream ecosystem following flash flooding. Ecological Monographs **52**:93-110.
Fisher, S. G. and G. E. Likens. 1973. Energy flow in bear brook, New Hampshire: An integrative approach to stream ecosystem metabolism. Ecological Monographs **43**:421-439.
Fleituch, T. 1998. Responses of benthic community metabolism to abiotic factors in a mountain river in southern Poland. Hydrobiologia **380**:27-41.
Flemer, D. A. 1970. Primary productivity of the North Branch of the Raritan River, New Jersey. Hydrobiologia **35**:273-296.
Fuss, C. L. and L. A. Smock. 1996. Spatial and temporal variation of microbial respiration rates in a blackwater stream. Freshwater Biology **36**:339-349.
Gawne, B., C. Merrick, D. G. Williams, G. Rees, R. Oliver, P. M. Bowen, S. Treadwell, G. Beattie, I. Ellis, J. Frankenberg, and Z. Lorenz. 2007. Patterns of primary and heterotrophic productivity in an arid lowland river. River Research and Applications **23**:1070-1087.
Genereux, D. P. and H. F. Hemond. 1992. Determination of gas exchange rate constants for a small stream on walker branch watershed, Tennessee. Water Resources Research **28**:2365-2374.
Gennings, C., L. A. Molot, and P. J. Dillon. 2001. Enhanced photochemical loss of organic carbon in acidic waters. Biogeochemistry **52**:339-354.
Gerbaud, A. and M. Andre. 1987. An evaluation of the recycling in measurements of photorespiration. Plant Physiology **83**:933-937.
Gilbert, O. L. and P. Anderson. 1998. Habitat creation and repair: woodland, scrub, and hedgerow. Oxford University Press, New York.
Gomi, T., R. C. Sidle, and J. S. Richardson. 2002. Understanding processes and downstream linkages of headwater systems. Bioscience **52**:905-916.
Graneli, W., M. Lindell, and L. Tranvik. 1996. Photo-oxidative production of dissolved inorganic carbon in lakes of different humic content. Limnology and Oceanography **41**:698-706.
GRCA. 2004. A Watershed Forest Plan for the Grand River. Grand River Conservation Authority (GRCA). Report. Cambridge, Ontario, Canada.
GRCA. 2012a. The Grand River Conservation Authority (GRCA): About the GRCA. From http://www.grandriver.ca/index/document.cfm?Sec=74&Sub1=5 Date accessed: Feb 01,2012.
GRCA. 2012b. The Grand River Conservation Authority (GRCA): Birding the Grand - Birding hot spots. From http://www.grandriver.ca/Birding/Birding%20hot%20spots.cfm?printer=true Date accessed: Feb 01,2012.
Griffiths, N. A., J. L. Tank, T. V. Royer, T. J. Warrner, T. C. Frauendorf, E. J. Rosi-Marshall, and M. R. Whiles. 2012. Temporal variation in organic carbon spiraling in Midwestern agricultural streams. Biogeochemistry **108**:149-169.
Grimm, N. B. and S. G. Fisher. 1984. Exchange between interstitial and surface water: Implications for stream metabolism and nutrient cycling. Hydrobiologia **111**:219-228.

Guasch, H., E. Marti, and S. Sabater. 1995. Nutrient enrichment effects on biofilm metabolism in a Mediterranean stream. Freshwater Biology **33**:373-383.
Guasch, H. and S. Sabater. 1995. Seasonal variations in photosynthesis-irradiance responses by biofilms in Mediterranean streams. Journal of Phycology **31**:727-735.
Gucker, B., I. G. Boechat, and A. Giani. 2009. Impacts of agricultural land use on ecosystem structure and whole-stream metabolism of tropical Cerrado streams. Freshwater Biology **54**:2069-2085.
Gucker, B., M. Brauns, and M. T. Pusch. 2006. Effects of wastewater treatment plant discharge on ecosystem structure and function of lowland streams. Journal of the North American Benthological Society **25**:313-329.
Gucker, B. and M. T. Pusch. 2006. Regulation of nutrient uptake in eutrophic lowland streams. Limnology and Oceanography **51**:1443-1453.
Hall, R. O. 2003. A stream's role in watershed nutrient export. Proceedings of the National Academy of Sciences of the United States of America **100**:10137-10138.
Hall, R. O. and J. L. Tank. 2003. Ecosystem metabolism controls nitrogen uptake in streams in Grand Teton National Park, Wyoming. Limnology and Oceanography **48**:1120-1128.
Hall, R. O. and J. L. Tank. 2005. Correcting whole-stream estimates of metabolism for groundwater input. Limnology and Oceanography-Methods **3**:222-229.
Hamilton, S. K., J. L. Tank, D. F. Raikow, W. M. Wollheim, B. J. Peterson, and J. R. Webster. 2001. Nitrogen uptake and transformation in a midwestern US stream: A stable isotope enrichment study. Biogeochemistry **54**:297-340.
Hanson, P. C., S. R. Carpenter, N. Kimura, C. Wu, S. P. Cornelius, and T. K. Kratz. 2008. Evaluation of metabolism models for free-water dissolved oxygen methods in lakes. Limnology and Oceanography-Methods **6**:454-465.
Harley, M. T. and S. Findlay. 1994. Photosynthesis-irradiance relationships for 3 species of submersed macrophytes in the tidal fresh-water Hudson river. Estuaries **17**:200-205.
Helman, Y., E. Barkan, D. Eisenstadt, B. Luz, and A. Kaplan. 2005. Fractionation of the three stable oxygen isotopes by oxygen-producing and oxygen-consuming reactions in photosynthetic organisms. Plant Physiol **138**:2292-2298.
Henderson, A. K. and B. N. Shuman. 2010. Differing controls on river- and lake-water hydrogen and oxygen isotopic values in the western United States. Hydrological Processes **24**:3894-3906.
Hickey, C. W. 1988. Benthic chamber for use in rivers: Testing against oxygen mass balances Journal of Environmental Engineering-Asce **114**:828-845.
Higgins, S. N., R. E. Hecky, and S. J. Guildford. 2008. The collapse of benthic macroalgal blooms in response to self-shading. Freshwater Biology **53**:2557-2572.
Hill, B. H., J. M. Lazorchak, F. H. McCormick, and W. T. Willingham. 1997. The effects of elevated metals on benthic community metabolism in a Rocky Mountain stream. Environmental Pollution **95**:183-190.
Hill, W. R. and H. L. Boston. 1991. Community development alters photosynthesis-irradiance relations in stream periphyton. Limnology and Oceanography **36**:1375-1389.
Hill, W. R. and S. E. Fanta. 2008. Phosphorus and light colimit periphyton growth at subsaturating irradiances. Freshwater Biology **53**:215-225.
Hill, W. R., S. E. Fanta, and B. J. Roberts. 2009. Quantifying phosphorus and light effects in stream algae. Limnology and Oceanography **54**:368-380.
Hill, W. R., M. G. Ryon, and E. M. Schilling. 1995. Light limitation in a stream ecosystem - responses by primary producers and consumers. Ecology **76**:1297-1309.

Hoellein, T. J., J. L. Tank, E. J. Rosi-Marshall, and S. A. Entrekin. 2009. Temporal variation in substratum-specific rates of N uptake and metabolism and their contribution at the stream-reach scale. Journal of the North American Benthological Society **28**:305-318.

Holtgrieve, G. W., D. E. Schindler, T. A. Branch, and Z. T. A'Mar. 2010. Simultaneous quantification of aquatic ecosystem metabolism and reaeration using a Bayesian statistical model of oxygen dynamics. Limnology and Oceanography **55**:1047-1063.

Holysh, S., J. Pitcher, and D. Boyd. 2000. Regional groundwater mapping: an assessment tool for incorporating groundwater into the planning process. Grand River Consevation Authority, Cambridge, Ontario.

Hood, L. A. J. 2012. The role of submersed macrophytes in river eutrophication and biogeochemical nutrient cycling. PhD Dissertation. University of Waterloo, Waterloo, ON, Canada.

Horita, J. and C. Kendall. 2004. Stable isotope analysis of water and aqueous solutions by conventional dual-inlet mass spectrometry. Pages 1-37 *in* P. A. d. Groot, editor. *Handbook of Stable Isotope Analytical Techniques*. Elsevier, Amsterdam.

Hornberger, G. M. 1980. Uncertainty in dissolved oxygen prediction due to variability in algal photosynthesis. Water Research **14**:355-361.

Hornberger, G. M. and M. G. Kelly. 1975. Atmospheric reaeration in a river using productivity analysis. Journal of the Environmental Engineering Division-Asce **101**:729-739.

Hornberger, G. M., M. G. Kelly, and B. J. Cosby. 1977. Evaluating eutrophication potential from river community productivity. Water Research **11**:65-69.

Hornberger, G. M., M. G. Kelly, and R. M. Eller. 1976. The relationship between light and photosynthetic rate in a river community and implications for water quality modeling. Water Resources Research **12**:723-730.

Hough, R. A. 1974. Photorespiration and productivity in submersed aquatic vascular plants. Limnology and Oceanography **19**:912-927.

Houser, J. N., P. J. Mulholland, and K. O. Maloney. 2005. Catchment disturbance and stream metabolism: patterns in ecosystem respiration and gross primary production along a gradient of upland soil and vegetation disturbance. Journal of the North American Benthological Society **24**:538-552.

Howarth, R. W., R. Marino, R. Garritt, and D. Sherman. 1992. Ecosystem respiration and organic carbon processing in a large, tidally influenced river: the Hudson River. Biogeochemistry **16**:83-102.

Hunt, R. J., T. D. Jardine, S. K. Hamilton, S. E. Bunn, and K. Tropical Rivers Coastal. 2012. Temporal and spatial variation in ecosystem metabolism and food web carbon transfer in a wet-dry tropical river. Freshwater Biology **57**:435-450.

Ivey, J. 2002. Grand River Watershed characteristisation report. Guelph Water Management Group, University of Guelph., Guelph, Ontario.

Iwakuma, T. and M. Yasuno. 1983. A comparison of several mathematical equations describing photosyntesis-light curve for natural phytoplankton populations. Archiv Fur Hydrobiologie **97**:208-226.

Izagirre, O., U. Agirre, M. Bermejo, J. Pozo, and A. Elosegi. 2008. Environmental controls of whole-stream metabolism identified from continuous monitoring of Basque streams. Journal of the North American Benthological Society **27**:252-268.

Jackson, W. A. and R. J. Volk. 1970. Photorespiration. Annual Review of Plant Physiology **21**:385-&.

Jamieson, T. S. 2010. Quantification of oxygen dynamics in the Grand River using a stable isotope approach. PhD Dissertation. University of Waterloo, Waterloo, ON, Canada.

Jamieson, T. S., S. L. Schiff, and W. D. Taylor. 2012. Using stable isotopes of dissolved oxygen for the determination of gas exchange in the Grand River, Ontario, Canada. Water Research **47**:781-790. doi: 710.1016/j.watres.2012.1011.1001. Epub 2012 Nov 1021.

Jassby, A. D. and T. Platt. 1976. Mathematical formulation of relationship between photosynthesis and light for phytoplankton. Limnology and Oceanography **21**:540-547.

Jones, J. B. 1995. Factors controlling hyporheic respiration in a desert stream. Freshwater Biology **34**:91-99.

Jones, J. B., S. G. Fisher, and N. B. Grimm. 1995. Vertical hydrologic exchange and ecosystem metabolism in a Sonoran desert stream. Ecology **76**:942-952.

Julian, J. P., M. W. Doyle, and E. H. Stanley. 2008. Empirical modeling of light availability in rivers. Journal of Geophysical Research-Biogeosciences **113**.

Julian, J. P., S. Z. Seegert, S. M. Powers, E. H. Stanley, and M. W. Doyle. 2011. Light as a first-order control on ecosystem structure in a temperate stream. Ecohydrology **4**:422-432.

Juranek, L. W. and P. D. Quay. 2010. Basin-wide photosynthetic production rates in the subtropical and tropical Pacific Ocean determined from dissolved oxygen isotope ratio measurements. Global Biogeochemical Cycles **24**.

Jyrkama, M. I. and J. F. Sykes. 2007. The impact of climate change on spatially varying groundwater recharge in the Grand River watershed (Ontario). Journal of Hydrology **338**:237-250.

Kaenel, B. R., H. Buehrer, and U. Uehlinger. 2000. Effects of aquatic plant management on stream metabolism and oxygen balance in streams. Freshwater Biology **45**:85-95.

Kaiser, J. 2011. Technical note: Consistent calculation of aquatic gross production from oxygen triple isotope measurements. Biogeosciences **8**:1793-1811.

Karim, A., K. Dubois, and J. Veizer. 2011. Carbon and oxygen dynamics in the Laurentian Great Lakes: Implications for the CO(2) flux from terrestrial aquatic systems to the atmosphere. Chemical Geology **281**:133-141.

Karlsson, J., P. Bystrom, J. Ask, P. Ask, L. Persson, and M. Jansson. 2009. Light limitation of nutrient-poor lake ecosystems. Nature **460**:506-U580.

Kaushal, S. S., G. E. Likens, N. A. Jaworski, M. L. Pace, A. M. Sides, D. Seekell, K. T. Belt, D. H. Secor, and R. L. Wingate. 2010. Rising stream and river temperatures in the United States. Frontiers in Ecology and the Environment **8**:461-466.

Kelly, M. G., N. Thyssen, and B. Moeslund. 1983. Light and the annual variation of oxygen- and carbon-based measurements of productivity in a macrophyte-dominated river. Limnology and Oceanography **28**:503-515.

Kendall, C. and T. B. Coplen. 2001. Distribution of oxygen-18 and deuterium in river waters across the United States. Hydrological Processes **15**:1363-1393.

Kilpatrick F.A., R. E. R., N. Yotsukura., et al. 1989. Determination of stream reaeration coefficients by use of tracers. Techniques of water resources investigations 3-A18. U.S. Geological Survey, Denver, Colorado, USA.

Kilpatrick, R. E. R., N. Yotsukura., et al. 1989. Determination of stream reaeration coefficients by use of tracers. Techniques of water resources investigations 3-A18. U.S. Geological Survey, Denver, Colorado, USA.

Kirk, J. T. O. 1994. Light and photosynthesis in aquatic ecosystems. 2nd edition. Cambridge University Press, Cambridge [England] ; New York, NY, USA.

Kool, D. M., N. Wrage, O. Oenema, D. Harris, and J. W. Van Groenigen. 2009. The O-18 signature of biogenic nitrous oxide is determined by O exchange with water. Rapid Communications in Mass Spectrometry **23**:104-108.

Kramer, D. L. 1987. Dissolved oxygen and fish behavior. Environmental Biology of Fishes **18**:81-92.

Kuntz, T. 2008. System and plankton metabolism in the lower Grand River, Ontario. Master Dissertation. University of Waterloo, Waterloo, ON, Canada.
Lamberti, G. A. and A. D. Steinman. 1997. A comparison of primary production in stream ecosystems. Journal of the North American Benthological Society **16**:95-104.
Lau, Y. L. 1972. Prediction equation for reaeration in open-channel flow. Journal of the Sanitary Engineering Division-Asce **98**:1063-&.
Laviale, M., J. Prygiel, Y. Lemoine, A. Courseaux, and A. Creach. 2009. Stream periphyton photoacclimation response in field conditions: Effect of community development and seasonal changes. Journal of Phycology **45**:1072-1082.
Lehman, J. T. and T. Naumoski. 1986. Net community production and hypolimnetic nutrient regeneration in a Michigan lake. Limnology and Oceanography **31**:788-797.
Lessard, J. L. and D. B. Hayes. 2003. Effects of elevated water temperature on fish and macroinvertebrate communities below small dams. River Research and Applications **19**:721-732.
Lester, W. W., M. S. Adams, and A. M. Farmer. 1988. Effects of Light and Temperature on Photosynthesis of the Nuisance Alga Cladophora-Glomerata (L) Kutz from Green-Bay, Lake-Michigan. New Phytologist **109**:53-58.
Levy, O., Z. Dubinsky, K. Schneider, Y. Achituv, D. Zakai, and M. Y. Gorbunov. 2004. Diurnal hysteresis in coral photosynthesis. Marine Ecology-Progress Series **268**:105-117.
Lloyd, N. D. H., D. T. Canvin, and D. A. Culver. 1977. Photosynthesis and photorespiration in algae. Plant Physiology **59**:936-940.
Logue, J. B., C. T. Robinson, C. Meier, and J. R. Van der Meer. 2004. Relationship between sediment organic matter, bacteria composition, and the ecosystem metabolism of alpine streams. Limnology and Oceanography **49**:2001-2010.
Loperfido, J. V., C. L. Just, and J. L. Schnoor. 2009. High-frequency diel dissolved oxygen stream data modeled for variable temperature and scale. Journal of Environmental Engineering-Asce **135**:1250-1256.
Lorenz, C. M., G. M. Van Dijk, A. G. M. Van Hattum, and W. P. Cofino. 1997. Concepts in river ecology: Implications for indicator development. Regulated Rivers-Research & Management **13**:501-516.
Luz, B. 1999. Triple-isotope composition of atmospheric oxygen as a tracer of biosphere productivity. Nature **400**:547-550.
Luz, B. and E. Barkan. 2000. Assessment of oceanic productivity with the triple-isotope composition of dissolved oxygen. Science **288**:2028-2031.
Luz, B. and E. Barkan. 2005. The isotopic ratios $^{17}O/^{16}O$ and $^{18}O/^{16}O$ in molecular oxygen and their significance in biogeochemistry. Geochimica Et Cosmochimica Acta **69**:1099-1110.
Luz, B. and E. Barkan. 2009. Net and gross oxygen production from O_2/Ar, $^{17}O/^{16}O$ and $^{18}O/^{16}O$ ratios. Aquatic Microbial Ecology **56**:133-145.
Luz, B. and E. Barkan. 2011. The isotopic composition of atmospheric oxygen. Global Biogeochemical Cycles **25**:Gb3001 3010.1029/2010gb003883.
Madsen, J. D., C. F. Hartleb, and C. W. Boylen. 1991. Photosynthetic Characteristics of Myriophyllum-Spicatum and 6 Submersed Aquatic Macrophyte Species Native to Lake George, New-York. Freshwater Biology **26**:233-240.
Maixandeau, A., D. Lefevre, H. Karayanni, U. Christaki, F. Van Wambeke, M. Thyssen, M. Denis, C. I. Fernandez, J. Uitz, K. Leblanc, and B. Queguiner. 2005. Microbial community production, respiration, and structure of the microbial food web of an ecosystem in the northeastern Atlantic Ocean. Journal of Geophysical Research-Oceans **110**:C07S17, doi:10.1029/2004JC002694.

Mandernack, K. W., C. T. Mills, C. A. Johnson, T. Rahn, and C. Kinney. 2009. The delta N-15 and delta O-18 values of N2O produced during the co-oxidation of ammonia by methanotrophic bacteria. Chemical Geology **267**:96-107.
Marcarelli, A. M., R. W. Van Kirk, and C. V. Baxter. 2010. Predicting effects of hydrologic alteration and climate change on ecosystem metabolism in a western U.S. river. Ecological Applications **20**:2081-2088.
Marzolf, E. R., P. J. Mulholland, and A. D. Steinman. 1994. Improvements to diurnal upstream-downstream dissolved oxygen change technique for determining whole-stream metabolism in small streams. Canadian Journal of Fisheries and Aquatic Sciences **51**:1591-1599.
Maurino, V. G. and C. Peterhansel. 2010. Photorespiration: current status and approaches for metabolic engineering. Current Opinion in Plant Biology **13**:249-256.
Mayer, T. and R. E. Delos. 1996. Phosphorus and metal contaminant transport in two southern Ontario rivers: the Grand River and its tributory, the Nith River. Water Quality Research Journal, Canada **31**:119-151.
McBride, G. B. 2002. Calculating stream reaeration coefficients from oxygen profiles. Journal of Environmental Engineering-Asce **128**:384-386.
McBride, G. B. and S. C. Chapra. 2005. Rapid calculation of oxygen in streams: Approximate delta method. Journal of Environmental Engineering-Asce **131**:336-342.
McCutchan, J. H., W. M. Lewis, and J. F. Saunders. 1998. Uncertainty in the estimation of stream metabolism from open-channel oxygen concentrations. Journal of the North American Benthological Society **17**:155-164.
McCutchan, J. H., J. F. Saunders, W. M. Lewis, and M. G. Hayden. 2002. Effects of groundwater flux on open-channel estimates of stream metabolism. Limnology and Oceanography **47**:321-324.
McDiffet, W. F., D. L. Young, and A. E. Carr. 1972. An estimate of primary productivity in a Pennsylvania Trout stream using a diurnal oxygen curve technique. American Midland Naturalist **87**:564-570.
McIntire, C. D. and H. K. Phinney. 1965. Laboratory studies of periphyton production and community metabolism in lotic environments. Ecological Monographs **35**:237-258.
McTammany, M. E., E. F. Benfield, and J. R. Webster. 2007. Recovery of stream ecosystem metabolism from historical agriculture. Journal of the North American Benthological Society **26**:532-545.
McTammany, M. E., J. R. Webster, E. F. Benfield, and M. A. Neatrour. 2003. Longitudinal patterns of metabolism in a southern Appalachian river. Journal of the North American Benthological Society **22**:359-370.
Melching, C. S. and H. E. Flores. 1999. Reaeration equations derived from US geological survey database. Journal of Environmental Engineering-Asce **125**:407-414.
Meyer, J. L. and R. T. Edwards. 1990. Ecosystem metabolism and turnover of organic-carbon along a Blackwater River Continuum. Ecology **71**:668-677.
Meyer, J. L., M. J. Paul, and W. K. Taulbee. 2005. Stream ecosystem function in urbanizing landscapes. Journal of the North American Benthological Society **24**:602-612.
Middelboe, A. L. and T. Binzer. 2004. Importance of canopy structure on photosynthesis in single- and multi-species assemblages of marine macroalgae. Oikos **107**:422-432.
Minshall, G. W. 1978. Autotrophy in stream ecosystems. Bioscience **28**:767-770.
Molles, M. C. and C. N. Dahm. 1990. A perspective on El Niño and La Niña: global implications for stream ecology. Journal of the North American Benthological Society **9**:68-76.
Molot, L. A. and P. J. Dillon. 1997. Photolytic regulation of dissolved organic carbon in northern lakes. Global Biogeochemical Cycles **11**:357-365.

Morse, N., W. B. Bowden, A. Hackman, C. Pruden, E. Steiner, and E. Berger. 2007. Using sound pressure to estimate reaeration in streams. Journal of the North American Benthological Society **26**:28-37.

Moss, M. R. and L. S. Davis. 1994. Measurement of spatial change in the forest component of the rural landscape of southern Ontario. Applied Geography **14**:214-231.

Mulholland, P. J., C. S. Fellows, J. L. Tank, N. B. Grimm, J. R. Webster, S. K. Hamilton, E. Marti, L. Ashkenas, W. B. Bowden, W. K. Dodds, W. H. McDowell, M. J. Paul, and B. J. Peterson. 2001. Inter-biome comparison of factors controlling stream metabolism. Freshwater Biology **46**:1503-1517.

Mulholland, P. J., J. N. Houser, and K. O. Maloney. 2005. Stream diurnal dissolved oxygen profiles as indicators of in-stream metabolism and disturbance effects: Fort Benning as a case study. Ecological Indicators **5**:243-252.

Mulholland, P. J., E. R. Marzolf, J. R. Webster, D. R. Hart, and S. P. Hendricks. 1997. Evidence that hyporheic zones increase heterotrophic metabolism and phosphorus uptake in forest streams. Limnology and Oceanography **42**:443-451.

Mulholland, P. J., E. R. Marzolf, J. R. Webster, D. R. Hart, and S. P. Hendricks. 1999. Evidence that hyporheic zones increase heterotrophic metabolism and phosphorus uptake in forest streams (vol 42, pg 443, 1997). Limnology and Oceanography **44**:230-231.

Mulholland, P. J., S. A. Thomas, H. M. Valett, J. R. Webster, and J. Beaulieu. 2006. Effects of light on NO3- uptake in small forested streams: diurnal and day-to-day variations. Journal of the North American Benthological Society **25**:583-595.

Murphy, J. L., P. A. Mackinnon, Y. Q. Zhao, R. M. Kalin, and T. Elliot. 2001. Measurement of the surface water reaeration coefficient using Kr as a gas tracer. Pages 505-514 *in* C. A. Brebbia, editor. Water Pollution Vi - Modelling, Measuring and Prediction. Wit Press, Southampton.

Naegeli, M. W. and U. Uehlinger. 1997. Contribution of the hyporheic zone to ecosystem metabolism in a prealpine gravel-bed river. Journal of the North American Benthological Society **16**:794-804.

Naiman, R. J. 1983. The Annual Pattern and Spatial Distribution of Aquatic Oxygen Metabolism in Boreal Forest Watersheds. Ecological Monographs **53**:73-94.

Naiman, R. J., J. M. Melillo, M. A. Lock, T. E. Ford, and S. R. Reice. 1987. Longitudinal patterns of ecosystem processes and community structure in a sub-Arctic river continuum. Ecology **68**:1139-1156.

Naimo, T. J., J. B. Layzer, and A. C. Miller. 1988. Benthic community metabolism in 2 northern Mississippi streams. Journal of Freshwater Ecology **4**:503-515.

Nelson, J. G., J. Porter, C. Farassoglou, S. Gardiner, C. Guthrie, C. Beck, and C. Lemieux. 2003. The Grand River watershed: a heritage landscape guide. Heritage Resources Centre, University of Waterloo., Waterloo, Ont.

O'Hare, M. T., R. T. Clarke, M. J. Bowes, C. Cailes, P. Henville, N. Bissett, C. McGahey, and M. Neal. 2010. Eutrophication impacts on a river macrophyte. Aquatic Botany **92**:173-178.

Odum, H. T. 1956. Primary production in flowing waters. Limnology and Oceanography **1**:102-117.

Odum, H. T. 1957a. Primary production measurements in eleven Florida Springs and a marine turtle-grass community. Limnology and Oceanography **2**:85-97.

Odum, H. T. 1957b. Trophic structure and productivity of silver springs, Florida. Ecological Monographs **27**:55-112.

Oliver, R. L. and C. J. Merrick. 2006. Partitioning of river metabolism identifies phytoplankton as a major contributor in the regulated Murray River (Australia). Freshwater Biology **51**:1131-1148.

OMI. 2006. Ontario Ministry of Infrastructure (OMI). Places to Grow: Growth Plan for the Greater Golden Horseshoe. From: http://www.placestogrow.ca. Ontario Ministry of Infrastructure.
Ongley, E. D. 1976. Sediment yields and nutrient loadings from Canadian watersheds tributary to Lake Erie - Overview. Journal of the Fisheries Research Board of Canada **33**:471-484.
Oreskes, N., K. Shraderfrechette, and K. Belitz. 1994. Verification, Validation, and Confirmation of Numerical-Models in the Earth-Sciences. Science **263**:641-646.
Ortiz-Zayas, J. R., W. M. Lewis, J. F. Saunders, J. H. McCutchan, and F. N. Scatena. 2005. Metabolism of a tropical rainforest stream. Journal of the North American Benthological Society **24**:769-783.
Parker, S. R., S. R. Poulson, C. H. Gammons, and M. D. Degrandpre. 2005. Biogeochemical controls on diel cycling of stable isotopes of dissolved O_2 and dissolved inorganic carbon in the Big Hole River, Montana. Environmental Science & Technology **39**:7134-7140.
Parkhill, K. L. and J. S. Gulliver. 1998. Application of photorespiration concepts to whole stream productivity. Hydrobiologia **389**:7-19.
Parkhill, K. L. and J. S. Gulliver. 1999. Modeling the effect of light on whole-stream respiration. Ecological Modelling **117**:333-342.
Parkhill, K. L. and J. S. Gulliver. 2002. Effect of inorganic sediment on whole-stream productivity. Hydrobiologia **472**:5-17.
Paul, B. J., K. E. Corning, and H. C. Duthie. 1989. An evaluation of the metabolism of sestonic and epilithic communities in running waters using an improved chamber technique. Freshwater Biology **21**:207-215.
Perkins, D. M., G. Yvon-Durocher, B. O. L. Demars, J. Reiss, D. E. Pichler, N. Friberg, M. Trimmer, and G. Woodward. 2012. Consistent temperature dependence of respiration across ecosystems contrasting in thermal history. Global Change Biology **18**:1300-1311.
Peterson, D. H., M. J. Perry, K. E. Bencala, and M. C. Talbot. 1987. Phytoplankton productivity in relation to light intensity: A simple equation. Estuarine Coastal and Shelf Science **24**:813-832.
Poff, N. L. and J. V. Ward. 1989. Implications of streamflow variability and predictability for lotic community structure - A regional analysis of streamflow patterns. Canadian Journal of Fisheries and Aquatic Sciences **46**:1805-1818.
Pollock-Ellwand, N. 1997. Planning for the Landscape Idea. PhD Dissertation. University of Waterloo, Waterloo, ON, Canada.
Potter, J. D., W. H. McDowell, J. L. Merriam, B. J. Peterson, and S. M. Thomas. 2010. Denitrification and total nitrate uptake in streams of a tropical landscape. Ecological Applications **20**:2104-2115.
Prezelin, B. B. and H. A. Matlick. 1980. Time-course of photoadaptation in the photosynthesis-irradiance relationship of a dinoflagellate exhibiting photosynthetic periodicity. Marine Biology **58**:85-96.
Prokopenko, M. G., O. M. Pauluis, J. Granger, and L. Y. Yeung. 2011. Exact evaluation of gross photosynthetic production from the oxygen triple-isotope composition of O(2): Implications for the net-to-gross primary production ratios. Geophysical Research Letters **38**.
Pusch, M. 1996. The metabolism of organic matter in the hyporheic zone of a mountain stream, and its spatial distribution. Hydrobiologia **323**:107-118.
Pusch, M. and J. Schwoerbel. 1994. Community respiration in hyporheic sediments of a mountain stream (Steina, Black-forest). Archiv Fur Hydrobiologie **130**:35-52.
Quay, P. D., C. Peacock, K. Bjoerkman, and D. M. Karl. 2010. Measuring primary production rates in the ocean: Enigmatic results between incubation and non-incubation methods at

Station ALOHA. Global Biogeochemical Cycles **24**:GB3014, doi:3010.1029/2009GB003665.
Quay, P. D., D. O. Wilbur, J. E. Richey, A. H. Devol, R. Benner, and B. R. Forsberg. 1995. The O^{18}:O^{16} of dissolved oxygen in rivers and lakes in the Amazon Basin: determining the ratio of respiration to photosynthesis rates in freshwaters. Limnology and Oceanography **40**:718-729.
Rae, R. and W. F. Vincent. 1998. Phytoplankton production in subarctic lake and river ecosystems: development of a photosynthesis-temperature-irradiance model. Journal of Plankton Research **20**:1293-1312.
Raghavendra, A. S., K. Padmasree, and K. Saradadevi. 1994. Interdependence of photosynthesis and respiration in plant cells: interactions between chloroplasts and mitochondria. Plant Science **97**:1-14.
Rasmussen, J. J., A. Baattrup-Pedersen, T. Riis, and N. Friberg. 2011. Stream ecosystem properties and processes along a temperature gradient. Aquatic Ecology **45**:231-242.
Rathbun, R. E. 1977. Reaeration coefficients of streams - State-of-the-art. Journal of the Hydraulics Division-Asce **103**:409-424.
Rebsdorf, A., N. Thyssen, and M. Erlandsen. 1991. Regional and Temporal Variation in Ph, Alkalinity and Carbon-Dioxide in Danish Streams, Related to Soil Type and Land-Use. Freshwater Biology **25**:419-435.
Rees, G. N., P. M. Bowen, and G. O. Watson. 2005. Variability in benthic respiration in three southeastern Australian lowland rivers. River Research and Applications **21**:1147-1156.
Regaudie-de-Gioux, A. and C. M. Duarte. 2012. Temperature dependence of planktonic metabolism in the ocean. Global Biogeochemical Cycles **26**:GB1015, doi:1010.1029/2010GB003907.
Reichert, P., U. Uehlinger, and V. Acuna. 2009. Estimating stream metabolism from oxygen concentrations: Effect of spatial heterogeneity. Journal of Geophysical Research-Biogeosciences **114**:G03016, doi:03010.01029/02008JG000917.
Reid, S. E., P. A. Mackinnon, and T. Elliot. 2007. Direct measurements of reaeration rates using noble gas tracers in the River Lagan, Northern Ireland. Water and Environment Journal **21**:182-191.
Roberts, B. J., P. J. Mulholland, and W. R. Hill. 2007. Multiple scales of temporal variability in ecosystem metabolism rates: Results from 2 years of continuous monitoring in a forested headwater stream. Ecosystems **10**:588-606.
Rosamond, M. S., S. J. Thuss, S. L. Schiff, and R. J. Elgood. 2011. Coupled cycles of dissolved oxygen and nitrous oxide in rivers along a trophic gradient in southern ontario, Canada. Journal of Environmental Quality **40**:256-270.
Rosenfeld, J. S. and R. J. Mackay. 1987. Assessing the food base of stream ecosystems: alternatives to the P/R ratio. Oikos **50**:141-147.
Ruggiero, A., A. G. Solimini, and G. Carchini. 2006. Effects of a waste water treatment plant on organic matter dynamics and ecosystem functioning in a Mediterranean stream. Annales De Limnologie-International Journal of Limnology **42**:97-107.
Russ, M. E., N. E. Ostrom, H. Gandhi, P. H. Ostrom, and N. R. Urban. 2004. Temporal and spatial variations in R:P ratios in Lake Superior, an oligotrophic freshwater environment. Journal of Geophysical Research-Oceans **109**:C10S12, doi:10.1029/2003JC001890.
Sanchez-Perez, J. M., M. Gerino, S. Sauvage, P. Dumas, E. Maneux, F. Julien, P. Winterton, and P. Vervier. 2009. Effects of wastewater treatment plant pollution on in-stream ecosystems functions in an agricultural watershed. Annales De Limnologie-International Journal of Limnology **45**:79-92.

Sand-Jensen, K., N. L. Pedersen, and M. Sondergaard. 2007. Bacterial metabolism in small temperate streams under contemporary and future climates. Freshwater Biology **52**:2340-2353.

Sandjensen, K. and T. V. Madsen. 1991. Minimum light requirements of submerged freshwater macrophytes in laboratory growth experiments. Journal of Ecology **79**:749-764.

Sarma, V. and O. Abe. 2006. Short-term variation of triple oxygen isotopes and gross oxygen production in the Sagami Bay, central Japan. Limnology and Oceanography **51**:1432-1442.

Sarma, V. V. S. S., O. Abe, M. Honda, and T. Saino. 2010. Estimating of Gas Transfer Velocity Using Triple Isotopes of Dissolved Oxygen. Journal of Oceanography **66**:505-512.

Sarma, V. V. S. S., O. Abe, and T. Saino. 2008. Spatial variations in time-integrated plankton metabolic rates in Sagami Bay using triple oxygen isotopes and O_2 : Ar ratios. Limnology and Oceanography **53**:1776-1783.

Sawyer, A., C. Cooke, P. J., and P. Laocevic. 2005. State of the Great Lakes: Groundwater dependant plant and animal communities. Grand River Consevation Authority, Cambridge, Ontario.

Schafer, R. B., M. Bundschuh, D. A. Rouch, E. Szocs, P. C. von der Ohe, V. Pettigrove, R. Schulz, D. Nugegoda, and B. J. Kefford. 2012. Effects of pesticide toxicity, salinity and other environmental variables on selected ecosystem functions in streams and the relevance for ecosystem services. Science of the Total Environment **415**:69-78.

Schindler, D. W. 1977. Evolution of phosphorus limitation in lakes. Science **195**:260-262.

Seibel, B. A. 2011. Critical oxygen levels and metabolic suppression in oceanic oxygen minimum zones. Journal of Experimental Biology **214**:326-336.

Servais, P., E. Debecker, and G. Billen. 1984. Annual cycle of gross primary production and respiration in the Viroin river (Belgium). Hydrobiologia **111**:57-63.

Shantz, M., E. Dowsett, E. Canham, G. Tavernier, M. Stone, and J. Price. 2004. The effect of drawdown on suspended solids and phosphorus export from Columbia Lake, Waterloo, Canada. Hydrological Processes **18**:865-878.

Sharkey, T. D. 1988. Estimating the rate of photorespiration in leaves. Physiologia Plantarum **73**:147-152.

Sobczak, W. V., J. E. Cloern, A. D. Jassby, B. E. Cole, T. S. Schraga, and A. Arnsberg. 2005. Detritus fuels ecosystem metabolism but not metazoan food webs in San Francisco estuary's freshwater Delta. Estuaries **28**:124-137.

Søndergaaard, M. 1988. Photosynthesis of aquatic plants under natural conditions. In: Vegetation of inland waters. Pages 63-111 *in* J. J. Symoens, editor. Handbook of Vegetation Science, The Hague, Netherlands.

Spence, J. A. and H. B. N. Hynes. 1971. Differences benthos upstream and downstream of impoundment. Journal of the Fisheries Research Board of Canada **28**:35-&.

Spivak, A. C., E. A. Canuel, J. E. Duffy, and J. P. Richardson. 2009. Nutrient enrichment and food web composition affect ecosystem metabolism in an experimental seagrass habitat. PLoS One **4**.

Stadnyk-Falcone, T. A. 2008. Mesoscale hydrological model validation and verification using stable water isotopes: The isoWATFLOOD Model. PhD Dissertation. University of Waterloo, Waterloo, ON, Canada.

Staehr, P. A. and K. Sand-Jensen. 2006. Seasonal changes in temperature and nutrient control of photosynthesis, respiration and growth of natural phytoplankton communities. Freshwater Biology **51**:249-262.

Stanley, E. H., S. M. Powers, and N. R. Lottig. 2010. The evolving legacy of disturbance in stream ecology: concepts, contributions, and coming challenges. Journal of the North American Benthological Society **29**:67-83.
Statzner, B. and B. Higler. 1985. Questions and Comments on the River Continuum Concept. Canadian Journal of Fisheries and Aquatic Sciences **42**:1038-1044.
Sterner, R. W., J. J. Elser, E. J. Fee, S. J. Guildford, and T. H. Chrzanowski. 1997. The light:nutrient ratio in lakes: The balance of energy and materials affects ecosystem structure and process. American Naturalist **150**:663-684.
Suarez, L. and R. Vidal-Abarca. 2001. Metabolism of a semi-arid stream of south-east Spain. Pages 756-761 *in* W. D. Williams, editor. International Association of Theoretical and Applied Limnology, Vol 27, Pt 2, Proceedings. E Schweizerbart'sche Verlagsbuchhandlung, Stuttgart.
Sumner, W. T. and S. G. Fisher. 1979. Periphyton production in Fort River, Massachusetts. Freshwater Biology **9**:205-212.
Suren, A. M. 2009. Using Macrophytes in Urban Stream Rehabilitation: A Cautionary Tale. Restoration Ecology **17**:873-883.
Tank, J. L., E. J. Rosi-Marshall, N. A. Griffiths, S. A. Entrekin, and M. L. Stephen. 2010. A review of allochthonous organic matter dynamics and metabolism in streams. Journal of the North American Benthological Society **29**:118-146.
Taylor, B. W., A. S. Flecker, and R. O. Hall. 2006. Loss of a harvested fish species disrupts carbon flow in a diverse tropical river. Science **313**:833-836.
Thorp, J. H. and A. D. Delong. 2002. Dominance of autochthonous autotrophic carbon in food webs of heterotrophic rivers. Oikos **96**:543-550.
Thorp, J. H., M. D. Delong, K. S. Greenwood, and A. F. Casper. 1998. Isotopic analysis of three food web theories in constricted and floodplain regions of a large river. Oecologia **117**:551-563.
Thuss, S. 2008. Nitrous oxide production in the Grand River, Ontario, Canada: new insights from stable isotope analysis of dissolved nitrous oxide. Thesis (MSc)-University of Waterloo, 2008. University of Waterloo,, Waterloo, Ont.
Tobias, C. R., J. K. Bohlke, and J. W. Harvey. 2007. The oxygen-18 isotope approach for measuring aquatic metabolism in high-productivity waters. Limnology and Oceanography **52**:1439-1453.
Tobias, C. R., J. K. Bohlke, J. W. Harvey, and E. Busenberg. 2009. A simple technique for continuous measurement of time-variable gas transfer in surface waters. Limnology and Oceanography-Methods **7**:185-195.
Townsend, C. R. 1989. The patch dynamics concept of stream community ecology. Journal of the North American Benthological Society **8**:36-50.
Tsivoglou, E. C. and L. A. Neal. 1976. Tracer measurement of reaeration. 3: Predicting reaeration capacity of inland streams. Journal Water Pollution Control Federation **48**:2669-2689.
Uehlinger, U. 1993. Primary production and respiration in the outlet of an eutrophic lake (River Glatt, Switzerland). Archiv Fur Hydrobiologie **128**:39-55.
Uehlinger, U. 2000. Resistance and resilience of ecosystem metabolism in a flood-prone river system. Freshwater Biology **45**:319-332.
Uehlinger, U. 2006. Annual cycle and inter-annual variability of gross primary production and ecosystem respiration in a floodprone river during a 15-year period. Freshwater Biology **51**:938-950.
Uehlinger, U. and J. T. Brock. 2005. Periphyton metabolism along a nutrient gradient in a desert river (Truckee River, Nevada, USA). Aquatic Sciences **67**:507-516.

Uehlinger, U., B. Kawecka, and C. T. Robinson. 2003. Effects of experimental floods on periphyton and stream metabolism below a high dam in the Swiss Alps (River Spol). Aquatic Sciences **65**:199-209.
Uehlinger, U., C. Konig, and P. Reichert. 2000. Variability of photosynthesis-irradiance curves and ecosystem respiration in a small river. Freshwater Biology **44**:493-507.
Uehlinger, U., M. Naegeli, and S. G. Fisher. 2002. A heterotrophic desert stream? The role of sediment stability. Western North American Naturalist **62**:466-473.
Uehlinger, U. and M. W. Naegeli. 1998. Ecosystem metabolism, disturbance, and stability in a prealpine gravel bed river. Journal of the North American Benthological Society **17**:165-178.
USGS. 2006. USGS water resources of Michigan: General climatology. From http://mi.water.usgs.gov/fdgenclim.php.
Uzarski, D. G., T. M. Burton, and C. A. Stricker. 2001. A new chamber design for measuring community metabolism in a Michigan stream. Hydrobiologia **455**:137-155.
Uzarski, D. G., C. A. Stricker, T. M. Burton, D. K. King, and A. D. Steinman. 2004. The importance of hyporheic sediment respiration in several mid-order Michigan rivers: comparison between methods in estimates of lotic metabolism. Hydrobiologia **518**:47-57.
Vallino, J. J., C. S. Hopkinson, and R. H. Garritt. 2005. Estimating estuarine gross production, community respiration and net ecosystem production: a nonlinear inverse technique. Ecological Modelling **187**:281-296.
Van de Bogert, M. C., S. R. Carpenter, J. J. Cole, and M. L. Pace. 2007. Assessing pelagic and benthic metabolism using free water measurements. Limnology and Oceanography-Methods **5**:145-155.
Van, T. K., W. T. Haller, and G. Bowes. 1976. Comparison of photosynthetic characteristics of 3 submerged aquatic plants. Plant Physiology **58**:761-768.
Vanderbijl, L., K. Sandjensen, and A. L. Hjermind. 1989. Photosynthesis and canopy structure of a submerged plant, Potamogeton Pectinatus, in a Danish lowland stream. Journal of Ecology **77**:947-962.
Vandijk, G. M. and W. Vanvierssen. 1991. Survival of a *Potamogeton Pectinatus L.* population under various light conditions in a shallow eutrophic lake (Lake Veluwe) in the Netherlands. Aquatic Botany **39**:121-129.
Vannote, R. L., G. W. Minshall, K. W. Cummins, J. R. Sedell, and C. E. Cushing. 1980. River continuum concept. Canadian Journal of Fisheries and Aquatic Sciences **37**:130-137.
Velasco, J., A. Millan, M. R. Vidal-Abarca, M. L. Suarez, C. Guerrero, and M. Ortega. 2003. Macrophytic, epipelic and epilithic primary production in a semiarid Mediterranean stream. Freshwater Biology **48**:1408-1420.
Velazquez, D., C. Rochera, A. Camacho, and A. Quesada. 2011. Temperature effects on carbon and nitrogen metabolism in some Maritime Antarctic freshwater phototrophic communities. Polar Biology **34**:1045-1055.
Venkiteswaran, J. J., S. L. Schiff, and L. I. Wassenaar. 2008. Aquatic metabolism and ecosystem health assessment using dissolved O-2 stable isotope diel curves. Ecological Applications **18**:965-982.
Venkiteswaran, J. J., L. I. Wassenaar, and S. L. Schiff. 2007. Dynamics of dissolved oxygen isotopic ratios: a transient model to quantify primary production, community respiration, and air-water exchange in aquatic ecosystems. Oecologia **153**:385-398.
Vilches, C. and A. Giorgi. 2010. Metabolism in a macrophyte-rich stream exposed to flooding. Hydrobiologia **654**:57-65.

Vink, S., M. Bormans, P. W. Ford, and N. J. Grigg. 2005. Quantifying ecosystem metabolism in the middle reaches of Murrumbidgee River during irrigation flow releases. Marine and Freshwater Research **56**:227-241.

Viviani, D. A., K. M. Bjoerkman, D. M. Karl, and M. J. Church. 2011. Plankton metabolism in surface waters of the tropical and subtropical Pacific Ocean. Aquatic Microbial Ecology **62**:1-12.

Von Schiller, D., E. Marti, J. L. Riera, M. Ribot, J. C. Marks, and F. Sabater. 2008. Influence of land use on stream ecosystem function in a Mediterranean catchment. Freshwater Biology **53**:2600-2612.

Wanninkhof, R., P. J. Mulholland, and J. W. Elwood. 1990. Gas exchange rates for a first-order stream determined with deliberate and natural tracers. Water Resources Research **26**:1621-1630.

Ward, J. V., C. T. Robinson, and K. Tockner. 2002. Applicability of ecological theory to riverine ecosystems. Pages 443-450 *in* R. G. Wetzel, editor. International Association of Theoretical and Applied Limnology, Vol 28, Pt 1, Proceedings. E Schweizerbart'sche Verlagsbuchhandlung, Stuttgart.

Warkentin, M., H. M. Freese, U. Karsten, and R. Schumann. 2007. New and fast method to quantify respiration rates of bacterial and plankton communities in freshwater ecosystems by using optical oxygen sensor spots. Applied and Environmental Microbiology **73**:6722-6729.

Warnaars, T. A., M. Hondzo, and M. E. Power. 2007. Abiotic controls on periphyton accrual and metabolism in streams: Scaling by dimensionless numbers. Water Resources Research **43**:DOI: 10.1029/2006WR005002.

Wassenaar, L. I. and G. Koehler. 1999. An on-line technique for the determination of the $\delta^{18}O$ and $\delta^{17}O$ of gaseous and dissolved oxygen. Analytical Chemistry **71**:4965-4968.

Wassenaar, L. I., J. J. Venkiteswaran, S. L. Schiff, and G. Koehler. 2010. Aquatic community metabolism response to municipal effluent inputs in rivers quantified using diel $\delta^{18}O$ values of dissolved oxygen. Canadian Journal of Fisheries and Aquatic Sciences **67**:1232-1246.

Webster, I. T., N. Rea, A. V. Padovan, P. Dostine, S. A. Townsend, and S. Cook. 2005. An analysis of primary production in the Daly River, a relatively unimpacted tropical river in northern Australia. Marine and Freshwater Research **56**:303-316.

Weiss, R. F. 1970. Solubility of nitrogen, oxygen and argon in water and seawater. Deep-Sea Research **17**:721-&.

Whitledge, G. W. and C. F. Rabeni. 2000. Benthic community metabolism in three habitats in an Ozark stream. Hydrobiologia **437**:165-170.

Wilcock, R. J. 1984. Methyl chloride as a gas-tracer for measuring stream reaeration coefficients. 2. stream studies. Water Research **18**:53-57.

Wilcock, R. J., J. W. Nagels, G. B. McBride, K. J. Collier, B. T. Wilson, and B. A. Huser. 1998. Characterisation of lowland streams using a single-station diurnal curve analysis model with continuous monitoring data for dissolved oxygen and temperature. New Zealand Journal of Marine and Freshwater Research **32**:67-79.

Wilde, F. D., D. B. Radtke, and Geological Survey (U.S.). 1998. Handbooks for water-resources investigations. National field manual for the collection of water-quality data. Field measurements. U.S. Geological Survey, Branch of Information Services [distributor], Denver, CO.

Wiley, M. J., L. L. Osborne, and R. W. Larimore. 1990. Longitudinal structure of an agricultural prairie river system and its relationship to current stream ecosystem theory. Canadian Journal of Fisheries and Aquatic Sciences **47**:373-384.

Wingler, A., P. J. Lea, W. P. Quick, and R. C. Leegood. 2000. Photorespiration: metabolic pathways and their role in stress protection. Philosophical Transactions of the Royal Society B-Biological Sciences **355**:1517-1529.
Winterbourn, M. J., J. S. Rounick, and B. Cowie. 1981. Are New Zealand stream ecosystems really different. New Zealand Journal of Marine and Freshwater Research **15**:321-328.
Wissmar, R. C., J. E. Richey, R. F. Stallard, and J. M. Edmond. 1981. Plankton metabolism and carbon processes in the Amazon River, its tributaries, and floodplain waters, Peru-Brazil, May-June 1977. Ecology **62**:1622-1633.
Wood, J. D. 1961. The woodland-oak plains transition zone in the settlement of western upper Canada. Canadian Geographer **5**:43-47.
Wright, J. C. and I. K. Mills. 1967. Productivity Studies on the Madison River, Yellowstone National Park. Limnology and Oceanography **12**:568-577.
WSC. 2001. Water Survey of Canada (WSC), Hydat CD-ROM: Surface water and sediment data. Ottawa, ON.
Xue, X. P., D. A. Gauthier, D. H. Turpin, and H. G. Weger. 1996. Interactions between photosynthesis and respiration in the green alga Chlamydomonas reinhardtii:Characterization of light-enhanced dark respiration. Plant Physiology **112**:1005-1014.
Young, R. 2006. Dissolved oxygen changes and ecosystem metabolism in the Motupipi Catchment - implications for river health assessment.
Young, R. G. and K. J. Collier. 2009. Contrasting responses to catchment modification among a range of functional and structural indicators of river ecosystem health. Freshwater Biology **54**:2155-2170.
Young, R. G. and A. D. Huryn. 1996. Interannual variation in discharge controls ecosystem metabolism along a grassland river continuum. Canadian Journal of Fisheries and Aquatic Sciences **53**:2199-2211.
Young, R. G. and A. D. Huryn. 1999. Effects of land use on stream metabolism and organic matter turnover. Ecological Applications **9**:1359-1376.
Young, R. G., C. D. Matthaei, and C. R. Townsend. 2008. Organic matter breakdown and ecosystem metabolism: functional indicators for assessing river ecosystem health. Journal of the North American Benthological Society **27**:605-625.
Yvon-Durocher, G., A. P. Allen, J. M. Montoya, M. Trimmer, and G. Woodward. 2010. The temperature dependence of the carbon cycle in aquatic ecosystems. Pages 267-313 *in* G. Woodward, editor. Integrative Ecology: From Molecules to Ecosystems.
Yvon-Durocher, G., J. M. Caffrey, A. Cescatti, M. Dossena, P. del Giorgio, J. M. Gasol, J. M. Montoya, J. Pumpanen, P. A. Staehr, M. Trimmer, G. Woodward, and A. P. Allen. 2012. Reconciling the temperature dependence of respiration across timescales and ecosystem types. Nature **487**:472-476.
Yvon-Durocher, G., J. M. Montoya, G. Woodward, J. I. Jones, and M. Trimmer. 2011. Warming increases the proportion of primary production emitted as methane from freshwater mesocosms. Global Change Biology **17**:1225-1234.

Appendix-A:

Reconstructed DO and δ^{18}O-DO Curves and cross plots of δ^{18}O-DO and O_2 saturations

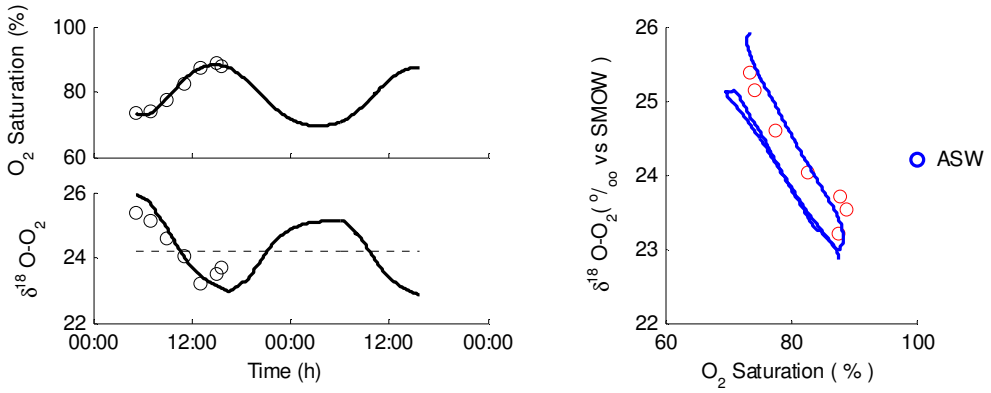

2F-1-1 (2008-July-15)

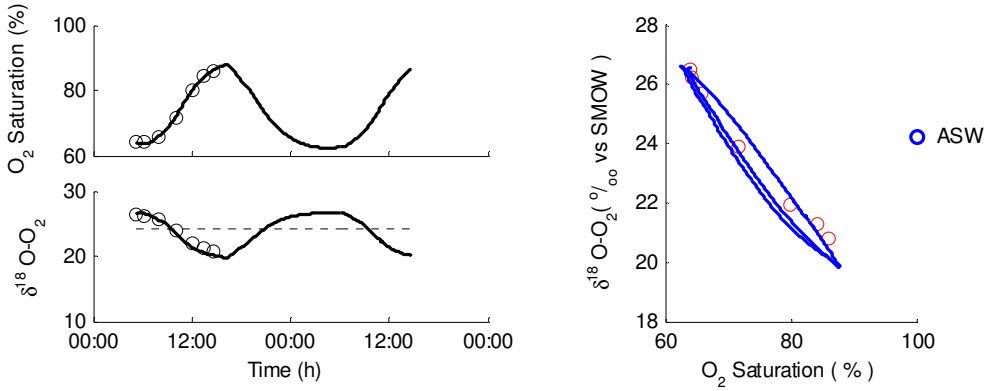

2F-2-0 (2008-August-19)

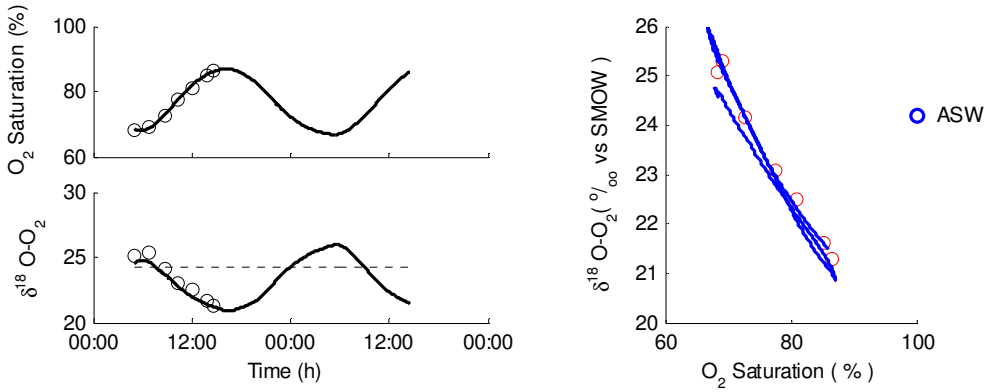

2F09-1-1 (2009-June-22)

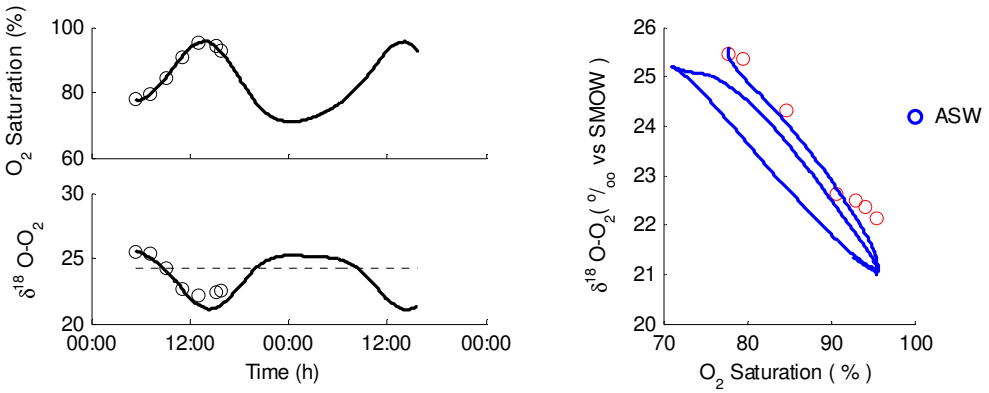

2NF-1-1 (2008-July-15)

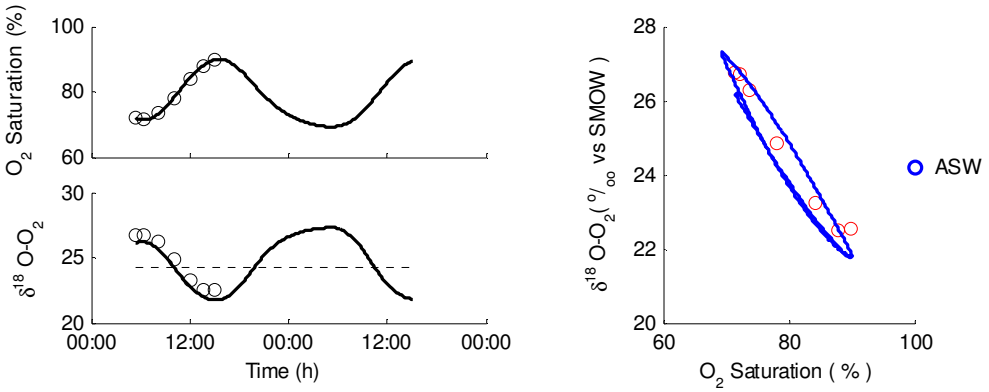

2NF-2-0 (2008-August-19)

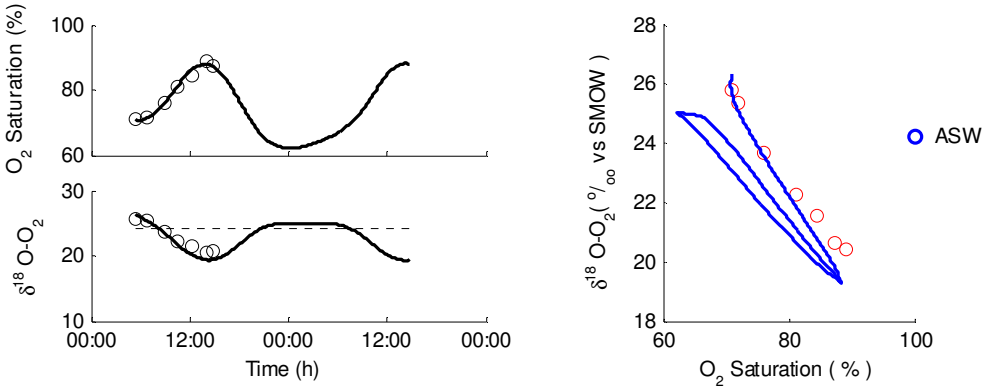

2NF09-1-1 (2009-June-22)

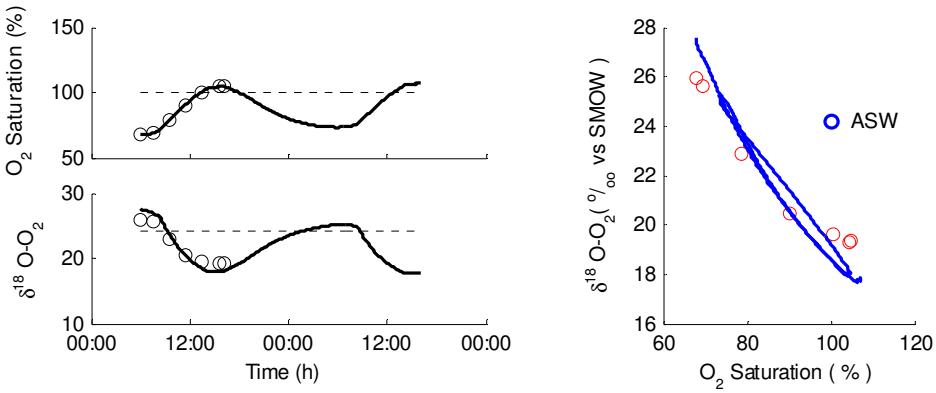

3F-1-1 (2008-July-15)

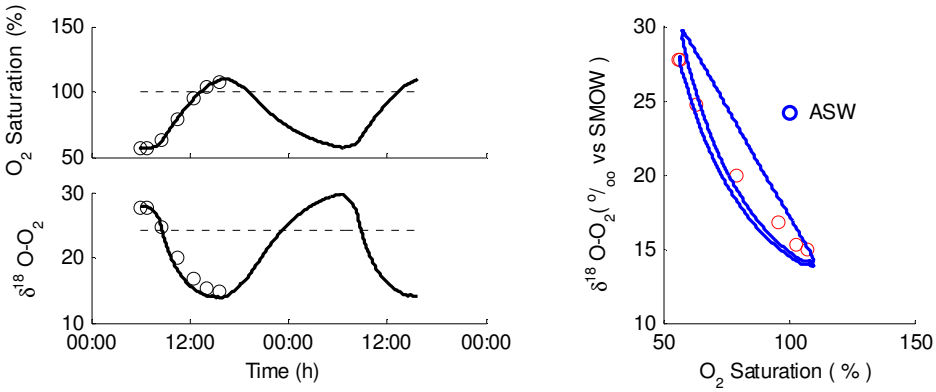

3F-2-0 (2008-August-19)

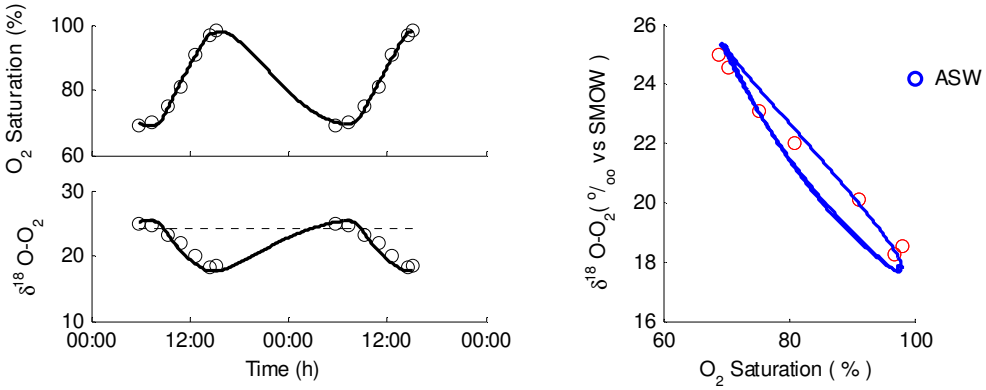

3F09-1-1 (2009-June-22)

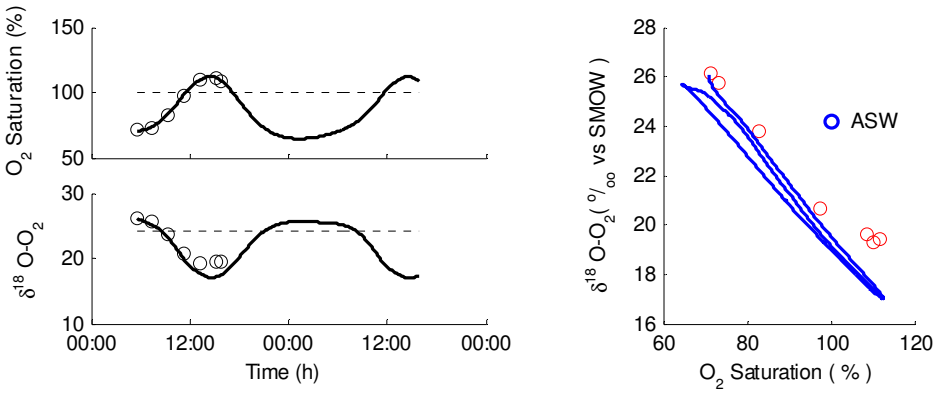

3NF-1-1 (2008-July-15)

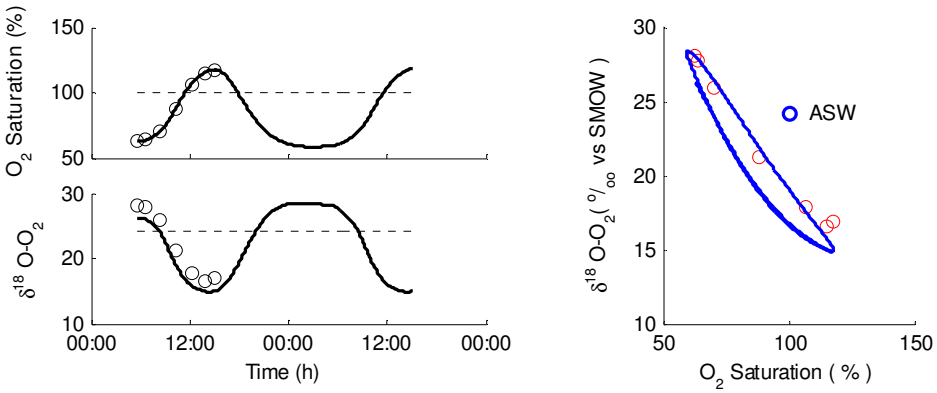

3NF-2-0 (2008-August-19)

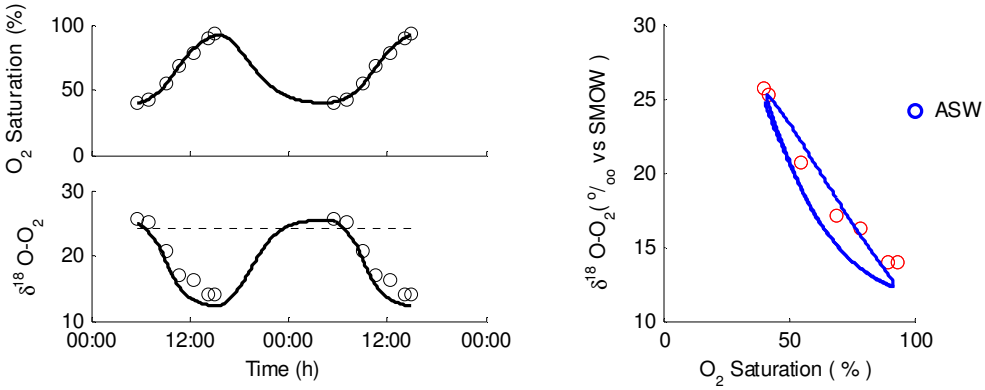

3NF09-1-1 (2009-June-22)

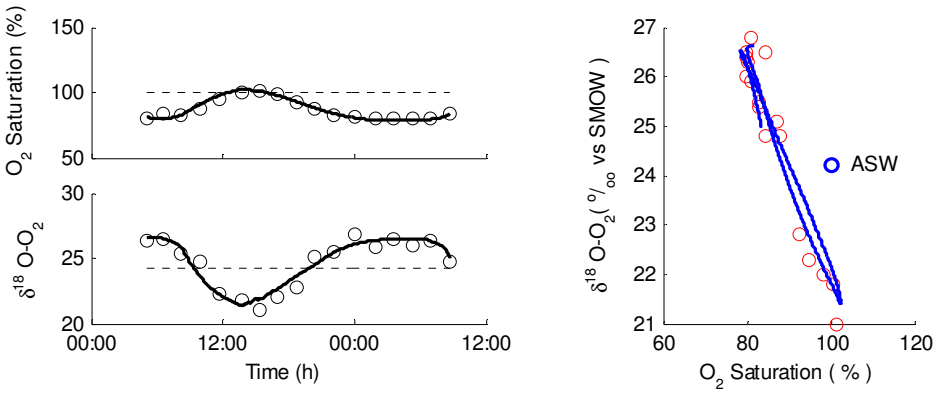

4F-2-1 (2007-July-22)

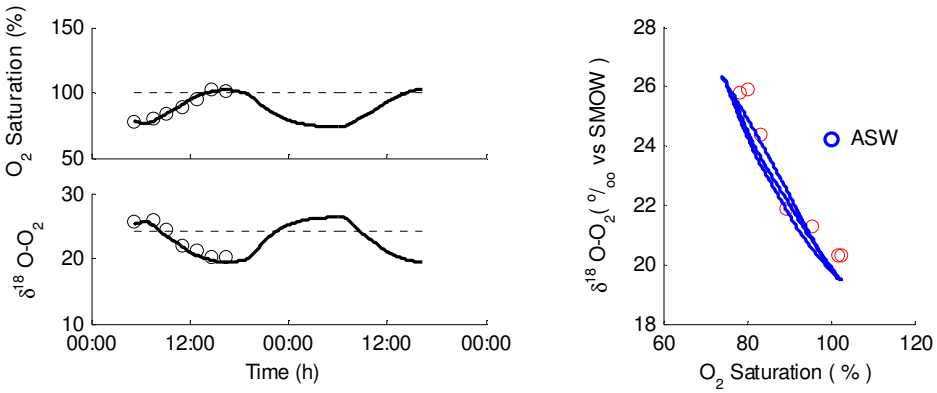

4F-3-1 (2007-August-27)

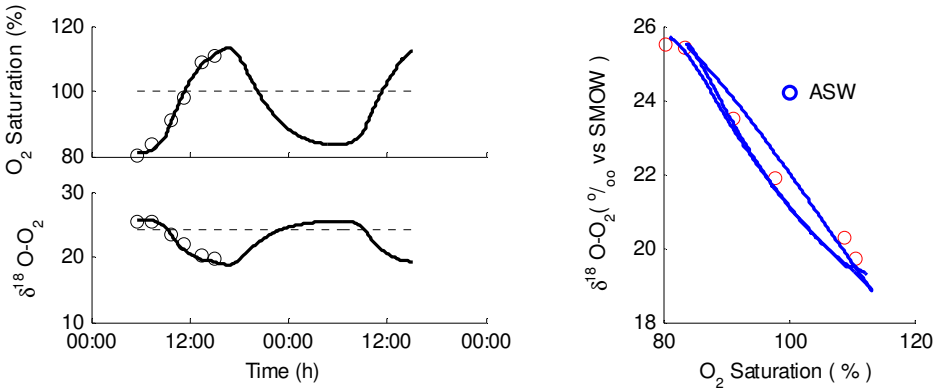

4F-4-1 (2007-Oct-07)

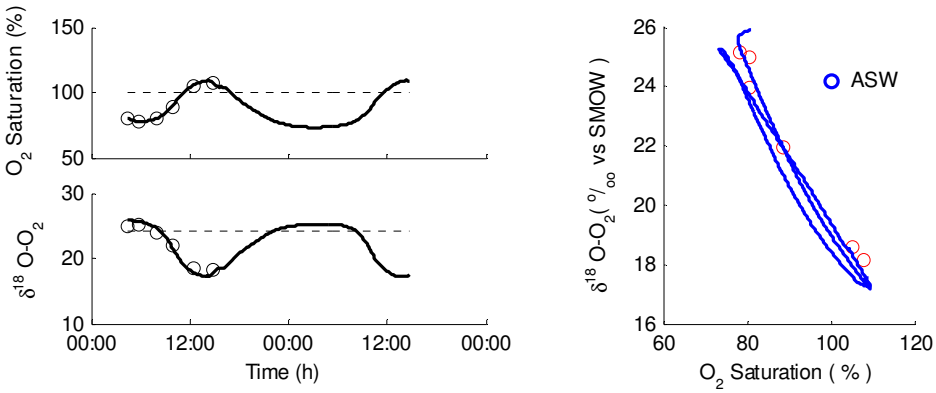

4F-09-1 (2009-June-23)

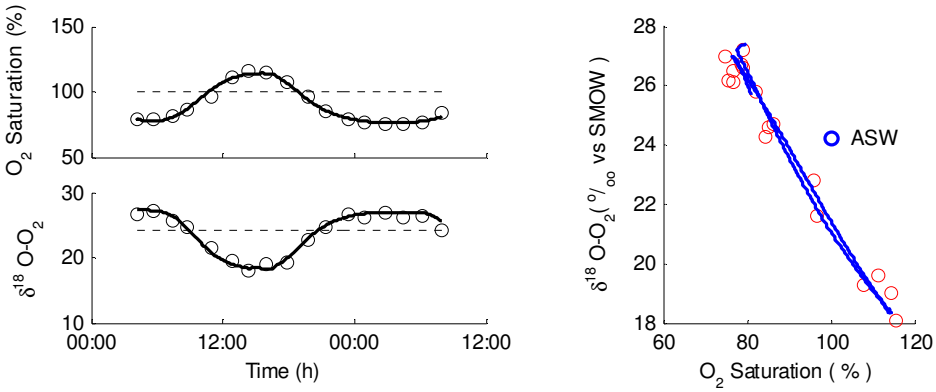

4NF-2-1 (2007-July-22)

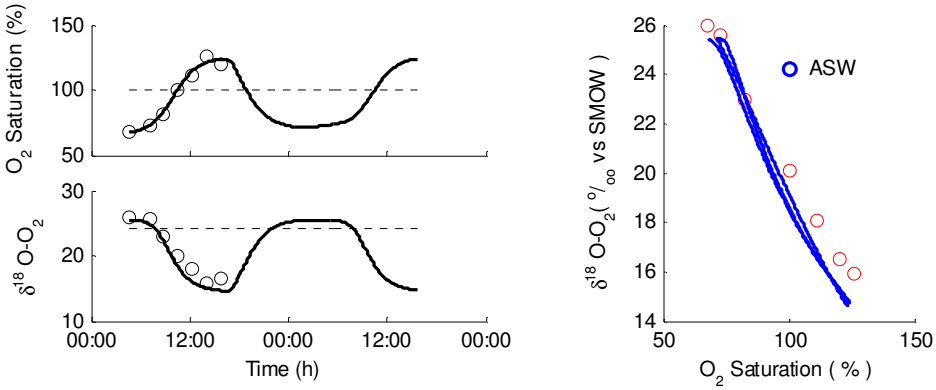

4NF-3-1 (2007-August-27)

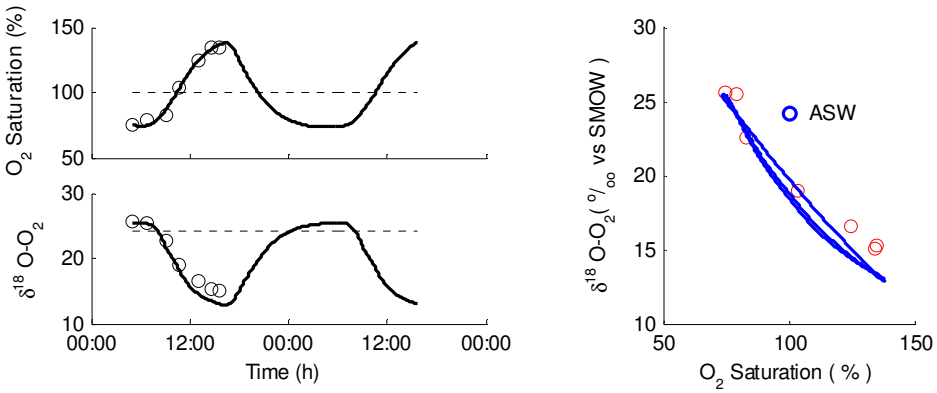

4NF-4-1 (2007-Oct-07)

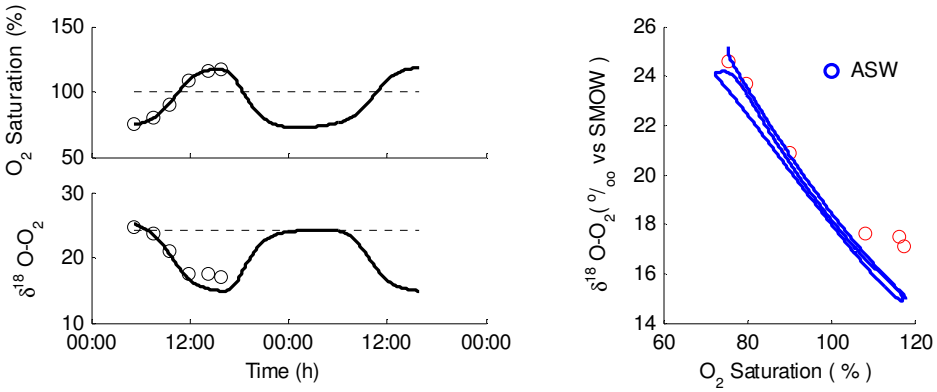

4NF-09-1 (2009-June-23)

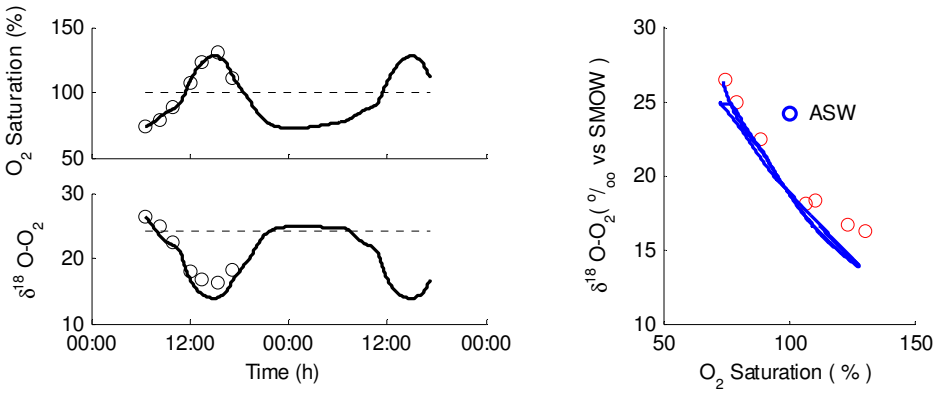

5F-3-1 (2007-August-27)

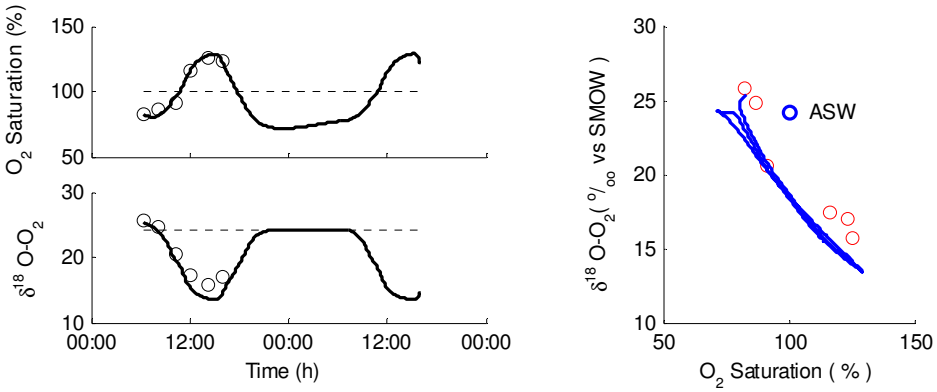

5F-4-1 (2007-Oct-07)

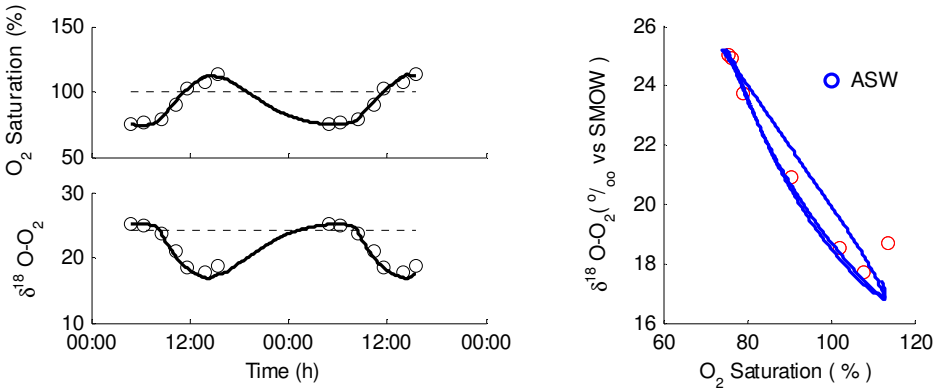

5F-09-1 (2009-June-23)

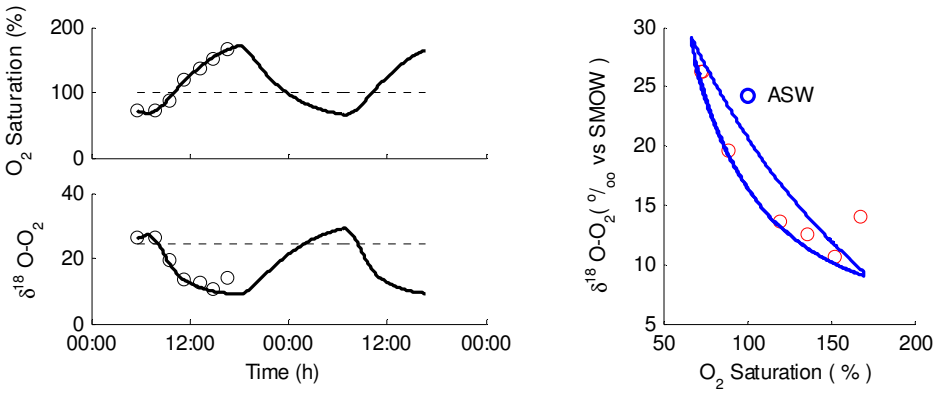

5NF-3-1 (2007-August-27)

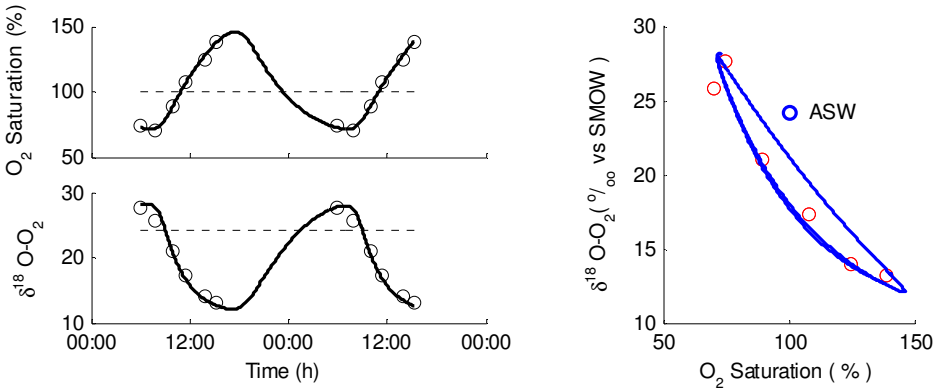

5NF-4-1 (2007-Oct-07)

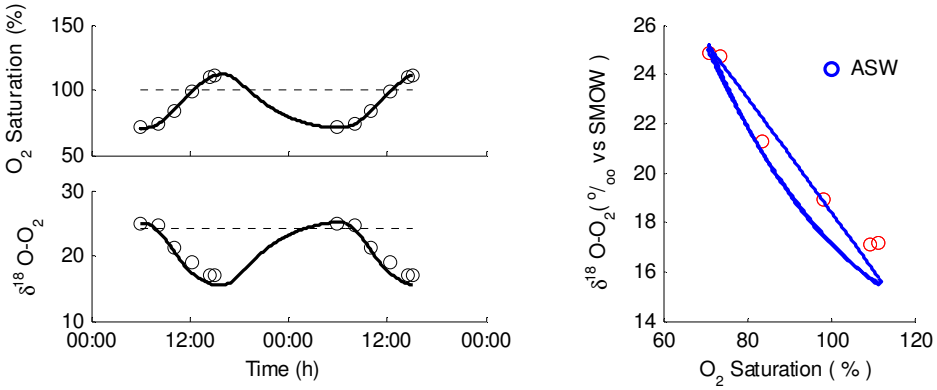

5NF-09-1 (2009-June-23)

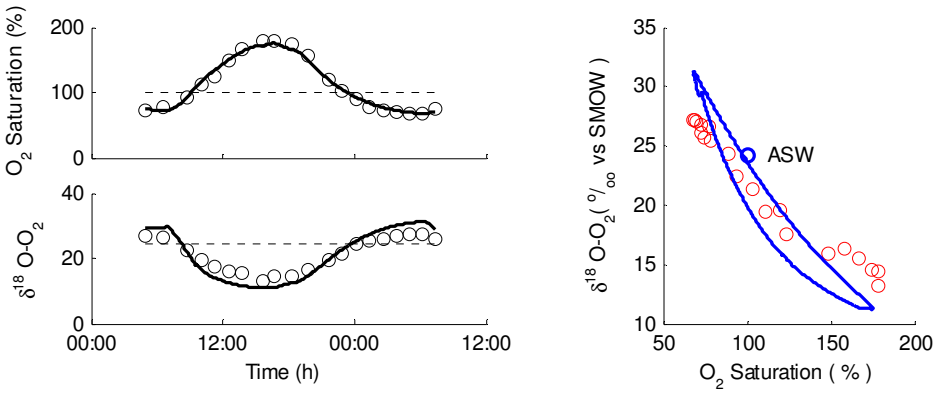

WM-1-2006 (2006-May-24)

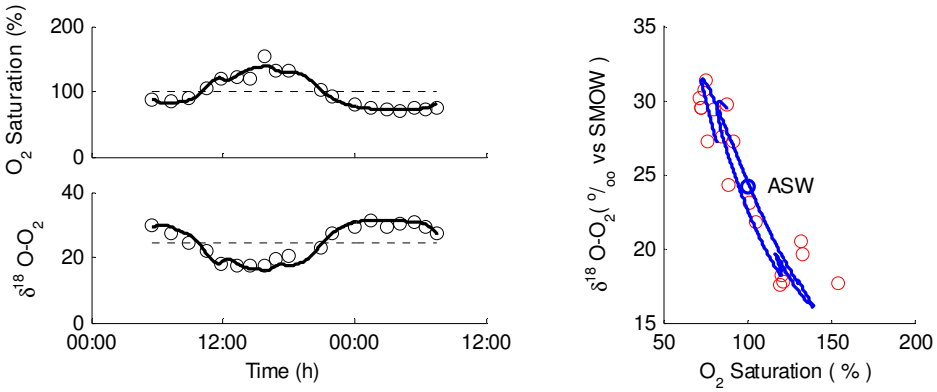

WM-2-2006 (2006-July-05)

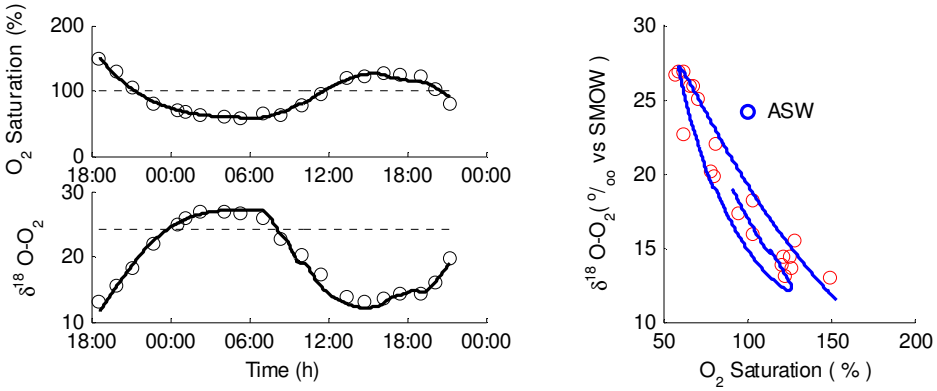

WM-3-2006 (2006-Aug-09)

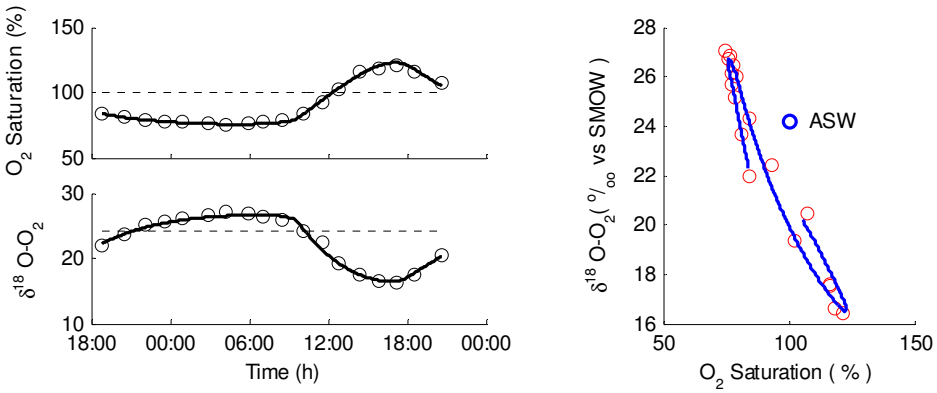

WM-4-2006 (2006-Oct-05)

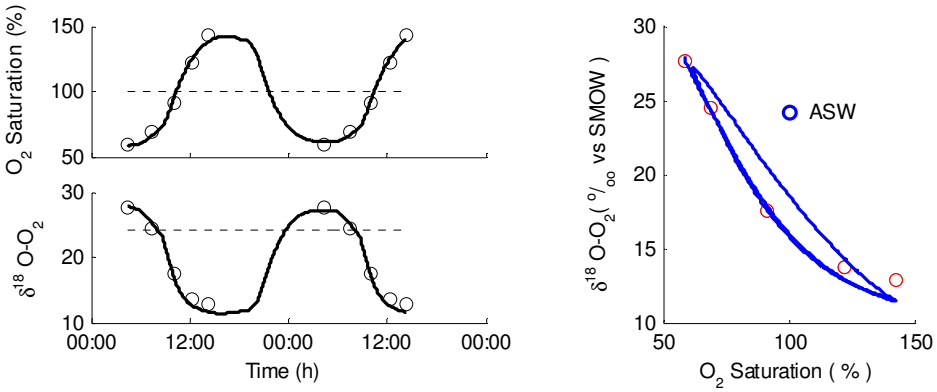

WM-5-2007 (2007-July-10)

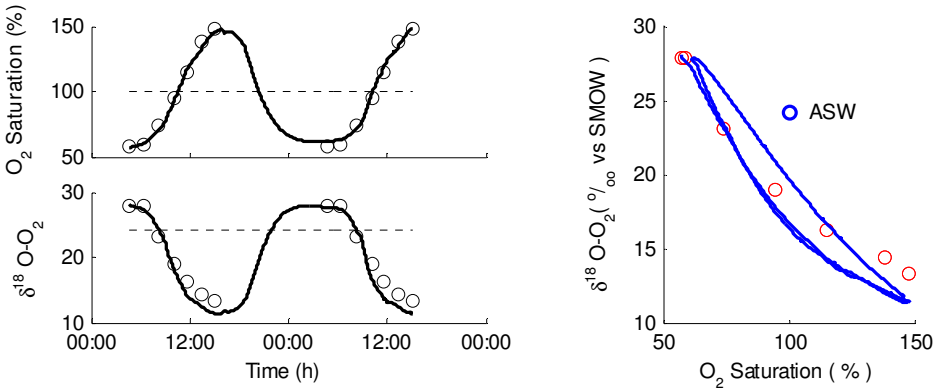

WM-6-2007 (2007-July-31)

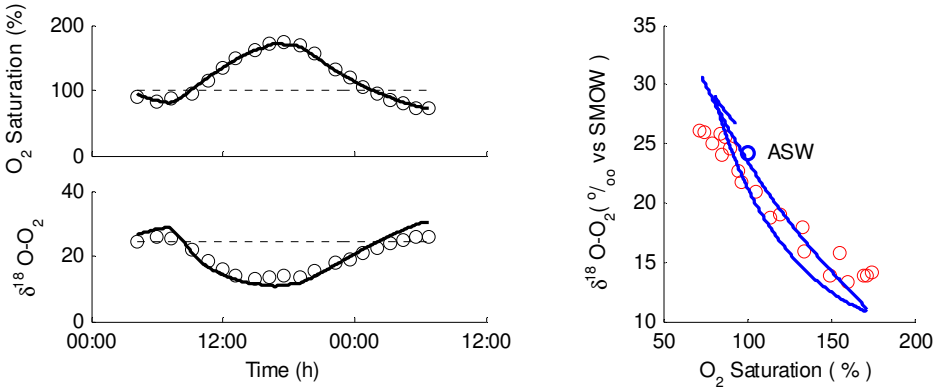

BP-1-2006 (2006-May-24)

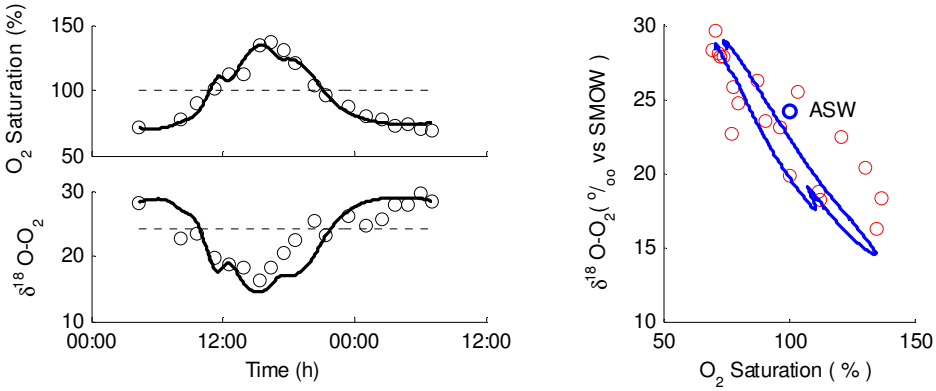

BP-2-2006 (2006-July-05)

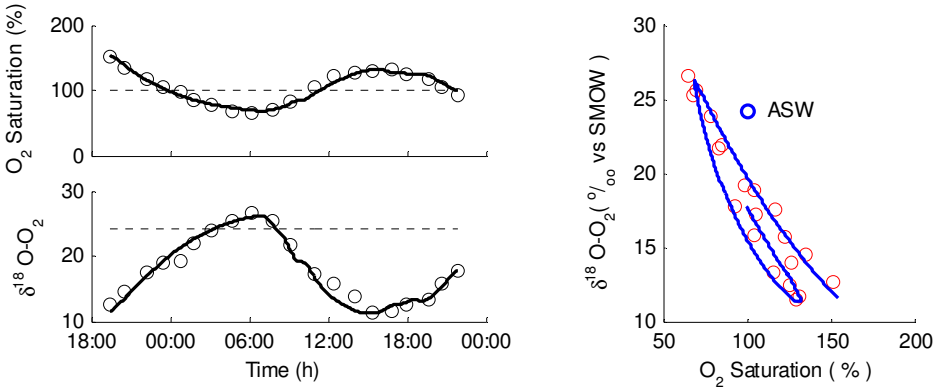

BP-3-2006 (2006-Aug-09)

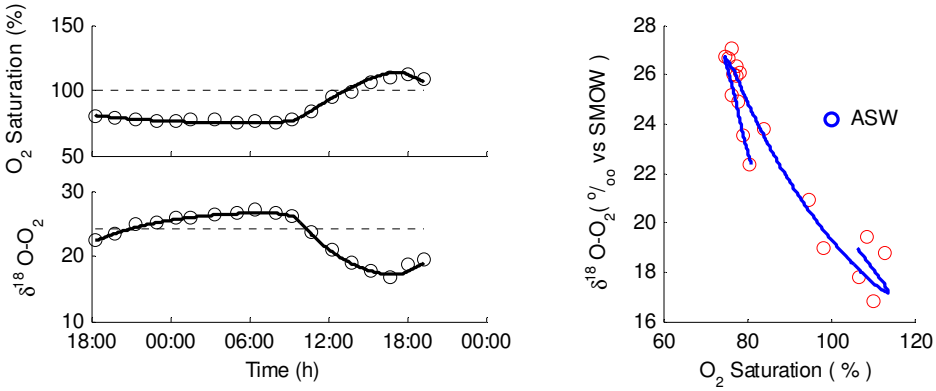

BP-4-2006 (2006-Oct-05)

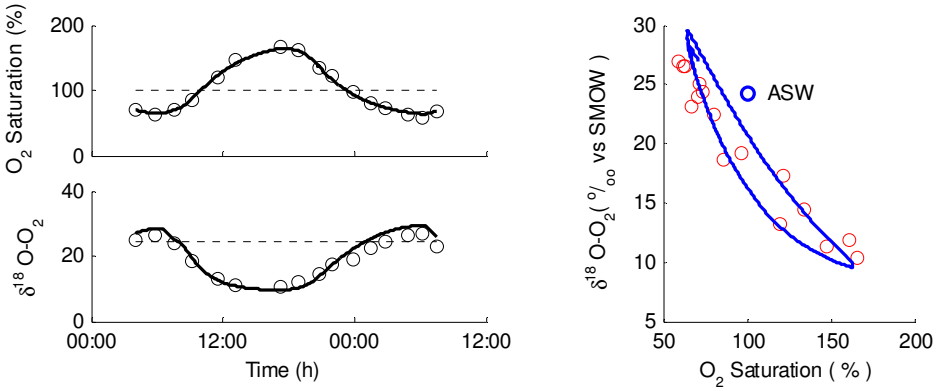

BP-5-2007 (2007-June-26)

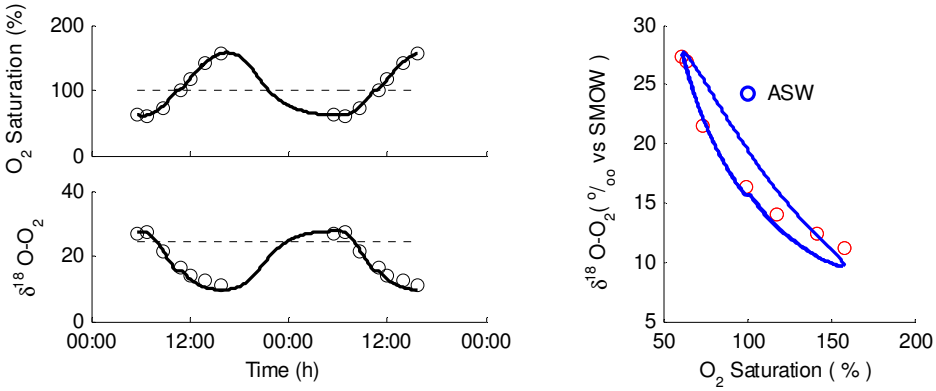

BP-6-2007 (2007-July-31)

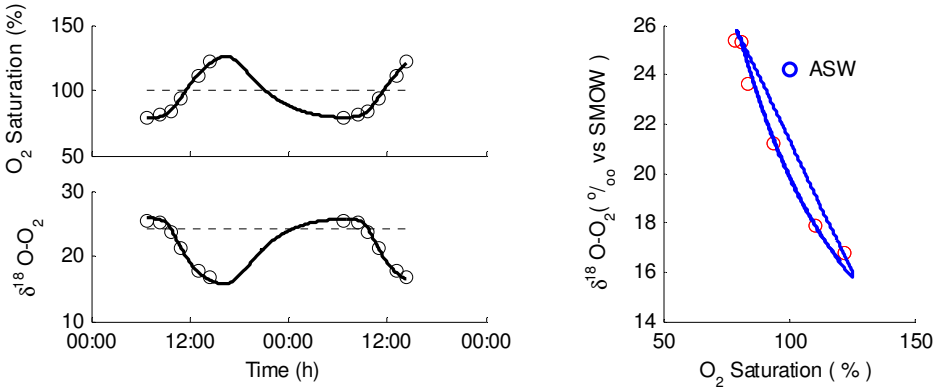

BP-8-2007 (2007-Oct-21)

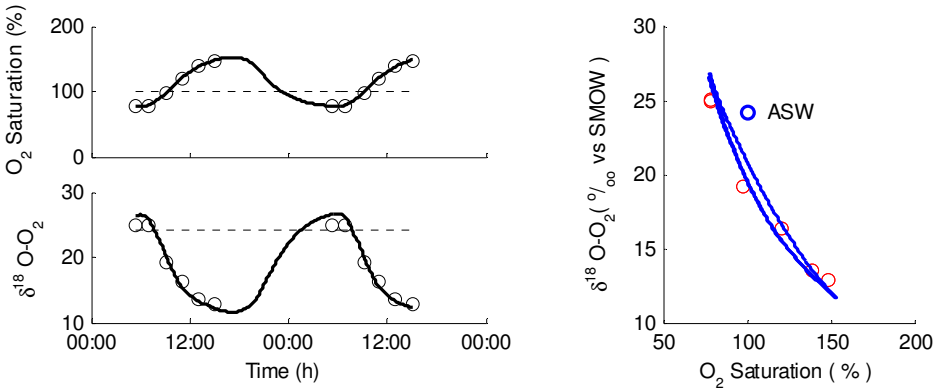

BP-10-2008 (2008-June-06)

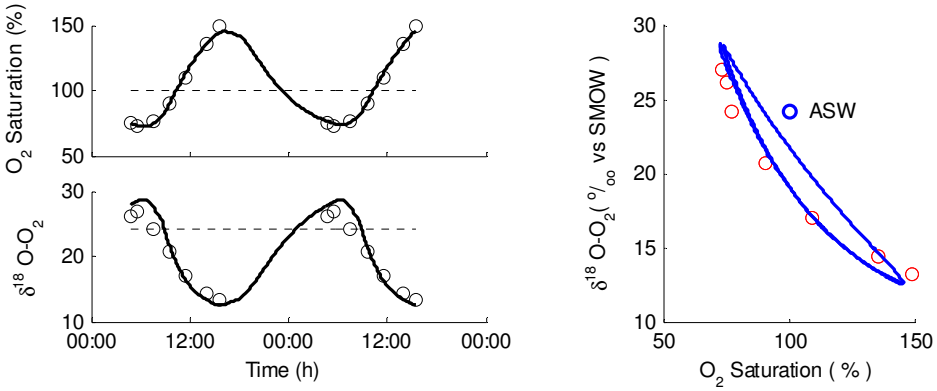

BP-08-1 (2008-June-24)

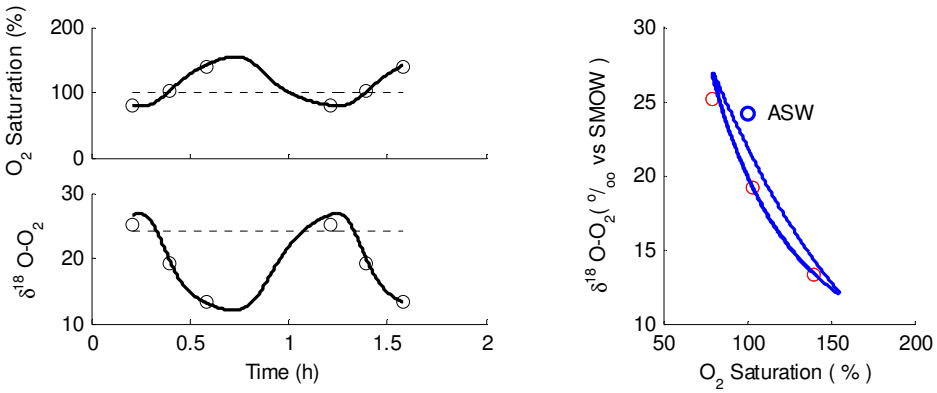

BP-08-2 (2008-July-04)

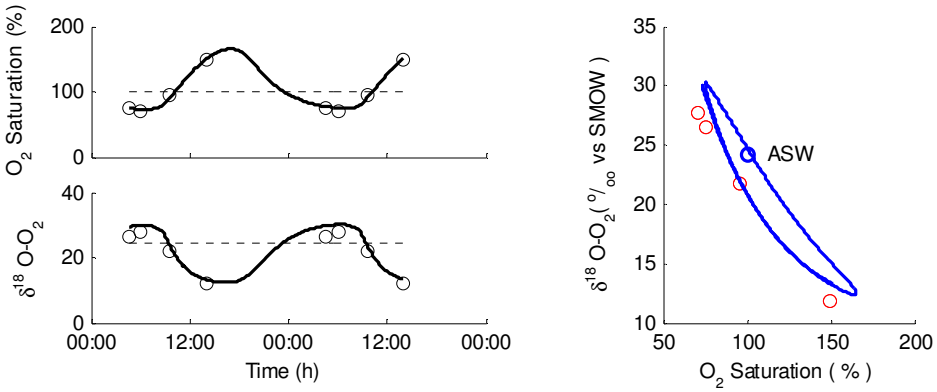

BP-08-3 (2008-Aug-20)

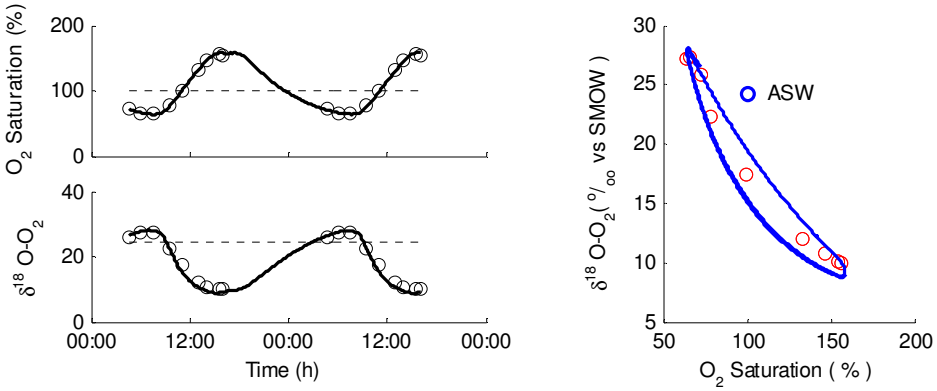

BP-08-4 (2008-Aug-21)

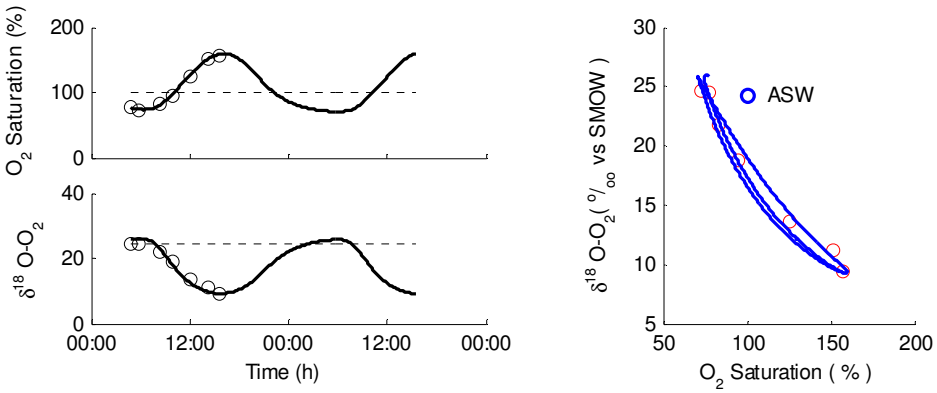

BP-09-1 (2009-May-20)

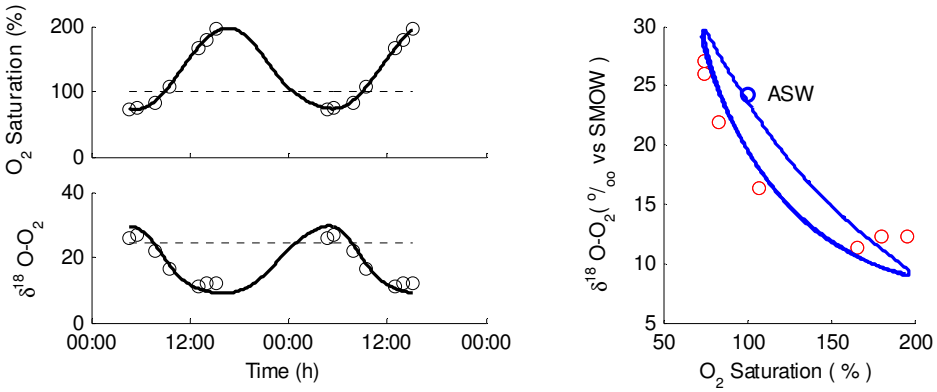

BP-09-2 (2009-May-21)

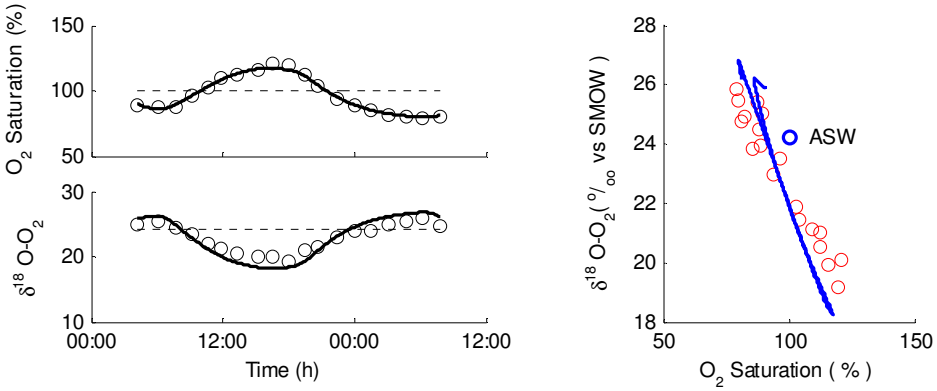

BL-1-2006 (2006-May-22)

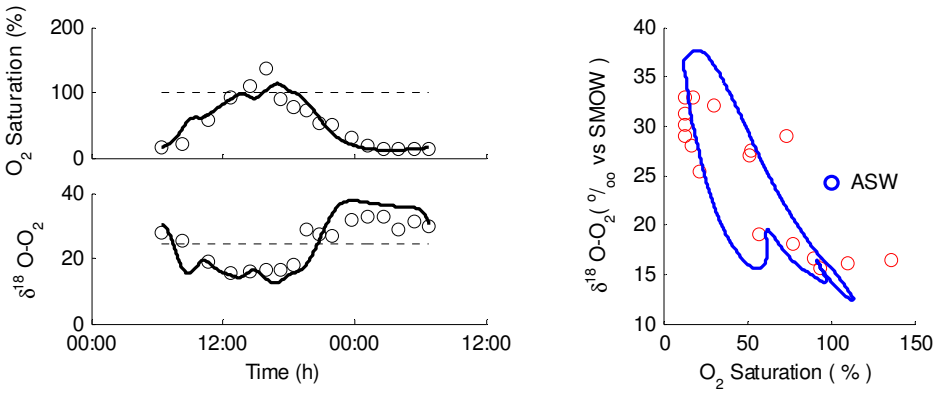

BL-2-2006 (2006-July-06)

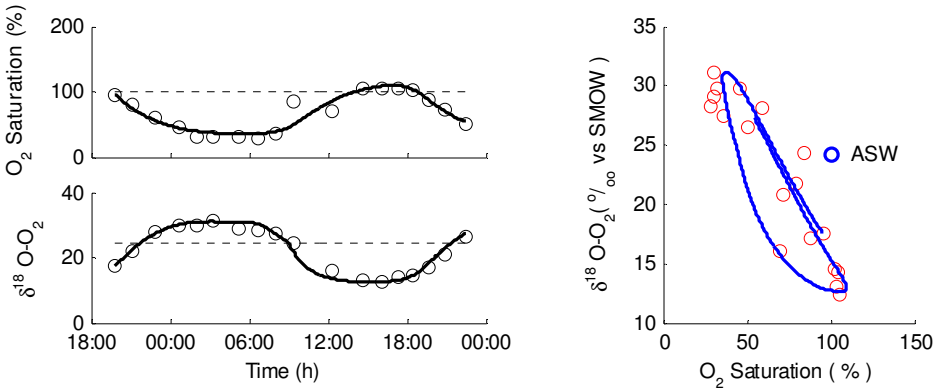

BL-3-2006 (2006-Aug-01)

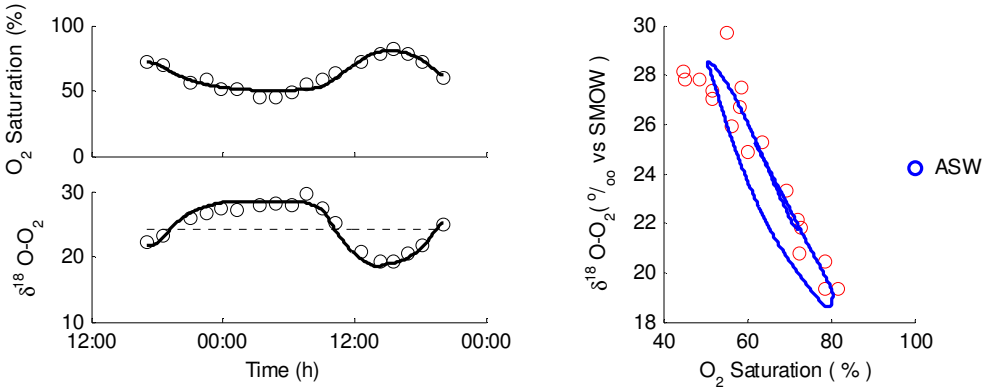

BL-4-2006 (2006-Oct-01)

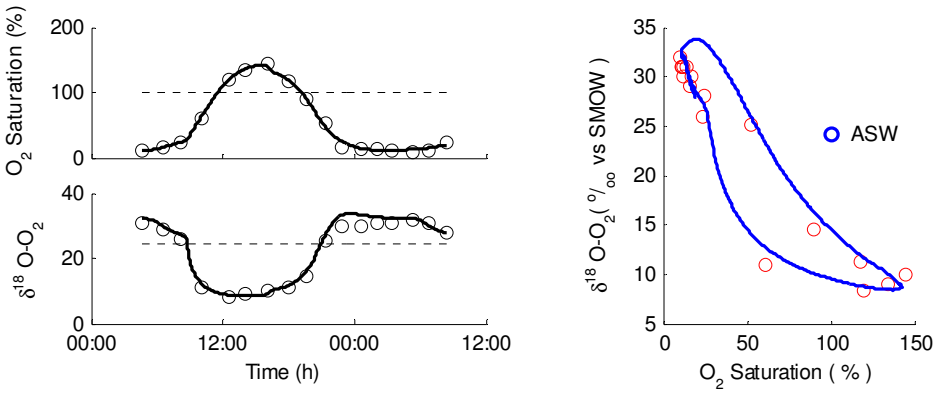

BL-5-2007 (2007-June-26)

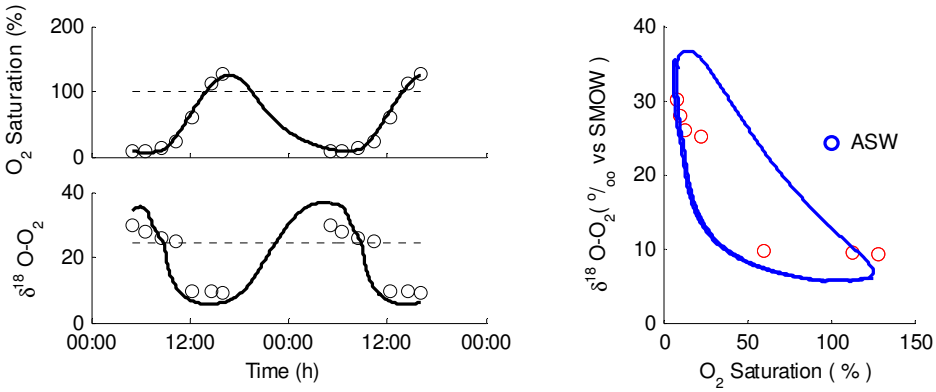

BL-6-2007 (2007-Aug-01)

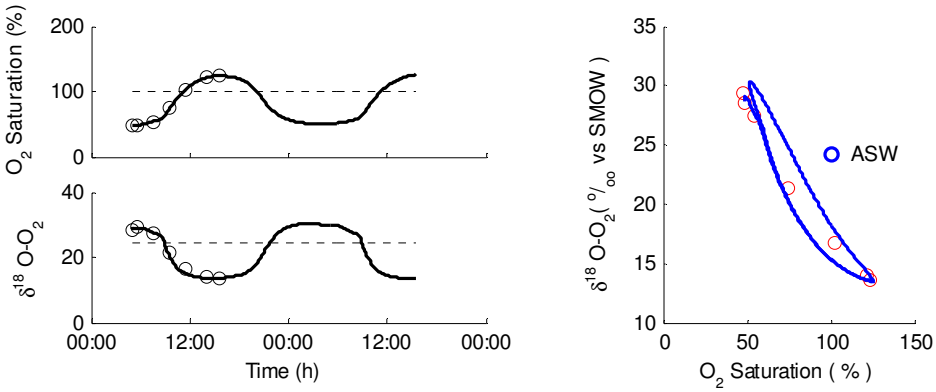

BL-08-1 (2008-July-01)

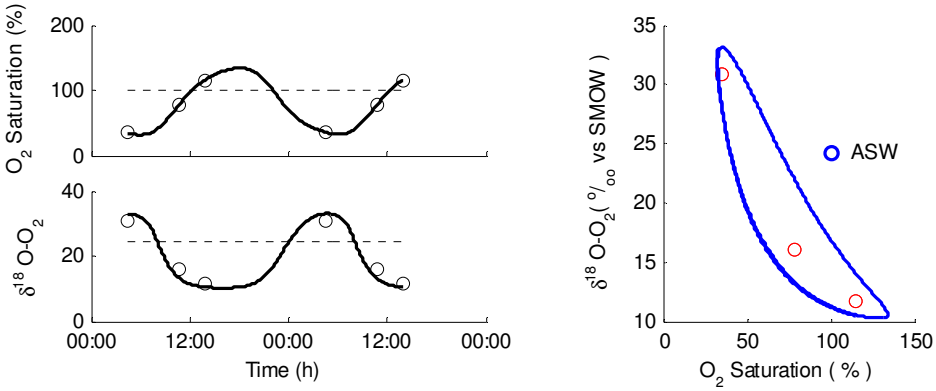

BL-08-2 (2008-July-03)

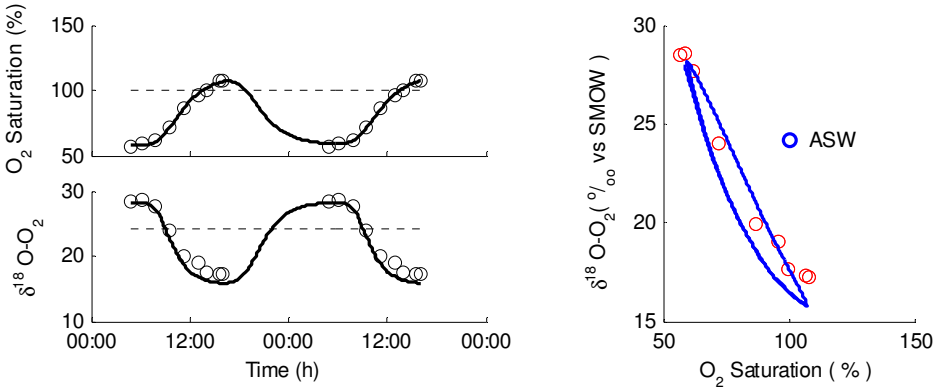

BL-08-3 (2008-Aug-22)

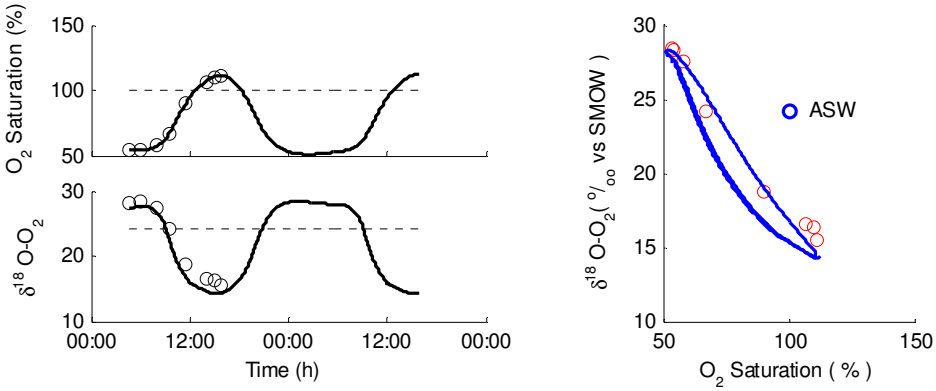

BL-08-4 (2008-Aug-23)

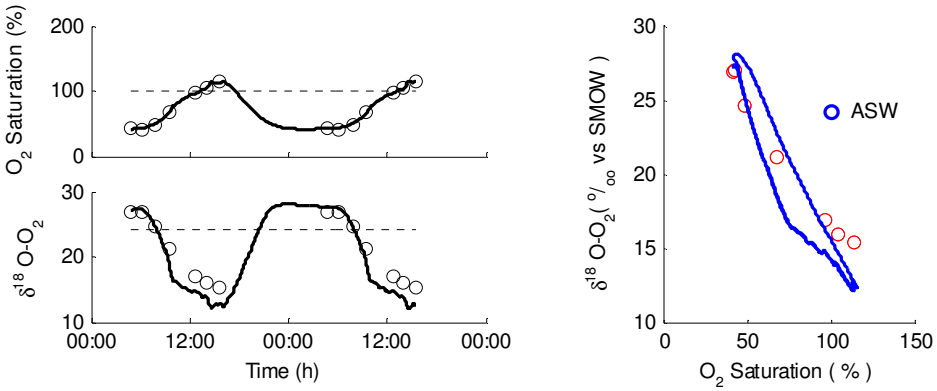

BL-09-1 (2009-May-22)

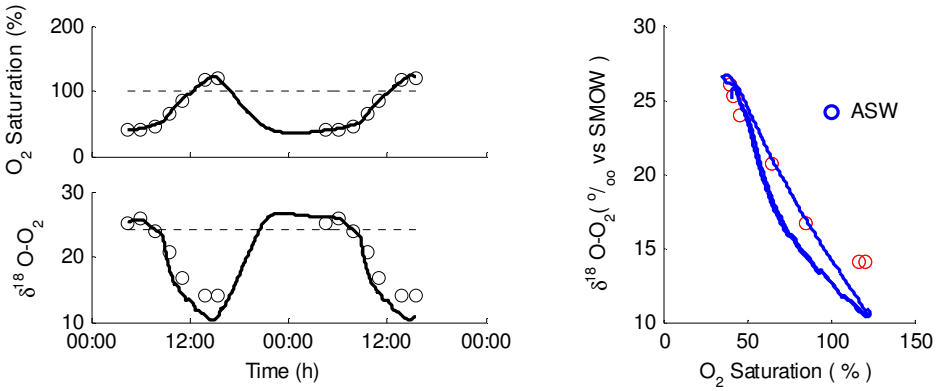

BL-09-2 (2009-May-23)

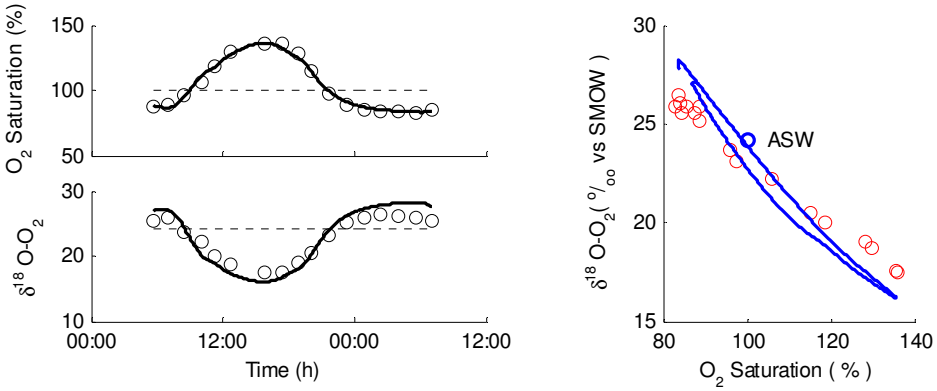

GM-1-2006 (2006-May-22)

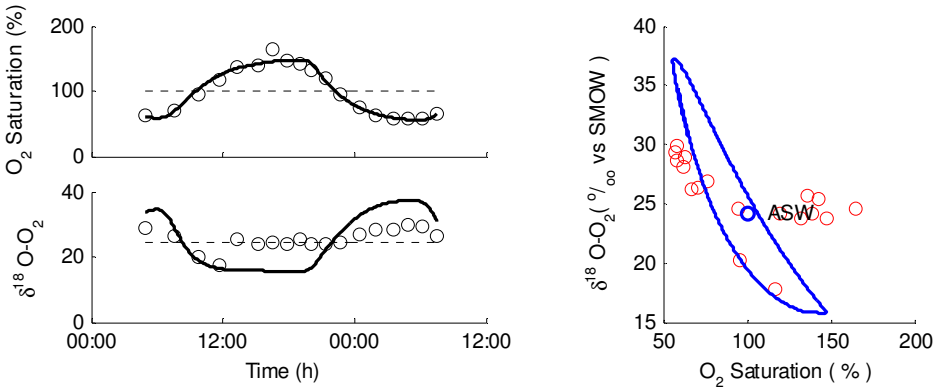

GM-2-2006 (2006-July-06)

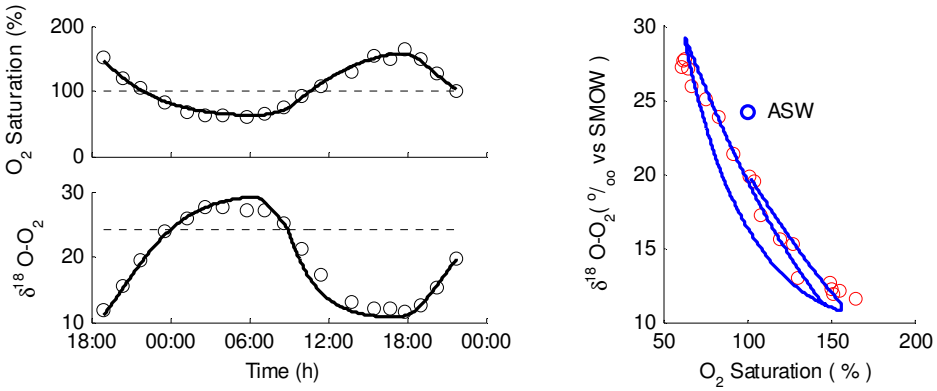

GM-3-2006 (2006-Aug-11)

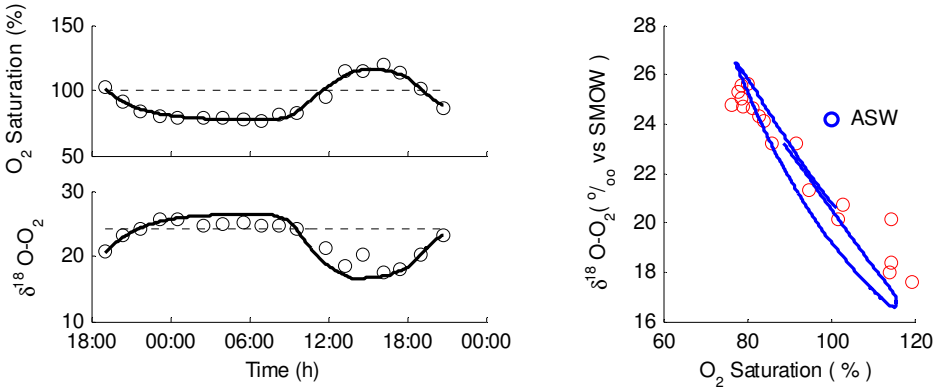

GM-4-2006 (2006-Oct-01)

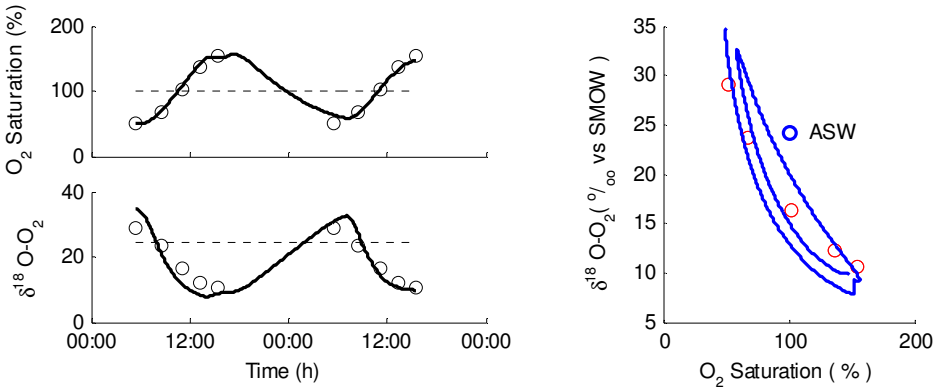

GM-5-2007 (2007-July-10)

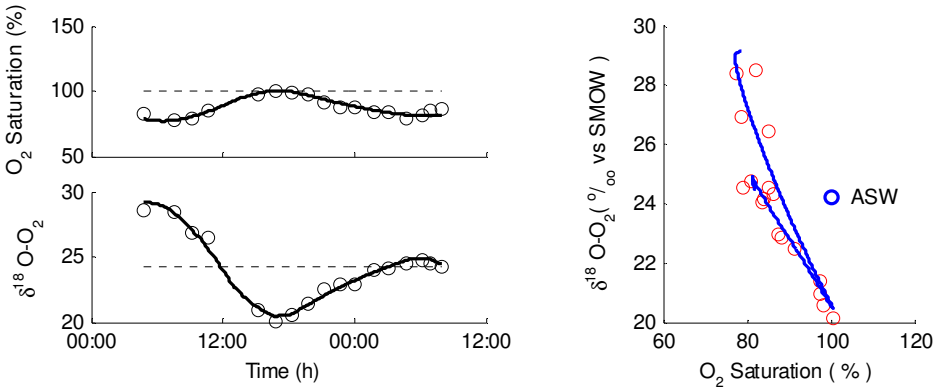

SPA-1-2006 (2006-07-19)

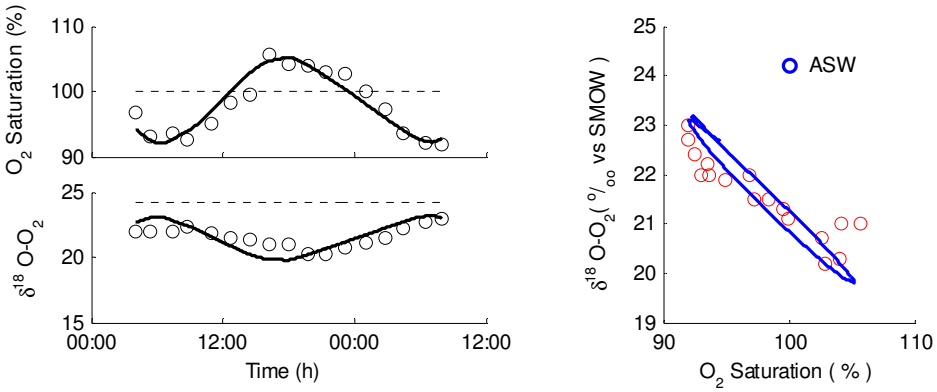

SPA-2-2007 (2007-07-23)

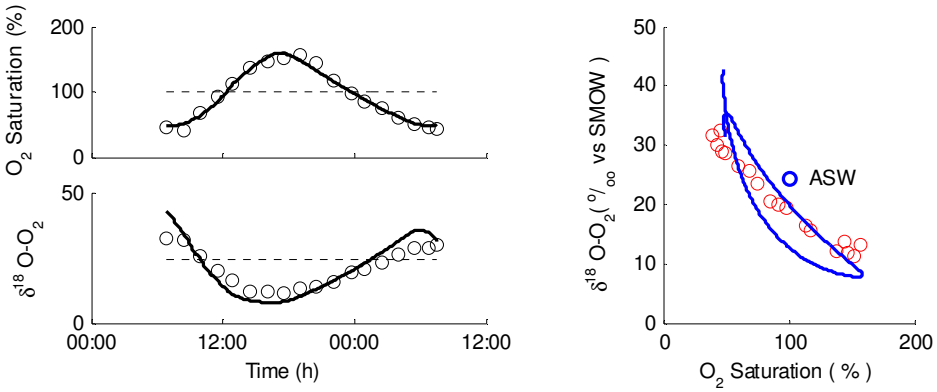

SPB-1-2006 (2006-07-19)

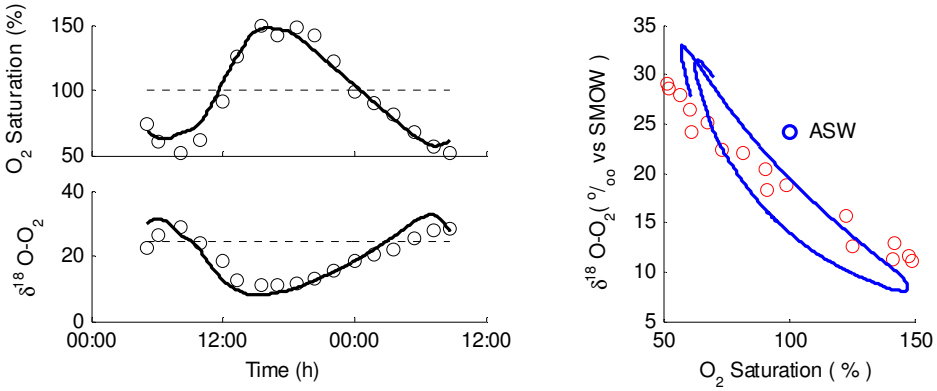

SPB-2-2007 (2007-07-23)